UNIVERSITY OF OXFORD

DOCTORAL THESIS

"Peptidoglycan recycling in the Gram-positive bacterium *Staphylococcus aureus* and its role in host-pathogen interaction"

Author:
Jack Dorling

Supervisor:
Prof. Petros Ligoxygakis

College:
St. Edmund Hall

A thesis submitted in fulfillment of the requirements for the degree of Doctor of Philosophy in Infection, Immunology and Translational Medicine

in the

Ligoxygakis lab
Department of Biochemistry

August 17, 2018

Declaration of Authorship

I, Jack Dorling, declare that this thesis titled, “"Peptidoglycan recycling in the Gram-positive bacterium *Staphylococcus aureus* and its role in host-pathogen interaction"” and the work presented in it are my own. I confirm that:

- This work was done wholly while in candidature for a research degree at the University of Oxford.
- No part of this thesis has previously been submitted for a degree or any other qualification at this University or any other institution.
- Where I have consulted the published work of others, this is always clearly attributed.
- Where I have quoted from the work of others, the source is always given. With the exception of such quotations, this thesis is entirely my own work.
- I have acknowledged all main sources of help.
- Where the thesis is based on work done by myself jointly with others, I have made clear exactly what was done by others and what I have contributed myself.

Signed:

Date:

Word count: 46450 (including Tables and Figure legends)

"Roses.
The flowers are easy to paint,
the leaves difficult."

- Masaoka Shiki (Translated by F. H. Blyth)

UNIVERSITY OF OXFORD

Abstract

Department of Biochemistry

Doctor of Philosophy in Infection, Immunology and Translational Medicine

"Peptidoglycan recycling in the Gram-positive bacterium *Staphylococcus aureus* and its role in host-pathogen interaction"

by Jack Dorling

Bacteria are enclosed by a peptidoglycan sacculus, an exoskeleton-like polymer composed of glycan strands cross-linked by short peptides. The sacculus surrounds the cell in a closed bag-like structure and forms the main structural component of the bacterial cell wall. As bacteria grow and divide, cell wall remodelling by peptidoglycan hydrolases results in the release of peptidoglycan fragments from the sacculus. In Gram-negative bacteria, these fragments are efficiently trapped and recycled. Gram-positive bacteria however shed large quantities of peptidoglycan fragments into the environment. For nearly five decades, Gram-positive bacteria were thus assumed not to recycle peptidoglycan and this process has remained enigmatic until recently. In this thesis, the occurrence and physiological role of peptidoglycan recycling in the Gram-positive pathogen *Staphylococcus aureus* was investigated. *S. aureus* is an important pathogen, and is becoming increasingly resistant to many antibiotics. Through bioinformatic and experimental means it was determined that *S. aureus* may potentially recycle components of peptidoglycan and novel peptidoglycan recycling components were identified and characterised. Though disruption of putative peptidoglycan recycling in *S. aureus* appears not affect growth or gross morphology of this bacterium, potential roles for peptidoglycan recycling in cell wall homeostasis and in virulence were identified. This is to my knowledge the first demonstration of a potential role of peptidoglycan recycling in either of these aspects of bacterial physiology in any Gram-positive bacterium. This is an important step forward in understanding the basic biology of Gram-positive bacteria, and in understanding the mechanisms of virulence in *S. aureus*. Future study of this process in *S. aureus* and other Gram-positive bacteria promises to reveal yet further facets of this process and its functions, potentially leading to the identification of novel therapeutic approaches to combat infections.

Acknowledgements

First and foremost I have to thank my supervisor Prof. Petros Ligoxygakis for giving the opportunity to work on this project and allowing me to design and carry out a research project that was truly my own. I have learned a great deal what it is to be a scientist during my time in your lab, and for that I am truly grateful. I also want to express my thanks to Prof. Sérgio Filipe, through whom I learned how to be a microbiologist, for his help and advice, and for allowing me to come and work with him in ITQB. Our discussions together were always a pleasure, and I hope to continue them in future. I would also like to extend my thanks to Prof. Mariana Pinho for valuable input on this project.

I also thank everyone from the Ligoxygakis, Filipe and Pinho labs that made this time so enjoyable and helped me to develop my ideas and grow as a scientist. My special thanks go first to Dr. Magda Atilano, [redacted]. Your drive and passion for science has inspired me and indeed it was your work that drew me to this field and this lab in the first place. Thank you for your help, advice, and all-round support. [redacted] To Marcus, thank you for your advice, checking my flies, and those rare conversations in the pub. To Ilias, my thanks for your help in everything lab management related and again, for your advice. To Megan, thanks for all of your help[redacted] I also owe special thanks to Gonçalo Covas, who taught me everything HPLC and made me feel at home in ITQB. Without you I doubt some of this work would have been possible. [redacted] To Denise, Rita and Joana thank you again for helping me out[redacted] To Trish, Raquel and Bruno, thank you all for your advice, technical assistance and general willingness to help with anything and everything. And to all the other members of the Pinho lab, thank you for making my time in ITQB so enjoyable.

Next I would like to thank my thesis committee, Prof. Colin Kleanthous and Prof. Jonathon Hodgkin, for your sound advice and your patience. I learned a lot from the meetings we had together. Also, I would like to thank Prof. Simon Foster, your advice and comments on my thesis were particularly illuminating.

I also want to express my thanks to all those who helped me to complete this work, and who are duly acknowledged within the text of this thesis. First, Gonçalo Covas, for all the mCherry::PGRP-SA, the PGN preps, and all the solutions and plates [redacted] Next, to Dr. Aino Jarvelin, for your help with the bioinformatics[redacted] To Erin Johnson and Ana Pielach of the Dunn School EM facility, for your preparation and imaging of those samples; they're beautiful. To Prof. James McCullagh and Elisabete Pires from the University of Oxford Chemistry Research Laboratory Mass Spectrometry Research Facility, for performing LC/MS-MS analyses. And finally, and very importantly, to the media kitchen and support staff at both the University of Oxford Department of Biochemistry and in ITQB UNL for all your help and support.

None of this work would have been possible without funding from the Wellcome Trust, for which I am incredibly thankful. Also, my thanks to EMBO for funding me as part of a short-term fellowship during my time in Portugal, and to St. Edmund Hall for help in covering expenses to make it to summer schools and to Bangkok. I would also like to thank the Infection, Immunology and Translational Medicine coordinators and staff, as well as the other students both past and present, for making this a great experience. I would also like to thank my past rotation supervisors; Prof. Keith Gull, Dr. Sam Dean, and Dr. Jeanne Salje for giving the opportunity to try some new science, and to learn all of those skills I have been using for the last few years. Also, my thanks to New Biochemistry, ITQB, the Sir William Dunn School of Pathology, and to MORU, for giving me a roof and four walls in which to do science.

To my friends, especially [redacted] and [redacted] without you these years would have been so dull, and your support during my thesis writing has been invaluable. My thanks for everything. [redacted]

x



Publications

Thesis publications:

No part of this thesis has yet been published.

Additional DPhil publications:

Sharanjeet Atwal, Suparat Giengkam, Suwittra Chaemchuen, **Jack Dorling**, Nont Kosaisawe, Michael Vannieuwenhze, Somponnat Sampattavanich, Peter Schumann and Jeanne Salje. "Evidence for a peptidoglycan-like structure in *Orientia tsutsugamushi*". In: Molecular Microbiology 105, 3 (2017), pp. 1–13. DOI: 10.1111/mmi.13709.

Contents

Declaration of Authorship iii

Abstract vii

Acknowledgements ix

Publications xi

List of Figures xvii

List of Tables xix

List of Abbreviations xxi

1 General Introduction 1
1.1 *Bacteria rule the world* . . . 1
1.2 *A brief history of cell wall research* . . . 1
1.3 *The biology and pathogenesis of Staphylococcus aureus* . . . 2
1.4 *The bacterial cell envelope* . . . 4
1.5 *Peptidoglycan structure and biosynthesis* . . . 6
1.5.1 Peptidoglycan composition and architecture . . . 6
1.5.2 Peptidoglycan biosynthesis and insertion into the sacculus . . . 11
1.5.3 Post-synthesis peptidoglycan modifications . . . 16
1.6 *Peptidoglycan hydrolysis and cell wall growth* . . . 17
1.6.1 PGN hydrolysis and its regulation . . . 17
1.6.2 Mechanisms of cell wall growth . . . 20
1.7 *Peptidoglycan turnover and recycling* . . . 26
1.7.1 Peptidoglycan turnover . . . 26
1.7.2 PGN recycling in Gram-negative bacteria . . . 28
1.7.3 Peptidoglycan recycling in Gram-positive bacteria . . . 30
1.7.4 Induction of β-lactamase production . . . 35
1.7.5 Peptidoglycan recognition, turnover and recycling in host-pathogen interactions . . . 35
1.8 *Drosophila melanogaster as a model host for Staphylococcus aureus infection* . . . 39
1.8.1 Recognition of peptidoglycan by *D. melanogaster* . . . 39
1.8.2 Use of *D. melanogaster* in studying the roles of peptidoglycan metabolism during *S. aureus* infection . . . 42
1.9 *Aims of the following work* . . . 42

2 Bioinformatic identification and analysis of putative peptidoglycan recycling machinery components in *Staphylococcus aureus* 45
2.1 *Introduction* . . . 45
2.2 *Results* . . . 47
2.2.1 *S. aureus* contains a suite of putative cell wall recycling genes . . . 47
2.2.2 Putative cell wall recycling genes are organised into operons and possess catabolite repression elements . . . 49
2.2.3 Domain structures of putative cell wall recycling proteins give insight into function and the nature of CWR in *S. aureus* . . . 49

2.2.4 Putative cell wall recycling genes are not evenly distributed in other Staphylococci . . . 52
2.2.5 Putative cell wall recycling genes were deleted from *S. aureus* NCTC8325-4 . . . 54
2.3 *Discussion* . . . 55

3 Vigour, morphology and aminosugar auxotrophy in putative *S. aureus* cell wall recycling mutants 61
3.1 *Introduction* . . . 61
3.2 *Results* . . . 63
3.2.1 Putative cell wall recycling mutants show little alteration in growth or morphology in rich media . . . 63
3.2.2 Putative cell wall recycling mutants display growth defects when supplied with cell wall amino sugars as the primary carbon source . . . 66
3.2.3 PtaA is a possible second GlcNAc transporter in *S. aureus* . . . 69
3.2.4 Optical density but not viable cell counts of PR mutants is altered in extended stationary phase . . . 71
3.3 *Discussion* . . . 71

4 NagA is a probable GlcNAc-6-P deacetylase and putative cell wall recycling mutants show possible cell wall ultrastructural alterations 75
4.1 *Introduction* . . . 75
4.2 *Results* . . . 77
4.2.1 NCTCΔ*nagA* and NCTCΔ*glcA*Δ*nagA* accumulate cytoplasmic GlcNAc-6-P . . . 77
4.2.2 Preliminary experiments reveal no major alterations to putative cell wall recycling mutant CW PGN molecular structure . . . 79
4.2.3 Preliminary transmission electron microscopy experiments reveal putative differences in cell wall ultrastructure and septal morphology 80
4.3 *Discussion* . . . 82

5 Putative roles for cell wall recycling and extracellular PGN degradation in *S. aureus* host-pathogen interaction 85
5.1 *Introduction* . . . 85
5.2 *Results* . . . 87
5.2.1 Putative cell wall recycling mutants do not differentially bind mCherry::PGRP-SA at the cell surface . . . 87
5.2.2 NCTCΔ*atl* spent supernatant, but not that of putative cell wall recycling mutants stimulates a PGRP-SA dependent immune response 88
5.2.3 Putative cell wall recycling mutants are impaired in virulence in *D. melanogaster* but *in vivo* bacterial growth is unaltered . . . 89
5.2.4 *S. aureus* cell wall recycling mutants appear to have an active virulence regulatory system, though haemolysis production by NCTCΔ*murQ* and NCTCΔ*murP* is altered . . . 90
5.3 *Discussion* . . . 92

6 General discussion and synthesis 97
6.1 *Putative PR and its functions in S. aureus* . . . 98
6.1.1 The putative peptidoglycan recycling pathways of *S. aureus* . . . 98
6.1.2 Possible physiological functions of peptidoglycan recycling in *S. aureus* 100
6.1.3 Peptidoglycan recycling may potentially play a role in *S. aureus* virulence, while Atl may have a novel role in immune evasion . . . 101
6.2 *Towards an broader understanding of the possible occurrence, nature and function of PR in S. aureus and other Gram-positive bacteria* . . . 101
6.2.1 Do Gram-positive bacteria really 'recycle' peptidoglycan? . . . 101
6.2.2 Aminosugar uptake and metabolism, and the possible regulatory functions of cell wall aminosugar-phosphates in *S. aureus* . . . 102
6.2.3 A re-evaluation of the possible functions of putative Gram-positive PR 104

6.3 *Concluding remarks and future perspectives* . . . 105

7 Materials and methods **107**
7.1 *Bioinformatics* . . . 107
7.1.1 Putative cell wall recycling gene identification in *S. aureus* . . . 107
7.1.2 Identification of putative peptidoglycan recycling operons, *cre* site regulatory elements and protein domains . . . 108
7.1.3 Identification of putative cell wall recycling protein orthologues in other Staphylococci . . . 108
7.1.4 Primer design . . . 108
7.2 *Molecular biology* . . . 109
7.2.1 *S. aureus* DNA extraction . . . 109
7.2.2 PCR, agarose gel electrophoresis, PCR product purification and gel imaging . . . 109
7.2.3 Restriction digests, vector construction and plasmid purification . . . 110
7.3 *Microbiological methods* . . . 110
7.3.1 Bacterial strains, general growth conditions, growth analyses and frozen stock preparation . . . 110
7.3.2 Preparation and transformation of *E. coli* DH5α competent cells . . . 111
7.3.3 Preparation and electroporation of *S. aureus* RN4220 electrocompetent cells . . . 113
7.3.4 Phage lysate preparation and phage transduction of NCTC8325-4 . . . 113
7.3.5 Construction of markerless gene deletion mutants in *S. aureus* NCTC8325-4 . . . 114
7.3.6 Streptozotocin resistance assay . . . 116
7.3.7 Stationary phase viable cell count assay . . . 116
7.3.8 Haemolysis assay . . . 117
7.4 *Microscopy* . . . 117
7.4.1 Live cell imaging of bacterial cells . . . 117
7.4.2 Live imaging of *Drosophila melanogaster* . . . 118
7.4.3 Transmission electron microscopy . . . 118
7.5 *Biochemical methods* . . . 119
7.5.1 Extraction of *S. aureus* cytoplasmic content . . . 119
7.5.2 CW PGN purification . . . 119
7.5.3 Purification of mCherry::PGRP-SA . . . 121
7.6 *Chromatography and mass spectrometry* . . . 122
7.6.1 Analysis of cytoplasmic GlcNAc-6-P levels by LC-MS/MS . . . 122
7.6.2 Analysis of cell wall peptidoglycan structure by RP-HPLC . . . 123
7.7 *Host-pathogen interaction* . . . 124
7.7.1 Drosophila culture . . . 124
7.7.2 Bacterial inoculate preparation, spent supernatant preparation and injection of *Drosophila melanogaster* . . . 124
7.7.3 Survival assays and determination of infection bacterial titres . . . 124
7.7.4 Assessment of Drosomycin::GFP production and *drs* transcription levels 125
7.8 *Statistical analyses* . . . 126

A Additional primers and strains used in this study **129**

B Sequencing primers and sequencing results **133**

C Supplementary data **135**

Bibliography **139**

List of Figures

1.1 A simplified schematic of the cell envelopes of Gram-positive and Gram-negative bacteria . . . 5
1.2 The basic chemical structure of peptidoglycan . . . 7
1.3 Classical models of peptidoglycan tertiary structure . . . 8
1.4 A comparison of cell envelope and peptidoglycan architectural features of *E. coli*, *B. subtilis* and *S. aureus* . . . 10
1.5 A generalised overview of peptidoglycan biosynthesis . . . 12
1.6 Hydrolysis of glycosidic, amide and peptide bonds of peptidoglycan by peptidoglycan hydrolases . . . 18
1.7 Models for the organisation of cell wall synthesis complexes and Gram-positive cell wall growth . . . 21
1.8 Septal cross-wall structure and development in *S. aureus* . . . 25
1.9 Peptidoglycan recycling pathways of Gram-negative bacteria . . . 29
1.10 Putative peptidoglycan recycling pathways in Gram-positive bacteria . . . 32
1.11 Mechanisms of carbon catabolite repression in Gram positive bacteria . . . 33
1.12 Recognition of peptidoglycan by the vertebrate innate immune system . . . 36
1.13 Peptidoglycan recognition in *D. melanogaster* . . . 40

2.1 The genomic context of putative cell wall recycling genes and putative regulatory elements in *S. aureus* . . . 50
2.2 Predicted functional domains of putative cell wall recycling proteins . . . 51
2.3 A highly conserved GlcA homologue is present in *S. saprophyticus* . . . 52
2.4 Genomic organisation of putative cell wall recycling genes is largely conserved in Staphylococci . . . 55
2.5 Putative cell wall recycling genes were deleted from *S. aureus* . . . 56

3.1 Growth of putative cell wall recycling mutants in rich media . . . 63
3.2 Putative cell wall recycling mutants show no obvious alteration to morphology 64
3.3 Putative cell wall recycling mutants show growth defects on cell wall aminosugars . . . 65
3.4 NCTCΔ*murQ* and NCTCΔ*murP* produce small colonies after growth in CDM(MurNAc) . . . 67
3.5 Streptozotocin resistance assays of putative cell wall recycling mutants . . . 69
3.6 Optical density and colony forming unit growth profiles of putative cell wall recycling mutants . . . 70

4.1 Profiling of cytoplasmic GlcNAc-6-P levels in putative cell wall recycling mutants implicated in GlcNAc uptake and reutilisation . . . 77
4.2 Cell wall peptidoglycan structure of putative cell wall recycling mutants . . . 78
4.3 Reference *S. aureus* cell wall peptidoglycan chromatogram and muropeptide structures . . . 79
4.4 Ultrastructure of the *S. aureus* cell envelope . . . 80
4.5 Cell wall ultrastructure of putative cell wall recycling mutants . . . 81

5.1 PGRP-SA binding to the surface of putative cell wall recycling mutants . . . 88
5.2 Drosomycin::GFP production in *DD1* flies upon injection with spent culture supernatant of putative cell wall recycling mutants and NCTCΔ*atl* . . . 89

5.3 Survival of *D. melanogaster* upon infection with putative cell wall recycling mutants and *in vivo* growth of bacterial strains 91
5.4 Haemolysis of sheep's blood is altered in NCTCΔ*murQ* and NCTCΔmurP . . 93

6.1 An overview of the putative peptidoglycan recycling pathways of *S. aureus* . 98

7.1 Construction of *S. aureus* deletion mutants 115
7.2 Elution profiles for ion chromatography and RP-HPLC 123

C.1 Enlargements of panels from Figure 3.3 to more clearly show stationary phase OD_{600} dynamics 135
C.2 Transmission electron microscopy field images of putative cell wall recycling mutants 137
C.3 Initial infection titres for *D. melanogaster* survival experiments 138
C.4 *In vivo* growth of NCTC8325-4 in *25174* flies in different experimental blocks . 138

List of Tables

2.1 Putative cell wall recycling proteins identified in *S. aureus* 48
2.2 Putative cell wall recycling protein orthologues identified in Staphylococci . . 53
2.3 Strains and plasmids produced in this study. 57

3.1 Mean maximum growth rates of putative cell wall recycling mutants from Figure 3.3 66

4.1 Descriptive statistics of cell wall layer thicknesses and peptidoglycan layer staining measurements determined by electron microscopy 82

7.1 Composition of chemically defined medium without carbon sources. 112
7.2 Summary of statistical models used for data analysis 128

A.1 Additional miscellaneous primers 129
A.2 Primers used to confirm integration of pMAD constructs 129
A.3 Primers used to create deletion constructs 130
A.4 Additional strains and plasmids used in this study 131

B.1 Sequencing primers used in this study 133
B.2 Results of sequencing of pMAD constructs 134
B.3 Results of sequencing of final mutant strains 134

C.1 Output of statitical analyses for r_0 and stationary phase OD_{600} in TSB and CDM(Glc) from Figure 3.3 and Table 3.1 136

List of Abbreviations

Abbreviation	Meaning
-6-P	-6-phosphate
ABC	ATP-binding cassette
ADP	Adenosine diphosphate
A_2pm	Diaminopimelic acid
AGE	Agarose gel electrophoresis
Ala	Alanine
AFM	Atomic force microscopy
aMLAA	*N*-acetylanhydromuramic acid-L-Alanine amidase
AMP	Antimicrobial peptide
Amp	Ampicillin
aPBP	Class A PBP
anhMurNAc	Anhydromuramic acid
ANODE	Analysis of Deviance
ANOVA	Analysis of Variance
ASC	Activating signal co-integrator
Asp	Aspargine
ATP	Adenosine triphosphate
BLAST	Basic logical alignment search tool
bp	base pair
bPBP	Class B PBP
BRB	Best Reciprocal Blast
C_{55}P	bactoprenol/undecaprenylpyrophosphate
CARD	caspase recruitment domain
CDS	Coding sequence
CCR	Carbon catabolite repression
CDM	Chemically defined medium
CERK	Ceramide kinase
CFU	Colony forming unit
CMOS	Complementary metal-oxide-superconductor
COG	Cluster of orthologous genes
CP	Carboxypeptidase
CPS	Capsular polysaccharide
cre	Catabolite responsive element
CW	Cell Wall
CWBD	Cell wall binding domain
CWR	Cell wall recycling
CWSC	Cell wall synthesis complex
DAP	Diaminopimelic acid
DEPC	Diethyl pyrocarbonate
DEPCW	DEPC-treated water
Di	Dif
DMC	Dunnett's multiple comparison
DMSO	Dimethylsulphoxide
DNA	Deoxyribonucleic acid
dNTPs	Deoxyribonucleotide-triphosphates
Ds	Dorsal

DTT	Dithiothreitol
DU	Disaccharide unit
EI/II	Enzyme I/II
EDTA	Ethylenediaminetetraacetic acid
EM	Electron microscopy
EP	Endopeptidase
ERK	Extracellular-signal-regulated kinase
Ery	Erythromycin
eSTPK	Eukaryotic-like serine-threonine kinase
Fru	Fructose
G6PD	Glucose-6-phosphate dehydrogenase
GIMP	Generic image manipulation program
Glc	Glucose
GlcN	Glucosamine
GlcNAc	*N*-acetylglucosamine
Glu	Glutamic acid
Gln	Glutamine
Gly	Glycine
GNBP	Gram negative binding protein
GOI	Gene of interest
GT	Glycosyltransferase
His	Histidine
HMM	Hidden Markov model
HMW	High molecular weight
HPr	Histidine protein
HPrK	Histidine protein kinase
IC	Ion chromatography
iE-DAP	isoGlutamic acid-diaminopimelic acid
iGlu	isoGlutamic acid
IM	Inner Membrane
IMD	Immune deficiency
IL	Interleukin
IPTG	isopropyl β-D-1-thiogalactopyranoside
IWZ	Inner wall zone
k(Da)	kilo(Dalton)
LBA	Luria-Bertani agar
LBB	Luria-Bertani broth
LC-MS/MS	Liquid chromatography-mass spectrometry/mass spectrometry
Ldt	L-D-transpeptidase
LMW	Low molecular weight
LOD	Libre Office Draw
LPS	Lipopolysaccharide
Lpo	Lipoprotein
Lpp	Braun's lipoprotein
LRR	Leucine-rich repeat
LRT	Likelihood ratio testing
LT	Lytic transglycosylase
LTA	Liopteichoic acid
Lys	Lysine
m-DAP	meso-diaminopimelic acid
m/z	mass/charge
MAMP	Microbial associated molecular pattern
MDP	Muramyl-dipeptide
MGcV	Microbial genome context viewer
MGT	monofunctional glycosyl trasnferase
MLAA	*N*-acetylmuramic acid-L-Alanine amidase
MLZ	Middle low-electron-density zone

MOPS	3-morpholinopropane-1-sulphonic acid
mRNA	Messenger RNA
MRSA	Methicillin-resistant *S. aureus*
MTP	Muramyl-tripeptide
MTtP	Muramyl-tetrapeptide
MurN	Muramic acid
MurNAc	*N*-acetylmuramic acid
NCBI	National Centre for Biotechnology Information
NEB	New England Biolabs
NFW	Nuclease-free water
NGD	*N*-acetylglucosaminidase
NLR	nucleotide oligomerisation domain like receptor
NLRP	NOD-, LRR- and pyrin domain-containing protein
NMD	*N*-acetylmuramidase
NMR	Nuclear magnetic resonance
NOD	nucleotide oligomerisation domain
OM	Outer membrane
OMP	Outer membrane protein
OWZ	Outer wall zone
PAMP	Pathogen associated molecular pattern
PASTA	PBP and STPK associated
PBP	Penicillin binding protein
PBS	Phosphate buffered saline
PCM	Putative cell wall recycling mutant
PCR	Polymerase chain reaction
P(EP)	phospho(enolpyruvate)
P	Phosphate (P_i; inorganic phosphate)
PGLYRP	Peptidoglycan recognition protein (mammalian)
PGN	Peptidoglycan
PGRP	Peptidoglycan recognition protein
PIPES	piperazine-N,N'bis[2-ethanesulfonic acid]
PPIase	Peptidyl-prolyl isomerase
PR	Peptidoglycan recycling
PRD	PTS-responsive domain
PRR	Pattern recognition receptor
PS	Polystyrene
PT	Peptidoglycan turnover
PTS	Phosphoenolpyruvate:carbohydrate transport system
qRT-PCR	Quantitative real time PCR
RBS	Ribosomal binding site
r_0	Maximum growth rate
Re	Relish
RE	Restriction endonuclease
RNA	Ribonucleic acid
RNS	Reactive nitrogen species
ROS	Reactive oxygen species
RP-HPLC	Reverse-phase high performance liquid chromatography
RT	Room temperature
SB	Solute binding
SCV	Small colony variant
SCW	Septal cross-wall
SDS	Sodium dodecyl sulphate
SEDS	Shape, elongation, division and septation
Ser	Serine
SLC	Solute carrier
SPR	Surface plasmon resonance
TCA	Trichloro-acetic acid

TCT	Tracheal cytotoxin
TE	Tris-EDTA
TEM	Transmission electron microscopy
TG	Transglycosylation
TKMC	Tukey-Kramer multiple comparison
TLR	Toll-like receptor
TLVR	Talon low viscosity resin
TM	Transmembrane
TNF	Tumour necrosis factor
TP	Transpeptidation
TSA	Tryptic soy agar
TSB	Tryptic soy broth
UDP	Uridine diphosphate
UMP	Uridine monophosphate
v/v	volume per unit volume
VRSA	Vancomycin-resistant *S. aureus*
w/v	weight per unit volume
WTA	Wall teichoic acid
X-gal	5-bromo-4-chloro-3-indolyl-β-D-galactopyranoside



Chapter 1

General Introduction

1.1 *Bacteria rule the world*

Bacteria are thought to be the oldest and most structurally simple living organisms on earth [1], capable of surviving and propagating in almost all environments found on this planet, ranging from deep sea vents to the digestive tract of humans, even inhabiting radioactive waste [2] among many other hostile environments. They have diverse metabolic capabilities encoded by a plethora of genetic elements that are exchanged between bacteria with ease, permitting their rapid colonisation of- and adaptation to novel environments. One of the most important metabolic capabilities that bacteria have is the ability to synthesise a complex and robust cell envelope, supported primarily by their cell wall (CW), a structure integral to their survival in diverse ecological niches and the main structural component of which is peptidoglycan (PGN).

1.2 *A brief history of cell wall research*

Even in the first microscopic observations of bacteria by Antonie van Leeuwenhoek in 1676 the varied shapes in which bacteria present were already evident. van Leeuwenhoek observed coccal, rod and spiral bacterial morphologies and insightfully anticipated the involvement of surface structures in determining such shapes [3], a function of the CW still recognised. After the isolation of individual bacterial species, made possible by the work of Pasteur and Koch in the late 18^{th} Century, the nature of the bacterial CW could begin to be determined. The development of Gram-staining by Hans Cristian Gram in 1884, enabled the division of bacteria into two broad groups; Gram-positive and Gram-negative, based on retention of crystal violet dye by the CW. Still in the eighteenth century, Vincenzy and Fisher attempted to determine the basic chemical nature of the CW through plasmolysis of cells and analysis of the resistant material, though this yielded little initial

information [4]. It was not until the 1940's, with the introduction of the electron microscope, that the cell wall was first clearly visualised as an empty sac like structure retaining the shape of the originating bacterium [5]. 1949 saw the first coccal CW, that of *Staphylococcus aureus*, visualised by Cooper *et al.* [6], which along with electron microscopy of thin sections of various other bacteria revealed that the bacterial cell envelope consisted of at least membranes and peptidoglycan (PGN).

The first biochemical insights into CW synthesis and the chemical nature of PGN in *S. aureus* came from observations of intracellular accumulation of uridine phosphate-containing compounds in the presence of penicillin [7]. Further characterisation of these compounds revealed the presence of *N*-acetyl muramic acid (MurNAc), D-alanine (D-Ala) and D-glutamic acid (D-Glu), components all found in PGN. In 1951 Salton and Horne prepared the first pure fractions of bacterial CW [8, 9], enabling the first determination of CW chemical composition by Salton [10] and a few years later by Cummins and Harris [11]. These discoveries gave birth to the field of bacterial CW biology and a flurry of key biochemical discoveries followed. Such discoveries provided insight into the chemical composition and organisation of the bacterial CW and important aspects of the mechanisms of CW synthesis, breakdown and recycling, paving the way to research on this topic in the modern day. Throughout these years of research, several laboratory model organisms have been utilised, though those studied in most detail have been the Gram-negative *Escherichia coli* and the Gram-positive *Bacillus subtilis*, examples from which will form the bulk of discussion in this Chapter, with special attention also given to the focus of this thesis; the Gram-positive *S. aureus*.

1.3 *The biology and pathogenesis of Staphylococcus aureus*

S. aureus is a Gram-positive coccus found within the Firmicutes, measuring around 0.5-1.5μm in diameter. Staphylococci divide in three orthogonal planes, leading to the formation of grape-like clusters of cells, but also occur singly, in pairs or in short cell chains [12]. Staphylococci are non-motile, non-spore forming and facultatively anaerobic [12]. *S. aureus* itself is an eminent human pathogen, occupying both commensal and pathogenic niches on and within the body. Under non-infectious conditions *S. aureus* primarily inhabits the moist, squamous epithelium of the anterior nares [13], but may also be found in the respiratory tract, on the skin, and as a normal component of vaginal microbiota [14]. Approximately 20% of the adult population carry *S. aureus* persistently in the nose, with another 20-30%

carrying the bacterium intermittently [15, 14]. Nasal carriage in children is around 45-70% [14].

Infections are most often derived from *S. aureus* already present in the colonising microbiota [14, 16] and upon breach of an epithelial barrier *S. aureus* may initiate superficial infections causing impetigo, folliculitis and cutaneous abscesses [16]. In nosocomial settings, *S. aureus* may also initiate infections at surgical sites or from implanted medical devices [16]. As infections progress bacteraemia may develop, resulting in the seeding of vital organs and leading to serious disseminated infections such as endocarditis, osteomyletis and descending urinary infections [16]. *S. aureus* is the most common cause of bacteraemia in hospitals in the USA, and in the UK over 12,500 cases are reported each year with an estimated mortality rate of 30% [17]. *S. aureus* is also able to persist on abiotic devices, making it particularly hard to eradicate from hospital settings. Once physical barriers have been breached by *S. aureus*, a strong inflammatory response is initiated during which neutrophils and macrophages migrate to the site of infection and attempt to engulf and dispose of the invading bacteria [18]. However, *S. aureus* expresses a plethora of virulence factors able to thwart this response, and secretes immunomodulatory proteins such as Staphylococcal protein A (SpA) that compromise humoral and cell mediated immunity [18, 19]. This often results in antibody titres too low to be protective and a lack of robust secondary responses upon re-infection due to depletion of T and B cells, perhaps explaining why many individuals suffer repeated infections. Neutrophil-mediated innate immune responses are thus the primary defence against *S. aureus* infection [20, 21].

Among the array of secreted and surface-associated virulence factors of *S. aureus* are proteins promoting adhesion to damaged tissue and the surface of host cells [22], immune evasion proteins binding humoral immune system components, and iron acquisition proteins [23]. Various proteases, lipases, a hyaluronidase and a nuclease facilitate tissue destruction, cytolitic toxins effect host cell and tissue damage and superantigens contribute to symptoms of septic shock [24]. Most strains of *S. aureus* also possess a protective polysaccharide capsule (CPS) [25]. *S. aureus* employs a number of strategies to avoid phagocytosis [26, 27, 28, 29, 30], can survive in the phagolysosome of host cells [31, 32, 30] and more recently has been shown to actively induce its uptake into non-phagocytic cells [33], potentially contributing to bacterial dissemination and persistence during chronic infections. Clearly capable of inhabiting multiple complex environments, the virulence of *S. aureus* is under careful control by a wide range of regulatory mechanisms, the complexity of which we are only just beginning to understand [34]. Several of these regulatory systems are also involved

in control of CW metabolism [35, 36]. Indeed, CW features and metabolism are intrinsically linked to *S. aureus* pathogenesis, and disruption of CW synthesis/hydrolysis components often results in attenuation of virulence e.g. [37, 38, 36, 39]. To further complicate matters, *S. aureus* is also resistant to many commonly used antibiotics, many of which act by disrupting CW metabolism [40, 41, 42, 43, 44]. Although promising new antimicrobials such as Teixobactin have recently been discovered [45], this presents a serious challenge in treating Staphylococcal infections, with multiple strains now resistant to last-resort antibiotics such as Methicillin and Vancomycin (MRSA and VRSA, respectively) [46]. As such, it is now of utmost importance that we explore novel aspects of *S. aureus*' biology, such as peptidoglycan recycling (PR), to better understand both its pathogenesis and to open up avenues for the development of novel antimicrobials.

1.4 *The bacterial cell envelope*

The cell envelope of bacteria completely surrounds the cell, protecting it from external challenges, governing interactions of the cell with its environment, and controlling the passage of molecules in and out of the cell. Gram-negative and Gram-positive bacteria each have a different cell envelope structure (Figure 1.1). Indeed, Gram-staining utilises such differences in cell envelope composition; crystal violet dye is retained by the thicker PGN layer of Gram-positive bacteria but lost from the thin PGN layer of Gram-negatives during alcohol washing.

The Gram-negative cell envelope consists of three principal layers; the inner membrane (IM), the largely mono-layered PGN sacculus of the CW, and the outer membrane (OM) (Figure 1.1, [50]). The PGN sacculus sits within the periplasm, the region between the IM and OM, and is the main structural component of the envelope (Figure 1.1). The IM is a symmetrical lipid bilayer composed of phospholipids, whereas the OM bilayer is asymmetrical, containing an inner leaflet of phospholipids and an outer leaflet composed largely of lipopolysaccharide (LPS) and is embedded with a large number of β-barrel proteins performing a variety of different functions [51]. The OM's structure is crucial to its function, and small alterations in this layer impact upon processes such as motility, attachment, and pathogenesis [51].

In contrast, Gram-positive bacteria do not possess an OM and sport a much thicker layer of PGN to which various CW polymers are are anchored ([52], Figure 1.1). These polymers include the wall teichoic acids (WTA's) [53] and in many cases a thick layer of CPS [52].

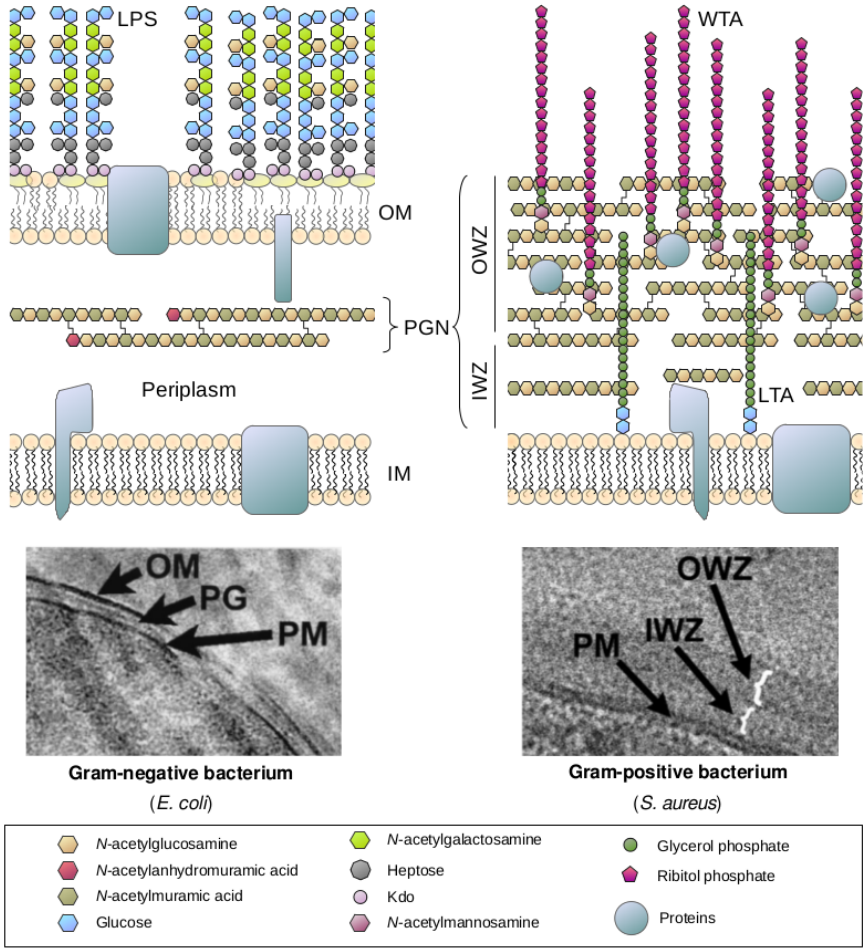


FIGURE 1.1: ***A simplified schematic of the cell envelopes of Gram-positive and Gram-negative bacteria displaying carbohydrate composition of major cell envelope polysaccharides.*** *The PGN layer ow the cell envelope is composed of repeating GlcNAc-MurNAc disaccharide units, cross-linked by short stem peptides (see Figure 1.2) and in Gram-negative PGN glycan chains are capped with anhydromuramic acid (anhMurNAc) at the reducing end. The Gram-negative outer membrane comprises an inner leaflet composed mainly of phospholipids and an outer leaflet containing LPS attached to lipid A, creating a thick polysaccharide layer at the cell surface. Gram-positive bacteria lack an OM and instead possess a much thicker layer of PGN with attached polysaccharide polymers such as WTA, comprised mainly of polyribitol phosphate. This is often surrounded by a thick layer of CPS (not shown). Also present in Gram-positive bacteria are membrane-bound LTA's comprised mainly of polyglycerol phosphate. Both WTA and LTA are joined to their respective anchoring substrates by short carbohydrate linkers. The PGN of Gram-positive bacteria has a distinct layered structure, comprising a lower density region at the inner surface (inner wall zone; IWZ) where nascent PGN is likely inserted into the sacculus and a higher density region of heavily cross-linked PGN at the outer surface (outer wall zone; OWZ) [47, 48]. Cryo-electron micrographs of E. coli [49] and S. aureus [48] have been included for comparison. Kdo; keto-deoxyoctulosonate. See text for other abbreviations.*

Interestingly, in Actinomycetales, such as *Corynebacterium* spp. and the Gram-positive-like *Mycobacterium tuberculosis*, branched polymers known as arabinogalactans are attached to the CW, and in turn covalently linked to a layer of corynemycolic acids or mycolic

acids, respectively, which forms a lipid layer at the surface of the cell [52, 54, 55] unique among Gram-positive bacteria. A plethora of proteins performing a variety of functions are anchored to the Gram-positive CW [56]. Membrane-anchored lipoteichoic acids (LTA's) may also protrude some way into the wall, though are thought not to be exposed at the surface [57]. In addition, further modifications may also be made to these polymers, such as the D-alanlylation of WTA's [58].

The cell envelope features of *S. aureus* are typical of Gram-positive bacteria, with a thick CW surrounding the cell around 20-40nm in thickness [48] constituting 20-60% of the dry cell weight [59] and with PGN as its main structural component. WTA's also comprise a significant proportion of the CW of *S. aureus* [53], alongside various proteins and the membrane anchored LTA [52]. In many strains, a thick coat of CPS is also present at the cell surface [60].

1.5 *Peptidoglycan structure and biosynthesis*

Almost all bacteria, with the notable exception of members of the Mollicutes, particularly mycoplasmas, possess a PGN CW [59, 61, 62, 63] and aside from some plant plastids [64] PGN is found only in bacteria. PGN biosynthesis is very well conserved in bacteria and occurs in three stages; the cytoplasmic synthesis of precursors [65], flipping of lipid-linked precursors to the outer leaflet of the plasma membrane [66], and the polymerisation of PGN and its incorporation into the growing sacculus [67, 68]. The resulting glycan-peptide heteropolymer forms the PGN sacculus, the structure and shape of which is referred to as PGN architecture. It is becoming clear that PGN architecture is both more complex than expected and of great physiological importance in bacteria [69]. What's more, PGN may also be modified by various enzymes that alter its chemical composition, or by attachment of additional CW polymers [70].

1.5.1 Peptidoglycan composition and architecture

Before considering the biosynthesis of PGN, it is first useful to understand its chemical nature and structure. PGN is a heteropolymer composed of glycan strands of alternating MurNAc and *N*-acetyl glucosamine (GlcNAc) subunits connected via β-1,4-glycosidic linkages, cross-linked by short peptides attached to the lactyl group of MurNAc (Figure 1.2, [71, 74]). The repeating GlcNAc-MurNAc-peptide unit is referred to as the PGN or muropeptide monomer and more generally, fragments of PGN containing glycans and

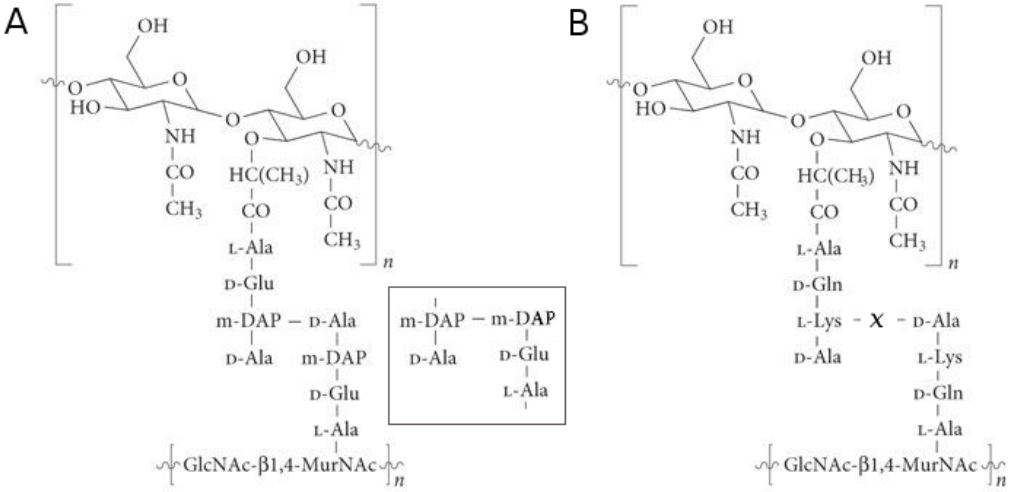


FIGURE 1.2: ***The basic chemical structure of peptidoglycan.*** *PGN is composed of repeating units of MurNAc and GlcNAc linked by β-1,4-glycosidic bonds. In Gram-negative bacteria as well as the Gram-positive Bacilli and Lysteria monocytogenes, the peptide side-chain contains meso-diaminopimelic acid (A_2pm, m-DAP or DAP) at the third position (A) and in other Gram-positive bacteria, this position is filled by* L*-lysine (*L*-Lys) (B). The third position amino acid is often cross-liked to the neighbouring 4th position* D*-Ala in both kinds of bacteria by an* L,D *peptide bond, though in Gram-positive bacteria, a bridging peptide (B; x) may also be present ranging from 1-7 amino acids in length [71]. In E. coli and B. subtilis* L-L *peptide bonds can be formed between two A_2pm residues [59] as depicted in the inset box of A, though other cross-linkage types between the second and fourth amino acids may also be observed in some species [71]. The second position amino acid of the Gram-positive muropeptide shown here is represented as* D*-glutamine (*D*-Gln) (B) as found in S. aureus and many other Gram-positive bacteria [59, 72, 73].*

peptides are known as muropeptides. The cross-linkage of glycan strands by peptides allows the molecule to form a mesh-like single-molecule polymer surrounding the cell in a closed bag-like structure, the PGN sacculus, though the higher order organisation of the sacculus is only partly understood [59, 69]. PGN glycan backbone structure is largely the same in Gram-negative and Gram-positive bacteria [75, 70] though variation in the exact chemical nature of monosaccharides, peptide composition, degree of cross-linking, and glycan chain length abounds between different bacterial species [59, 69].

PGN of *E. coli* and other Gram-negative bacteria, as well as the Gram-positive Bacilli [71] contains peptides of the sequence L-Ala-γ-D-Glu-*m*-A_2pm-D-Ala-D-Ala, known as 'DAP-type' PGN whereas in most Gram-positive bacteria the third position amino acid is substituted for L-Lys ('Lys-type' PGN) [59]. The primary L-Ala is joined via an amide bond to the D-lactyl group of MurNAc with a resulting D-L-D-L peptide sequence beginning with the D-lactyl group of MurNAc and ending with the L-centre of m-DAP / Lys. This arrangement prevents the formation of an α-helical peptide structure [80, 59] producing

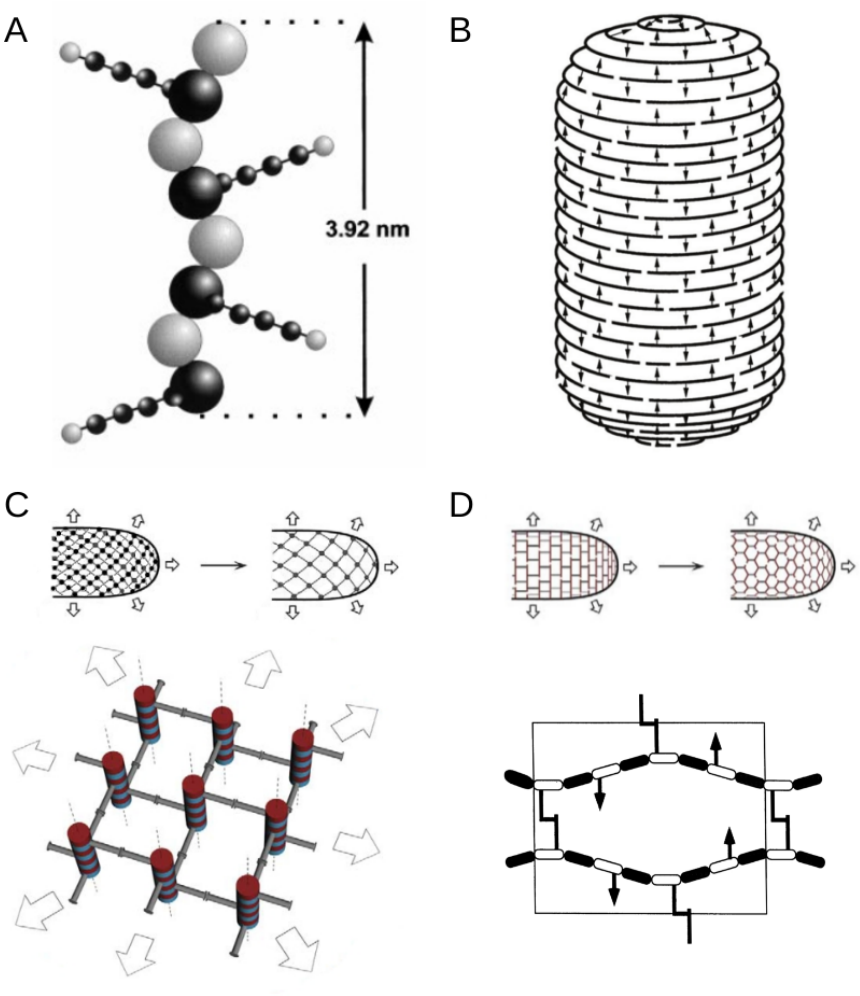


FIGURE 1.3: ***Classical models of peptidoglycan tertiary structure.*** *Glycan strands exhibit a helical confirmation from which attached stem peptides would protrude at approximately 90^o to one another (A), allowing for the formation of a cross-linked in a meshwork (e.g. C). In the 'layered' model (B) glycan strands (horizontal lines) run parallel to the plasma membrane of the cell around the cell circumference, and in the 'scaffold' model (C) glycan strands are positioned perpendicular to the plasma membrane. Panels C and D depict how the sacculus would expand under turgor pressure for the scaffold and horizontal models, respectively. In C, the plasma membrane would be found below the depicted meshwork. In panel A, large black balls represent MurNAc residues, and large grey balls GlcNAc residues. Smaller balls represent amino acids. In panel B horizontal lines represent glycan strands, and arrowheads cross-linked peptides. Non-cross-linked peptides are not shown. In panels C and D, white arrowheads represent tensile forces acting upon the PGN sacculus and the lower images represent fully stretched PGN. In the upper panel of C, black dots represent end-on glycan strands and black lines stem peptides. In the lower panel of C, red discs represent MurNAc residues, and blue discs those of GlcNAc, while dotted lines indicate the continuation of these strands above and below the plane in view. Grey arms represent cross-linked stem peptides. In the upper panel of D, vertical lines represent glycan strands and horizontal lines stem peptides. In the lower panel of D, the black arrowheads represent un-cross-linked stem peptides and solid black lines are cross-linked peptides. Black units represent MurNAc residues and white units GlcNAc residues. Panel A is taken from [76]. Panel B is taken from [77]. Panel C is adapted from [78]. Panel D is adapted from [78] and [79].*

flexible stem-peptides that can stretch up to four-times their relaxed length [79]. DAP-type PGN is cross-linked via the transpeptidation of A_2pm of one peptide side chain and the fourth position D-Ala of the neighbouring side chain to form a D,D-peptide bridge, though

less frequently L,D-cross-linkages may be formed between two A_2pm residues (Figure 1.2). In Lys-type Gram-positive bacteria cross-linkage is normally made between L-Lys and the and the neighbouring fourth position D-Ala via a variable number of bridging amino acids, ranging from the pentaglycine bridge of *S. aureus* to the single D-asparagine (D-Asp) of *Streptococcus faecium* [59]. The terminal D-Ala-D-Ala motif is relatively well conserved within bacteria as it is required for cross-linking, but may also vary. Many additional variations in peptide composition too numerous to document here are reviewed in [71].

E. coli exhibits degrees of cross-linking varying from 31-61% [69] whereas *B. subtilis* cells possess around 56%-64% cross-linked stem peptides and *B. subtilis* spore cortex PGN contains only 3% [81, 82]. In *S. aureus*, cross-linkage reaches 74-92% [83, 84, 85, 86]. Generally, PGN cross-linking in Gram-negative species is lower than that of Gram-positives. Stem-peptides are thought to protrude perpendicularly to one another (Figure 1.3 A) [87, 88] meaning that in a planar arrangement of glycan strands such as that found in the Gram-negative sacculus, every second stem peptide becomes unavailable for cross-linkage leaving many available stem peptides uncross-linked in mature PGN. However, NMR (nuclear magnetic resonance) studies have also predicted a three-fold symmetry of small peptidoglycan fragments (tetrasaccharide, two pentapeptides), which would theoretically prevent a fully planar arrangement of cross-linked glycan strands [89].

Most Gram-negative species examined have an average glycan chain length of 10-30 disaccharide (GlcNAc-MurNAc) units (DU's) (Table 1 in [69]), though this may vary depending on bacterial strain and growth conditions. In *E. coli* newly synthesised glycan strands are on average 50-60 DU's long whereas older glycan strands are only around ~17 DU's [91, 95], though some strands of ~200nm (~200 DU's) are present [96]. *B. subtilis* possesses glycan strands >500 DU's long and some upward of 5000 [92], while *S. aureus* has glycan strands of a predominant mean length of only 3-10 DU's (85-90% of strands), with a small proportion (3-14%) of strands longer than 50 disaccharides [86, 97]. It seems that larger proportions of long glycan strands may be a feature of Gram-positive bacteria [97, 69], though *S. aureus* is a notable exception. Instead, the high level of cross-linking in *S. aureus* PGN [83, 84, 85, 86] produces multimeric muropeptides containing up to 20 connected peptides [83, 69] creating 10–100nm long peptides connecting multiple short glycan strands [69].

Two major models have been put forward for PGN tertiary arrangement; the 'layered' or 'horizontal' model in which glycan strands and peptide cross-linkages run parallel to the membrane of the cell [98, 99, 77, 87], and the 'scaffold' model, in which glycan strands run

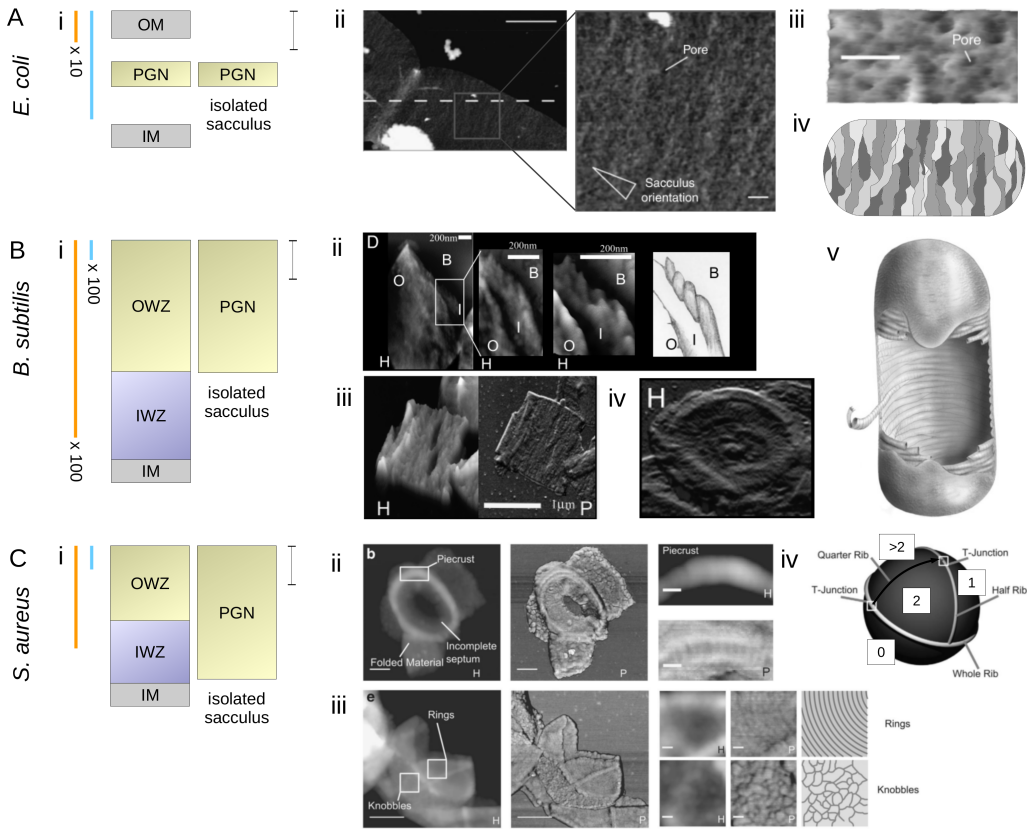


FIGURE 1.4: ***A comparison of cell envelope and peptidoglycan architectural features of E. coli, B. subtilis and S. aureus.*** *The dimensions of cell envelope layers and isolated PGN sacculi are given to scale in panel i) of A-C (scale bar 10nm). Glycan strand length is also indicated to scale, with blue lines representing average glycan strand length and orange lines the longest strand length recorded for each bacterium. Data from [49, 47, 48, 90, 91, 86, 92]. The E. coli PGN sacculus exhibits a fine 'filigree' structure (A ii) in which many pores are present (A, ii and iii). Glycan strands are arranged in a roughly horizontal-type architecture (A ii) in patches of more or less dense material. This is represented schematically in A iv in which differing shades of grey represent different densities of material across the sacculus surface (not to scale). Images (A ii and iii) were generated by tapping-mode AFM (atomic force microscopy) and are taken from [93]. Scale bars: A ii left-hand panel; 500nm, right hand panel; 50nm, A iii; 50nm. The characteristic 'cabled' architecture of the inner surface (I) of the B. subtilis PGN sacculus can be seen in B ii (with accompanying interpretive diagram) and the rough, disorganised texture of the outer surface (O) in B iii. B iii also shows a tear along a cable interface. Images show fragmented sacculi. Scale bars: 200nm. B. subtilis septal architecture viewed from the cell pole is shown in B iv, with cables and cross-striations visible. Scale bar: 500nm. 'B' denotes background in the images, 'H'; height, and 'P'; phase. Images are again generated by AFM. A schematic representation of B. subtilis architecture is shown in B v. Images from B ii-v are taken from [92]. The stereotypical 'piecrust' and 'rib' architectural features of S. aureus PGN can be observed in AFM images in C ii and iii, and the characteristic 'ring' and 'knobble' textures of the outer surface can be observed in detail in C iii. The sacculus in C iii shows an apparent incomplete septum, parallel to the image plane, encircled by a piecrust feature shown in detail in the enlargements. C iii shows a broken sacculus. Enlargements show details of rings and knobbles with interpretative diagrams. B iv shows the architectural subdivisions of the S. aureus cell surface, with age of the PGN sacculus in generations shown in boxes. Also marked are 'rib' and 'junction' architectural features involved in determining the plane of cell division in this bacterium. All images in C ii-iv are taken from [94].*

perpendicular to the membrane and peptide cross-linkages again run in parallel [76, 100, 101, 78, 89] (Figure 1.3 B and C, respectively). Both models present mechanisms by which the sacculus may form a single cell-encompassing network while allowing for expansion

of the sacculus as the cell increases in volume through stretching of stem peptides [79, 78], bending of glycan strands (layered model) or compression and expansion of glycan helices (scaffold model) [79, 76] (Figure 1.3 C and D, respectively). Both models assume roughly even distribution of cross-linkages and material density across the cell surface. The scaffold model has met considerable opposition, and in *E. coli* the length of glycan strands in this organism exceed the thickness of the PGN sacculus, precluding a scaffold-type arrangement [102, 103] (see Figure 1.4). Direct assessment of *E. coli* PGN architecture by AFM also revealed a roughly horizontal model type architecture [93], in accordance with previous data [104, 105, 103]. However, rather than a strictly perpendicular arrangement of glycan strands and uniform distribution of material across the sacculus (horizontal model; Figure 1.3), more disordered bands of material and regions of differing density were detected across the sacculus (Figure 1.4 Aiii, iv), [93].

The scaffold model could not immediately be discounted for organisms like *S. aureus* [101, 86] where short glycan strands form a thick sacculus. However, even *S. aureus* contains 3-14% glycan chains >50 DU's long unaccounted for in the scaffold model [97]. In fact, *S. aureus* and a variety of other Gram-positive bacteria have been recently shown to exhibit a variety of much more complex PGN architectures neither scaffold-like or akin to a simple 'layering-up' of the horizontal model (Figure 1.4, [92, 94, 106, 93]). The inner surface of the *B. subtilis* PGN sacculus is composed of thick ~50nm cables running circumferentially and perhaps helically around the cell, likely made up of coiled 'ropes' of glycan strands further coiled to form cables [92] (Figure 1.4 Biii, v, vi) surrounded by an external layer of rough, disordered material (Figure 1.4 Biv [92]). Similar circumferential bands, 25nm in diameter, are found around cells of *Lactococcus lactis* and other Ovococci, in hoops or helices around the cell, though it is unclear if these structures are PGN based [107, 97]. In *S. aureus* circumferential 'ring' features are also observed in nascent PGN [108, 94], though these rings are rapidly converted to a 'knobble' type architecture presumably by the activity of PGN hydrolases [94, 90, 109] (Figure 1.4 Civ), along with thick ridge or 'piecrust' type features (Figure 1.4 Ciii) formed at the initiation of septation [94]. How these bacteria construct such features is still uncertain, but these architectures clearly differ from a layered horizontal-type architecture.

1.5.2 Peptidoglycan biosynthesis and insertion into the sacculus

The synthesis of PGN in both Gram-negative and Gram-positive bacteria occurs in essentially the same way [59]. This occurs in three stages; first, soluble activated nucleotide precursors (UDP-MurNAc-pentapeptide and UDP-GlcNAc, UDP; uridine diphosphate) are

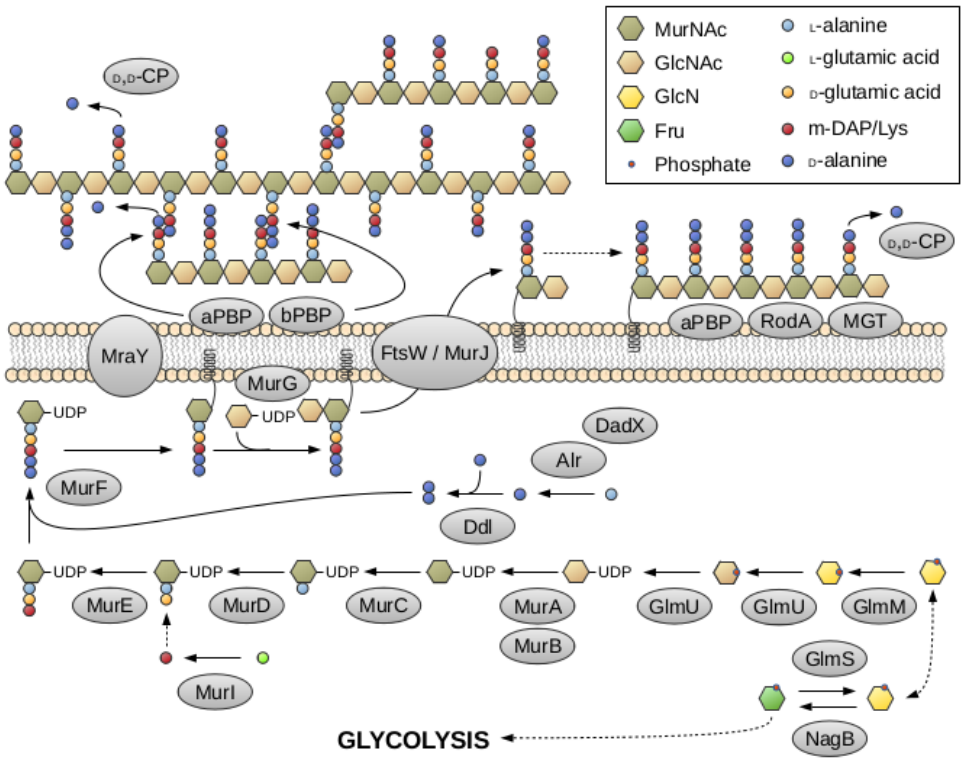


FIGURE 1.5: ***A generalised overview of peptidoglycan biosynthesis.*** *PGN biosynthesis begins with the synthesis of nucleotide-linked precursors (UDP-GlcNAc and UDP-MurNAc) to which amino acids are added in a processive manner to build a pentapeptide side chain linked to the lactyl group of muramic acid (MurNac-pentapeptide). MurNAc-pentapeptide is attached to bactoprenol, forming membrane-bound Lipid I. GlcNAc is then transferred from UDP-GlcNAc to Lipid I to form Lipid II, after which it is then flipped from the inner to outer leaflet of the plasma membrane. In Gram-positive bacteria, further modification of lipid II may occur, as in S. aureus where a pentaglycine bridge is added before flipping across the membrane. Glycan strands are polymerised and then inserted into the PGN sacculus by cross-linkage of stem peptides. PGN may be modified in several ways during precursor synthesis, or more extensively after polymerisation and insertion into the sacculus (see text). No OM is depicted here as the biosynthesis pathway presented is a general representation of PGN biosynthesis steps shared between Gram-positive and Gram-negative bacteria. See text for references and abbreviations.*

synthesised cytoplasmically [65]. Secondly, at the inner leaflet of the cytoplasmic membrane these nucleotide precursors are linked to undecaprenyl phosphate (bactoprenol) to form a lipid anchored disaccharide-peptide monomer subunit (GlcNAc-MurNAc-pentapeptide) before being flipped to the outer leaflet of the membrane [66]. Lastly, lipid II is polymerised, concomitant with the release of bactoprenol, to form glycan strands with peptide branches that are then inserted into the PGN sacculus via the action of both synthetic and hydrolytic enzymes [67, 68] (Figure 1.5).

PGN precursor synthesis begins with the conversion of fructose-6-phosphate (Fru-6-P) to UDP-GlcNAc, catalysed by the activity of GlmS; an amidotransferase using L-Gln as a

nitrogen source [110], GlmM; a phosphomutase [111, 112], and GlmU; a bi-functional (acetyl/UDP) transferase [113, 114] (Figure 1.5). UDP-MurNAc is synthesised in a two-step reaction requiring MurA and MurB, beginning with an enolpyruvyl transfer from phosphoenolpyruvate (P(EP)) to an OH group of GlcNAc to form GlcNAc-3-EP by MurA [115] and followed by the reduction of EP by MurB to form the characteristic lactyl group of UDP-MurNAc [116]. Specific racemases convert L-amino acids to their respective D-amino acid counterparts, and the synthesis of D-Ala-D-Ala is carried out by the D-Alanine ligase; Ddl [117]. The four ATP-dependent ligases MurC-F polymerise stem peptides by sequentially adding L-Ala, D-Glu, either m-DAP or L-Lys (see Figure 1.2) and finally the dipeptide D-Ala-D-Ala [118].

The transmembrane (TM) protein MraY catalyses the transfer of the phospho-MurNAc-pentapeptide moiety of UDP-MurNAc-pentapeptide to the lipid carrier undecaprenylpyrophosphate (C_{55}P or bactoprenol) at the inner leaflet of the cytoplasmic membrane [119], generating C_{55}PP-MurNAc-pentapeptide, or Lipid I, as well as uridine monophosphate (UMP). In *E. coli* and *B. subtilis*, the IM-located MurG transferase then adds GlcNAc derived from UDP-GlcNAc to Lipid I to form Lipid II [120], which is then flipped to the outer leaflet of the plasma membrane. However, in *S. aureus* and other Gram-positive bacteria, further modification of Lipid II occurs before flipping [59]. In *S. aureus* five glycine (Gly) residues are added to the stem peptide L-Lys residue at the ϵ-amino group by three further enzymes; FmhB (FemX) (Gly_1), FemA ($Gly_{2,3}$) and FemB ($Gly_{4,5}$) [121, 122, 123, 124, 56]; steps apparently integral to Methicillin resistance in this organism [125]. In *S. aureus* the second position D-Glu residue is also amidated to produce D-Gln by the enzymes GatD and MurT [72, 73], presumably at one of the the Lipid II / Lipid II-L-Gly_x intermediate stages. Amidation of second and third position amino acids, such as m-DAP in *B. subtilis*, is a common modification observed in Gram-positive bacteria [75, 126].

Lipid II must be flipped across the cytoplasmic membrane by a flippase. The essential integral shape, elongation, division and septation (SEDS) membrane protein FtsW was first proposed as the primary Lipid II flippase in *E. coli* [127, 128], based on *in vitro* Lipid II flipping activity in membrane vesicles [127]. However, it was subsequently demonstrated *in vivo* that MurJ is the primary, if not the only flippase active in *E. coli* under standard laboratory conditions [129]. *S. aureus* MurJ [130], but not FtsW, is required for septal PGN synthesis [131], pointing to MurJ as the major if not only Lipid II flippase in this organism. Amj (alternative to MurJ) is a second Lipid II flippase in *B. subtilis* [132], though it bears no sequence or structural homology to MurJ. Amj may thus transport Lipid II in a

mechanistically distinct manner [132], and is expressed under the control of the cell envelope stress-response transcription factor σM and at elevated levels in MurJ mutants, perhaps to compensate for loss of MurJ activity [132].

In the final stage of PGN synthesis, at the external surface of the cytoplasmic membrane, polymerisation of Lipid II-linked precursors by transglycosylation (TG) [133, 134] and insertion of nascent PGN into the sacculus by transpeptidation (TP) is carried out by a variety of membrane-associated PGN synthases [135, 68]. The TG step of PGN synthesis is primarily accomplished using bi-functional (glycosyltransferase; GT and TP domain-containing) high molecular weight (HMW) class A penicillin-binding proteins (aPBP's) [68], catalysed by the *N*-terminal GT domain of these proteins. Most bacteria require the presence of at least one aPBP for viability. *E. coli* has a total of 12 PBP's, three of which are bi-functional aPBP's; aPBP1a, aPBP1b and aPBP1c of which aPBP1a and aPBP1b form a synthetically lethal pair, while aPBP1c alone cannot sustain growth [136]. OM lipoproteins (Lpo's) regulate PBP activity, traversing the PGN layer to induce PBP activity via interaction with non-catalytic PBP domains [74, 137]. In *E. coli*, aPBP1a and aPBP1b possess cognate Lpos; LpoA and LpoB, respectively, that may only be deleted in tandem with their respective PBP [74, 137]. *S. aureus* contains only four PBP's (PBP1-4), though MRSA strains also contains PBP2A, a β-lactam insensitive HMW class B PBP (bPBP; TP only) [39, 138]. PBP2 is the only aPBP of *S. aureus* and its TP function is essential [139]. PBP2's TG function also becomes essential in MRSA treated with β-lactams, when cooperation between its GT domain and the TP domain of PBP2A is required for survival [140]. To my knowledge, only one example of a regulator of PBP activity is known in Gram-positive bacteria; CozE of *S. pneumoniae*, which directs and governs activity of aPBP1a in this organism [141]. However, CozE homologues are widespread in bacteria, and may represent a common regulator of PBP activity [141].

Mono-functional glycosyltransferases (MGT's) also play a role in glycan chain polymerisation in some species [142, 143, 144, 145], though in others such as *B. subtilis* [146] and some Enterococci [147] such enzymes are apparently absent and in *E. coli* are dispensable [142]. In *S. aureus* however, two MGT's; MGT (SgtB) [144, 148] and SgtA [149, 145] are known to exhibit *in vitro* TG activity [144, 145] and in a strain lacking the GT domain of PBP2, SgtB becomes essential [140]. Despite lacking any identifiable MGT's, strains of *B. subtilis* lacking all aPBP's are still viable [150]. Instead, RodA and potentially other SEDS proteins are thought to be the GT's performing this function [151, 152, 153] and are now thought to form a previously unknown class of essential GT's playing key roles in CW synthesis in many bacteria

[135, 152, 153]. Unlike aPBP's, RodA is unaffected by the GT inhibitor Moenomycin, explaining why *B. subtilis* is resistant to this antibiotic [150]. Like Amj, RodA expression is induced by σM [154]. *S. aureus* possesses a RodA homologue [155], but its function is unknown. In *E. coli*, RodA contributes considerable TG activity, but is not able to compensate for the loss of aPBP's [156]; depletion or inhibition of aPBP's in Gram-negative bacteria typically leads to halting of growth, lysis or death [157].

In addition to the vital role played by aPBP's in TG, these enzymes also possess a C-terminal transpeptidase domain, as do the monofunctional bPBP's [68]. Both catalyse the cross-linking of PGN. The transpeptidase domains of PBP's are also their namesake, after their affinity for β-lactam antibiotics such as Penicillin which share structural similarity with D-Ala-D-Ala termini of pentapeptide side chains [68]. As the normal TP substrate required for cross-linking is the terminal D-Ala-D-Ala motif of the peptide side-chain, cleavage of this bond by D,D-carboxypeptidases (D,D-CP's) can also act to regulate the degree of cross-linking in mature PGN [95]. L,D-transpeptidases (Ldt's) are another group of transpeptidase enzymes, forming non-canonical 3,3 L,D cross-links found in many bacterial species [158, 159, 160, 161, 162]. Ldts belong to a family of transpeptidases separate from the PBP's and can confer resistance to β-lactams [163, 164, 160].

In addition to mechanisms mentioned above, protein phosphorylation may be also used to regulate activities of various different PGN synthases. Gram-positive bacteria do so extensively, via eukaryotic-like serine-threonine protein kinases (eSTPK's) [165, 166]. An ultraconserved family of eSTPK's found solely in Gram-positive bacteria contain several PBP and STPK associated (PASTA) domains in the extracellular region and a cytoplasmic kinase domain, the former of which binds muropeptide fragments or nascent PGN, as well as having a weak affinity for β-lactam antibiotics [167]. For example, the eSTPK of *M. tuberculosis*, PknB, binds specific muropeptides thought to recruit the protein to CW growth sites [168], where it then phosphorylates various proteins including GlmU, MurJ, an aPBP; PonA1 and a cytoplasmic protein CwlM that is homologous to PGN amidases [169, 170, 171, 172]. It is not known how phosphorylation affects TG or TP activity of PonA1, but phosphorylated CwlM activates MurA under high-nutrient conditions, stimulating PGN precursor synthesis [172].

1.5.3 Post-synthesis peptidoglycan modifications

In addition to the attachment in Gram-positive bacteria of CW glycopolymers and proteins, as well as variations in peptide composition and glycan strand length, PGN sacculi show extensive internal modification of the glycan backbone itself [70, 173]. These modifications include the *O*-acetylation of MurNAc, *N*-deacetylation of GlcNAc, *N*-glycolylation of MurNAc and the production of anhydromuropeptides or δ-lactams [70]. These modifications may regulate the activity of PGN hydrolases [174], confer resistance to host immune effectors such as lysozyme [173], limit host immune recognition [175], promote survival within phagocytic cells [176] or provide resistance to β-lactam antibiotics [177, 178]. Indeed, no known species of bacteria has completely unmodified PGN [70] and PGN of pathogenic bacteria is often more heavily modified [173]. In *Bacillus* spp. for example; *B. subtilis*, *B. cereus* and *B. anthracis*, each posses deacetlyated GlcNAc (GlcN), whereas only the latter two pathogenic species possess deacetlyated MurNAc (MurN), with both modifications known to decrease lysozyme susceptibility [179].

Modifications of the glycan backbone appear to be more prevalent in Gram-positive bacteria [70], likely as their PGN is more exposed than the membrane-enclosed sacculus of Gram-negative bacteria. The production of δ-lactams appears to be largely restricted to the spore forming Bacilli and Clostridia, where they are thought to mark spore PGN for specific spore PGN hydrolases involved in spore germination, although some are also found in the PGN of *Micrococcus lysodeikticus* [70]. Similarly, N-glycolylation of MurNAc is also restricted in its distribution, largely to the Actinomycetales, though it's exact *in situ* function is unclear. Anhydromuropeptides are found in both Gram-positive and Gram-negative bacteria, though are clearly more prevalent in Gram-negative bacteria where they are generated by lytic transglycosylases (LT's) (see Subsection 1.6.1). *B. subtilis* carries a mere 0.4% anhydromuropeptides in its PGN [82] and *S. aureus* none at all [86]. *N*-deacetylation and *O*-acetylation of PGN are widespread among bacteria, though the former modification is restricted to Gram-positives [70]. Both the *N*-deacetylation of MurNAc and GlcNAc have been observed in Gram-positives, whereas *O*-acetylation is present throughout both Gram-positive and Gram-negative bacteria [70]. Both modifications confer resistance to lysozyme and can regulate the activity of bacterial PGN hydrolases, potentially affecting processes such as cell division [180]. Resistance to lysozyme through *N*-deacetylation or *O*-acetylation is of dual importance for pathogenic bacteria, preventing solubilisation of the PGN sacculus, and potentially modulating the amount of immunostimulatory fragments produced as a result (see Subsection 1.7.5). Indeed *S. aureus* employs high levels of *O*-acetylation, and

combined with extensive cross-linking and WTA attachment makes it especially resistant to lysozyme [173]. The degree of *O*-acetlyation, lysozyme resistance and pathogenicity in a range of Staphylococci is highly correlated, demonstrating the importance of this modification during infection [181].

Modification of peptide side chains, through incorporation of D-amino acids secreted by a bacterium or other bacteria in the environment, either via Ldt's, Ddl, MurF, or in *E. coli* by aPBP1a, can give rise to modified pentapeptide side-chains [182, 183]. This can change cell shape [184], disperse biofilms [185], and may act as a common strategy for rapid adaptation to changing environmental conditions. Furthermore, in Gram-negative bacteria Ldt's also attach Braun's lipoprotein (Lpp) which performs the important function of covalently linking the PGN sacculus to the outer membrane [95].

1.6 *Peptidoglycan hydrolysis and cell wall growth*

PGN biosynthesis alone is not enough to build the complex structure that is the PGN sacculus (see Subsection 1.4), and PGN hydrolases facilitate CW growth by cleaving existing bonds in PGN to make way for new material [186]. PGN hydrolases and synthases, along with their regulatory elements, are thought to work together in CW synthesis complexes (CWSC's) [187], guided by various cytoskeletal components that play both structural and regulatory roles and provide the spatio-temporal coordination required for PGN sacculus assembly [188, 189, 190]. However, the exact mode by which new material is inserted into the PGN sacculus is still somewhat unclear, though several models are in existence [190] and recent studies directly examining PGN insertion mode have clarified important aspects of this process [94, 93, 191, 192, 96]. Many other regulatory mechanisms also act to maintain CW homeostasis during CW growth, and though the sheer diversity and complexity of CW growth regulation precludes a full discussion here several excellent reviews covering the subject are in existence [193, 187, 190, 157].

1.6.1 PGN hydrolysis and its regulation

The PGN sacculus is not a static but highly dynamic structure. In order to grow and divide bacteria must not only synthesise PGN but must also incorporate this into the sacculus, tailor polymerised PGN and separate dividing cells, all while maintaining cell shape and sacculus integrity [186]. Crucial to these processes are the PGN hydrolases, or autolysins [186, 194, 195] (See Figure 1.6). There are examples of PGN hydrolase that cleave every

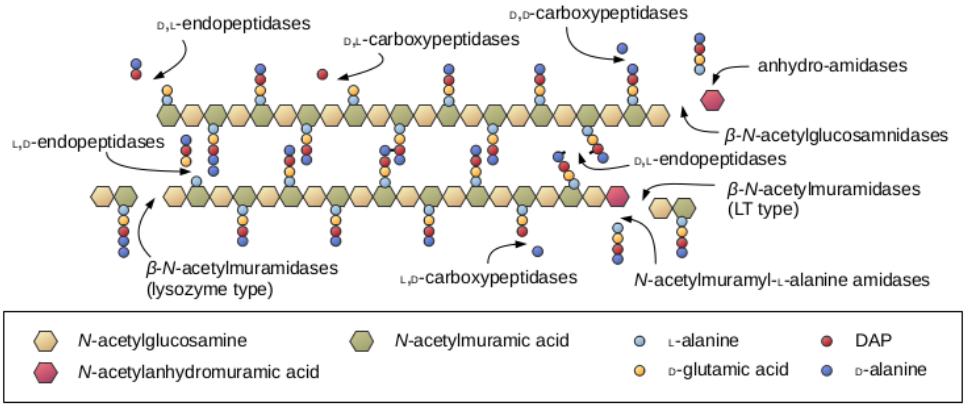


FIGURE 1.6: ***Hydrolysis of glycosidic, amide and peptide bonds of peptidoglycan by peptidoglycan hydrolases.*** *The PGN structure given is of E. coli or B. subtilis, and displays all activities of PGN hydrolases except those specific for other PGN structures. MLAA's cleave the bonds between MurNAc and the first-position* L*-Ala of the stem peptide to release peptides of varying length, though there are specific anhydro MLAA's (anhMLAA's) that specifically cleave at 1,6-anhMurNAc residues. Several species of EP also cleave PGN at specific positions within peptide side chains including* D,L*-EP's,* D,D*-EP's and* L,D*-EP's. These enzymes may cleave such bonds in both momomeric muropeptides and multimeric muropeptides. CP's cleave terminal amino acids from peptide side chains, again including enzymes that cleave* D,L*,* D,D *and* L,D *peptide bonds. Glycosidases known as NGD's cleave the glycosidic bond between GlcNAc and either MurNAc or anhMurNAc residues while β-N-acetylglucosaminidases (NMDs) cleave bonds between MurNAc and GlcNAc. lysozyme-type NMDs produce free unreduced MurNAc residues, whereas LT type NMDs cleave MurNAc-GlcNAc bonds with the concomitant formation of a 1,6-anhydro ring, producing anhMurNAc characteristic of the ends of Gram-negative glycan strands. Figure adapted and expanded from [186]. See text for abbreviations.*

glycosidic or amide bond in PGN (see Figure 1.6), though not every specificity is found in every species and it is often hard to assign functions to individual enzymes due to their apparent redundancy [186]. PGN hydrolase activity is often specific for a certain PGN type [75], PGN modified in a certain way [70] or for either HMW (CW) or LMW material (soluble muropeptides) [186]. Those PGN hydrolases binding a HMW substrate often have CW binding domains (CWBDs) that can help target hydrolases and greatly enhance enzymatic activity, such as LysM domains that bind directly to PGN [196], and GW domains that bind LTA [197]. Repeat domains of Atl, the major autolysin of *S. aureus* also target processed forms of the enzyme to the division septum [198], where a lack of WTA's allows binding [199].

PGN hydrolases are intimately involved in the enlargement of the PGN sacculus, breaking existing bonds to make way for insertion of new material. Accordingly, it would be expected that inactivation of certain hydrolases would hinder bacterial growth [186]. For example, when the *B. subtilis* autolysins CwlO and LytE are inactivated cell elongation halts [200]. PGN hydrolases are also involved in cell enlargement in *S. aureus*, where three *β-N*-acetylglucosaminidases (NGD's); SagA, ScaH and SagB are involved in reduction of glycan

chain length and cell wall stiffness [191], while LytM (Gly_5 endopeptidase; EP) and SsA (*N*-acetylmuramyl-L-Ala amidase; MLAA) are implicated in PGN cross-linking relaxation [201]. Atl, which is proteolytically cleaved to form an NGD and an MLAA [202], is also involved in CW homeostasis and cell shape maintenance in *S. aureus*, as is Sle1 (MLAA) [109]. PGN hydrolases also have well established roles in division septum formation and cell separation. Atl [202, 203, 204, 205] and Sle1 [37], along with LytN [206] are also involved in cell separation in *S. aureus*, and in their absence, cell clustering results. In *E. coli* the most important hydrolases involved in cell separation are the amidases AmiA-C, though several other hydrolases including CP's, LT's and EP's also contribute and their removal results in varying degrees of cell chaining [207, 208]. One further class of PBP, the LMW PBP's actually act as D,D-CP's and D,D-EP's rather than transpeptidases or GT's. Most are seemingly non-essential and enzymatically redundant, and in *E. coli*, deletion of D,D-CP's under typical lab conditions has little influence on phenotype, aside from that of PBP5, which causes kinking, bending or even branching of cells [209, 210]. As D,D-CP's remove terminal D-Ala residues, and thus the substrate for TP, this is likely as a result of aberrant PBP activity utilising untrimmed donor stem peptides from the sacculus rather than those from nascent PGN for cross-linking. Other functions of PGN hydrolases include morphogenesis and germination of spores in some species [211, 212], insertion of trans-envelope structures such as macromolecular transport systems [213] and formation and dispersal of biofilms [214], among others [194, 186].

As PGN hydrolases degrade the CW, tight control must be exerted over PGN hydrolysis to prevent cell lysis. One way in which bacteria can do so is by direct inhibition of hydrolases under certain circumstances, as with IseA of *B. subtilis* which inhibits cell separation EP's [215], or *Pseudomonas aeruginosa* Ivy, which inhibits both lysozyme and the LT MltB [216]. Conversely, in *E. coli*, EnvC and NlpD act as activators of AmiA and AmiB (EnvC) and AmiC (NlpD) [217]. EnvC and NlpD arrive at the division site before the onset of PGN synthesis, and the amidases are unable to localise in their absence, thus creating a 'fail-safe' mechanism to prevent premature amidase activation and cell lysis [218]. Furthermore, EnvC is itself activated by the FtsEX ABC (ATP-binding casette) transporter-like complex [219, 220], thought to allow modulation of PGN hydrolysis activity and controlled by cytoplasmic ATP hydrolysis. FtsEX also modulates PcsB activity in *S. pneumoniae*, an example of a singly essential PGN hydrolase [221, 222]. Other mechanisms of hydrolase regulation include proteolytic cleavage for activation [204], substrate modification, both of glycans or peptides [223, 180, 126], alteration of cell surface charge [224], control of hydrolase abundance at the

protein level [225] and transcriptional regulation of hydrolase genes (see Subsection 1.6.2).

1.6.2 Mechanisms of cell wall growth

PGN hydrolases may also be included in CWSCs, theoretically ensuring safe expansion of the sacculus by incorporation of nascent material before existing bonds are broken, the so called 'make-before-break' strategy of CW growth (Figure 1.7 B, [226]). Indeed, *B. subtilis* LytE is associated with MreB, a cytoskeletal protein coordinating such complexes [227] and when catalytically inactive PBP1B is overproduced in wild-type *E. coli*, complexes lacking PGN polymerisation activity are formed and cells lyse [228]. However, subsequent models incorporating more recent data have described a 'break-before-make' strategy (Figure 1.7 C, [157]). In the simplest hypothetical scenario a CWSC should contain proteins possessing a GT domain for PGN polymerisation, an EP domain to cleave existing cross-linkages, and 1-2 TP domains to cross-link nascent material to the sacculus (Figure 1.7 A, [68, 190]). *E. coli* uses at least one mode of PGN polymerisation involving just these few enzymatic activities when normal PGN polymerisation is blocked by β-lactam antibiotics [229] but CWSCs are generally thought to involve more components [188, 189, 190] (Figure 1.7 B, C). The precise nature of CWSCs and CW growth is still unclear, but protein interaction data, mutant phenotypes, and protein localisations support their existence, at least in Gram-negative bacteria [189, 230, 190]. Furthermore, several structural and regulatory proteins that guide the assembly, disassembly, positioning and regulation of putative CWSCs have been identified, most notably the cytoskeletal components MreB and FtsZ [231, 232, 233, 193, 187].

MreB is a homologue of eukaryotic actin, forming dynamic filament patches that move in a helical motion, circumferentially around the cell in rod-shaped bacteria and driven by RodA and/or bPBP mediated PGN synthesis [231, 235, 236, 232]. This ensures uniform distribution of new PGN insertion sites and maintains rod shape during cell elongation [237, 238, 239, 240, 231]. In *B. subtilis* and the Gram-negative *Caulobacter crescentus* MreB is essential, though in *E. coli* MreB phenotypes are only apparent when MreC and MreD are also removed [241]. aPBPs also interact with MreB [242, 243, 232], though are not necessary for cell elongation and may also operate outside of MreB guided complexes [156, 244] (see Figure1.7 C). MreB also interacts with cytoplasmic PGN precursor synthesis proteins [245, 246, 247, 248] perhaps to coordinate precursor availability, though it is unknown if MreB also interacts with a lipid II flippase. The eukaryotic tubulin homologue FtsZ also interacts with MreB, initialising cell division [249, 250], and cells lacking FtsZ form filaments due to an

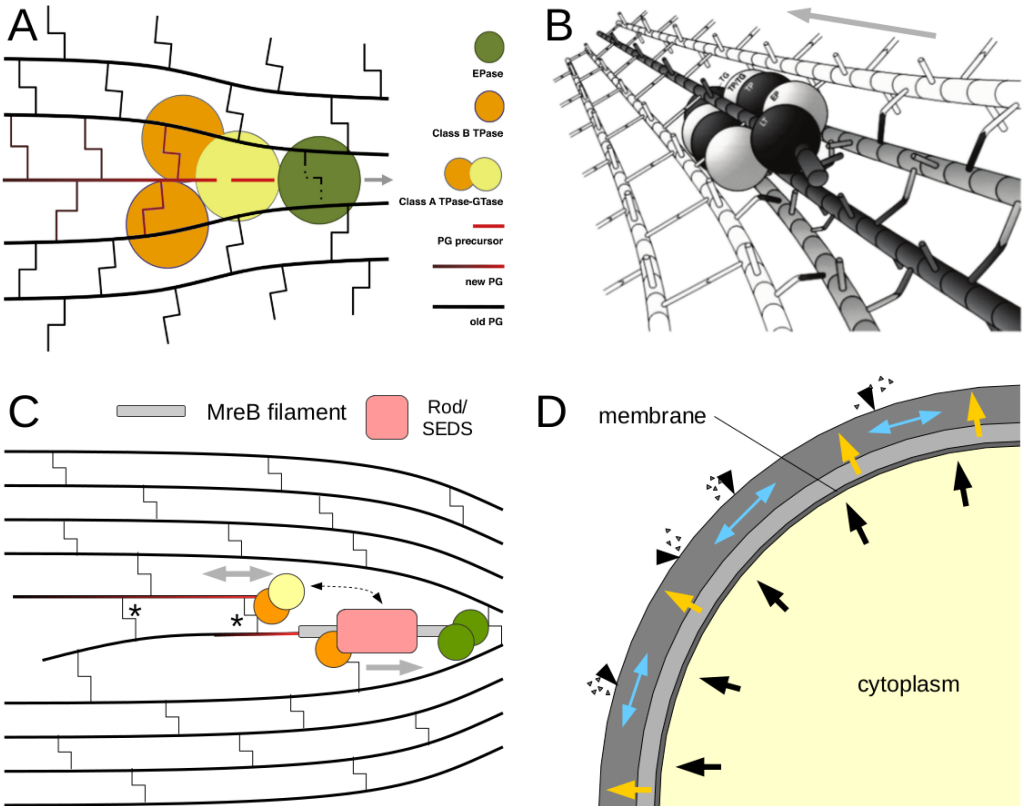


FIGURE 1.7: ***Models for the organisation of cell wall synthesis complexes and Gram-positive cell wall growth.*** *The simplest (A) and more complex (B-D) models of PGN synthesis complexes in E. coli, are depicted. In (A) cooperation of just 3-4 enzymatic activities allows polymerisation of PGN strands with their concomitant insertion into the PGN sacculus. Figure from [68, 190]. Panel B shows the more complex scenario originally proposed by Holtje [77] in which a 'three-for-one', 'make-before-break' scenario is envisaged where three PGN strands (cables) are synthesised and cross-linked as the complex slides along the 'docking strand' (dark grey strand), which is removed as the new strands are inserted. A mono-functional transglycosylase synthesises the central strand of the triplet (dark grey strand flanked by light grey strands), while two bi-functional transglycosylase/transpeptidase enzymes synthesise the flanking two strands and cross-link them to the central strand and to the rest of the PGN sacculus (white strands). Following this, hydrolases including a lytic transglycosylase (LT) and endopeptidases (EPs) and/or two amidases remove the docking strand. Figure from [77]. Panel C shows an updated model incorporating new data suggesting that aPBPs operate somewhat autonomously from the MreB associated Rod/SEDS complex [156] involved in PGN insertion. In this model a 'break-before-make' scenario is presented in which Rod/SEDS/MreB associated EPs cleave cross-links in existing PGN to allow insertion of new material, which is synthesised by RodA and cross-linked by bPBPs to the existing sacculus. Although only a single strand is shown here, this could also consist of a raft-like structure of several strands. aPBPs then generate additional glycan strands (in parallel or anti-parallel direction) cross-linking nascent and existing PGN to ensure structural integrity. Whether the Rod/SEDS/MreB complex and aPBPs interact (dotted arrow) is as yet undetermined. Cross-links between nascent PGN strands may contain pentapeptide-tetrapeptide cross-links (*). Figure modified from [157], see panel A for key. Grey arrows in panels A-C represent the direction of complex/aPBP movement. Panel D depicts a end-on cross-section of a Gram-positive bacterium showing the 'inside-outside' growth model [234, 226]. PGN is deposited in the IWZ (light grey area) in a relaxed form, gradually moves outwards (orange arrows) and matures to form the OWZ (dark grey) where it becomes stretched (blue arrows) as a result of turgor pressure from within the cell (black arrows). PGN is then hydrolysed by PGN hydrolases (black arrow heads) in the outermost layers, releasing PGN fragments (small grey triangles) to release tension and allow expansion of the sacculus.*

inability to divide properly. Early 'divisome' proteins including FtsZ, FtsA and ZipA [251] assemble before constriction begins forming a stable FtsZ 'Z-ring' to which Lipid II synthesis enzymes and presumably PGN synthases for pre-septal elongation are recruited [252, 253] with further PGN synthases and flippases arriving later [254, 255, 256, 131]. Rather than PGN synthesis, a GTP-dependent treadmilling mechanism drives FtsZ patch movement around the closing division ring [257, 233]. However, although FtsZ treadmilling appears to provide force to initiate constriction [258, 259], completion of septum closure appears to be driven by PGN polymerisation and FtsZ rotation coincides with PGN deposition at the leading edge of the closing septum in *E. coli* and *B. subtilis* [260, 261, 262, 233, 263]. However, *B. subtilis* FtsZ controls not just the spatio-temporal distribution of PGN synthesis during septum formation, but also its rate [233]. Gram-positive bacteria, such as *S. aureus* and *B. subtilis* also employ two further noteworthy cytoskeletal components; EzrA and GpsB [264, 265]. In *B. subtilis* EzrA and GpsB control the localisation of aPBP1 during the cell cycle, as well as ensuring proper Z-ring formation and division [264], while in *S. aureus*, EzrA is required for PGN synthesis, assembly of the divisome and cytokinesis [265].

Alongside CWSC scaffolding functions, CWSC component interactions themselves have many other functions [193, 187]. In *E. coli*, the divisome component FtsN is thought to simultaneously signal to both early and late arriving proteins (see above) through its periplasmic interaction with FtsA and cytosolic interaction with FtsQLB, initiating cell division [266, 267]. FtsN is also directly involved in control of PGN synthesis during division through interaction with the membrane proximal portion of PBP1B, increasing the rate of TG in synergism with LpoB [193]. The total extent of interactions within CWSCs are too numerous to document here, but as the above example demonstrates can have profound effects on PGN synthesis and CW growth. CWSC complex composition may also be environmentally dependent, transient, and variable to ensure robust growth under varied environmental conditions such as changes in pH or osmolarity [190]. Environmental conditions also influence bacterial cell size, with nutrient-rich environments producing larger cells and *vice-versa* [268, 269]. As the PGN sacculus dictates morphology, bacteria must coordinate PGN synthesis and hydrolysis with changes in cell size to ensure sufficient available space for cytoplasmic components. Though regulation of PBP activity by Lpos may contribute to this indirectly (see Subsection 1.6.1), bacteria also appear to regulate CW growth via central metabolism [187]. In *B. subtilis* the glucosyltransferase UgtP is a metabolic sensor recognising UDP-Glc, mediating cell size increase under nutrient-rich conditions by inhibiting Z-ring formation, allowing more time for cell growth before division [270, 271].

Other candidates for coordination of CW growth and metabolism have also been identified in several bacteria, such as *B. subtilis* YvcK, associated with the functions of MreB and PBP1 [272, 273].

PGN insertion in Gram-negative bacteria is also thought to be coordinated to some extent by PGN architecture, in that regions of more porous material (Figure 1.4 A) are thought to be more permissive to insertion than those more densely populated by glycan strands [93]. OM-localised Lpos, essential for the activities of IM-localised aPBPs [74, 137] must traverse the PGN layer to initiate PGN synthesis and more porous regions of PGN are potentially more permissive to these interactions [189, 93]. This would ensure that a given CWSC would stretch from the IM to OM, potentially incorporating OM anchored or periplasmically located hydrolases [186] in a CWSC such as that originally envisioned by Holtje (Figure 1.7 B, [77]). However, this is obviously impossible in Gram-positive bacteria, and the greater thickness and complexity of the Gram-positive CW have made understanding CW growth more difficult. The 'inside-to-outside' growth model (Figure 1.7, [234, 226]) proposed for rod-shaped Gram-positive bacteria suggests that relaxed, nascent PGN is deposited in the innermost layers of the CW before migrating outward as continued PGN polymerisation forces it to do so. Concomitantly, migrating material would become stretched and eventually degraded by PGN hydrolases in the outermost stress-bearing CW layers, with a time lag of ~1 generation between synthesis and release of PGN during peptidoglycan turnover (PT; see Subsection 1.7.1) [234]. Given the complexity of Gram-positive sacculi so far examined (Figure 1.4 and Section 1.5.1), this seems a simplistic scenario, and was likely originally intended to apply to a layered-up horizontal model type architecture. However, in *B. subtilis* a progressive outward decrease in CW density (observed by EM and expected of outer-surface hydrolase activity) [47, 48], the architecture of the its CW PGN [92], and a ~1 generation time lag between PGN deposition and turnover all fit this general framework [274], as does the observation that labelled PGN precursors are incorporated close to the cytoplasmic membrane [226].

The spatial separation of PGN synthesis and hydrolysis implicitly assumed by the inside-outside model would appear to preclude the formation of CWSC's in Gram-positive bacteria, and though synthases and hydrolases appear to work closely together in cell division [109, 192] interactions between synthases, hydrolases and regulators have been reported far less frequently [39, 141]. Interestingly however, upon PGN synthesis inhibition in *S. aureus* the CW becomes weaker but hydrolase gene expression is also reduced [275]. This belies the influence of another regulatory mechanism found exclusively in low-GC

Gram positive bacteria; the WalKR two-component system (TCS) [35]. WalKR is practically ubiquitous within the Firmicutes, a phylum to which it is also restricted [35] and unlike many TCSs WalKR is essential to many of the bacteria that possess it [276, 277, 278]. WalKR, comprising the WalR response regulator and the WalK histidine kinase, has a major role in regulating CW metabolism [35]. WalR orthologues in several species regulate genes encoding a variety of cell wall hydrolases, WTA biosynthesis enzymes, PGN modifying enzymes, fatty acid metabolism enzymes and FtsAZ [279, 35, 201]. WalK localises to the division septum [280] and is thought to recognise Lipid II at the outer leaflet of the cytoplasmic membrane [35] thus regulating CW growth and division through monitoring Lipid II abundance and concordantly modulating expression of its target genes. WalKR also engages in cross-talk with PknB (Stk1) in *S. aureus*, a highly conserved and septally localised eSTPK that also interacts with Lipid II [281], controls hydrolase expression [282] and may modulate FtsZ activity [281]. Several other *S. aureus* TCS's including AirSR, GraSR and VraSR also control hydrolase expression and CW synthesis [283, 284, 285], but will not be discussed in detail here.

Intriguingly, *S. aureus* does not show a hallmark decrease in CW density [48], nor a lag between PGN deposition and turnover [288] stipulated by the inside-to-outside growth model. *S. aureus* grows by in part by gradual increase in size throughout the cell cycle [109, 287] but primarily by cell division (Figure 1.8) and posseses only one major CWSC [289, 290] recruited from the cell periphery to the septum during cell division [109]. During division, FtsZ treadmilling causes initial, slow membrane constriction while subsequent FtsZ-treadmilling-independent PGN synthesis drives septum closure [131]. MurJ recruitment coincides with the FtsZ-treadmilling-independent stage, and the almost exclusive septal localisation of MurJ during septum closure is thought to restrict Lipid II flipping to the mid-cell region, recruiting aPBP2 via substrate affinity [131, 291] and redirecting PGN synthesis to the septum in the absence of an MreB-like cytoskeleton. During this process, a septal cross-wall (SCW) comprising two OWZs separated by a middle zone of low-electron density (MLZ) is formed [48, 90], protected from the outside environment (Figure 1.8 A). PGN biosynthesis begins at the tip of the inward-growing SCW and after annulus fusion synthesis continues across the septum, unlike the leading-edge-restricted septal synthesis of *B. subtilis* and *E. coli* (Figure 1.8 B, [192, 233, 263]). Once the uniform-thickness septum is complete, daughter cells then rapidly 'pop' apart upon hydrolysis of the peripheral bridge (Figure 1.8) and along the MLZ [109, 287, 206]. Thus, PGN synthesis does not proceed from inside-outside (Figure 1.8 B), though outer surface remodelling certainly occurs in *S. aureus* [292,

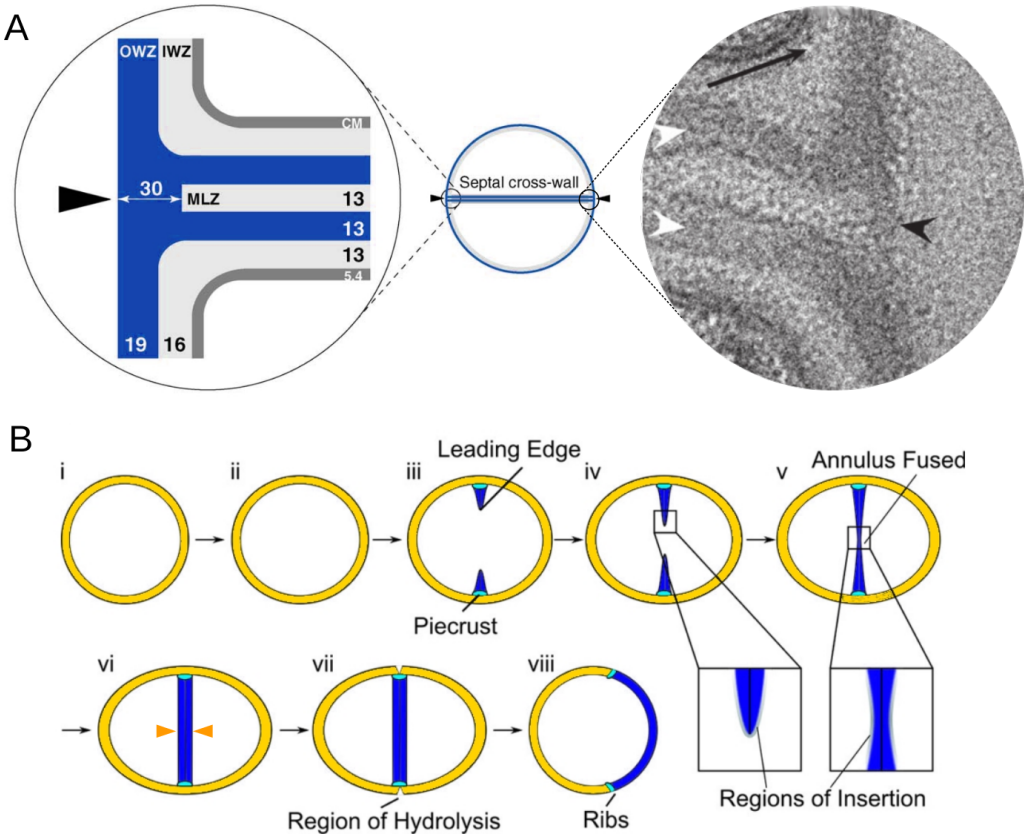


FIGURE 1.8: ***Septal cross-wall structure and development in S. aureus.*** *During cell division in S. aureus a SCW is formed (A) consisting of 2 IWZs, 2 OWZs and a middle low-density zone (MLZ), the dimensions of which are given in nm in the left-hand circle [69]. An electron micrograph of the S. aureus SCW [90] is shown in the right-hand circle with the peripheral bridge marked by a black arrowhead (see also left-hand circle) and OWZs marked by white arrow heads. The black arrow designates the cutting direction of the section. Hydrolysis along the septum-proximal edge of the OWZ and within the MLZ, along with degradation of the peripheral bridge allow cytokinesis. Panel B shows a conceptual model for the development of the S. aureus septum in which cell size and aspect ratio first increase [109] (i, ii) followed by the formation of pie-crust features [94] (light blue) and the initiation of septum synthesis (iii) showing the characteristic thin septal leading edge [90]. New PGN is inserted at the leading edge (iv) and across the rest of the cell surface, and after annulus fusion (v) PGN insertion continues across the septum until it reaches constant thickness (v, vi), forming the inner surface of the wall (orange arrowheads). Nicks/cracks in the peripheral bridge appear (region of hydrolysis) [286] (vii) likely as a result of the activity of Atl, the major autolysin of S. aureus [204] before daughter cells rapidly 'pop' apart [287] (viii). Scars, or ribs remain, marking the division site, and possibly providing spatial cues for subsequent orthogonal divisions [94]. Figure from [192].*

94, 293, 191]. Maturation of the CW outer surface however, does include 'trimming' of loose PGN [292, 293], perhaps removing evidence of other outer surface cleavage, and it seems possible that material trapped in the MLZ from OWZ and MLZ PGN hydrolysis could be rapidly released during cell popping, perhaps explaining why no lag is observed between PGN deposition and turnover [288].

1.7 *Peptidoglycan turnover and recycling*

Concomitant with the cleavage of PGN during cell elongation, division and sacculus remodelling is the release of muropeptide, glycan or peptide products. This process is referred to as PGN turnover [186, 194, 294] and was first discovered in the Gram-positive *Bacillus megaterium* [295, 296, 297]. In Gram-negative bacteria, such turnover products are largely trapped in the periplasmic space by the OM and recovered by the cell for reuse in CW biosynthesis or for other cellular processes such as glycolysis in a process termed PGN recycling (PR) [194, 294, 298]. PR is far less well understood in Gram-positive bacteria, though a recent renewal of interest in this topic has emerged. Though other parts of the cell wall, such as WTAs [274, 288, 299] and CPS [300] of Gram-positive bacteria are also turned-over and potentially recycled, the discussion here will focus on PGN specifically. This topic has also been reviewed in [194, 294, 298].

1.7.1 Peptidoglycan turnover

The activity of extracytoplasmic PGN hydrolases results in extensive PT in both Gram-negative and Gram-positive bacteria [194, 294, 298]. In *E. coli* ~40-50% of sacculus PGN is turned-over each generation by the combined action of LT's, NGD's, D-D-EP's and MLAA's [301, 302] with 30% of newly synthesised septal PGN degraded during septation, primarily by LT's [303]. However, the cell poles remain metabolically inactive [304]. In *E. coli* the major LT is Slt70 [305], and EPs such as PBP4, PBP7 and MepA [208, 306] are responsible for cleaving cross-linkages between strands. The soluble *E. coli* MLAAs AmiA, AmiB and AmiC release stem peptides from MurNAc residues along with the lipoprotein MLAA AmiD [307]. Combined, this results mainly in the production of GlcNAc-β-1,4-anhMurNAc-L-Ala-γ-D-Glu-*m*-A_2pm-D-Ala (GlcNAc-anhMurNAC-tetrapeptide), as well as smaller amounts of disaccharide-tripeptide, trace amounts of disaccharide-pentapeptide, GlcNac-β-1,4-anhMurNAc disaccharides and released stem peptides [308, 309].

Gram positive bacteria display various rates of CW turnover [310, 311, 312]; up to 50% per generation in *B. subtilis* [274, 313], and 15-25% per generation in *S. aureus* [288, 314, 299], with a lag of ~1 generation between PGN synthesis and turnover in many species [310, 311, 312, 274, 313]. *S. aureus* however, turns-over both new and old PGN at similar rates during exponential growth (see Subsection 1.6.2, [288]) but preferentially old PGN during autolysis [315]. Of the >30 putative or known PGN hydrolases in *B. subtilis* [316] the MLAA LytC is primarily responsible for turnover, with LytC mutants displaying either

an increase in turnover lag time with no change in turnover rate [317] or septal thickening with a considerable decrease in turnover rate [318]. LytD (NGD) and LytF (D,L-EP) are also involved in PGN turnover in *B. subtilis* [318, 319], and released fragments are further processed by NagZ (NGD) and AmiE (MLAA), presumably before recovery [320]. In *S. aureus* there are 14 confirmed or putative PGN hydrolases, predominantly NGDs [202, 203, 191], and MLAAs [202, 203, 321, 201, 206], though some are EPs [206, 322] and putative LTs [323]. Removal of Atl (NGD, MLAA) [202, 203] almost completely abolishes turnover [324], and indeed Atl is the main cell separation hydrolase [204] and trims material from the outer surface of the cell [292, 293]. Of the other characterised hydrolases, Sle1 (MLAA) and LytN (MLAA, EP) may also contribute to turnover due to their roles in cell separation [37, 206]. *S. aureus* LytM has unique Gly_5-L,L-EP activity, and is involved in cleavage of PGN anchors of Protein A [322] while SagA, ScaH and SagB (all NGDs) are involved in CW relaxation during growth, likely removing glycans in the process [191]. *S. aureus* IsaA and SceD are also two putative LT's [323]. To my knowledge, only one inconclusive attempt to partially characterise released PGN fragments in any Gram-positive bacterium has been made, from *B. subtilis* [320].

NGDs, MLAAs and EPs seem to be most important in Gram-positive bacterial PT, while LTs predominate in Gram-negative PT [316, 294], though both LTs [316, 323] and non-LT NMDs that cleave PGN or muropeptides are also frequently found in Gram-positive bacteria [325, 326, 327, 328, 329, 330, 316]. Bacilli and Clostridiae release anhydromuropeptides during forespore engulfment in sporulation [331, 332], but mature *B. subtilis* and *S. aureus* PGN contains no, or almost no anhydromuropeptides [82, 86]. It seems therefore, that the overall character of material released by PT may differ between Gram-negative and Gram-positive bacteria. Additionally, while displaying similar rates of turnover, large quantities of turnover products are found in the culture medium of Gram-positive bacteria [274, 288, 314], while only 6-8% of turnover products are lost by *E. coli* [302], which led investigators to believe Gram-positive bacteria could not recover and recycle PGN. However, such a loss of material seems to be far from adaptive, especially when considering that the Gram-positive CW generally constitutes >20% of the dry cell weight [59], as opposed to 2% in *E. coli* [194]. However, the apparent Gram-negative-Gram-positive dichotomy in turnover rate is not a rule. The Gram-positive *Enterococcus faecalis* [333], *Streptococcus mutans* [312] and *Streptococcus pneumoniae* [334] all shed only very small amounts of PGN, despite having readily detectable autolytic activity [333], while the Gram-negative *Neisseria gonnorhoeae* and *Neisseria meningitidis* shed large amounts of turnover products [335, 336, 337].

1.7.2 PGN recycling in Gram-negative bacteria

Turnover products are efficiently trapped and recycled in most Gram-negative bacteria, and ~50% of PGN is recycled in *E. coli* each generation, approximately equal to that turned-over [301]. PR pathways employ specific enzymes involved in the breakdown, recovery and reutilisation of products of PT [194, 294, 298] and *E. coli* possesses three inter-linked pathways involving the recycling of muropeptides, aminosugars, and peptides (Figure 1.9). The main recycling pathway is concerned with the recycling of GlcNAc-anhMurNAc-tetrapeptide [338, 339] and begins with the uptake of this molecule via the major facilitator family transporter, AmpG [338]. The tetrapeptide is then removed by the AmpD (MLAA) [338, 339, 340] and the resulting GlcNAc-anhMurNac disaccharide is cleaved by the NagZ (NGD) to produce GlcNAc and anhMurNAc [341] before their conversion to GlcNAc-6-P and MurNAc-6-P by the aminosugar kinases NagK and AnmK, respectively [342, 343]. GlcNAc-6-P and MurNAc-6-P may also be generated through the recovery and concomitant phosphorylation of GlcNAc by the enolpyruvate-phosphotrasferase system (PTS) components NagE or ManXYZ [344], and of MurNAc/anhMurNAc by another PTS transporter, MurP [345]. MurNAc-6-P is then converted to GlcNAc-6-P by the etherase MurQ [346, 347] and GlcNAc-6-P to GlcN-6-P by NagA [348, 349], before entry back into the PGN biosynthesis pathway. GlcN-6-P may also be generated during uptake of GlcN by ManXYZ [344]. Peptides released by AmpD are cleaved by the the L,D-CP LdcA [340] releasing D-Ala and L-Ala-γ-D-Glu-*m*-A_2pm, the latter of which may then be re-ligated to UDP-MurNAc by Mpl [350], where it then re-enters the PGN biosynthesis pathway. Mpl may also ligate MurNAc-tripeptide directly to UDP [350, 340], prior to AmpD cleavage, but following removal of D-Ala by LdcA. Peptides released by AmiD [307] in the periplasm may also be directly recovered via the general oligopeptide transporter OppA via recruitment of the specific oligopeptide binding protein MppA [351, 352] before being processed as described above.

Of all of the known PR proteins in *E. coli* none show a phenotype when removed under standard laboratory conditions apart from LdcA [340], with Δ*ldcA* mutants forming thick oval cells in late exponential phase before lysing in stationary phase, a result recapitulated under inhibition of LdcA [353]. The fact that this phenotype presented only in stationary phase points toward an importance of PR during this phase of growth, perhaps due to nutrient scarcity at this point, or due to a possible role of PR in CW homeostasis. In the absence of LdcA, accumulated tetrapeptide may then be ligated to UDP-MurNAc by Mpl, later forming Lipid II missing the terminal stem-peptide D-Ala. As tetrapeptide

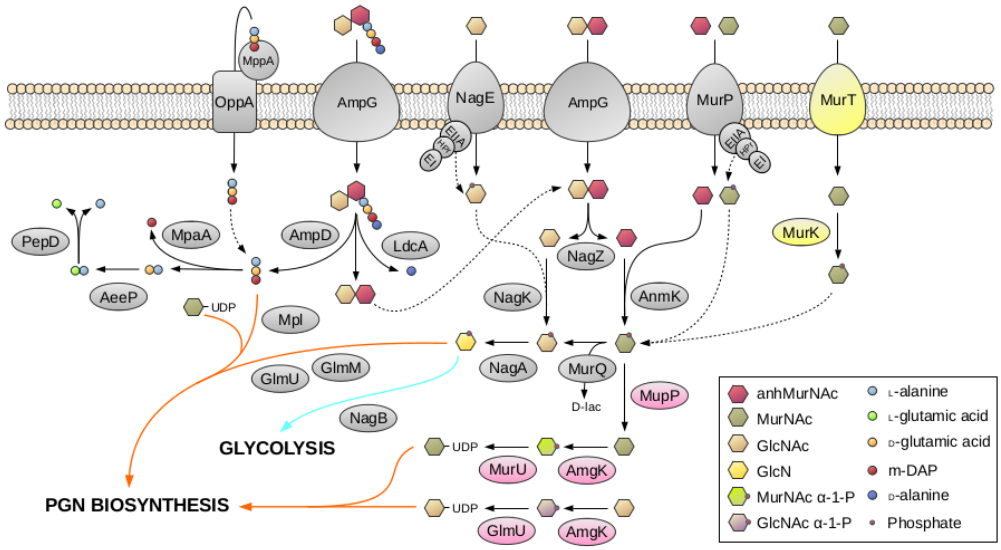


FIGURE 1.9: ***Peptidoglycan recycling pathways of Gram-negative bacteria.*** *Fragments of PGN released by the action of PGN hydrolases are sequestered in the periplasm of Gram-negative bacteria, before being recovered by a number of plasma-membrane localised transporters. Those utilised by E. coli are shown in grey. A novel MurNAc uptake mechanism employed by T. forsythia is shown in yellow (MurT; TfMurT, MurK; TfMurK). Various catabolic cytoplasmic enzymes then process recovery products before material then either re-enters the PGN biosynthesis pathway (see Figure 1.5), or is passed to the glycolytic pathway. Those utilised by E. coli are again depicted in grey. P. putida is able to by-pass the normal PGN recycling pathway and thus MurA (see Figure 1.5), allowing for Fosfomycin resistance in this bacterium. P. putida recovers turnover products via AmpG and MurNAc-6-P produced by degradation of recovery products in the cytoplasm is then processed by those enzymes depicted in pink. Here recovery of tripeptide by OppA is depicted, but tetrapeptide and pentapeptide fragments may also be recovered. OM, PGN, and degradation of PGN by hydrolases has been omitted for clarity, see text for details and references.*

may not be used by PBPs as a TP substrate, reduced PGN cross-linking and eventual bacterial lysis results. Studies of other species of Gram-negative bacteria have also revealed additional routes by which PT-derived material may be recycled not present in *E. coli*. In many Gram-negative species the MurNAc 6-phosphate etherase (MurQ) is absent [294, 354], and the normal catabolic pathway involving the removal of the D-lactyl group from MurNAc-6-P to produce GlcNAc-6-P is bypassed via an alternative anabolic route [354, 355]. In *Pseudomonas putida* this involves a novel MurNAc-6-P phosphatase MupP [355, 356] which converts MurNAc-6-P to MurNAc, followed by the formation of MurNAc-α-1-P via the enzyme AmgK and production of UDP-MurNAc by the enzyme MurU [354] (Figure 1.9). Cytoplasmic GlcNAc may also be converted to GlcNAc-α-1-P by AmgK followed by the formation of UDP-GlcNAc by MurU [355] (Figure 1.9). UDP-MurNAc may then re-enter the PGN biosynthesis pathway downstream of MurA and MurB. The fastidious oral anaerobe *Tannerella forsythia* is auxotrophic for both MurNAc and GlcNAc, and is thought to obtain these aminosugars solely through scavenging muropeptides from other cohabiting

bacteria [357] and contains functional homologues of AmpG and MurQ [358, 357]. Although aminosugars are taken up primarily by PTS transporters [359], *T. forsythia* also utilises a novel non-PTS MurNAc uptake system consisting of an integral membrane transporter (TfMurT) and a cytoplasmic MurNAc kinase (TfMurK), generating MurNAc-6-P which is then processed by MurQ [358] (Figure 1.9). The genes encoding these proteins in *T. forsythia* were found in a putative PR operon [358, 357], and although at present unique to *T. forsythia*, it is exciting to speculate that similar PR components may be found in other Gram-negative and indeed Gram-positive bacteria where orthologues of canonical PR genes are absent [294].

Though all Gram-negative bacteria appear to recycle PGN, it is not always highly efficient; some species, most notably *Neisseria gonorrhoeae* [360, 361] and *Bordatella pertusis* [362], release considerable quantities of turnover products into the external environment. In fact, several different species of *Neisseria* release PGN fragments to varying degrees, including the human pathogen *N. meningitidis* and the human commensal species *N. siccia* and *N. mucosa* [363]. Released PGN fragments are generated by the LT AtlA [364], largely in the form of GlcNAc-anhMurNAc-tetrapeptide. It appears that this trait has evolved via crippling of AmpG [335, 363] and is thought to be of advantage to *N. gonorrhoeae* in establishing infection [336]. The variation in *Neisseria* spp. PR suggests that PR efficiency may be altered during adaptation to certain niches, and that highly efficient PGN recycling may not always be present or indeed advantageous.

1.7.3 Peptidoglycan recycling in Gram-positive bacteria

PR in Gram-positive bacteria is far less well understood, with only a few reports directly addressing this prospect [320, 365, 366, 367, 368]. Gram-positive PR was long assumed not to occur, first because of the large scale shedding of PGN-derived material to the medium during growth by numerous Gram-positive bacteria [295, 296, 297, 274, 313, 288, 299, 310, 311, 312] and the lack an outer membrane which might trap turnover products (Section 1.4). CW-linked polymers such as CPS or surface layer proteins [52] have been hypothesised to help compensate for the lack of an outer membrane [294], though WTA's and CPS are themselves shed to the medium [274, 288, 299, 300]. However, some Actinomycetales such as *M. tuberculosis* and *C. glutamicum* possess a lipid layer at the cell surface composed of mycolic or corynemycolic acids [54, 55] which may act to trap material. Interestingly, a periplasmic-like space between the lower density IWZ and the cytoplasmic membrane has

also been observed in *B. subtilis* and *S. aureus*, of 16nm and 22nm respectively, using cryo-transmission EM [47, 48, 90]. Turnover products may potentially be accumulated in this space, where they may be imported for recycling, though the mechanism by which this may occur is unknown.

Indirect evidence also hints at an ability of Gram-positive bacteria to recover turnover products. *Bacillus licheniformis* responds to the CW derived dipeptide fragment; γ-D-Glu-*m*-A_2pm, upon its binding to the cytoplasmic BlaI repressor, BlaI is released from DNA and β-lactamase expression is induced [369]. The BlaI orthologue MecI of *S. aureus* also binds γ-D-Glu-L-Lys, though *in vivo* activity has not yet been demonstrated [369]. Furthermore, *Streptococcus pneumoniae* sheds only very little PGN [334, 333, 312], potentially as a result of efficient PR. An alternative interpretation is simply reduced PT in this species, and indeed stable hemispheres of unhydrolysed PGN persist over generations at the old poles of dividing cells [334]. However, PT a result of hydrolase activity during cell separation still seems likely, and resulting turnover products may well be recycled.

PR may also involve extracytoplasmic breakdown of turnover products before more piecemeal recovery, and recovered products may require further processing before they can be accepted by cytoplasmic recycling enzymes. Indeed, *B. subtilis* possesses two hydrolases, NagZ and AmiE, found in a putative PR operon [320] that appear to process turnover products in the medium (Figure 1.10). *Clostridium acetobutylicum* on the other hand, possesses two cytoplasmic enzymes, an *N*-acetyl transferase (GlmA) and an aminosugar kinase (MurK), which may function in recovery of non-*N*-acetylated and general muropeptide/aminosugar recovery, respectively [366, 367] (Figure 1.10). Furthermore, the PTS component MurP and MurNAc-etherase (MurQ), of *B. subtilis*, *S. aureus* were recently demonstrated to be involved in uptake and processing of MurNAc [368]. This demonstrated for the first time that Gram-positive bacteria may potentially recycle CW derived aminosugars [368], though this may also be interpretted as MurNAc scavenging, as in *T. forsythia* [358, 357]. It was also shown that slightly fewer viable Δ*murQ* cells could be recovered from late stationary phase [368], again suggesting that PR may be most important in this phase of growth.

Bioinformatic identification of *E. coli* PR protein orthologues in multiple Gram-positive bacteria [294] also suggests that PR may be more widespread in this group. Orthologues of the PR proteins MurP, NagE, MurQ, NagA and LdcA were found in most, though not all of the species examined, while NagZ and AeeP (an LdcA-like L,D-CP) orthologues were also be found in some species [294]. However, there is a conspicuous absence of

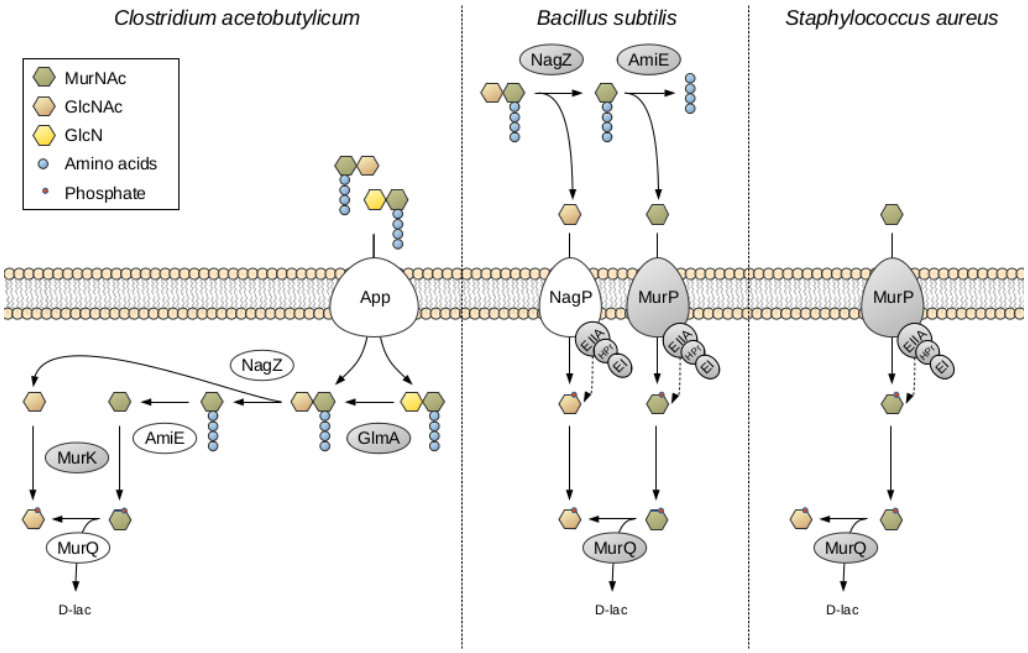


FIGURE 1.10: ***Putative peptidoglycan recycling pathways in Gram-positive bacteria.*** *Several proteins are hypothesised to be involved in peptidoglycan recycling in different species of Gram-positive bacteria; C. acetobutylicum, B. subtilis and S. aureus. Here they are depicted in putative recycling pathways in these organisms. The cytoplasmic proteins GlmA and MurK are thought to be involved in recovery of deacetylated and acetylated muropeptide monomers (disaccharide-peptide fragments), [366, 367, 370] though it is possible that this pathway may only recycle aminosugars. GlmA is thought to re-acetylate de-acetylated GlcN residues, to allow cleavage by NagZ. MurK then phosphorylates aminosugar monosaccharides to allow their processing by MurQ (MurNAc-6-P) and downstream of this, NagA (GlcNAc-6-P) (see Figure 1.9). In B. subtilis, the secreted peptidoglycan hydrolases NagZ and AmiE have been characterised and shown to cleave muropeptides to allow their possible recovery by the transporters MurP and NagP [320]. It has also been shown that MurP and MurQ are responsible for the recovery and processing of MurNAc [368] in this organism. These same proteins in S. aureus are also responsible for the recovery and processing of MurNAc [368]. Those proteins that are shown in white are hypothesised to be involved in these putative peptidoglycan recycling pathways, but have not yet been characterised [320, 366, 367].*

AmpG orthologues in Gram-positive bacteria [294]. As it also seems that the nature of turnover products may differ (see Subsection 1.7.1), that the CW of some Gram-positive bacteria contain few or no anhydromuropeptides [82, 86], and that anhydromuropeptide processing MLAA orthologues are also absent from examined Gram-positive bacteria [307, 371, 294], it seems likely that putative PR mechanisms of Gram-positive bacteria would be quite different to those employed by Gram-negative bacteria. It seems likely that uptake of CW aminosugars by the PTS transporter orthologues of NagE and MurP and of CW-derived peptides by Mpp/Opp-like ABC transporter systems, both of which are well-conserved among examined Gram-positive bacteria [294], may constitute the major turnover product uptake routes. Anhydromuropeptide recycling may be only a minor pathway,

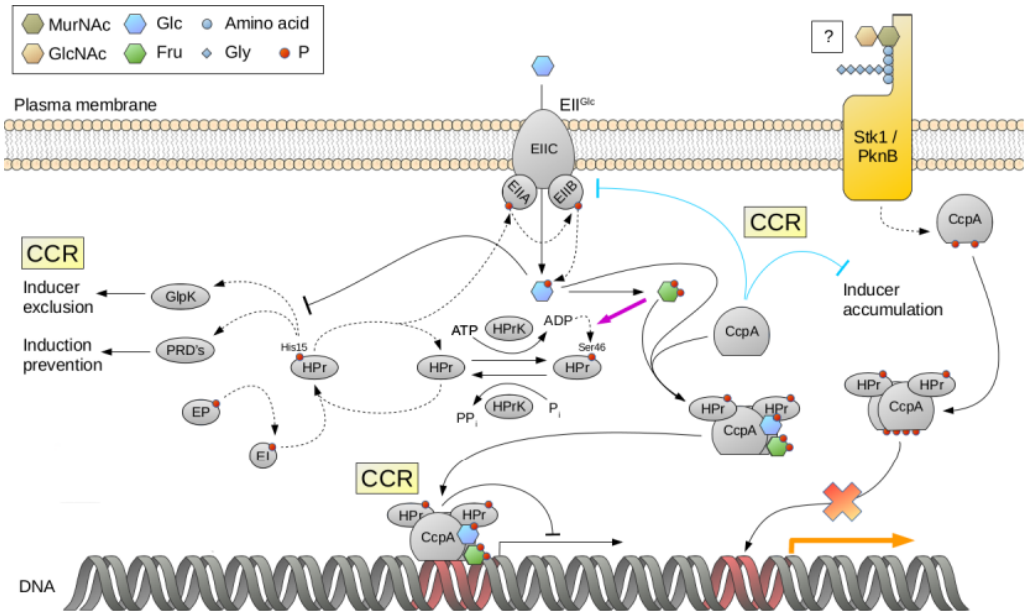


FIGURE 1.11: ***Mechanisms of carbon catabolite repression in Gram-positive bacteria.*** *A schematic representation of CCR mechanisms in Firmicutes, with specific details from S. aureus (Stk1/PknB). Here, CCR is depicted involving glucose uptake and metabolism, though this may also be caused by other carbohydrates. Stimulation of HPrK activity by Fru-1,6-PP is represented by the purple arrow. Blue arrows denote indirect effects of CcpA on prevention of Glc uptake and inducer exclusion. Prevention of CcpA binding to DNA following phosphorylation by Stk1 is represented by an orange cross and subsequent alteration to gene expression by the orange angled arrow. Red regions of DNA represent cre sites. Dashed arrows represent phosphate transfer, pointed arrowheads represent activities of proteins/molecules and flat arrowheads represent inhibition. Angled arrows on the DNA represent gene transcription. Question marks denote hypothetical or uncertain phenomena. Figure adapted and expanded from [372]. P; phosphate, P_i; inorganic phosphate, ATP; adenosine triphosphate, ADP; adenosine diphosphate, EP; enolpyruvate.*

except perhaps during sporulation of some species [331, 332]. Indeed, orthologues of AnmK, which converts anhMurNAc to MurNAc [343] were found in *Bacillus cereus* and *Streptomyces avermitilis*, both of which sporulate.

Despite multiple lines of evidence pointing toward the potential for PR in Gram-positive bacteria, there is still the problem of the seemingly unabated turnover of PGN to the extracellular milieu [274, 288, 312]. This is not necessarily disadvantageous [373], but does bring into question the potential function and/or significance of Gram-positive PR. As we have seen, rates of PGN shedding vary considerably within and between species [312], and although some reported variation may be attributable to experimental error, this may also be due to variation in bacterial strain, mutations, or growth conditions. The vast majority of measurements of PT have been made during exponential growth, and as discussed above, it seems PR may be most important during stationary phase. Pertaining to this, and the lower availability of carbon-containing nutrients during this stage of growth, it has been

suggested that carbon catabolite repression (CCR) may play a role in regulating PR in Gram-positive bacteria [294]. The main regulator of CCR in low-G/C Gram-positive bacteria like *B. subtilis* and *S. aureus* is the catabolite control protein (CcpA) [374] which binds carbon repression element (*cre*) sites in the promoter region of repressed genes [375], preventing their transcription in the presence of glucose or other preferred carbon sources in order to maximise growth rate and fitness [376] (Figure 1.11).

When glucose is taken up via a PTS transporter it is concomitantly phosphorylated by the PTS enzyme II B (EIIB) subunit to produce Glc-6-P. Phosphate for this reaction originates from P(EP) passed to the EII complex via a series of phosphorylation reactions [359, 377, 378] (see Figure 1.11). Intracellular Fru-1,6-PP, produced from Glc-6-P as a product of glycolysis, acts a signal of preferred carbon source presence and stimulates the activity of the histidine protein kinase HPrK, resulting in phosphorylation of HPr which then binds to CcpA. CcpA-Hpr complexes then dimerise and bind *cre* sites located primarily in promoter regions of genes or operons along the chromosome [377, 378]. CcpA-Hpr complexes are further stabilised by binding of Glc-6-P and Fru-1,6-PP [379]. The glycerol kinase, GlpK, and PTS-regulatory domain (PRD) containing catabolic gene/operon transcription factors are also phosphorylated by HprK [378]. Inhibition of this phosphorylation leads to exclusion of inducers of catabolic operons (inducer exclusion, via GlpK) and prevention of catabolic gene/operon transcription (induction prevention), which also contribute to CCR (Figure 1.11). CcpA may also indirectly prevent glucose uptake and inducer accumulation [380].

If indeed many of the genes involved in PR are under the control of CCR, then this could provide some explanation as to why efficient PR has not been observed frequently in Gram-positives. Initial studies that were performed on PT in Gram-positive bacteria were carried out in presence of relatively high concentrations of glucose (e.g. [274, 299, 288]), and it has been recently demonstrated that *cre* (catabolite responsive element) sites are present in the promoter region of putative MurNAc recycling genes in Gram-positive bacteria [368]. Thus, PR may become active in environments where nutrients are less abundant. Interestingly however, CcpA is also phosphorylated by the CW metabolism regulator Stk1 (PknB, an eSTPK) in *S. aureus*, which affects it's DNA binding capacity [381, 282]. Stk1 contains several extracellular PASTA (penicillin-binding protein and serine/threonine kinase associated) domains which may bind PGN fragments as they do in other bacteria [382, 383]. This suggests that CCR may be overcome in the presence of high concentrations of PGN fragments, for example when cell wall turnover is accelerated, stimulating PR.

1.7.4 Induction of β-lactamase production

In many Gram-negative Enterobacteriaceae, though not *E. coli*, PR is closely connected to AmpC-type β-lactamase induction [338]. Bacteria lacking AmpD accumulate cytoplasmic anhMurNAc-tripeptide, triggering expression of the β-lactamase AmpC [338, 339], whereas mutants lacking AmpG cannot recover muropeptides and lack AmpC expression entirely [338]. This is an important signal of CW damage by β-lactams, and an important function of PR alongside the recovery and re-utilisation of CW derived material. It has even been suggested that the primary function of PR in Gram-negative bacteria is to assess the integrity of their CW and respond accordingly [373]. In Gram-positive bacteria, induction of β-lactamase resistance has also been putatively linked to recovery and intracellular recognition of PGN fragments, though in the form of γ-D-Glu-*m*-A_2pm or γ-D-Glu-L-Lys (See Section 1.7.3, [369]).

1.7.5 Peptidoglycan recognition, turnover and recycling in host-pathogen interactions

Due to its widespread nature within- and restriction largely to bacteria, PGN is a microbial/pathogen associated molecular pattern (MAMP/PAMP) [384] and an important target for recognition by the innate immune system of eukaryotic hosts [385]. PGN may be recognised extracellularly by a host as a HMW polymer at the bacterial cell surface or as LMW PGN fragments released as a result of PT or degradation by host lytic enzymes. Recognition may be modulated both by modification of PGN (see Section 1.5.3), and the degree of PGN shedding and/or recovery. PGN fragments may also be released by intracellular bacteria [386], injected by bacteria, or actively transported into host cells [387, 388, 389] where they are recognised by intracellular receptors, such as mammalian NOD1 [390, 391, 392] (Figure 1.12). As Gram-positive bacteria generally shed higher quantities of turnover products, they could reasonably be expected to be more immunogenic than Gram-negative bacteria. Indeed, *Bacllius* spp. culture supernatants elicit greater NOD1-dependent immune responses in mammalian cell cultures than those of *E. coli* [393, 394], despite both species having comparable turnover rates. In eukaryotes, PGN is directly or indirectly recognised by a variety of pattern recognition receptors (PRRs, see Figure 1.12) [395], such as nucleotide-binding oligomerisation domain-like receptor (NLR) proteins [391, 390, 396] and Toll-like receptor (TLR) proteins [397] of mammals, Lysin-motif domain containing (LysM) proteins of plants [398] and peptidoglycan recognition proteins (PGRPs) found in many taxa [399, 385].

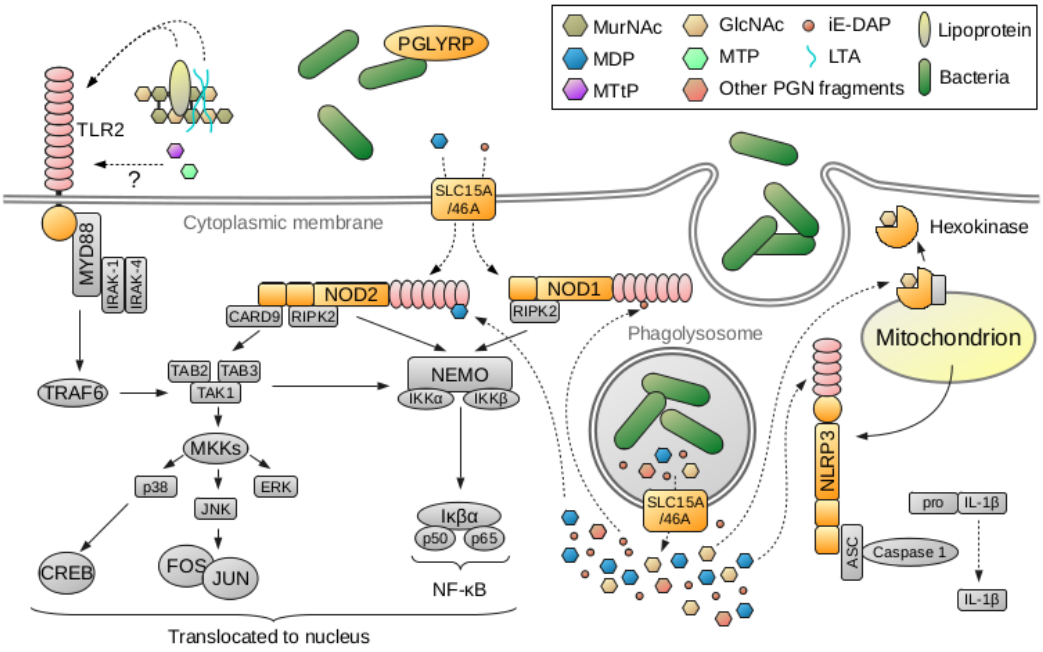


FIGURE 1.12: ***Recognition of peptidoglycan by the vertebrate innate immune system.*** *Multiple pathways for the recognition of various PGN-derived molecules exist in mammals. Receptors and PGN transporters are depicted in orange, with receptor LRR domains in pink. Both innate immune cells and non-haematopoietic cells secrete PGLYRPs where they interact with bacterial CW PGN and induce lysis. Small PGN-derived molecules may enter the cells via solute carrier family proteins (SLC15A/SLC46A2), though particulate PGN internalised by phagocytosis may activate signalling more efficiently. Following degradation of PGN in the phagolysosome, PGN derived small molecules such as MDP and γ-D-glutamyl-meso-diaminopimelic acid (iE-DAP), among others, stimulate a panel of cytosolic NLRs including nucleotide-binding oligomerisation domain-containing protein 1 (NOD1), NOD2 and NLRP3 (NOD-, LRR- and pyrin domain-containing protein 3). Membrane-bound TLR2 may potentially recognise muramyl-tripeptide (MTP) and/or muramyl-tetrapeptide (MTtP), and PGN acts as a vehicle for other TLR2 ligands such as lipoproteins and LTA. GlcNAc also binds hexokinase, releasing it from the mitochondrial membrane and inducing NLRP3 inflammosome activation. Figure adapted and expanded from [400, 401]. See text for references. ASC; Activating signal co-integrator, CARD9; caspase recruitment domain-containing protein 9, CREB; Cyclic AMP-responsive element-binding protein, ERK; extracellular-signal-regulated kinase, FOS; proto-oncogene c-Fos, IKKα/β; inhibitor of nuclear factor-κB α/β, IRAK-1/4; Interleukin-1 receptor-associated kinase 1/4; JNK; JUN N-terminal kinase, JUN; transcription factor AP-1, MKK's; dual specificity mitogen-activated protein kinase kinases, MYD88; myeloid differentiation primary response protein, NEMO; NF-κB essential modulator, NF-κB; nuclear factor-κB, RIPK2; receptor-interacting serine/threonine-protein kinase 2, TAB1/2; TGF-β-activated kinase 1/2, MAP3K7-binding protein, TAK1(MAP3K7); mitogen-activated protein kinase kinase kinase 7, TLR2; Toll-like receptor 2, TRAF6; TNF receptor associated factor 6.*

In mammals, the intracellular NLR NOD1 preferentially senses DAP-type PGN, and not Lys-type PGN (Figure 1.2) [396] while the minimal structure sensed by NOD2 is the general PGN motif muramyl-dipeptide (MDP; MurNAc-L-Ala-γ-D-Glu or MurNAc-L-Ala-γ-D-Gln) [390, 392], both via leucine-rich repeat (LRR) domains (Figure 1.12). PGN monomers from *S. aureus* stimulate NOD2, and likely represent a natural ligand [397]. NLRP3 and NLRP1 (NACHT, LRR and PYD domain-containing protein 1) also recognise MDP in some

circumstances [402, 403]. Another intracellular enzyme hexokinase, binds GlcNAc released by the degradation of Gram-positive PGN in macrophage and dendritic cell phagosomes, releasing it from the mitochondrial surface and stimulating downstream activation of the NLRP3 inflammosome by an unknown mechanism (Figure 1.12, [404]). The LRR domain containing TLR2 has a more controversial role in PGN recognition. TLR2 was originally thought to recognise polymeric PGN, but this was later attributed to commonly co-purified lipoprotein and/or LTA contaminants [405]. However, polymeric, lipoprotein-free *S. aureus* PGN associates with both NOD2 and TLR2 in cultured HEK293 cells, stimulating and inducing intracellular accumulation of both proteins, with concomitant stimulation producing an enhanced immune response [406]. LTAs may have however underlain this response. Subsequent studies also suggested that uncross-linked, soluble PGN fragments may indeed stimulate TLR2 (Figure 1.12, [407]) and that synthetic muramyl-tripeptide and muramyl-tetrapeptide fragments associate with TLR2 in surface plasmon resonance (SPR) experiments whereas pure cross-linked PGN does not [408]. Regardless of its direct stimulatory activity, PGN also serves as a vehicle for lipoproteins/LTA [397], and the degree of its degradation may dictate accessibility of these ligands to TLR2. PGN recognition via these pathways induces secretion of pro-inflammatory cytokines such as tumour necrosis factor alpha (TNF-α), interleukin 6 (IL-6), IL-1β and IL-18 [402, 409, 404] which play key roles in controlling bacterial infections and stimulate antimicrobial responses such as production of reactive oxygen/nitrogen species (ROS/RNS) and antimicrobial peptides (AMPs) [410, 411].

Plants recognise PGN using plasma-membrane localised PRRs, triggering local immune responses [412] and recognise glycan backbone structures, rather than muropeptides [413, 390]. HMW PGN of both Gram-positive and Gram-negative bacteria, as well as a mix of oligomeric LMW PGN structures stimulate immune responses in *Arabidopsis thaliana* via LysM domain containing proteins that act as general sensors for GlcNAc-containing MAMPs [413, 414, 398]. LysM domains were originally identified in bacterial PGN hydrolases [415]. In *A. thaliana* a plasma-membrane localized, tripartite PGN recognition system is employed, comprising the membrane-tethered LysM domain proteins LYM1 and LYM3 and the trans-membrane LysM receptor kinase CERK1 (Chitin elicitor receptor kinase 1), likely required for transducing the extracellular signal to intracellular signalling pathways [416]. All three proteins are required to produce a response. Orthologous proteins LYP4, LYP6 and OsCERK1 are involved in PGN recognition in rice (*Oryza sativa*) [417].

PGRPs are involved in physiological processes ranging from control of endosymbionts, to

directly fending off infection [418], and are present in many metazoan taxa from mammals to insects [399]. PGRPs come in two forms, the short (PGRP-S) and long (PGRP-L) proteins [399], and can be further categorised by their ability hydrolyse PGN, with some cleaving the MurNAc-L-Ala amide bond like the MLAAs of bacteria [419, 418] while others simply stimulate downstream signalling cascades [420]. PGRPs that degrade PGN sometimes help to control immune activation by removing ligands [420], or may release PGN fragments to be recognised by other receptors [399]. Though mammalian PGLYRPs do not stimulate further immune responses, they are able to kill Gram-positive bacteria directly by binding to septal PGN and either preventing TP [421], or causing massive disruption to cellular processes such as PGN, DNA and RNA biosynthesis, membrane depolarisation and production of hydroxyl radicals though interference with TCSs normally involved in mis-folded protein export [422].

Trapping of turnover products during PR may aid Gram-negative pathogens in their avoidance of host immune recognition. Gram-positive pathogens may have also evolved mechanisms to reduce turnover product release, though these possibilities still await investigation. However, modification of PGN and extracytoplasmic degradation of turnover products may also reduce immune stimulation by modifying the structures of released compounds (Subsection 1.5.3), [320]). *S. aureus* Atl, Sle1, LytN and LytM are involved in releasing SpA from the CW, and shape the PGN anchor structure of this protein [322] potentially reducing its immunogenicity. Stem peptide modifications such as *meso*-A_2pm or glutamic acid amidation, or substitution of *meso*-A_2pm with L-ornithine alter NOD1 PGN recognition [396, 175] and hypothetically, modification of MurNAc residues (see Subsection 1.5.3) could also directly alter NOD2 sensing of MurNAc-containing PGN fragments [373]. *N*-glycolylated PGN of *Mycobacterium* spp. for example elicits higher NOD2 dependent immune responses [423] and NOD2 responses may also be modified via fragment interaction with Nalp1, another NLR involved in NOD2-mediated PGN recognition [424]. Enhancement of immune responses may sometimes be advantageous [423], and PGN fragments can be used to cause damage to a host [362]. Both *Bordatella pertusis* and *Neisseria gonorrhoeae* release large quantities of tracheal cytotoxin (TCT; GlcNAc-anhMurNAc-tetrapeptide) which causes ciliated cell death when applied to a human fallopian tube organ culture model [362, 336]. Both species utilise an alternative PR pathway not found in *E. coli* [354], and *N. gonorrhoeae* has actually evolved to reduce efficiency of PR via AmpG [363], potentially facilitating recognition to attract immune cells for invasion [425]. The secretion of *N*-glycolylated muropeptides by *M. tuberculosis* may also attract

host immune cells within which they can then replicate [423, 386]. Bacteria may also use muropeptides to signal to other microbes to enhance infection. *S. aureus* is often found in biofilms alongside the fungal pathogen *Candida albicans* [426], in which they induce *C. albicans* hyphal formation [427]. *C. albicans* hyphal induction is stimulated by both Gram-positive and Gram-negative bacterial PGN, and aids invasion of host tissues by *S. aureus* [428]. PR may potentially be used to modulate these phenomena, but in the Gram-negative *Salmonella typhimurium* intracellular accumulation of turnover products during PR is thought to influence virulence directly [429]. *S. typhimurium* AmpG mutants were not attenuated in their virulence in a mouse model, nor affected in assays of immune stimulation or host cell invasion, but AmpD mutants in which intracellular PGN recovery products accumulate were found to be less virulent, more immunogenic and defective in host cell invasion [429]. This bears similarity to mechanisms of AmpC-type β-lactamase induction [338, 339], and suggests that PR may have roles in regulating bacterial virulence and perhaps other cellular processes important during infection.

1.8 *Drosophila melanogaster as a model host for Staphylococcus aureus infection*

In order to study pathogenic interactions with a host, tractable animal models are required. It is often impractical and unethical to compare large numbers of strains in mammalian models and various alternative animal models have been developed to study *S. aureus* pathogenesis and/or virulence, including larval *Danio rerio* (zebra fish; [20]) and invertebrate models such as *Tenebrio molitor* (flour beetle; [430, 431]) and *Drosophila melanogaster* (fruit fly; [432, 433, 434]). *D. melanogaster* in particular offers an attractive model host, with short generation times, ease of culture, genetic tractability, a long history of research into the mechanisms of immune activation and defense [420], and a relatively good correlation between pathogenicity of *S. aureus* in this host and severity of human clinical outcomes [433].

1.8.1 Recognition of peptidoglycan by *D. melanogaster*

D. melanogaster has been a key model in studying PGN recognition by PRRs and has 19 transcribed members of this family [418]. *D. melanogaster* 'catalytic' PGRPs contain a conserved Zn^{2+} binding domain within the active site [418, 435], crucial for PGN hydrolytic activity and down-regulation of PGN-mediated immune responses, whereas those involved in immune recognition lack key zinc-coordinating residues [435]. The catalytic PGRPs

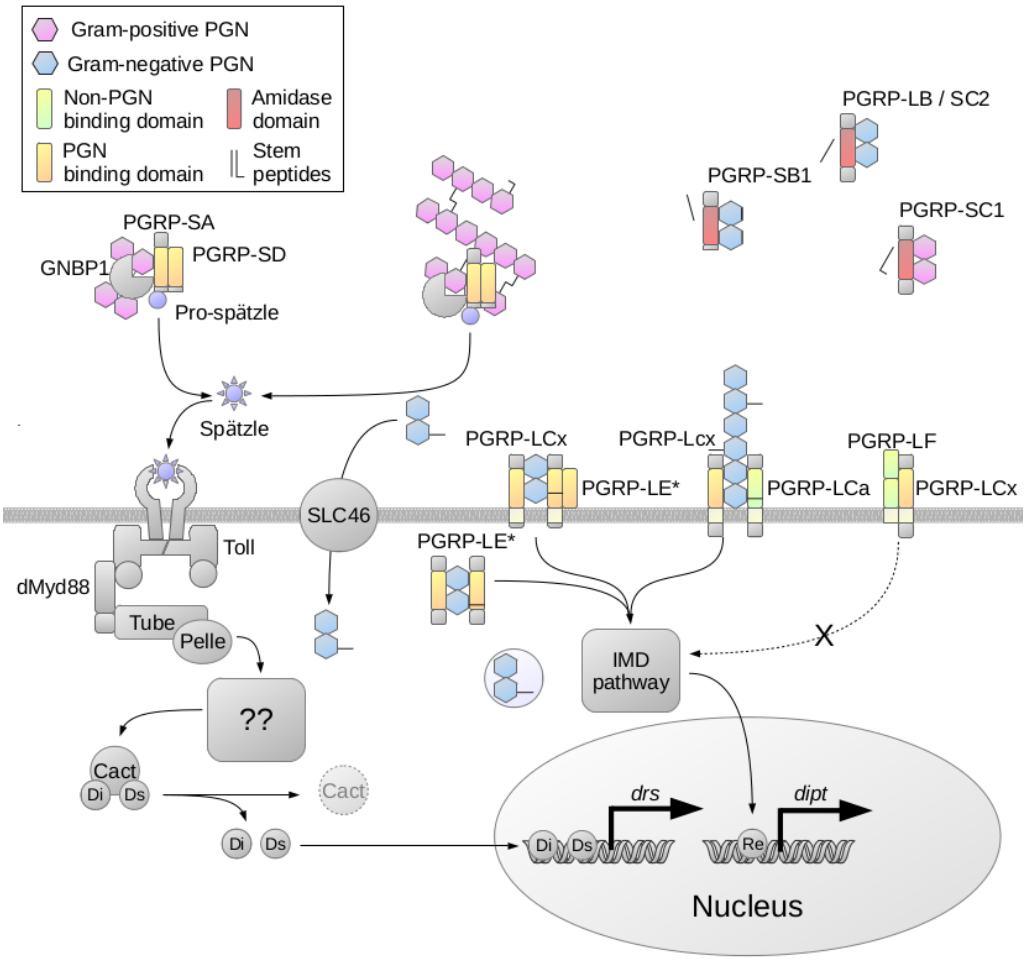


FIGURE 1.13: ***Peptidoglycan recognition in D. melanogaster.*** *Drosophila uses PGRPs to recognise PGN, recognising both fragments of PGN released by PGN turnover and also higher molecular weight PGN, such as that exposed at the surface of Gram-positive bacteria. Focus here is given to recognition of Gram-positive bacteria. Gram-positive (Lys-type) PGN is recognised by a complex consisting of PGRP-SA, PGRP-SD and GNBP1. Gram-negative (DAP-type) PGN is sensed primarily by PGRP-LCx a transmembrane-spanning PGRP, which forms dimers and interacts with PGRP-LE to recognised polymeric DAP-type PGN and activate the IMD-pathway. PGRP-LE is also found intracellularly where it recognises fragments of PGN in the cytoplasm, supplied in autophagiosomes or perhaps via transporters of the SLC46 family. PGRP-LCx also interacts with PGRP-LCa in order to recognised monomeric DAP-type PGN and with PGRP-LF, which plays a role in suppression of IMD signalling. Drosophila also possesses amidase domain containing PGRP's which may also down-regulate immune signalling by degrading PGN-derived ligands. PGRP-SC1 degrades Lys-type PGN and PGRP-SB1 and LB/SC2 degrade DAP-type PGN. See text for references and further detail.*

include PGRP-LB, SB1, SB2 SC1A, SC1B and SC2, of which PGRP-SC1A/B, LB and SC1 are responsible for removing peptides from glycan strands to reduce or eliminate immunostimulatory activity of PGN [436, 437] (Figure 1.13). The non-catalytic PGRPs include PGRP-SA, SD, LCx, and LE [418, 399] (Figure 1.13). PGRP-LC and LE act as PRRs upstream of the immune deficiency (IMD) pathway [438, 439], with PGRP-LC recognising

DAP-type PGN (Figure 1.13). PGRP-LC is a TM receptor with two interacting forms; PGRP-LCx and LCa [440]; PGRP-LCx binds PGN but LCa does not. PGRP-LCx also interacts with PGRP-LF, another PGRP without PGN binding activity, blocking IMD activation [441] and with PGRP-LE to enhance activation [442]. The various associations of LCx with other PGRPs facilitates the recognition of polymeric and monomeric DAP-type PGN [443], while PGRP-LE also mediates recognition of intracellular monomeric DAP-type PGN fragments to induce autophagy, dimerising upon its recognition [440, 444]. *D. melanogaster* SLC46 family transporters take up GlcNAc-anhMurNAc-tetrapeptide, facilitating its recognition [389], as in humans [388]. Following recognition of Gram-negative PGN the IMD pathway is stimulated and a signalling cascade results, culminating in the translocation of the NFκB transcription factor Relish (Re) to the nucleus, and the expression of AMP genes such as *diptericin dipt* [420].

Two further non-catalytic PGRPs; PGRP-SA and PGRP-SD ciculate freely in *D. melanogaster* haemolymph (blood) and are responsible for Gram-positive Lys-type PGN recognition [445, 446] (Figure 1.13). Both HMW Lys-type PGN and muropeptide components derived thereof activate the *Drosophila* immune system via PGRP-SA [445, 447]. The crystal structure of PGRP-SA sports a muropeptide-binding hydrophilic groove [448] which binds strongly to Lys-type PGN, but also weakly to DAP-type PGN [448]. PGRP-SA also possesses CP activity for DAP-type PGN, cleaving A_2pm from stem tripeptides, thus preventing stimulation of the Toll pathway by this ligand [449]. PGRP-SD's role in PGN recognition is more subtle. PGRP-SD is involved in recognition of some Gram-positive bacteria such as *S. aureus* and *Streptococcus pyogenes* [450], though its crystal structure suggests binding to DAP-type PGN [451]. PGRP-SD forms a complex with PGRP-SA and another protein, GNBP1 (Gram-negative binding protein 1), mediating recognition of *S. aureus* PGN and stimulation of the Toll pathway [446]. GNBP1 cleaves Lys-type HMW PGN when in complex with PGRP-SA, producing muropeptide dimers (tetrasaccharides with two stem peptides), enhancing recognition of Lys-type PGN by PGRP-SA [452, 447]. PGN recognition by PGRP-SA induces cleavage of pro-spaetzle to produce the Toll-ligand Spaetzle which in turn binds to Toll, activating an intracellular proteolytic cascade (Figure 1.13, [453, 445, 420, 446]). The Toll signalling cascade is highly homologous to that of TLR/IL-1 in mammals, and TLRs have been found in all metazoans [454, 385]. Toll interacts with the highly conserved dMyD88 (c.f. mammalian MyD88), Tube (IκB) and Pelle (IRAK) forming a complex which induces the phosphorylation of Cactus by an unknown mechanism [420, 385]. Phosphorylation of Cactus then leads to its degradation by the proteasome, and the release of the NF-κB

transcription factors Dif and Dorsal [455]. Dif and Dorsal translocate to the nucleus where they induce the expression of immune effector genes such as *drs* (Drosomycin), a Gram-positive targetting antimicrobial peptide (AMP) [456].

1.8.2 Use of *D. melanogaster* in studying the roles of peptidoglycan metabolism during *S. aureus* infection

Although not a natural host, *D. melanogaster* has been employed extensively to study *S. aureus* virulence [432, 433, 434], PGN recognition [457, 293, 458, 452, 446] and the impact of different aspect of CW metabolism on pathogenesis [457, 293, 39]. Using this model, roles of WTA and the major autolysin (Atl) of *S. aureus* in preventing recognition of PGN at the bacterial cell surface have been uncovered [457, 293], and non-essential PBPs (all but bPBP1 and aPBP2) were implicated in pathogenesis despite having seemingly no importance during *in vitro* growth in rich media. *Drosophila* is able to recognise PGN sacculi and soluble sacculus-derived muropeptides from *S. aureus* and *S. pneumoniae* via PGRP-SA [447]. Interestingly however, although PGRP-SA is evidently able to bind monomeric muropeptides from *S. aureus* and *S. pneumoniae*, only those of *S. pneumoniae* elicit an immune response, though higher molecular weight muropeptides of both species also produce a response [447]. The muropeptides used were generated using mutanolysin from *Streptomyces globisporus* [447] and it remains to be seen if natural turnover products of *S. aureus* behave in a similar manner.

1.9 *Aims of the following work*

PR in Gram-positive bacteria remains enigmatic, and its potential role(s) in host-pathogen interaction remain almost completely unexplored. As such, my first aim was to determine if the Gram-positive pathogen *S. aureus* might have the capacity to recycle PGN, first through bioinformatic identification of potential PR components followed by *in vitro* characterisation of corresponding *S. aureus* deletion mutants. I also aimed to understand how PR might affect various aspects of *S. aureus* physiology and PGN metabolism. The results pertaining to these aims are presented in Chapters 2 - 4. Chapter 2 includes bioinformatic analyses and details of mutant construction. Chapter 3 details the basic characterisation of these mutants in terms of growth, morphology and ability to grow on CW aminosugars. Chapter 4 contains the further characterisation of a subset of these mutants with regards to the possible function of NagA and a preliminary investigation of the potential effects of PR on CW characteristics. My final aim, was to try and understand what role PR might play in the host pathogen

interaction of *S. aureus*. Chapter 5 contains initial characterisation of the interaction of *S. aureus* mutants lacking putative PR components with the model host *D. melanogaster* along with a preliminary assay of virulence factor production. The work undertaken for Chapter 5 also revealed a possible new role for *S. aureus* Atl. To my knowledge this thesis represents the first attempt to characterise the possible role of Gram-positive PR in host-pathogen interaction.

Chapter 2

Bioinformatic identification and analysis of putative peptidoglycan recycling machinery components in *Staphylococcus aureus*

2.1 *Introduction*

Many Gram-positive species shed PGN at relatively high rates during vegetative growth [310, 311, 312, 274, 313, 288, 314, 299]. Given the considerable proportion of bacterial dry-cell-weight taken up by the Gram-positive CW and the considerable loss of resources this would represent, it seems likely that some portion of this material may be recovered and recycled under certain environmental conditions [294]. However, it is also possible that PGN shedding may also serve several different functions (see Section 1.7). Aside from resource recovery [368], Gram-positive PR may hypothetically play roles in antibiotic resistance [369], virulence [429], or indeed simply in regulating PGN shedding itself [337], as it does in Gram-negative bacteria. One previous bioinformatic analysis identified several putative *E. coli* PR protein orthologues in a number of Gram-positive bacteria, including *S. aureus* [294]. Several of the analysed species possessed a core set of putative PR proteins, largely those thought to be involved in aminosugar recycling [294], though none possessed orthologues of AmpG, the primary permease responsible for PGN fragment recovery in Gram-negative bacteria [338]. Similarly, none of the species investigated contained orthologues of the two main peptidoglycan hydrolases employed in PR in *E. coli*; AmiD and AmpD, both of which are anhMurNAc-L-Ala amidases (anhMLAAs) [339, 307]. Orthologues of the anhMurNAc kinase AnmK [343] were also found in only 2 out of 10 species. Together, this suggests recycling of anhMurNAc-containing PGN fragments is not likely to be a major pathway in Gram-positive bacteria [294], consistent with the relative paucity of LTs in this group and

the minimal quantities of anhMurNAc found in the PGN of some Gram-positive species [82, 86].

Though the presence of some putative PR proteins had already been identified in *S. aureus* [294], little further information was provided. Here, a more in-depth bioinformatic analysis was undertaken to establish a full list of putative PR components for this organism, to determine the organisation of encoding genes within the genome, and to generate hypotheses pertaining to their likely function. It was hoped that this would shed further light on the potential PR capabilities of *S. aureus*, and indeed similar analyses have preceded discovery of novel PGN biosynthetic capabilities in other bacteria [459, 63]. In addition to the identification of putative PR components by orthology, further putative PR genes may also be found through analysis of neighbouring regions of the chromosome [320, 366, 367, 370, 368] and several putative PR operons have been identified in this manner. Indeed, it was recently discovered that *S. aureus* and *B. subtilis* are able to take-up and metabolise MurNAc from the environment, utilising the PTS transporter MurP and the MurNAc-1-P etherase MurQ [368]. The encoding genes sit within four-gene and six-gene putative PR operons in *S. aureus* and *B. subtilis* respectively [368]. Several further proteins thought to be involved in recovery and reutilisation of PGN fragments have also been characterised in *B. subtilis* and *C. acetobutylicum*, all of which are encoded by genes found in similar operons [320, 366, 367, 370].

Notwithstanding these discoveries, the fact that Gram-positive bacteria release large quantities of turnover material to the medium during vegetative growth remains [288, 274]. As discussed in Chapter 1, this may be due CCR of PR gene expression [294, 334, 460]. Early studies of PT in both *S. aureus* and *B. subtilis* employed media containing relatively high concentrations of glucose, and thus PR gene expression may well have been considerably lower than in environments with scarce preferred carbon sources. PR in Gram-negative bacteria has also been shown to be regulated by CCR [460, 348]. Recent studies have shown that PR in Gram-positive bacteria also appears to be most important in the stationary phase of growth [368] when most preferred carbon sources have been used up. It therefore seemed likely that putative PR gene expression could be subject to CCR in Gram-positive bacteria, and PR genes should therefore sport *cre* sites to which the catabolite control protein CcpA may bind, either within promoter regions of genes, or the genes themselves [374]. Thus, the occurrence of *cre* sites within or around identified PR genes was also investigated.

Presented here is the identification of 17 putative aminosugar and peptide recycling components in *S. aureus*, 9 of which were organised into two putative operons consisting

of 4 and 5 genes each, revealing expanded aminosugar recovery/recycling potential in this organism. However, as GlcNAc residues are also present in CW glycopolymers such as WTA or CPS [52], PTS components predicted to be involved in GlcNAc uptake and metabolism should more correctly be considered as CW recycling (CWR) components, and henceforth the identified proteins / genes will be referred to as CWR components where appropriate. Additionally, *cre* elements were identified that may be involved in control of expression of several of these genes. The identification of an RpiR-like regulatory protein encoded by a gene within a putative MurNAc recycling operon suggests a further level of regulation of MurNAc recycling in particular [460]. With the help of Dr Aino Jarvelin a CWR component search was extended to other Staphylococci, revealing variation in putative PR capabilities within this Genus. Following bioinformatic analysis, deletion vectors for the identified genes were constructed and a total of 9 markerless deletion mutants produced for use in further laboratory-based studies.

2.2 *Results*

2.2.1 *S. aureus* contains a suite of putative cell wall recycling genes

Protein sequences of known PR proteins from *E. coli* [194] were used as queries to search the proteome of *S. aureus* NCTC8325-4 using NCBI's `blastp` algorithm (protein-protein basic logical alignment search tool; BLAST) in a Best Reciprocal Blast (BRB) approach. This identified orthologues of MurQ, MurP, NagA, MppA and NagE from *E. coli* (Table 2.1). Despite not being detected as orthologues in these initial searches, several other PTS components showed relatively high sequence coverage (60-70%) and identity (30-40%) to MurP and NagE. Thus, using the Hidden Markov Model (HMM) search tool HMMER [461], which allows detection of remote homologues with high sensitivity, a search for further putative orthologues of GlcNAc and MurNAc specific PTS components was made. Gram-negative GlcNAc and MurNAc specific EIIBC PTS component domain sequences downloaded from the CATH protein structure classification database (FunFam2607; GlcNAc, FunFam2608; MurNAc) [462] and sequence alignments made to use as queries for HMMER. This identified 6 further PTS components that may play a role in CW aminosugar recovery (Table 2.1). Though not a direct orthologue of *E. coli* MppA, *S. aureus* OppA was retained as a putative PR component as of the multiple oligopeptide transporters in this organism only OppA showed similarity to MppA, an

TABLE 2.1: Putative cell wall recycling proteins identified in *S. aureus*

Query [1]	Protein / CATH annotation	*S. aureus* protein [2]	Protein annotation[3]	Method[4]	% CV[5]	% ID[6]	E-value
JW2421 (MurQ)	*N*-acetylmuramic acid 6-phosphate etherase	SAOUHSC_00157 (MurQ)	*N*-acetylmuramic acid 6-phosphate etherase	BRB	98	46.758	$1.34x10^{-91}$
JW2422 (MurP)	PTS system *N*-acetylmuramic acid specific EIIBC component	SAOUHSC_00158 (MurP)	PTS system EIIBC component	BRB	98	37.219	$1.41x10^{-81}$
JW0663 (NagA)	*N*-acetylglucosamine-6-phosphate deacetylase	SAOUHSC_00710 (NagA)	*N*-acetylglucosamine-6-phosphate deacetylase	BRB	97	28.756	$3.97x10^{-45}$
JW1322 (MppA)	Periplasmic murein peptide-binding protein	SAOUHSC_00927 (OppA[7])	Oligopeptide ABC transporter substrate-binding protein (putative)	BRB	93	27.652	$1.03x10^{-51}$
JW0665 (NagE)	PTS system *N*-acetylglucosamine-specific EIICBA component	SAOUHSC_01836 (PtaA)	Uncharacterized protein	BRB	99	41.566	$2.23x10^{-101}$
FunFam2607	GlcNAc_EIIBC_PTS	SAOUHSC_00155 (GlcA)	PTS system glucose-specific EIICBA component	HMM	NA	NA	$4.1x10^{-15}$
FunFam2607	GlcNAc_EIIBC_PTS	SAOUHSC_00209 (PtsG)	PTS system glucose-specific IIBC component (putative)	HMM	NA	NA	$1.0xx10^{-12}$
FunFam2608	MurNAc_EIIBC_PTS	SAOUHSC_00437 (TreP)	Uncharacterized protein	HMM	NA	NA	$1.1x0^{-12}$
FunFam2607	GlcNAc_EIIBC_PTS	SAOUHSC_02597 (GlvC)	PTS system component (putative)	HMM	NA	NA	$6.7x10^{-9}$
FunFam2608	MurNAc_EIIBC_PTS	SAOUHSC_02661 (ScrA)	PTS system sucrose-specific IIBC component (putative)	HMM	NA	NA	$2.0x10^{-12}$
FunFam2607	GlcNAc_EIIBC_PTS	SAOUHSC_02848 (GlcB)	PTS system glucoside-specific EIICBA component	HMM	NA	NA	$1.6x10^{-15}$

[1]*E. Coli* K-12 W3110 locus tag and common name or CATH FunFam alignment, [2]*S. aureus* NCTC8325-4 locus tag and common names taken from AureoWiki (http://aureowiki.med.uni-greifswald.de/Main_Page), [3]Protein annotation from UniProt (http://www.uniprot.org/), [4]Method of identification; BRB - Best Reciprocal BLAST, HMM - Hidden Markov Model search (`hmmsearch`, http://www.ebi.ac.uk/Tools/hmmer/search/hmmsearch), [5]ID; identity, [6]CV; coverage, [7]Not a direct orthologue (see text)

extracytoplasmic peptide-specific PR component found in *E. coli* [352]. For further details of the methodology used here and throughout the rest of this thesis, please refer to Chapter 7.

2.2.2 Putative cell wall recycling genes are organised into operons and possess catabolite repression elements

Following putative CWR protein identification, the genomic context of the encoding genes was mapped, using the Microbial Genome-context Viewer (MGcV; http://mgcv.cmbi.ru.nl/, [463]) (Figure 2.1). This enabled the identification of two putative PR operons in *S. aureus*. The first includes the genes *murQ* and *murP*, along with two further genes; *SAOUHSC_00156* and *murR* (*SAOUHSC_00160*). This same operon was identified in a recent publication [368]. A second operon was identified containing 4 genes upstream of *oppA*; *oppBCDF*. None of the additional genes found in these two operons were identified in previous analyses. A further operon was also identified downstream of *treP*, but was not taken for further analysis as the two accompanying genes *treC* and *treR*, are annotated as being involved in trehalose uptake and thus were deemed unlikely to be involved in PR. Though *treP* is similarly annotated it may still be involved in CW aminosugar uptake as PTS components may be involved in uptake of multiple carbohydrates [359]. In order to address the question of whether the identified putative CWR genes may be regulated by CCR, the occurrence of *cre* sites in or around the identified genes was undertaken. Using the consensus sequence for *cre* sites in *B subtilis* [464] alignments were made with the coding sequence (CDS) and flanking 200bp regions of the genes of interest (GOIs) using ClustalOmega [465] and identified *cre* sites mapped onto genomic context maps. This revealed that all except two of these genes possessed *cre* elements within the gene / operon, or immediately upstream of the gene in the putative promoter region (Figure 2.1). This suggests that control of gene expression by CcpA may be widespread among these putative CWR genes. Following this, the genomic context and presence of *cre* sites was also investigated for *ccpA* itself, identifying a *cre* site upstream of *cppA* and suggesting CcpA may auto-regulate (Figure 2.1). The short CDS upstream of *ccpA* appears only to encode for a short peptide with no annotated function and may represent a pseudogene.

2.2.3 Domain structures of putative cell wall recycling proteins give insight into function and the nature of CWR in *S. aureus*

All PTS components contained domains indicative of a membrane localisation (EII subunits), as expected. Domain structures of the PTS components TreP and PtaA give clues to their

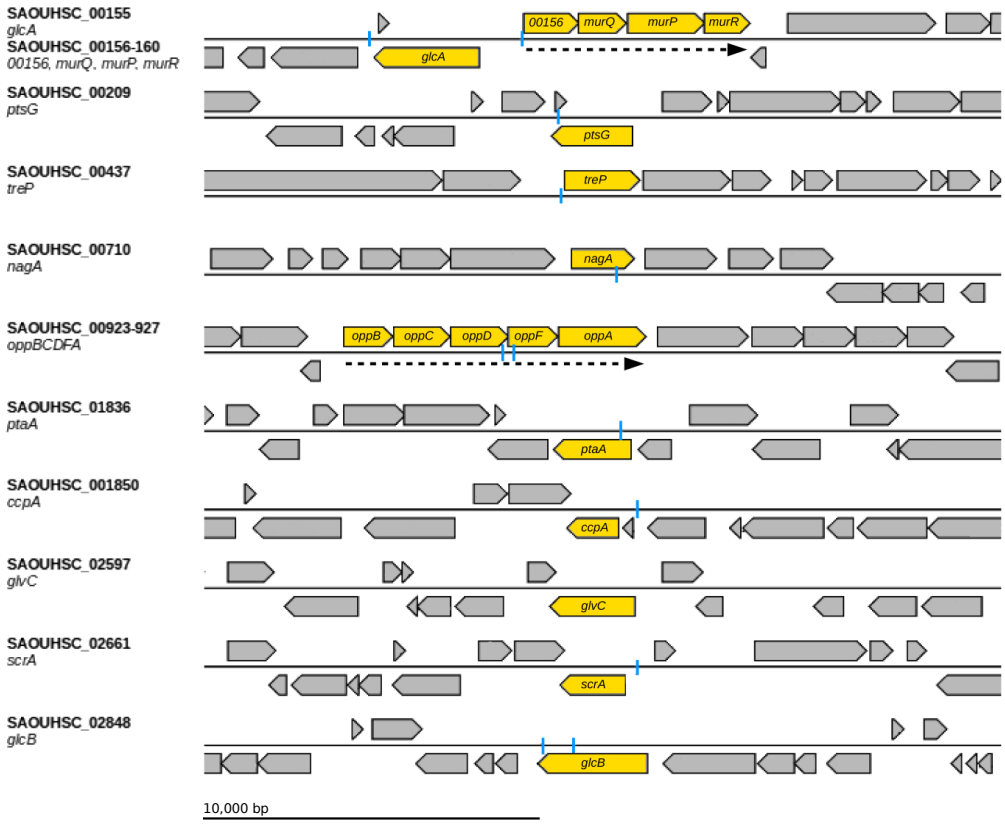


FIGURE 2.1: ***The genomic context of putative peptidoglycan recycling genes and putative regulatory elements in S. aureus*** *The genomic context of genes encoding proteins identified in Table 2.1 were mapped to enable the identification of putative PR operons and to map potential cre sites around these genes. The identified GOI's are highlighted in yellow, putative PR operons are denoted by dashed arrows, and putative cre sites are marked by blue tick marks. A scale bar is provided in the bottom left of the figure. Units; base pairs (bp).*

likely substrate specificity (Figure 2.2, A), reaffirming PtaA as a likely GlcNAc transporter and suggesting that TreP is likely responsible for the uptake of trehalose, though it may also transport CW aminosugars [359]. ScrA appears to lack the IIB PTS component subunit present in all of the other identified PTS transporters, suggesting a further protein may be required for its function [359]. OppABCDF may form a similar system to the OppBCDF/MppA system of *E. coli* for the recovery of stem peptides [352]. OppA contains a signal peptide at its *N*-terminus suggesting that like MppA it may be secreted, while OppBCDF likely form an ABC-type peptide or amino acid transporter. Indeed OppBCDF contain domains similar to other such transporters including D-methionine transport system permease-like (MetI-like) TM domains [468], OppC-like domains [469] and ATP binding and hydrolysis domains (Figure 2.2, B). The solute binding (SB) domain of OppA is part of the SB protein family 5 (Interpro domain: IPR000914) that includes many peptide binding proteins including MppA of *E. coli* and other oligopeptide or dipeptide binding proteins of *E. coli*

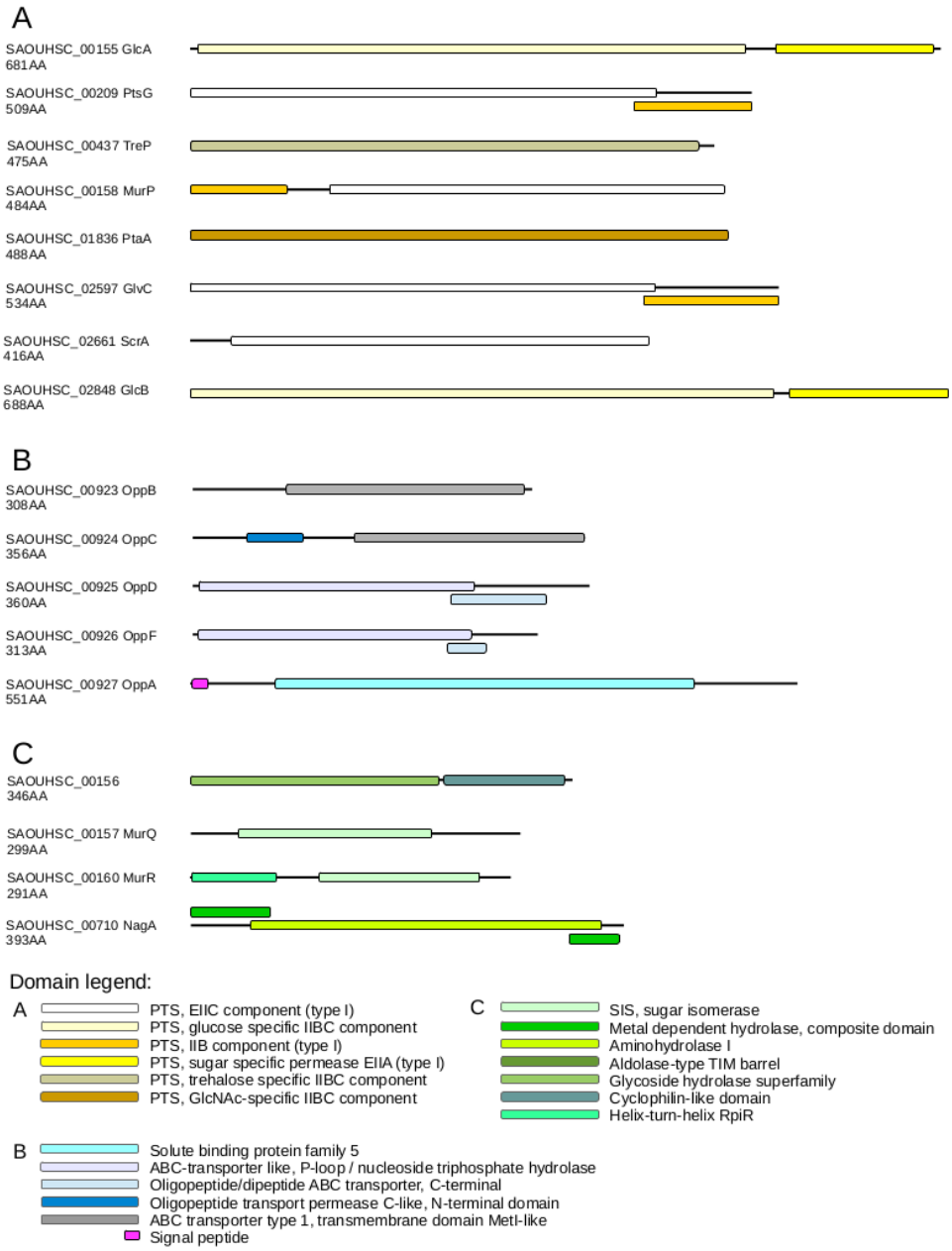


FIGURE 2.2: ***Predicted domain structures of putative PGN recycling proteins.*** *All of the identified proteins contained domains which may play roles in aminosugar transport (A), peptide transport (B) metabolism of aminosugars (MurQ, NagA) or muropeptides (SAOUHSC_00156) (C) or MurNAc metabolism regulation (MurR) (C). All proteins in group A contain PTS domains, which in turn contain several transmembrane (TM) domains, and likely these proteins are localised to the plasma-membrane. Similarly, group B proteins OppB and OppC seem to form the two TM subunits of an ABC transporter, while OppD and OppF are likely cytoplasmic ATP hydrolysing subunits. OppA is likely to be secreted due to the presence of a signal peptide at its N-terminus. Group C proteins contain neither TM domains nor any indication of domains that would signal their secretion and are most likely cytoplasmic. Predicted domain structures were taken from Interpro [466] and Pfam [467]. Proteins are orientated with the N-terminus on the left. Annotations from Interpro can be found in the Domain legend.*

and *B. subtilis* [470]. Indeed, both OppD and OppF contain domains annotated as being specifically involved in dipeptide transport (Figure 2.2, B).

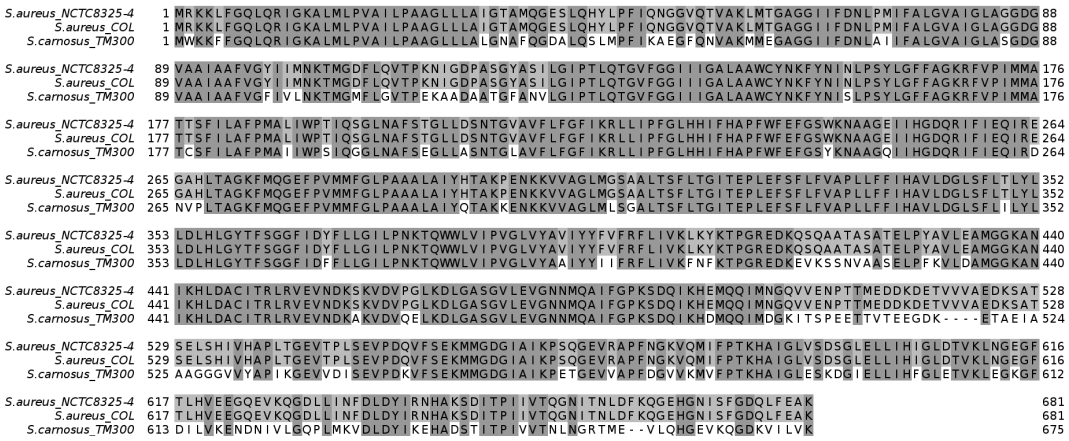


FIGURE 2.3: ***A highly conserved GlcA homologue is present in S. saprophyticus.*** *GlcA has previously been designated as an S. aureus-specific protein [474]. Orthologue searching (Table 2.2) identified a second homologue of E. coli NagE in S. carnosus which shows high sequence conservation when compared to S. aureus GlcA. Shades of grey denote percentage identity: dark grey, 100%, light grey: 66%.*

The remaining identified proteins appear to be cytoplasmically located (Figure 2.2, C) including both MurQ and NagA, orthologues of the cytoplasmic enzymes of the same name in *E. coli* (Table 2.1). Of these proteins, MurQ is now thought to be responsible for the metabolism of MurNAc-6-P to produce GlcNAc-6-P in *S. aureus* [368] and NagA may be responsible for the deacetylation of GlcNAc-6-P as it is in *E. coli* [471, 349]. MurR and SAOUHSC_00156, found together in a putative MurNAc recycling operon with MurQ and MurP (Figure 2.1) encode what appears to be an RpiR-like regulatory protein [472] and a cytoplasmic PGN hydrolase, respectively. MurR contains a RpiR-like helix-turn-helix DNA binding domain and a sugar isomerase domain, like MurQ (Figure 2.2, C), suggesting it may act as a transcriptional regulator of the operon as in *E. coli* [460]. SAOUHSC_00156 contains a glycoside hydrolase domain (Interpro domain: IPR017853) potentially involved in the cleavage of glycosidic bonds between two carbohydrates or a carbohydrate and another moiety, such as those formed between GlcNAc and MurNAc or MurNAc and stem peptides. Alongside this, SAOUHSC_00156 also contains a cyclophilin-like domain (Interpro domain: IPR029000) at the the C terminus of the protein. These domains are normally involved in the cis-trans isomerisation of peptides at proline residues[473].

2.2.4 Putative cell wall recycling genes are not evenly distributed in other Staphylococci

The occurrence of *E. coli* PR protein orthologues in other Staphylococci was investigated to determine if this was a ubiquitous feature of the Genus, and thus to better understand the significance of putative PR in *S. aureus* (Table 2.2). Furthermore, as several new PR

TABLE 2.2: Putative cell wall recycling protein orthologues identified in Staphylococci

Protein	Spp[1]	COG[2]	Hit	*Sau*	COL	*Sho*	*Sca*	*Sep*	*Sha*	*Slu*	*Ssa*	*Swa*	*Scp*
AmpG	*Ec*	5EYM	-	-	-	-	-	-	-	-	-	-	-
AmiD	*Ec*	8VBV	-	-	-	-	-	-	-	-	-	-	-
AmpD	*Ec*	8VBV	-	-	-	-	-	-	-	-	-	-	-
LdcA	*Ec*	5EBE	+	-	-	-	-	-	-	-	1	-	-
NagZ	*Ec*	7QPA	-	-	-	-	-	-	-	-	-	-	-
NagK	*Ec*	5EZX	-	-	-	-	-	-	-	-	-	-	-
AnmK	*Ec*	5ED7	-	-	-	-	-	-	-	-	-	-	-
MurP	*Ec*	5C5Y	+	1	1	-	1	1	1	1	1	1	1
NagE	*Ec*	5CI1	+	1	1	1	2	1	1	1	1	1	1
MurQ	*Ec*	5E15	+	1	1	-	1	1	1	1	1	1	1
NagA	*Ec*	5CE4	+	1	1	1	1	1	1	1	1	1	1
MppA	*Ec*	7QSI	+	0[a]	0[a]	1	-	-	-	-	0[a]	-	-
Mpl	*Ec*	5DFU	+	0[b]	0[b]	-	-	-	-	-	-	-	-
MpaA	*Ec*	5KXI	-	-	-	-	-	-	-	-	-	-	-
AeeP	*Ec*	7S8C	-	-	-	-	-	-	-	-	-	-	-
08375	*Tf*	NA	-	-	-	-	-	-	-	-	-	-	-
08380	*Tf*	NA	-	-	-	-	-	-	-	-	-	-	-
AmgK	*Pp*	5EHM	-	-	-	-	-	-	-	-	-	-	-
MurU	*Pp*	8S0S	-	-	-	-	-	-	-	-	-	-	-
MupP	*Pp*	8VXP	-	-	-	-	-	-	-	-	-	-	-

[1] Spp; query species, [2] COG; Cluster of Orthologous Genes, [a] As described above, no direct orthologue of MppA apparently exists in *S. aureus*, though a protein of likely similar function was found in both *S. aureus* NCTC8325-4 and COL as well as *S. saprophyticus*, while a direct orthologue was found in *S. hominis*, [b] Mpl showed high sequence similarity to the PGN biosynthesis protein MurC of both *S. aureus* NCTC8325-4 and COL (84.0% coverage, 29.5% identity).

Species key:
Ec; *E. coli*, ***Tf***; *T forsythia*, ***Pp***; *P. putida*, ***Sau***; *S. aureus* NCTC8325-4, **COL**; *S. aureus* COL (MRSA), ***Sho***; *S. hominis*, ***Sca***; *S. carnosus*, ***Sep***; *S. epidermidis*, ***Sha***; *S. haemolyticus*, ***Slu***; *S. lugdunensis*, ***Ssa***; *S. saprophyticus*, ***Swa***; *S. warneri*, ***Scp***; *S. caprae*

components have recently been discovered in Gram-negative bacteria [354, 355, 356, 358, 357], their occurrence in *S. aureus* and other Staphylococci was also investigated. All of the Staphylococcal species present in the EggNOG 4.5.1 database used for analysis [475].

Not all analysed Staphylococci possess the same set of *E. coli* PR protein orthologues found in *S. aureus*, though all except *S. hominis* contained a core set of PR protein orthologues; MurP, NagE, MurQ and NagA. Where it was possible to map genomic context of the encoding genes, *murQ* and *murP* always resided within putative MurNAc operons, though a putative cytoplasmic hydrolase was lacking in *S. warneri* (Figure 2.4). As *S. hominis* lacks both MurQ and MurP orthologues, this suggests that either that this bacterium does not recycle MurNAc or that it employs an alternative pathway. The fact that *S. hominis* also contains a true orthologue of MppA, unlike any of the other species examined, suggests further

idiosyncrasies in PR may exist in this species. An OppA protein similar to that found in *S. aureus* was also identified in *S. saprophyticus* (Table 2.2), the encoding gene of which resides in a similar operon (Figure 2.4).

S. saprophyticus also possesses an orthologue of LdcA not found in *S. aureus*, which contains a murein tetrapeptide CP domain and appears to be cytoplasmic (data not shown). *Staphylococcus carnosus* (Sc, Table 2.2) was found to contain 2 direct orthologues of *E. coli* NagE, a GlcNAc-specific PTS component (Table 2.1). One orthologue is highly homologous to *S. aureus* GlcA (Figure 2.3), previously reported to be a unique PTS component found only in *S. aureus* [474]. However, *S. carnosus glcA*, did not share the same genomic location as *S. aureus glcA*, instead located upstream of *glcB* (data not shown). No orthologues of *P. putida* or *T. forsythia* PR components were found with the analysed Staphylococci, and indeed the result was the same for other Gram-positive taxa in which other PR proteins had previously been identified [294] (results not shown).

2.2.5 Putative cell wall recycling genes were deleted from *S. aureus* NCTC8325-4

Following the bioinformatic identification of putative CWR genes, attempts were made to produce markerless gene deletion mutants using the pMAD cloning system developed by Arnaud *et al.* (see Chapter 7, [476]). Deletion vectors were successfully produced for all of the identified genes except *murR* and *SAOUHSC_00156* (Table 2.3) and for the *opp* operon. Deletion mutants for all except *murR*, *SAOUHSC_00156*, *ptaA*, *glcB*, *oppBCDF* and *oppABCDF* (Figure 2.5) were then constructed. Missing vectors or mutants were the result of unsuccessful cloning rather than selective omission. In addition, a *glcA* / *nagA* double mutant was later constructed (see Chapters 3 and 4). All resulting strains and plasmids were sequenced confirming that no additional mutations had been introduced around the cloning sites (see Tables B.2 and B.3). Curiously however, while producing these mutants it originally appeared that several polymorphisms and deletions had been introduced into the *scrA* gene and surrounding region of *S. aureus* NCTC8325-4 (see Table B.3). On further analysis, these mutations were found to exist between *S. aureus* NCTC8325 (the reference strain genome available from NCBI; https://www.ncbi.nlm.nih.gov/) and NCTC8325-4, the strain used in this study, rather than being mutations introduced as a result of genetic manipulation. NCTC8325-4 is a derivative of NCTC8325 cured of 3 prophages [477].

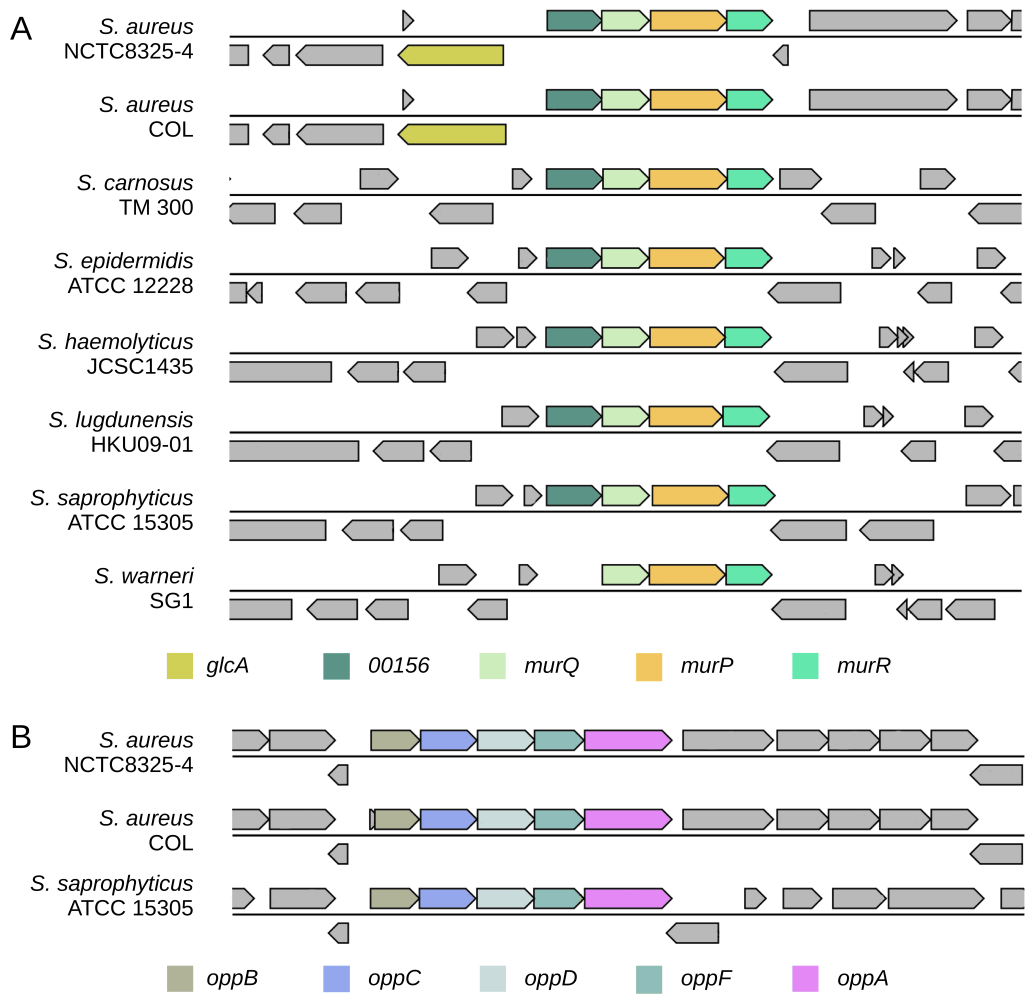


FIGURE 2.4: ***Genomic organisation of putative cell wall recycling genes is largely conserved in Staphylococci.*** *Both of the putative PR gene operons found in S. aureus are also found in the other Staphylococci examined for which genome context maps were able to be built. S. warneri however seems to lack a gene encoding the putative PGN hydrolase (SAOUHSC_00156). This may simply be an annotation error as the spacing of genes in the genome of S. warneri is close to identical of that found in other Staphylococci, or may represent the pseudogenisation of this gene through alteration of stop or start codons. Despite the presence of orthologues of several of these genes in S. hominis and S. caprae, it was not possible to include them in analyses of genomic organisation. The genome sequences of these species are currently incomplete and exist only as contigs not useful for assembly with MGcV [463].*

2.3 *Discussion*

Only a few previous studies have searched for the presence of putative CWR components in Gram-positive bacteria [294, 366, 367, 320], and no comprehensive bioinformatic analysis of putative CWR components in any Gram-positive bacterium has been presented previously. Through a combination of techniques, it is shown here that *S. aureus* possesses a larger arsenal of putative CWR components than previously assumed, and analysis of the

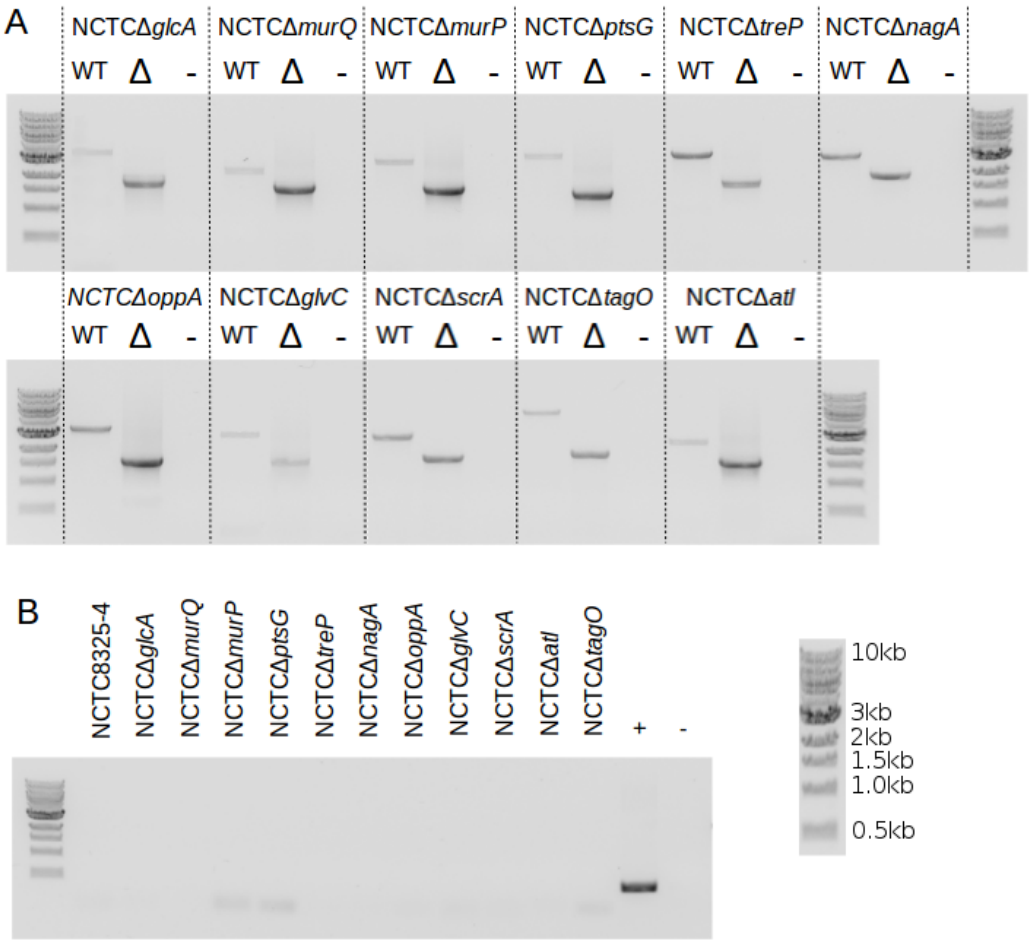


FIGURE 2.5: ***Putative cell wall recycling genes were deleted from S. aureus.*** *Agarose gel electrophoresis of polymerase chain reaction (PCR) products generated using integration primers (see Chapter 7 and Table A.2) demonstrates the absence of the indicated putative PR genes in NCTC8325-4 deletion mutants (A). The absence of pMAD derivatives in final mutants was also confirmed (B). Predicted fragment sizes are listed in Table 2.3. WT; NCTC8325-4, Δ; mutant, +; pMAD positive control, -; negative control.*

repertoire of identified components raises interesting questions about the nature of PR in this organism. Furthermore, analysis of the presence of conserved regulatory elements involved in CCR indicate that this process may play a role in regulating putative CWR gene expression, as previously hypothesised [294, 298]. Finally, the occurrence of putative CWR protein orthologues was confirmed in a range of different Staphylococcal species, suggesting that this is a widespread trait among this group though variation in the potential mechanisms of PR is present even within the Genus.

As with other Gram-positive bacteria, *S. aureus* does not possess any orthologue of AmpG, nor do any of the other Staphylococci examined in this Chapter. This reaffirms that *S. aureus* and other Gram-positive bacteria are unlikely to employ the same major recycling pathway as Gram-negative bacteria. Instead, *S. aureus* possesses an expanded repertoire

of putative aminosugar-transporting PTS components, alongside an oligopeptide transport system similar to that found in *E. coli* [351, 352] (See Table 2.1). PTS components are transport systems that catalyse the uptake of numerous carbohydrates and convert them to their respective phosphoesters during transport [377] (see Figure 1.11). They were originally discovered as a system using P(EP) to phosphorylate a number of hexose sugars including *N*-acetyl mannosamine, Glc, mannose, GlcN and GlcNAc [478] and are involved in CW aminosugar uptake in *E. coli* and other bacteria [194, 368]. Indeed, the PTS component MurP is now implicated as the sole MurNAc transporter in *S. aureus* [368], though two possible alternative MurNAc PTS components were identified here. MurR, which is encoded in the same operon as MurP, contains both DNA binding and sugar isomerase (phosphosugar binding) domains and may perhaps act as transcriptional regulator of its operon and may sense MurNAc-6-P generated during MurNAc recovery by MurP in much the same way as MurR of *E. coli* [460]. MurR is also known as RpiRB and has been implicated in pentose phosphate pathway regulation, as well as virulence gene expression in *S. aureus* [472, 479]. GlcA has also now been implicated in GlcNAc uptake, validating the HMM searching approach used to identify this protein as a putative GlcNAc transporter (Table 2.1).

TABLE 2.3: Strains and plasmids produced in this study.

Strain / Plasmid	Relevant characteristics	WT*	Mutant*	Source
NCTC8325-4	*S. aureus* reference strain	-	-	R. Novick
NCTCΔ*glcA*	NCTC8325-4 *glcA* null mutant	3865	1891	This study
NCTCΔ*murQ*	NCTC8325-4 *murQ* null mutant	2797	1945	This study
NCTCΔ*murP*	NCTC8325-4 *murP* null mutant	3330	1920	This study
NCTCΔ*ptsG*	NCTC8325-4 *ptsG* null mutant	3218	1727	This study
NCTCΔ*treP*	NCTC8325-4 *treP* null mutant	3511	2089	This study
NCTCΔ*nagA*	NCTC8325-4 *nagA* null mutant	3290	2123	This study
NCTCΔ*oppA*	NCTC8325-4 *oppA* null mutant	3342	1692	This study
NCTCΔ*glvC*	NCTC8325-4 *glvC* null mutant	3398	1799	This study
NCTCΔ*scrA*	NCTC8325-4 *scrA* null mutant	3113	1892	This study
NCTCΔ*glcA*Δ*nagA*	NCTC8325-4 *glcA*/*nagA* null mutant	-	-	This study
pMADΔ*glcA*	pMAD + *glcA* deletion fragment	-	-	This study
pMADΔ*murQ*	pMAD + *murQ* deletion fragment	-	-	This study
pMADΔ*murP*	pMAD + *murP* deletion fragment	-	-	This study
pMADΔ*ptsG*	pMAD + *ptsG* deletion fragment	-	-	This study
pMADΔ*treP*	pMAD + *treP* deletion fragment	-	-	This study
pMADΔ*nagA*	pMAD + *nagA* deletion fragment	-	-	This study
pMADΔ*oppA*	pMAD + *oppA* deletion fragment	-	-	This study
pMADΔ*oppBCDF*	pMAD + *oppBCDF* deletion fragment	-	-	This study
pMADΔ*oppABCDF*	pMAD + *oppABCDF* deletion fragment	-	-	This study
pMADΔ*ptaA*	pMAD + *ptaA* deletion fragment	-	-	This study
pMADΔ*glvC*	pMAD + *glvC* deletion fragment	-	-	This study
pMADΔ*scrA*	pMAD + *scrA* deletion fragment	-	-	This study
pMADΔ*glcB*	pMAD + *glcB* deletion fragment	-	-	This study

*Fragment size; Fragment size produced using integration primers (see Chapter 7 and Table A.2) to screen for the absence of the GOIs.

However, in *S. aureus*, the GlcNAc-specific PTS domain-containing PtaA, not GlcA, is the direct orthologue of the main GlcNAc transporter in *E. coli*, NagE (Table 2.1). A GlcA homologue also forms part of the putative PR machinery of *S. saprophyticus* (Figure 2.3), a fact that stands in opposition to the idea that GlcA is unique to *S. aureus* [474].

Alongside aminosugar recycling, *S. aureus* may have the capacity to recover stem peptide or muropeptide fragments via the OppABCDF system identified here (Figure 2.1, Figure 2.2), such as the dipeptide γ-D-Glu-L-Lys thought to be involved in β-lactamase induction in *S. aureus* [369]. *E. coli* OppBCDF form a general ABC oligopeptide transporter that functions with the muropeptide-specific SB protein MppA to recover PGN-derived tripeptides [301, 351, 352]. OppA of *S. aureus* may play a similar role, but it remains possible that PGN-derived peptides may not be specifically recovered in *S. aureus* and that OppA may function in more general oligopeptide recovery. Despite the lack of putative specific muropeptide permeases, the presence of SAOUHSC_00156 in *S. aureus* hints at the possibility that more complex fragments of PGN may be recovered by this bacterium. SAOUHSC_00156 contains a glycoside hydrolase domain, which suggests that this protein may function as a cytoplasmic hydrolase akin to AmpD or NagZ of *E. coli* [338, 339, 341]. When then reconsidering the potential function of OppA and OppBCDF, it seems that these proteins may possibly function together to recover MurNAc containing muropeptides. Indeed *opp* null mutants of *Shigella flexneri* have been shown to release anhMurNAc-pentapeptides, suggesting its involvement in their uptake [480], though it remains possible that a further unidentified transporter may also fill this role.

Taken together, this data paints a more complex picture of the putative PR capacity of *S. aureus* than previously established. Previous analysis has also revealed that the repertoire of putative CWR components varies largely from Genus to Genus in Gram-positive bacteria [294] as it does in Gram-negative bacteria [194], and new pathways for PR continue to be discovered as more non-model species are investigated [354, 355, 356, 357, 358]. Upon examination of other members of the Staphylococci, it became evident that the putative PR pathways of *S. aureus* are a more general feature of this genus, suggesting that all Staphylococci may potentially recycle PGN, though in different ways, and that these capabilities may well have evolved in a common ancestor inhabiting environments unlike that currently inhabited by *S. aureus*. Intriguingly, the lack of orthologues of MurQ and MurP and the presence of a true orthologue of MppA in *S. hominis* suggests that perhaps that this organism does not recycle MurNAc in monosaccharide form, but may perhaps recycle muropeptides [301, 351, 352, 480]. The presence in *S. saprophyticus* of an orthologue of *E.*

coli LdcA, a murein tetrapeptide CP [340], is similarly suggestive of muropeptide recovery capabilities.

Chapter 3

Vigour, morphology and aminosugar auxotrophy in putative *S. aureus* cell wall recycling mutants

3.1 *Introduction*

Despite the emerging possibility that Gram-positive bacteria might recover and/or recycle components of PGN, the components involved are largely unknown or uncharacterised and the putative functions of these processes are still enigmatic. In Gram-negative bacteria, recovery of PGN fragments during PR plays a major role in the induction of β-lactamase expression [338, 339], but may also play a role in signalling when to enter stationary phase [481], may provide nutrients to complete a final round of division while doing so [194], or may confer a survival advantage in environments where competition for nutrients is high [194]. In the case of pathogenic Gram-negative bacteria, PR also plays roles modulating host immune recognition [335, 482], release of cytotoxic muropeptides [483, 363], and in regulation of virulence [429]. PR may also play a role in the governance of symbiotic relationships where bacteria use muropeptide shedding to signal to the host [484, 485]. However, under standard laboratory conditions no *E. coli* PR mutants display a growth or morphological phenotype save for *ldcA* mutants which become ovoid and lyse during stationary phase [340, 481]. Indeed, it seems PR is largely non-essential for Gram-negative bacteria [194]. Some bacteria however, must acquire rather than synthesise essential PGN components. The Gram-negative, fastidious oral anaerobe *T. forsythia* is auxotrophic for the PGN aminosugar MurNAc and relies on muropeptide/MurNAc scavenging as a source of this aminosugar, using canonical PR proteins such as AmpG, MurQ and NagA as well as a novel MurNAc transport system to do so [358, 357].

Nevertheless, CWR components of Gram-positive bacteria also seem to be largely non-essential under standard laboratory conditions as large quantities of turnover product is often shed during normal vegetative growth [274, 288]. The current limited volume of published work on Gram-positive PR is inconclusive as to what its physiological roles may be, though it gives some clues. In *B. subtilis*, deletion of *nagZ*, a gene encoding one of two PGN hydrolases thought to be involved in muropeptide recovery, results in a drop in optical density in the stationary phase of growth [320]. Deletion of *murQ* from *S. aureus* and *B. subtilis* also results in a small difference in stationary phase cell viability [368]. Furthermore, while addition of exogenous MurNAc boosted wild-type *S. aureus* and *B. subtilis* stationary phase cell viability, the same effect was not observed in strains carrying the Δ*murQ* mutation [368]. These results are suggestive of a putative role of Gram-positive PR in maintaining bacterial viability when nutrients are limiting, such as during the prolonged stationary phase in which many natural bacterial communities likely exist [486, 487]. However, whether Gram-positive bacteria truly recycle PGN, or rather scavenge shed PGN-derived material from the extracellular milieu, is an open question.

Though there are now several papers reporting some degree of putative CWR component characterisation in *S. aureus* [471, 368, 474], at the outset of this study only *S. aureus* NagA had been implicated GlcNAc-6-P metabolism [471]. Thus, in order to identify which of the putative CWR components identified in Chapter 2 were most likely to be involved in *S. aureus* PR, and to get an idea of their possible importance in bacterial viability, a number of basic characterisations of their corresponding mutants were made. *S. aureus* mutants lacking putative CWR genes (putative cell wall recycling mutants; PCM's) were initially characterised in terms of their general vigour during growth, basic cell morphology and their ability to sustain growth when provided with the PGN aminosugars GlcNAc and MurNAc as the primary carbon source. These studies revealed several deficiencies in growth of these mutants on PGN aminosugars, though only small alterations to growth in rich media and no obvious morphological phenotypes. PCM's were also examined for their ability to grow in the presence of the antibiotic Streptozotocin, a GlcNAc analog, identifying one further potential route for GlcNAc uptake. A subset of mutants was selected based on the outcome of these experiments, and their stationary phase cell viability examined. However, this yielded no further information.

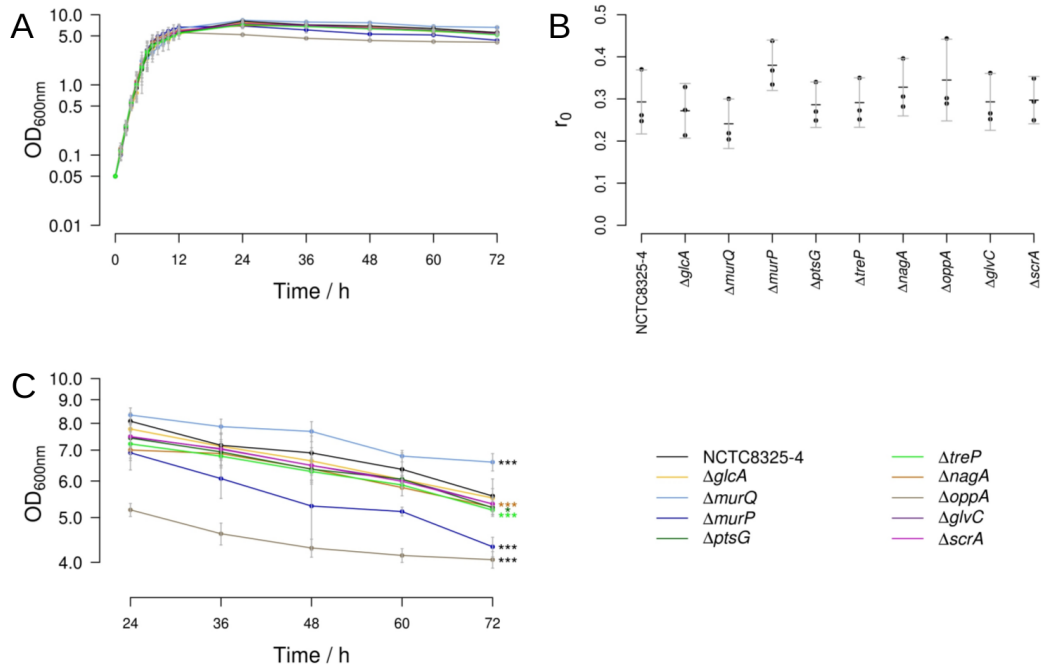


FIGURE 3.1: ***Growth of putative cell wall recycling mutants in rich media*** *NCTC8325-4 and PCM's were grown in tryptic soy broth (TSB) for 72h and optical density (OD_{600}) monitored (A). Maximal growth rates (r_0) were calculated from the growth profiles in panel A using the* `R` *package* `grofit` *(B). Panel C shows a magnified portion of the data from panel A, to better show differences in stationary phase OD_{600} values. Analyses for panel C were conducted on OD_{600} data from 24-72h to specifically examine stationary phase density dynamics. All data points (panels A, B and C) are representative of 3 independent biological replicates and error bars represent 95% confidence intervals. Significance levels; * $p < 0.05$, ** $p < 0.01$, *** $p < 0.001$. In panel C asterisks are representative of Dunnett's multiple comparisons (DMC's) between strains. Where strains were clustered close together, coloured asterisks were used to distinguish which significance levels belong to strains NCTCΔnagA, NCTCΔptsG and NCTCΔtreP. All strains were compared to the wild-type; NCTC8325-4.*

3.2 *Results*

3.2.1 Putative cell wall recycling mutants show little alteration in growth or morphology in rich media

S. aureus PCM's were examined for their general vigour by first analysing growth in rich media (tryptic soy broth; TSB). It should be noted here that in this thesis *S. aureus* were grown at at 30°C, rather than the usual 37°C, to keep *in vitro* and *in vivo* infection experiments consistent (See Chapter5 and Chapter 7). Using the `grofit` package for `R` [488, 489] maximal growth rate (r_0) was measured for each strain, but no alterations in r_0 of any mutant relative to NCTC8325-4 were observed (Analysis of variance (ANOVA); $F_{10,12} = 1.33$, $p = 0.277$, Figure 3.1). Analysis of OD_{600} data from 24-72h showed that all bacterial strains dropped in OD_{600} with time (ANOVA; $F_{1,153} = 744.26$, $p < 0.001$) and that differences in stationary phase density between strains were evident (ANOVA; $F_{10,153} = 93.87$, $p < 0.001$).

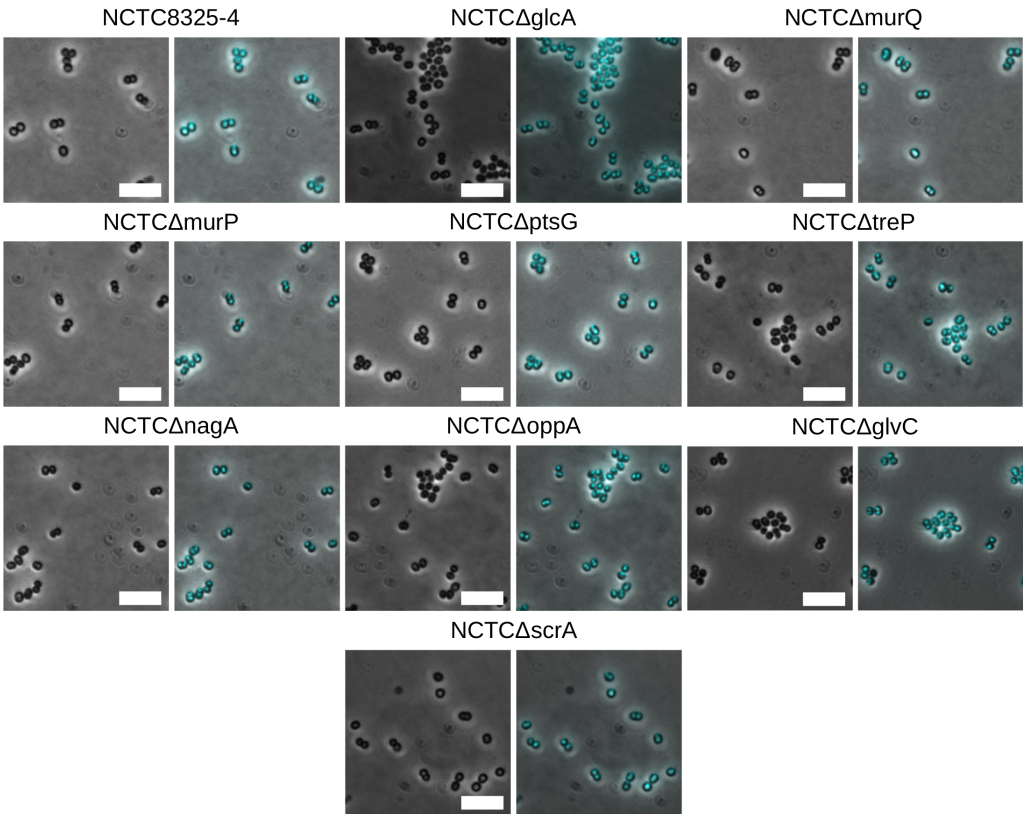


FIGURE 3.2: ***Putative cell wall recycling mutants show no obvious alteration to morphology.*** *NCTC8325-4 and PCM's were grown until an OD_{600} of 0.5 (mid-exponential phase), washed with phosphate-buffered saline (PBS) and imaged by wide-field microscopy on PBS-agarose slides. Left-hand panels for each mutant are phase-contrast images and right-hand-panels show hoechst staining overlaid. Representative images were chosen. Scale bars represent 5µm.*

Multiple comparison testing (DMC's) revealed that NCTCΔ*murQ* had an overall higher stationary phase OD_{600} than NCTC8325-4 and that NCTCΔ*nagA*, NCTCΔ*ptsG*, NCTCΔ*treP*, NCTCΔ*murP* and NCTCΔ*oppA* all exhibited lower overall stationary phase optical densities (Figure 3.1 C). However, though differing statistically, the magnitude of differences between NCTC8325-4 and NCTCΔ*nagA*, NCTCΔ*ptsG* and NCTCΔ*treP* were quite small. Overall, little major alteration to the growth profiles of PCM's was observed though some differences in stationary phase density were evident. Examination of exponential phase cell morphology by light microscopy also revealed no obvious differences in shape, size or clustering of any PCM's when grown in TSB when compared to NCTC8325-4, in keeping with the majority of studies of *E. coli* PR mutants [194]. It remains possible that alterations to morphology may occur in stationary phase, but this was not tested here.

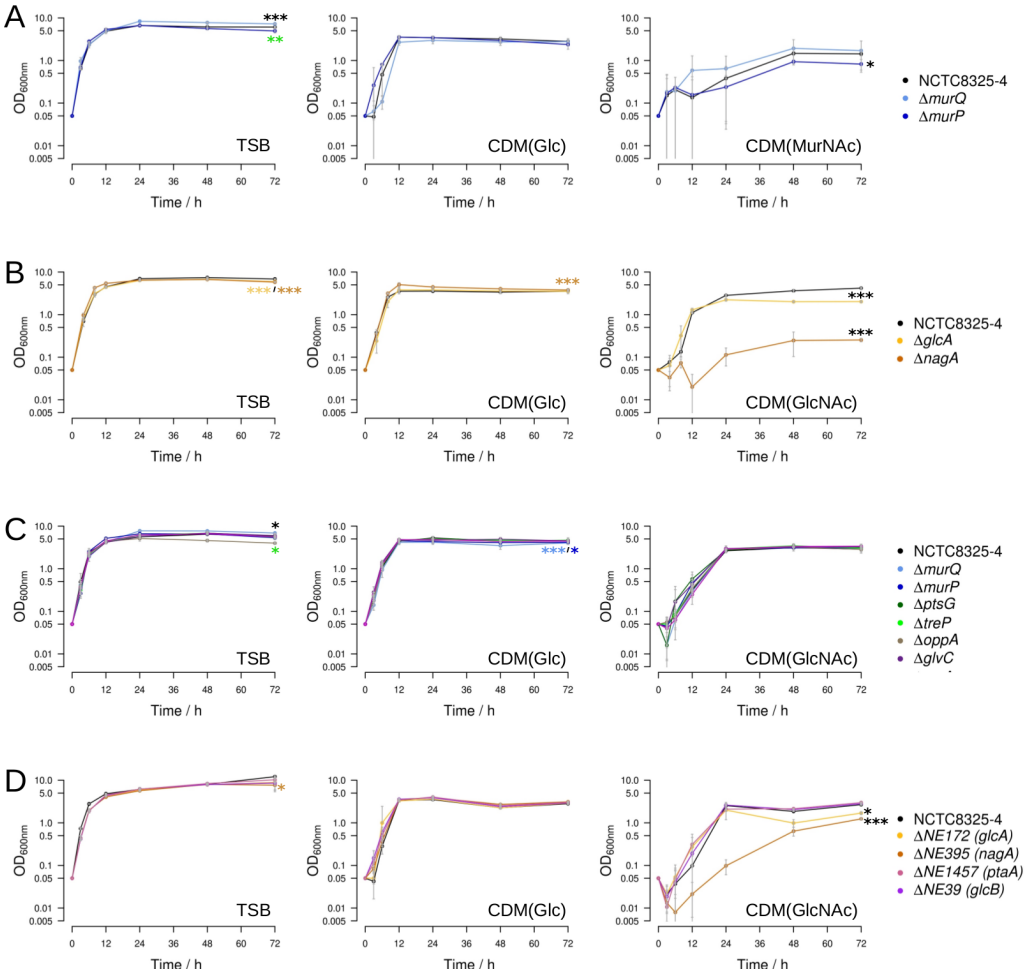


FIGURE 3.3: ***Growth of putative cell wall recycling mutants on cell wall aminosugars.*** *NCTC8325-4 and all PCM's were tested for growth in TSB, CDM containing glucose CDM(Glc) or CDM containing CW aminosugars (GlcNAc or MurNAc) for 72h and OD_{600} monitored (A-C). NCTC8325-4, NCTCΔmurQ and NCTCΔmurP were tested for growth on MurNAc (A). NCTC8325-4 and all PCM's were tested for growth on GlcNAc (B-C). As NCTC8325-4 deletion mutants for ptaA or glcB were unavailable to examine growth on GlcNAc, S. aureus USA300 JE2 NTIML mutants [490] (see Table A.4) with insertions in these genes were used instead (D). NTIML mutants containing transposons in glcA and nagA were also used to verify that phenotypes seen in NTIML mutants could recapitulate what is seen in NCTC8325-4 deletion mutants, and JE2 used as a reference strain (D). All JE2-derived strains were also examined for growth in TSB and CDM(Glc) (D). The maximal growth rates of mutants were again calculated using* `grofit` *[489] and the results of these analyses may be found in Table 3.1. As in Figure 3.1, stationary phase densities were also analysed (see Figure C.1 for an enlarged Figure), and asterisks are representative of the outcome of these analyses. All data points are representative of 3 independent biological replicates and error bars represent 95% confidence intervals. Variable low OD_{600} readings produced some negative errors bars that were trimmed at 0.005 as negative errors are not permissible on a logarithmic scale. Significance levels; * $p < 0.05$, ** $p < 0.01$, *** $p < 0.001$. Black asterisks denote DMC's comparing PCM's to their respective parental strain, and green asterisks denote orthogonal contrasts (OC's) representing interaction effects between time and strain, again relative to the parental strain. Where strains are clustered close together, the colours of the respective strains were used for asterisks (B; TSB and C; CDM(Glc)) and represent DMC's. Analyses of stationary phase OD_{600} were conducted on OD_{600} data from 24-72h to specifically examine stationary phase density dynamics, except for CDM(MurNAc), for which data from 48-72h was used. Glc, GlcNAc and MurNAc were supplied at 25mM. NTIML mutants (NEx) were grown in the presence of 25μg mL^{-1} Erythromycin, JE2 was not.*

TABLE 3.1: Mean maximum growth rates (r_0) of putative cell wall recycling mutants from Figure 3.3.

		TSB		G[1]		GN[2]		MN[3]	
Strain	**E[4]**	**r_0**	**± C.I.[5]**	**r_0**	**± C.I.[5]**	**r_0**	**± C.I.[5]**	**r_0**	**± C.I.[5]**
NCTC	A	0.143	0.0079	0.106	0.0047	-	-	0.0175	0.0019
8325-4	B	0.146	0.0011	0.128	0.0047	0.0638	0.0012	-	-
	C	0.137	0.0042	0.124	0.0098	0.0554	0.0011	-	-
Δ*glcA*	B	0.145	0.0068	0.126	0.0089	0.0634	0.0031	-	-
Δ*murQ*	A	0.145	0.0049	**0.0898****	0.0068	-	-	0.0230	0.0069
	C	0.136	0.00096	0.118	0.0071	0.0580	0.0015	-	-
Δ*murP*	A	0.152	0.0034	0.107	0.0022	-	-	**0.0108****	0.0014
	C	**0.149** *	0.0021	0.126	0.00091	0.0595	0.0059	-	-
Δ*ptsG*	C	0.138	0.0025	0.125	0.0087	0.0583	0.0022	-	-
Δ*treP*	C	0.137	0.0053	0.129	0.0030	0.0588	0.0049	-	-
Δ*nagA*	B	**0.161*****	0.0016	**0.150****	0.0046	**0.00575****	0.0016	-	-
Δ*oppA*	C	0.137	0.0043	0.128	0.0019	0.0580	0.0053	-	-
Δ*glvC*	C	0.133	0.0091	0.130	0.0052	0.0590	0.0056	-	-
Δ*scrA*	C	0.140	0.0055	0.128	0.0036	0.0580	0.00070	-	-
JE2	D	0.145	0.0029	0.104	0.0026	0.0525	0.0016	-	-
NE172	D	**0.133*****	0.0020	0.111	0.017	0.0475	0.0055	-	-
NE395	D	**0.131*****	0.0014	0.106	0.0036	**0.0163*****	0.0015	-	-
NE1457	D	**0.135*****	0.0037	0.106	0.0030	0.0488	0.013	-	-
NE39	D	**0.134*****	0.0016	0.108	0.0028	0.0548	0.0040	-	-

[1] G; Glucose, [2] GN; GlcNAc, [3] MN; MurNAc, [4] E; Experiment - corresponding to panels in Figure 3.3, [5] C.I.; 95% confidence interval. All data are representative of 3 independent biological replicates. Significance levels; * $p < 0.05$, ** $p < 0.01$, *** $p < 0.001$. Asterisks are representative of DMC's and all comparisons were made to NCTC8325-4 or JE2. Values significantly different to that of NCTC8325-4 / JE2 are marked in bold. Analyses were conducted for each medium within each experimental group. All r_0 values are given to 3 significant figures (S.F.) and 95% C.I's to 2 S.F's.

3.2.2 Putative cell wall recycling mutants display growth defects when supplied with cell wall amino sugars as the primary carbon source

As a first attempt to determine if any of the identified putative CWR components (Chapter 2) were involved in the uptake or metabolism of GlcNAc or MurNAc, the growth profiles of the available respective mutants was assessed when supplied with these aminosugars as the primary carbon source (Figure 3.3). In order to do so, a chemically defined medium (CDM) was employed (modified from [491], see Chapter 7) to enable manipulation of the composition of the growth medium. The ability of NCTC8325-4 and PCM's to grow in CDM with glucose (Glc) as the primary carbon source had already been established (data not shown), and as the central panels of Figure 3.3 show, they grew well and in similar fashion to when grown in TSB. r_0 and stationary phase OD_{600} characteristics of PCM's in TSB were similar to what was seen previously (Figure 3.1), though some mutants showed differences in r_0 (see Table 3.1) not previously observed, and NCTCΔ*glcA* showed a slightly lower stationary phase density than NCTC8325-4 (Figures 3.1 B and C.1 B). JE2 grew more

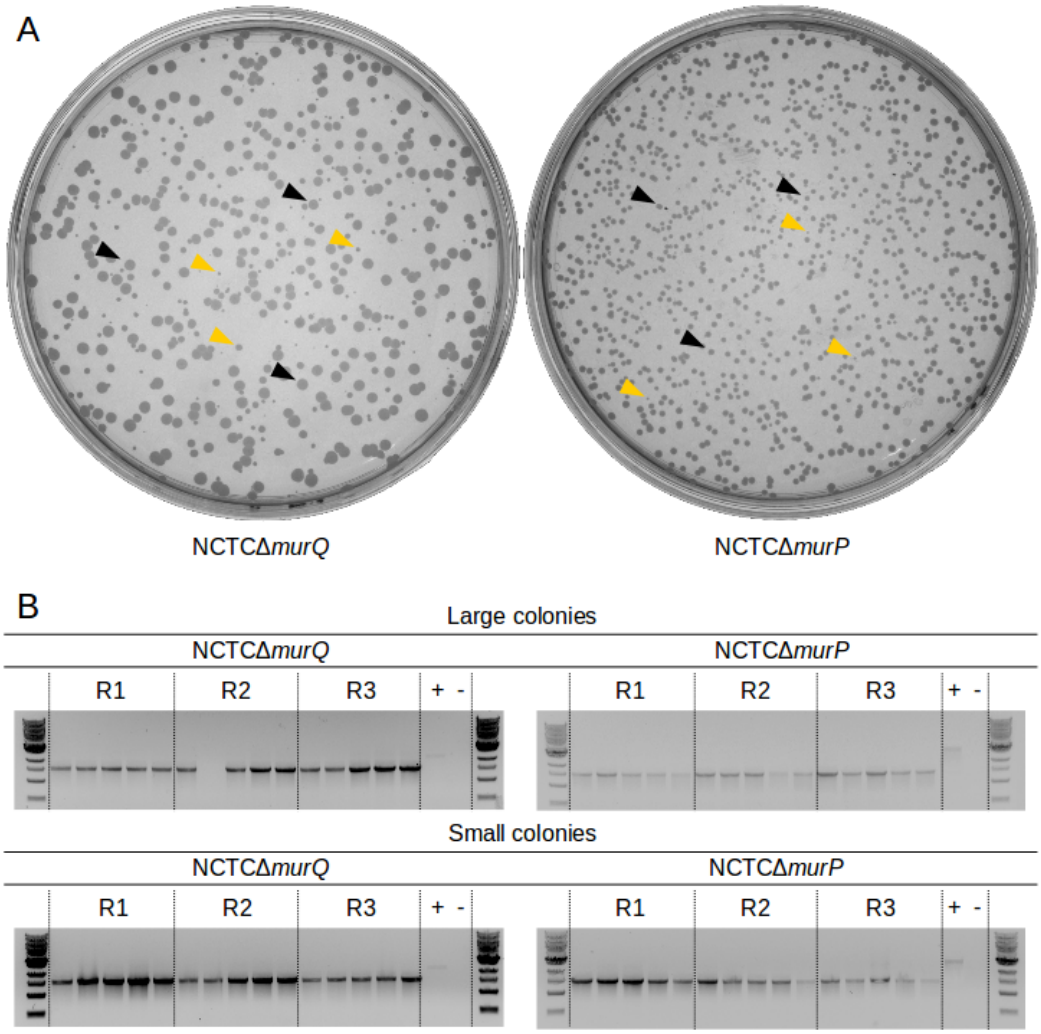


FIGURE 3.4: ***NCTCΔmurQ and NCTCΔmurP produce small colonies after growth in CDM(MurNAc).*** *72h cultures of NCTCΔmurQ and NCTCΔmurP grown in CDM(MurNAc) (Figure 3.3 A) were plated on tryptic soy agar (TSA) and incubated at 30°C for 24h before imaging (A). Colonies were then screened for the correct mutation by colony PCR (see Chapter 7) and products separated by agarose gel electrophoresis (AGE) (B). Colonies were screened using p1/p4 primers (see Chapter 7 and Table A.3, 5 per replicate; R1, R2, R3) and all contained the correct mutation except for one NCTCΔmurQ colony which DNA extraction likely failed (see Chapter 7) (B). Black arrowheads; large colonies, orange arrowheads; small colonies. +; NCTC8325-4 control, -; negative control. DNA ladders are shown either side of the bands of screened colonies, refer to Figure 2.5 for size markers.*

quickly than any of the NTIML mutants (Table 3.1) though this is almost certainly due to the fact that the NTIML mutants were grown with Erythromycin to maintain their transposon insertions [490] while JE2 is susceptible to Erythromycin and was not. NE395 (*nagA*) also showed a slightly lower stationary phase OD_{600} (Figures 3.1 D and C.1 D). Similarly, in CDM(Glc) some minor alterations to the growth rates of PCM's was observed (Table 3.1), as with stationary phase OD_{600} (Figures 3.3 and C.1). A full description of statistical output from these analyses and those from TSB is given in Table C.1.

When turning to the growth of mutants in CDM containing CW aminosugars, more obvious differences were apparent. NCTC8325-4, NCTCΔ*murQ* and NCTCΔ*murP* all showed long lag phases in CDM(MurNAc) as previously reported for *E. coli* [345]. However, NCTCΔ*murQ* appeared to show no growth defects when compared to NCTC8325-4 (Figure 3.3 A and Table 3.1) though assessment of this was difficult as the variation in OD_{600} readings was very high and growth of NCTCΔ*murQ* was particularly erratic (see C.I. in Table 3.1 and Figure 3.3 A). NCTCΔ*murP* however, displayed both a statistically significant decrease in r_0 (Analysis of Deviance (ANODE); ${\chi^2}_8^{strain}$ = 0.83, p < 0.001, see Table 3.1) and a lower stationary phase OD_{600} (ANOVA; ${F_{2,\,14}}^{strain}$ = 7.41, p < 0.01, see Figures 3.3 A and C.1 A). As these mutants were not expected to grow [368], 72h cultures of these cultures were plated on TSB to check the identity of the cultured strains. This revealed the presence of small colonies reminiscent of small colony variants (SCVs) of *S. aureus* [492] (Figure 3.4, A) not normally present when these mutants are grown on solid media (data not shown). The presence of the correct mutations in these colonies was confirmed by PCR (Figure 3.4, B).

Most of the PCM's showed no phenotype when grown on GlcNAc (Figure 3.3, C). Growth rates of mutants in CDM(GlcNAc) from panel C did not differ from that of NCTC8325-4 (ANODE; ${\chi^2}_7^{strain}$ = 0.0097, p = 0.91, Table 3.1), nor did stationary phase optical densities (ANOVA; ${F_{7,\,63}}^{strain}$ = 1.22, p = 0.31). However, NCTCΔ*glcA* displayed a considerably lower stationary phase OD_{600} relative to NCTC8325-4, as did NCTCΔ*nagA* (ANOVA; ${F_{2,\,23}}^{strain}$ = 289.13, p < 0.001, Figures 3.3 B C.1 B) when grown on GlcNAc. In the case of NCTCΔ*glcA* this appeared to be due to the continued increase of NCTC8325-4 OD_{600} while that of NCTCΔ*glcA* began to decline (ANOVA; ${F_{1,\,23}}^{time}$ = 8.60, p <0.01). In the case of NCTCΔ*nagA* however, this was due to a massively decreased growth rate in CDM(GlcNAc) (ANODE; ${\chi^2}_7^{strain}$ = 7.91, p < 0.001, Figure 3.3 B, Table 3.1). Deletion mutants for *ptaA* and *glcB*, two further PTS components potentially involved in GlcNAc uptake (Table 2.1), were unavailable. Thus, *S. aureus* JE2 (USA300) Nebraska Transposon Insertion Library (NTIML) mutants [490] for the corresponding genes (NE1457; *ptaA* and NE39; *glcB*) were used instead, comparing growth to JE2. NE172 and NE395, NTIML mutants containing transposons in *glcA* and *nagA* respectively were also included to establish whether phenotypes seen in the NCTC8325-4 background were comparable to those in a JE2 background. The phenotypes observed for NCTCΔ*glcA* and NCTCΔ*nagA* were mirrored in the growth rates (ANODE; ${\chi^2}_4^{strain}$ = 2.48, p < 0.001, Table 3.1) and stationary phase OD_{600} (ANODE; ${\chi^2}_4^{strain}$ = 15.6, p < 0.001, Figure 3.3 D) of the corresponding NTIML mutants. However, neither NE1457 or NE39 showed any growth defect on GlcNAc (Figure 3.3 D, Table 3.1).

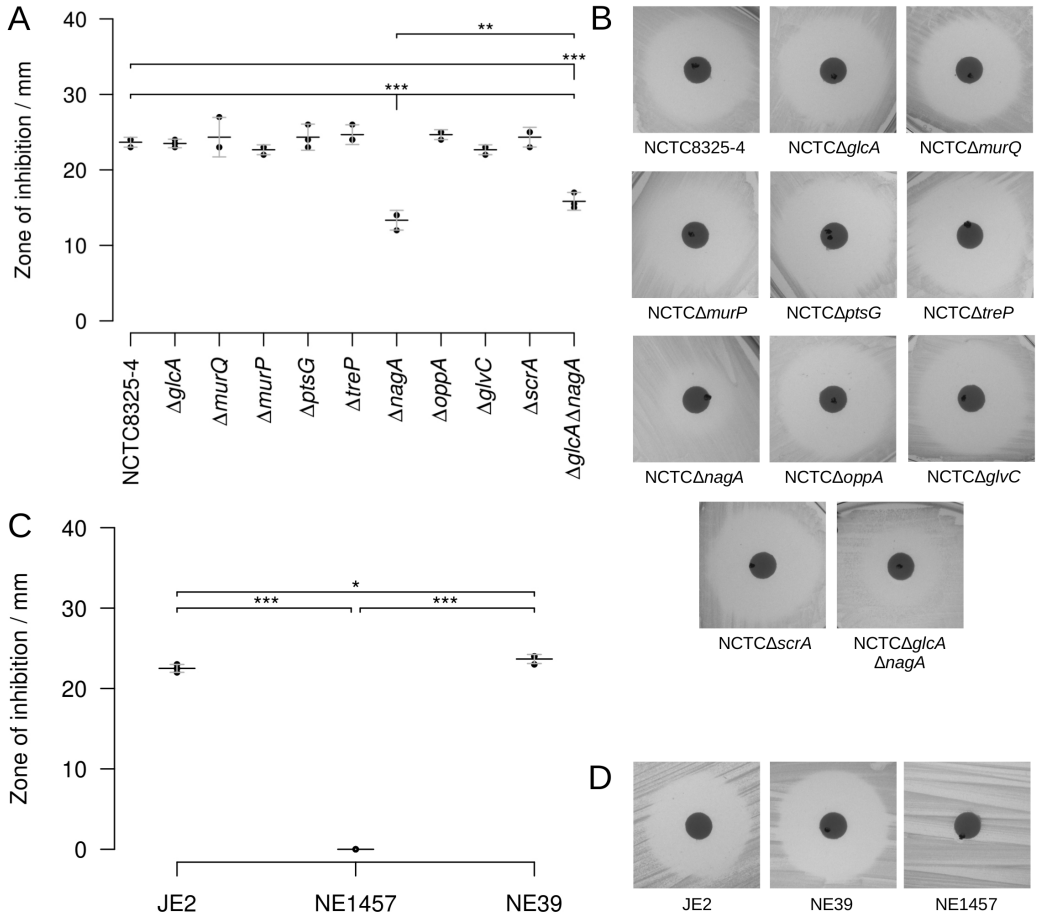


FIGURE 3.5: ***Streptozotocin resistance assays of putative cell wall recycling mutants.*** *NCTC8325-4 (A, B) and NTIML (C, D) PCM's were grown in the presence of Streptozotocin, a GlcNAc analogue and antibiotic [493, 494, 495], supplied on paper discs on TSA plates for 24h. Panels A and C are graphical representations of measured zones of inhibition, while panels B and D show corresponding images for panels A and C, respectively. Data are representative of 3 independent biological replicates and error bars represent 95% confidence intervals. Significance levels; * $p < 0.05$, ** $p< 0.01$, *** $p < 0.001$. Asterisks are representative of Tukey-Kramer multiple comparisons (TKMCs).*

3.2.3 PtaA is a possible second GlcNAc transporter in *S. aureus*

Despite the stationary phase growth phenotype of NCTCΔ*glcA* in CDM(GlcNAc) it is apparent that GlcA cannot be the only GlcNAc transporter in *S. aureus* as this mutant was still capable of growth. Furthermore, the closest orthologue of the *E. coli* GlcNAc transporter NagE in *S. aureus* is not GlcA, but PtaA (Table 2.1). To investigate further if any of the identified genes may fill this role, resistance to the antibiotic Streptozotocin was assessed via disc diffusion assay for all of the NCTC8325-4 PCM's and NTIML *ptaA* and *glcB* mutants, NE1457 and NE39. Streptozotocin (*N*-methyl-*N*-nitroso-acetyl-glucosamine) shares close structural analogy with GlcNAc and is taken up via unidentified PTS transporters of both Gram-negative and Gram-positive bacteria [493, 494, 495]. It was therefore hypothesised

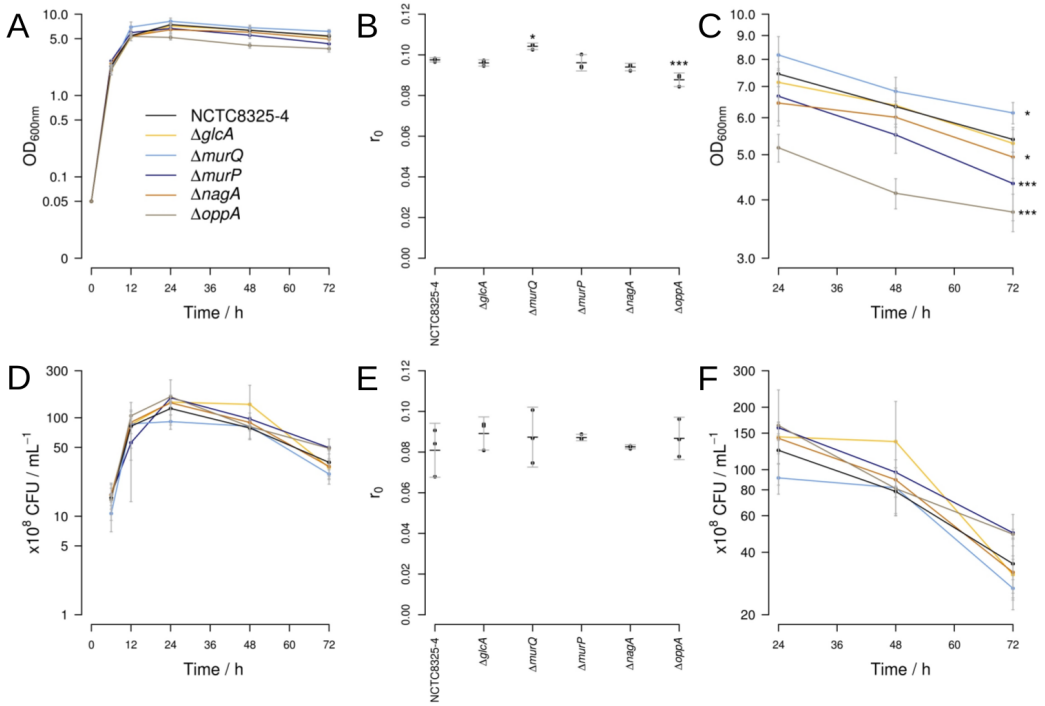


FIGURE 3.6: ***Optical density and colony forming unit growth profiles of putative cell wall recycling mutants.*** *NCTC8325-4 and PCM's were grown in TSB for 72h and both OD_{600} measurements (A, C) and viable CFU counts (D, F) were taken at several time-points by plating on TSA. r_0 values were calculated for both OD_{600} (B) and CFU (E) using* `grofit` *[489]. Data in all panels are representative of 3 independent biological replicates and error bars represent 95% confidence intervals. Significance levels; * $p < 0.05$, *** $p < 0.001$. In panels B and C asterisks are representative of Dunnett's multiple comparisons (DMC's) between strains. Panels C and F are magnified portions of the data from panels A and D, respectively, to better show differences in stationary phase OD_{600} values. Analyses for panels C and F were conducted on OD_{600} data from 24-72h to specifically examine stationary phase density dynamics.*

that mutants lacking functional PTS components normally used for the uptake of GlcNAc would show increased resistance to this antibiotic.

Several of the assayed mutants displayed resistance to Streptozotocin, but most spectacularly was NE1457 (*ptaA*) (Figure 3.5, C and D), suggesting that PtaA is in fact a GlcNAc transporter. This was confirmed statistically through analysis of the diameter of the zone of inhibition (ZOI) (ANOVA; $F_{2,6}{}^{strain} = 2745.6$, $p < 0.001$, Figure 3.5). Interestingly, both NCTCΔ*nagA* and the double mutant NCTCΔ*glcA*Δ*nagA* also showed decreased resistance to Streptozotocin (ANODE; $\chi^2{}_{11}{}^{strain} = 1.3102$, $p < 0.001$, Figure 3.5). NCTCΔ*glcA*Δ*nagA* also appeared to be slightly less resistant than NCTCΔ*nagA*.

3.2.4 Optical density but not viable cell counts of PR mutants is altered in extended stationary phase

As reported in a recent publication, Δ*murQ* mutants of both *S. aureus* and *B. subtilis* show a drop in viable colony forming units (CFUs) during prolonged stationary phase [368], and thus here it was decided to investigate if this was true of the PCM's generated in this study. Following the above assays, NCTCΔ*glcA*, NCTCΔ*murQ*, NCTCΔ*murP*, NCTCΔ*nagA* and NCTCΔ*oppA* were selected for analysis, based on their growth profiles in either TSB or CDM containing CW aminosugars (see Discussion 3.3). Some small alterations to r_0 calculated from OD_{600} values were observed (ANOVA; $F_{5, 12}{}^{strain} = 17.72$, $p < 0.001$, Figure 3.6 B) and differences in stationary phase density previously observed were evident (ANOVA; $F_{5, 47}{}^{strain} = 42.42$, $p < 0.001$, Figure 3.6 C). Here however, no difference in CFU r_0 (ANOVA; $F_{5, 12}{}^{strain} = 0.40$, $p = 0.84$) was evident when compared to NCTC8325-4, and though differences in stationary phase CFU counts were evident between some strains (ANODE; ${\chi^2}_{5}{}^{strain} = 1.11x10^{10}$, $p < 0.001$) no difference was observed between any of the PCM's and NCTC8325-4 (DMC's, Figure 3.6 F).

3.3 *Discussion*

At the outset of this study no characterisation of components potentially involved in uptake of PGN derived material had been made in any Gram-positive bacterium, though three cytoplasmic enzymes [471, 366, 367] and two PGN hydrolases [320] potentially involved in CWR in various species were already identified. Here, genetic evidence is presented suggesting the involvement of two PTS components in uptake of GlcNAc; GlcA and PtaA (Figures 3.3, C.1 and 3.5), and of the cytoplasmic enzyme NagA (Figure 3.3, Table 3.1) in its subsequent cytoplasmic processing as GlcNAc-6-P. Similar evidence is now published regarding GlcA [474], and NagA had previously been implicated in GlcNAc metabolism [471]. Evidence is also presented in this chapter suggesting the role of MurP in MurNAc uptake, consistent with published data [368], though is was less clear whether MurQ may be involved in processing of recovered MurNAc-6-P. However, it has now been established that this is the likely role of MurQ [368]. Though deletion of putative CWR genes was associated with growth defects of their respective mutants on CW aminosugars, there appeared to be only subtle effects on growth in TSB or CDM(Glc) (Figures 3.1 and 3.3). No difference in the exponential phase cell morphology (Figure 3.2) or ability to maintain viable cell counts in prolonged stationary phase of PCM's relative to NCTC8325-4 was observed (Figure 3.6).

It is now known that in the absence of *murQ*, MurNAc-6-P accumulates in the cytoplasm of *S. aureus*, and that in the concomitant absence of *murP* (along with *SAOUHSC_00156* and *murR*) such accumulation does not occur. This suggested that these were the only components responsible for MurNAc uptake and metabolism in *S. aureus* [368]. Here however, both NCTCΔ*murQ* and NCTCΔ*murP* were able to grow on MurNAc, suggesting contrary to the above study that these are not the only components able to recover and metabolise this aminosugar [368]. As other PTS component mutants were not tested for their growth on MurNAc here, it is not possible to say if one or more may complement the role of MurP, but they represent candidates for future study. It may also be possible that a non-PTS component-mediated route may be used for MurNAc recovery and metabolism, such as that employed by *T. forsythia* [358, 357].

Interestingly, although both NCTCΔ*murQ* and NCTCΔ*murP* grew, there appeared to have been some change to their physiology during culture in CDM(MurNAc), as signified by the presence of a sub-population of small colonies on plates grown from 72h CDM(MurNAc) cultures of these mutants. Such small colonies were not normally observed during growth of these mutants on solid media and were reminiscent of *S. aureus* SCV's, of which slow growth rate, atypical colony morphologies and unusual biochemical properties are characteristic [492]. The small colonies are likely indicative of a slower growth rate of the bacteria that produced them, a trait suggestive of altered metabolic activity or other pleiotropic effects of mutations selected for under the given growth conditions. At present, it is not possible to say what these potential alterations may be, but it seems that whatever bacteria may be using some mechanism to compensate for the loss of these components and that this may come at a cost. Thus, import and metabolism of MurNAc via MurP and MurQ likely represents the main, but not only, route for MurNAc recycling / uptake and metabolism [368]. Plating of NCTC8325-4 was however not performed and production of small colonies may be a more general effect of culturing *S. aureus* with MurNAc as the primary carbon source.

Data published during the course of this study similarly suggested that GlcA was the sole transporter of GlcNAc in *S. aureus*, due to the inability of the NTIML strain NE172 (*glcA*) to grow in a CDM containing GlcNAc as the primary carbon source [474]. The experiments in question were very similar to those presented here (Figure 3.3) and employed the one of the same strains (NE172) [474]. This same study reported that NE1457 (*ptaA* NTIML mutant) had no growth phenotype on GlcNAc [474], in agreement with the results in this Chapter. However, it was demonstrated here that both NCTCΔ*glcA* and NE172 (*glcA*) can grow with GlcNAc as the primary carbon source (Figure 3.3) and that PtaA is likely a

second GlcNAc transporter (Figure 3.5). The only major difference between CDM growth experiments performed in this study and that of Vitko *et al.* [474] was the temperature at which the assays were performed (30°C vs. 37°C). It may be that expression or activity of *ptaA* is temperature dependent. If PtaA were active only at the lower temperature of 30°C, this could explain the discrepancy between the data presented here and that of Vitko *et al*. The fact that the stationary phase optical density of NCTCΔ*glcA* and NE172 fell in CDM(GlcNAc) relative to that of their respective parental strains (Figure 3.3 B, D) also suggests that GlcA may be primarily active as a GlcNAc transporter during this growth phase, potentially working to complement primary GlcNAc uptake by PtaA. Indeed, GlcA is one of an expanded repertoire of glucose transporters [474], and during exponential phase is likely primarily involved in glucose uptake.

Streptozotocin resistance assays support this idea. Assays were made on bacteria growing exponentially on glucose-containing TSA in which NCTCΔ*glcA* and NE172 showed no resistance phenotype (i.e. took-up Streptozotocin, likely via PtaA) while NE1457 (*ptaA)* showed complete resistance (Figure 3.5). The Streptozotocin resistance assays also showed for the first time that Streptozotocin may interact with NagA, and were suggestive of a role of NagA in GlcNAc metabolism (Figure 3.5). This also suggests that in order for Streptozotocin to be fully active it may require processing by NagA, a facet of its mode of action not previously documented [494, 493, 495]. Why NCTCΔ*glcA*Δ*nagA* showed slightly decreased resistance to Streptozotocin when compared to NCTCΔ*nagA* is unclear, but may be due to increased transport activity of PtaA in compensation for GlcA's absence. Combined with the almost complete lack of growth of NCTCΔ*nagA* and NE395 (*nagA*) in CDM(GlcNAc), this suggests that NagA may be involved in GlcNAc metabolism as previously reported [471].

Despite demonstration that several of the assayed mutants exhibited growth defects when supplied with CW aminosugars all strains grew well in TSB with little or no alteration in maximum exponential phase growth rate (Figure 3.1, Figure 3.3, Table 3.1) or morphology (Figure 3.2). Furthermore, though several mutants displayed some alteration in their stationary phase optical densities when grown in TSB (Figure 3.1, Figure 3.3, Figure 3.6), this was not recapitulated in the number of viable cells in the culture. Indeed previous reports of this phenomenon in Gram-positive bacteria either did not examine cell viability [320] or reported only small differences in the number of viable cells found in stationary phase [368]. As the magnitudes of differences in TSB stationary phase optical density were not large, this may be potentially indicative of different sizes of cells present in stationary phase cultures rather than differences in viability. Mutants with lower optical density but the same number

of viable cells may be smaller overall and *vice versa*. Most mutants with altered stationary phase OD_{600} showed a drop in OD_{600}, particularly NCTCΔ*oppA* and NCTCΔ*murP*, which if indicative of smaller size would be consistent with a possible role of PR in supplementing carbon intake in nutrient poor environments as nutrient deprivation tends to produce smaller bacterial cells [194, 294, 268, 269]. However, NCTCΔ*murQ* showed consistently higher OD_{600} values, which may indicate larger cells in stationary phase cultures of this mutant, perhaps as a result of a weaker CW less able to withstand the internal turgor pressure of the cell. Unfortunately, data on the stationary phase morphology of cells was not obtained here to address this proposition.

No evidence was thus far found for the potential involvement of PtsG, TreP, GlvC or ScrA in aminosugar uptake, though testing was not exhaustive, nor were the respective mutants found to have any major alterations to growth or morphology. Thus, these mutants were excluded from stationary phase CFU analyses, and indeed further testing in this study. Despite identification of PtaA as a potential second GlcNAc transporter, this was also henceforth dropped from the study as no NCTC8325-4 *ptaA* deletion mutant was available, as was the case for *glcB*. However, although no assay of the possible function of OppA in peptide/ muropeptide uptake was made here, NCTCΔ*oppA* was retained for study due to its considerable and reproducible drop in stationary phase optical density characteristic of other PR/CWR mutants in various species [340, 481, 320] and as the only potential candidate involved in recycling non-aminosugar components of PGN (see Chapter 2). Finally, one major caveat of the results presented in this Chapter, and indeed the rest of this thesis, is that the PCM's generated and studied during the course of this study were not complemented. This means that the results obtained may also potentially be due to other mutations present in the generated strains rather than being attributable to the introduced mutation in question. However, given the agreement of results in this Chapter with the independent validation of the potential functions of GlcA [474], MurQ and MurP [368], and NagA [471], the results presented here regarding the potential functions of these components in PR / aminosugar recovery and metabolism seem relatively robust.

Chapter 4

NagA is a probable GlcNAc-6-P deacetylase and putative cell wall recycling mutants show possible cell wall ultrastructural alterations

4.1 *Introduction*

Bacterial cells are surrounded by a mesh-like network of PGN, the PGN sacculus [77, 59] which performs a number of vital functions [59]. Despite its importance the PGN sacculus is a highly dynamic structure which is constantly remodelled by PGN hydrolases as the cell grows and divides, resulting in PT [194, 74, 301, 302, 274, 288]. The Gram-negative PGN sacculus is enclosed by an OM which allows them to trap turnover products in the periplasmic space for recovery and re-use during PR [194, 294, 298]. Gram-positive bacteria on the other hand do not possess an outer membrane and thus cannot trap PGN fragments in the same way, though other surface structures present in Gram-positive bacteria might compensate for this to some extent [52, 294]. Gram-positive bacteria also possess a periplasm-like space, or IWZ in which fragments could be sequestered [47, 48]. However, many Gram-positive species shed large quantities of turnover products, alongside other CW components such as WTAs and CPS [288, 312, 300, 496, 497]. This would at first glance suggest that Gram-positive bacteria do not recycle PGN, or indeed other CW components. However, loss of up to 50% of the thick PGN layer found in the Gram-positive CW each generation would represent a considerable loss of resources [59, 294, 298] and in the case of pathogenic species such as *S. aureus* may also result in increased immune stimulation as PGN is a potent immune elicitor [498, 173]. It seems likely that PR might function in providing feedback to Gram-positive bacteria about the status of their CW as it does in Gram-negative species [338, 339, 429]. It is also known, albeit rarely, that alterations to PR may also have a direct impact on the CW PGN structure of Gram-negative bacteria.

Mutation of the cytoplasmic hydrolase LdcA of *E. coli* results in improper catabolism of recovered muropeptides, resulting in the accumulation of MurNAc-tetrapeptide which is then used by Mpl to form UDP-MurNAc-tetrapeptide [340]. This leads to the incorporation of MurNAc-tetrapeptide into PGN precursors instead of MurNAc-pentapeptide, which cannot be cross-linked to existing PGN. This results in reduced PGN cross-linking, loss of cell shape and lysis in the stationary phase of growth [340].

It is possible that past experimental conditions have not been favourable of Gram-positive PR [294], and it is also apparent that the mechanism by which PR may occur in Gram-positive bacteria varies considerably from species to species [320, 294, 366, 367, 370, 368, 334]) as does the rate of PGN fragment release [288, 274, 313, 312, 333, 334]. To date, it has been established that *S. aureus*, *B. subtilis* and *Streptomyces coelicolor* and able to recover and metabolise MurNAc recovered from the environment [368] (see also Chapter 3), that *B. subtilis* produces extracellular PGN hydrolases thought to be involved in muropeptide degradation prior to recovery [320] and that *C. acetobutylicum* possesses enzymes thought to be involved in recovery of deacetylated muropeptides or aminosugars [366, 367]. *S. aureus* GlcA, PtA and NagA have also been implicated in GlcNAc uptake (GlcA and PtaA) and metabolism (NagA) (Chapter 3, [474, 471]).

In Gram-negative bacteria impairment of PR or inactivation of PGN hydrolases results in increased rates of PGN fragment release [338, 339, 194] and/or release of different PGN fragment structures [364]. One of the original aims of this Chapter was to establish if those PCM's selected in Chapter 3 showed alteration to PGN turnover, to assess the potential influence of PR on determining extracellular turnover product shedding [234]. Unfortunately, due to unforeseen difficulties it was not possible to address this aim. However, further characterisation of PCM's was still undertaken. A second aim of this chapter was to establish more definitively what roles each of the selected putative CWR components might play in PR / PGN fragment recovery and metabolism, and how this may alter cytoplasmic recovery product accumulation. To this end, evidence supporting the role of NagA as a GlcNAc-6-P deacetylase was obtained and the proposition that GlcA plays little role in GlcNAc uptake during exponential phase was reaffirmed. Additionally, as disruption of PR in *E. coli* can also cause fatal abnormalities in the structure of CW PGN [340], preliminary assessments of CW PGN molecular structure and CW ultrastructure of the selected PCM's were made. This revealed little or no alteration in CW PGN molecular structure though some potential abnormalities in CW ultrastructural characteristics.

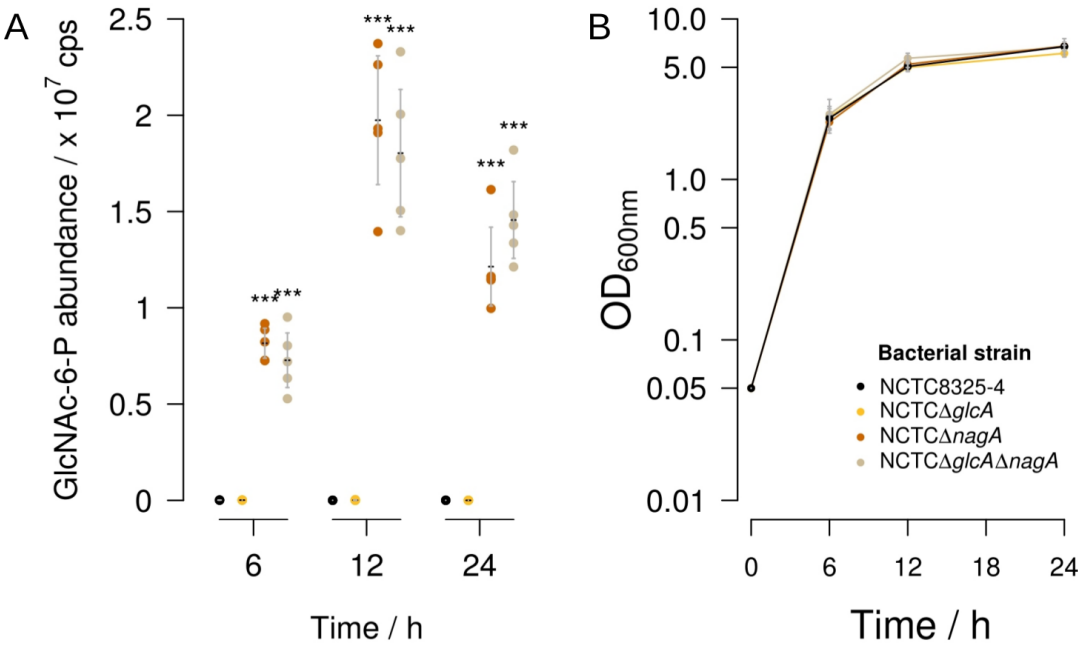


FIGURE 4.1: ***Profiling of cytoplasmic GlcNAc-6-P levels in putative cell wall recycling mutants implicated in GlcNAc uptake and reutilisation.*** *PCM's were grown in parallel in TSB and sampled at 6h (exponential phase), 12h (transition phase) and 24h (stationary phase) (B) before extraction of cytoplasmic content. Cytoplasmic metabolite content samples were standardised and subjected LC-MS/MS. GlcNAc-6-P peaks were identified using a standard profile generated using purified GlcNAc-6-P, allowing extraction of raw GlcNAc-6-P abundance data (A). Data are representative of 5 independent biological replicates and error bars represent 95% confidence intervals. Significance levels; *** $p < 0.001$. Asterisks in panel A are representative of TKMC's but here denote only the differences between the indicated strains and NCTC8325-4 and NCTCΔglcA. No statistically significant differences were found between NCTC8325-4 and NCTΔglcA or between NCTCΔnagA and NCTCΔglcAΔnagA. cps; counts per second.*

4.2 *Results*

4.2.1 NCTCΔ*nagA* and NCTCΔ*glcA*Δ*nagA* accumulate cytoplasmic GlcNAc-6-P

Given the observed growth and Streptozotocin resistance phenotypes of Δ*glcA*, Δ*nagA* and Δ*glcA*Δ*nagA* mutants (see Chapter 3) it was postulated that these putative CWR components were involved in GlcNAc uptake and its subsequent cytoplasmic processing as GlcNAc-6-P. Thus, examination of cytoplasmic GlcNAc-6-P levels of NCTC8325-4, NCTCΔ*glcA*, NCTCΔ*nagA* and NCTCΔ*glcA*Δ*nagA* was undertaken at the University of Oxford Chemistry Research Laboratory Mass Spectrometry Research Facility with the help of Prof. James McCullagh and Elisabete Pires.

Indeed it appears that deletion of *nagA* is associated with accumulation of GlcNAc-6-P in the cytoplasm (ANODE; ${\chi^2}_3{}^{strain}$ = 1789.79, p < 0.001, Figure 4.1 A), but deletion of *glcA* seems

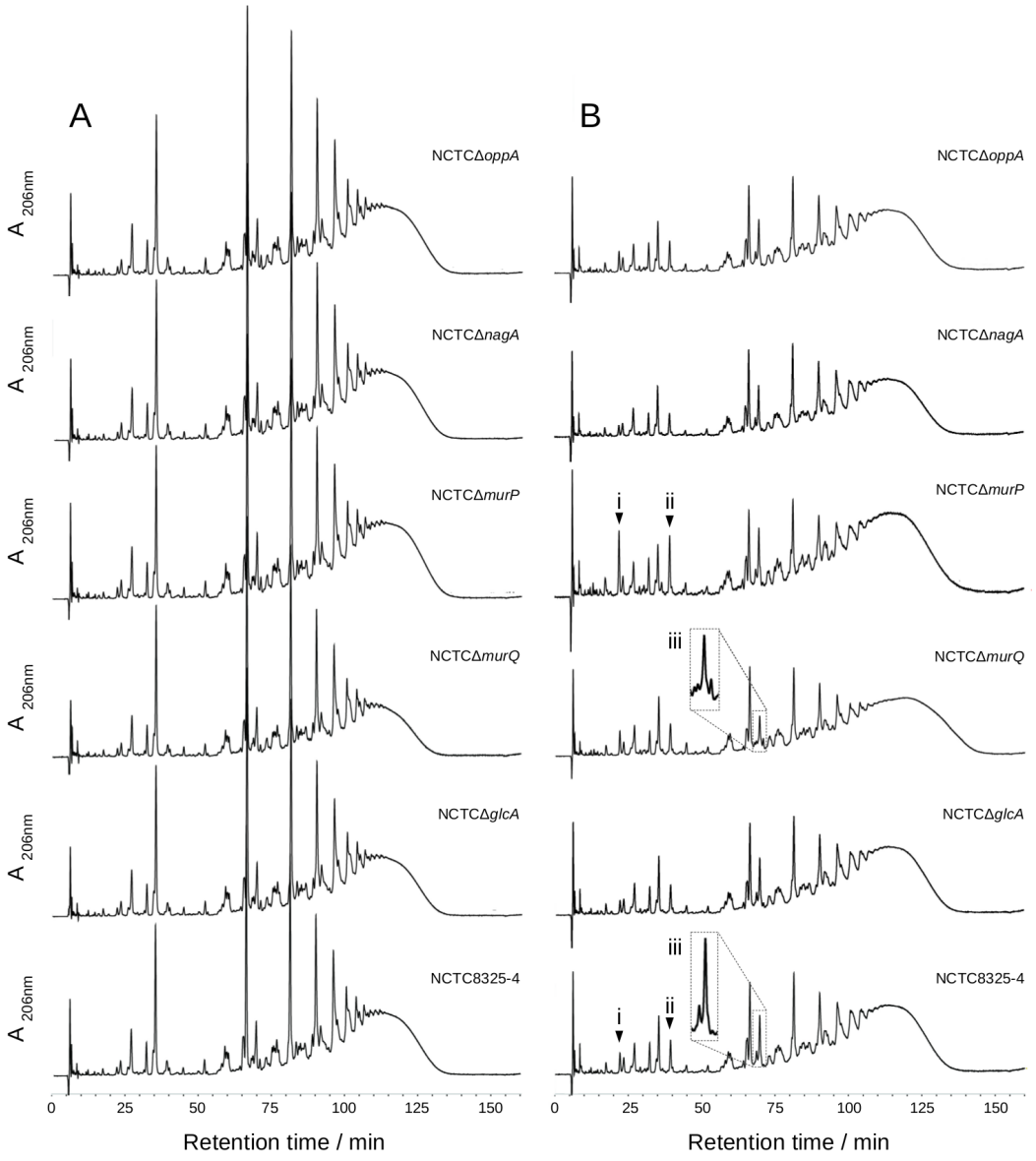


FIGURE 4.2: ***Cell wall peptidoglycan structure of putative cell wall recycling mutants.*** *PCM's were grown in parallel in TSB and sampled at 6h (exponential phase; A) and 24h (stationary phase; B) before purification of CW PGN. CW PGN structure was analysed by digesting purified PGN with Mutanolysin and subsequent analysis by RP-HPLC coupled with detection of analytes using UV radiation at 206nm (A_{206}). Peaks which appeared to be altered are labelled i-iii, with peak iii depicted in an inset. Corresponding peaks are also labeled in stationary phase NCTC8325-4 samples, and the reference chromatogram used for interpretation of profiles is supplied in Figure 4.3 (from [84, 85]). Data presented here are representative of a single biological replicate and all CWR mutant chromatograms are normalised to the abundance of the muropeptide dimer (peak 11 in Figure 4.3) of NCTC8325-4 in each respective growth phase.*

not to affect GlcNAc-6-P accumulation (Figure 4.1 A). Despite apparent blocking of GlcNAc-6-P metabolism in mutants lacking *nagA*, no effects on growth were observed in any PCM tested here (Figure 4.1, B, see also Chapter 3). Interestingly, GlcNAc-6-P accumulation began in exponential phase, unlike accumulation of MurNAc-6-P in *S. aureus* Δ*murQ* mutants [368]

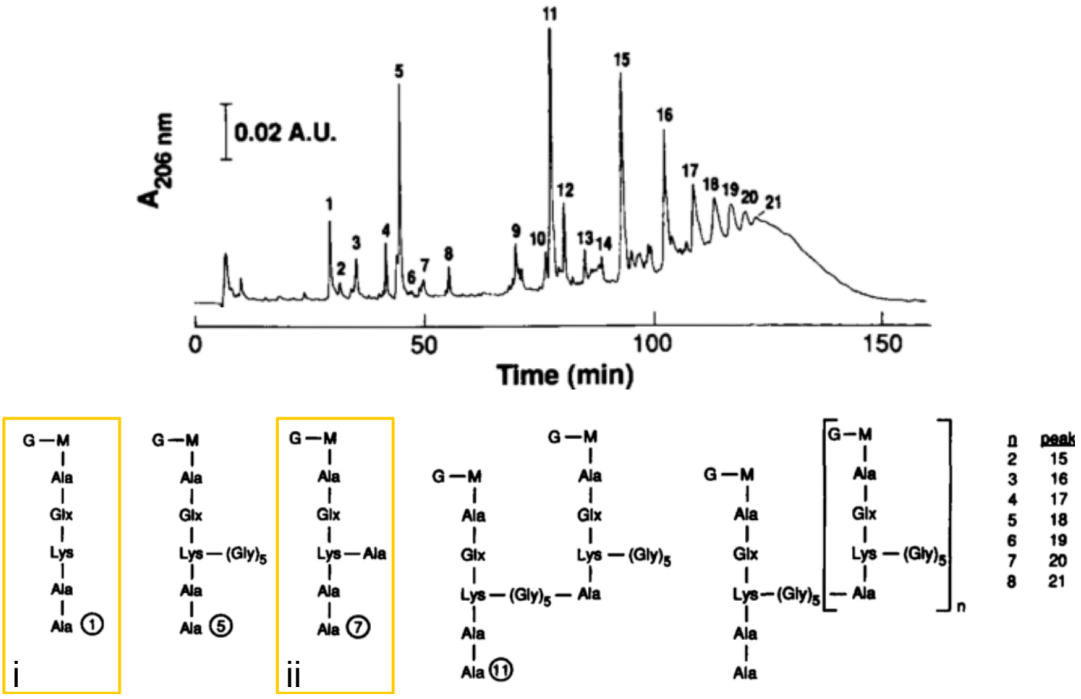


FIGURE 4.3: ***Reference S. aureus CW PGN chromatogram and muropeptide structures.*** *The above cell wall peptidoglycan chromatogram is derived from S. aureus COL (taken from [84, 85]) and was used to identify peaks in Figure 4.2. Peaks 1 and 7 correspond to peaks i and ii from Figure 4.2, respectively. Peak 5 represents the S. aureus muropeptide monomer (GlcNAc-MurNAc-pentapeptide-pentaglycine), peak 11 the muropeptide dimer, and peaks 15-21 various oligomers of the muropeptide monomer, as denoted in the bottom right of the figure.*

and appeared to decline slightly in stationary phase following a peak in transition phase (ANODE; $\chi^2{}_1{}^{time} = 8.68$, $p < 0.01$, Figure 4.1 A).

4.2.2 Preliminary experiments reveal no major alterations to putative cell wall recycling mutant CW PGN molecular structure

The exponential and stationary phase CW PGN structure of the selected *S. aureus* PCM's was assessed using Reverse-Phase High Performance Liquid Chromatography (RP-HPLC; Figure 4.2) [84, 85]. Overall, little alteration to the molecular structure of PCM CW PGN was observed, though some small alteration to satellite peaks was observed in the chromatograms of NCTCΔ*murQ* and NCTCΔ*murP* (see Figure 4.2 B, i-iii and Figure 4.3). These peaks represent the PGN monomer of *S. aureus* lacking the characteristic pentaglycine bridge (peak i), the alanyl derivative thereof (peak ii) and an unidentified peak (peak iii) that in NCTCΔ*murQ* appears to have been split into several smaller peaks.

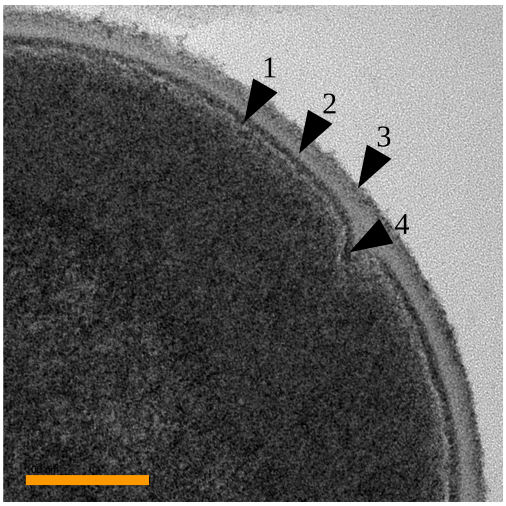


FIGURE 4.4: ***Ultrastructure of the S. aureus cell envelope.*** *Several differentially stained regions can be observed at the cell surface of S. aureus. (1) A heavily stained region immediately above the plasma-membrane represents the 'periplasmic-like space' or IWZ, (2) a much less intensely stained region outside of the IWZ represents the PGN sacculus, also containing proteins and other polysaccharide polymers (3) an outer heavily stained region composed of a dense layer of WTA and cell surface proteins though probably also some PGN. It is also possible to observe the beginning of membrane constriction in this cell (4). Layers were assigned their identity based on comparison with previously published data [47, 48, 499]. Scale bar; 200nm.*

4.2.3 Preliminary transmission electron microscopy experiments reveal putative differences in cell wall ultrastructure and septal morphology

Though some insight can be gained into the molecular structure of CW PGN by RP-HPLC analysis of purified PGN digests, this does not allow assessment of the ultrastructure of the CW. Thus analysis of CW ultrastructure in stationary phase (24h) cultures grown in TSB was examined by transmission electron microscopy (TEM). Fixation and imaging of samples was performed by Erin Johnson and Ana Pielach of the Dunn School EM facility, University of Oxford. A reference guide depicting the identities of CW layers is given in Figure 4.4. CW layer thicknesses quoted in Table 4.1 were measured using Fiji [500].

The most striking observation was that NCTCΔ*murQ* cells seemed to have thicker CW's than NCTC8325-4, attributable to a seemingly thicker, less well-stained PGN layer (Figure 4.5 Ci-Cx, Table 4.1). However, this was not true of all cells measured, and CW thickness was particularly variable between cells in this sample, as well as in the NCTC*δnagA* sample (Table 4.1). NCTCΔ*murQ* samples also contained a seemingly increased number of lysed cells when compared to NCTC8325-4 and the other CWR mutants (See Figure C.2), and what appeared to be abnormal nascent septa (Figure 4.5 Ciii, Civ, Cix). Abnormal-looking septa can also be observed in NCTCΔ*nagA* and NCTCΔ*oppA* (Figure 4.5 Ev, Evi, Evii, Eix and Fiv-Fviii, respectively). Both NCTCΔ*glcA* and NCTCΔ*murP* also seemed to show an increase in staining of the CW PGN layer (Table 4.1), while NCTCΔ*murP* samples also contained a seemingly increased number of cells in which poorly stained material seems to have accumulated at the inner surface of the plasma membrane (Figure 4.5D; blue arrowheads, Figure C.2). This same layer may be observed in NCTC8325-4 and all of the other mutants, as a thin pale layer directly beneath the IWZ (Figure 4.5, Figure C.2).

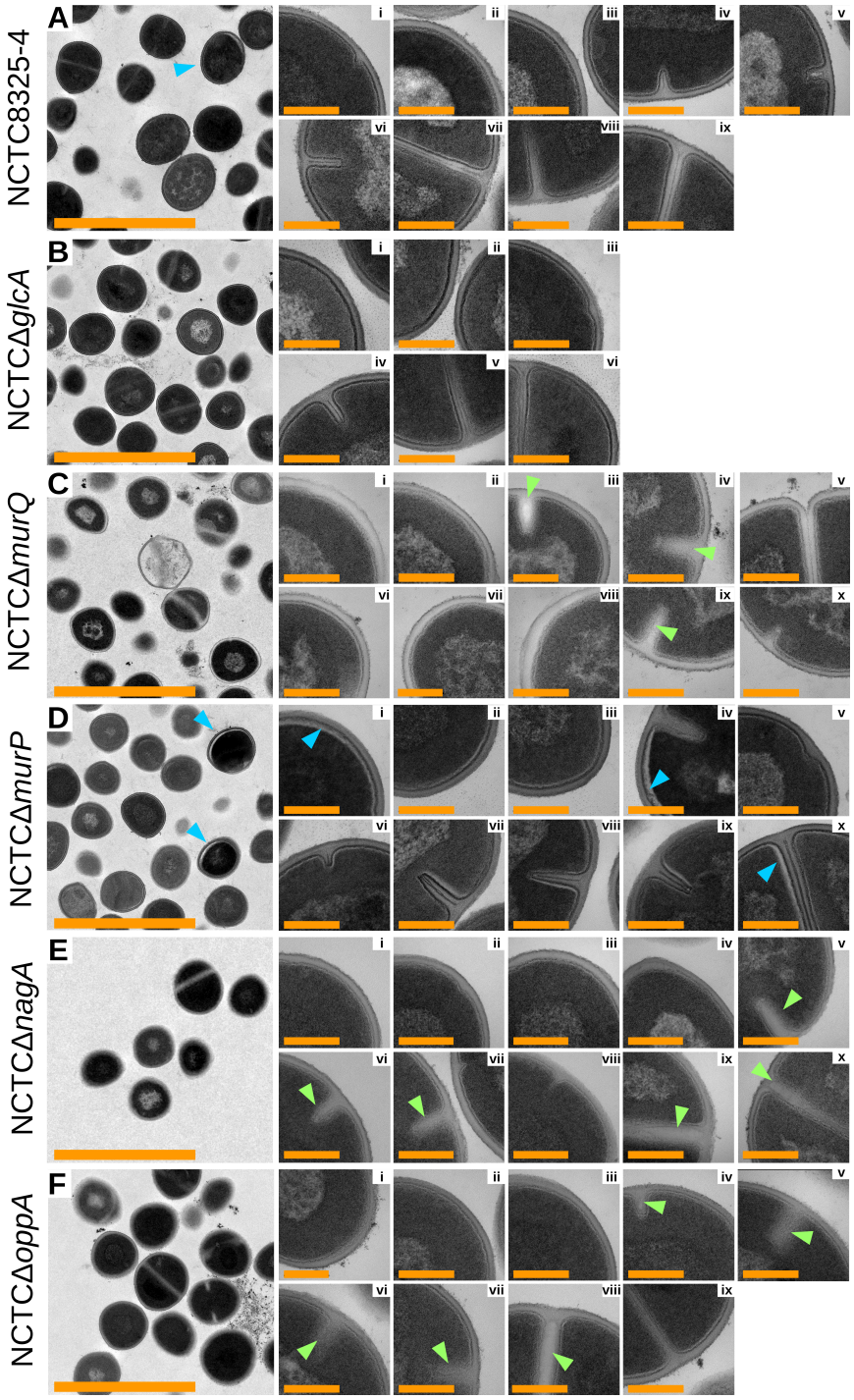


FIGURE 4.5: ***Cell wall ultrastructure of putative cell wall recycling mutants.*** *Bacteria were grown in TSB until stationary phase (24h), pelleted by centrifugation, fixed, stained and imaged using TEM. For identification of CW layers see Figure 4.4. The leftmost images of panels A-F show a small field of cells, and images i-x in each panel show high magnification images of single or dividing cells. Scale bars in the leftmost images represent 5µm, and in images i-x, 200nm. Green arrowheads indicate abnormal septa and blue arrowheads indicate accumulation of poorly stained material below the plasma membrane. Data presented here are representative of one biological replicate, and all high magnification images obtained are presented here. See Figure C.2 for larger images of cell fields. Measurements of mean CW layer thicknesses and staining intensity are given in Table 4.1.*

TABLE 4.1: Descriptive statistics of cell wall layer thicknesses and peptidoglycan layer staining measurements determined by electron microscopy (from Figure 4.5.)

Strain[2]	N[3]	Thickness / nm[1]							
		CW		SL[4]		PGN		PS[5]	
		$\bar{x}$	±C.I.	$\bar{x}$	±C.I.	$\bar{x}$	±C.I.	$\bar{x}$	±C.I.
NCTC	7	20.7	1.53	9.80	1.59	10.8	1.74	122	6.95
Δ*glcA*	6	20.8	1.70	10.4	1.80	10.1	1.63	108	4.36
Δ*murQ*	10	28.1	4.13	9.80	1.80	18.3	3.31	160	8.27
Δ*murP*	10	22.6	1.46	10.3	1.52	12.3	1.01	97.7	5.09
Δ*nagA*	10	21.5	3.02	7.89	1.69	13.6	2.36	126	6.88
Δ*oppA*	9	20.3	1.83	6.86	1.19	13.5	2.10	117	3.54

[1] $\bar{x}$; mean, C.I.; 95% confidence interval, [2] NCTC; NCTC8325-4, Δ*x*; NCTC8325-4 deletion mutants, [3] N; Number of cells per strain measured, [4] SL; surface layer, [5] PS; PGN layer staining, measured here as the image grey value (0-255). Lower values represent more intense staining. Data were obtained from the high magnification images of cells from Figure 4.5. See Figure 4.4 for CW layer identification.

4.3 *Discussion*

It is well established that many Gram-negative bacteria such as *E. coli* recycle their CW PGN, and that they do so efficiently [301, 302, 194, 298]. Released material trapped by the OM in the periplasm is recovered via a number of transporters [345, 344, 338, 339] and once inside the cytoplasm is processed by a well characterised series of catabolic enzymes [194] including the MurNAc-6-P etherase MurQ [346, 347] and the GlcNAc-6-P deacetylase NagA [501]. It has recently been demonstrated that *S. aureus* MurQ likely performs the same function as *E. coli* MurQ [368] and *S. aureus* NagA had previously been implicated in GlcNAc utilisation [471]. The accumulation of GlcNAc-6-P in the cytoplasm of Δ*nagA* mutants reported here (Figure 4.1) suggests that *S. aureus* NagA is most likely also a GlcNAc-6-P deacetylase. However, complementation of this mutation is required to confirm this result. The fact that GlcNAc-6-P did not accumulate to any lesser degree in the cytoplasm of NCTCΔ*glcA*Δ*nagA* however, suggests the contribution to the cytoplasmic pool of GlcNAc-6-P by GlcA under during exponential growth in rich media is rather limited (Figure 3.3 and 4.1). GlcNAC-6-P began to accumulate in Δ*nagA* mutants in exponential phase and seemed to fall in stationary phase, suggesting that unlike MurNAc [368] this sugar is not taken up primarily in stationary phase. This is is also consistent with the proposition put forward in Chapter 3 that PtaA may be involved in uptake of GlcNAc in the exponential phase of growth.

Disruption of PR in *E. coli* has been shown in one case to influence CW structure and integrity [340]. Thus, initial assessments were made of CW molecular structure (Figure 4.2) and

ultrastructure (Figure 4.5 and Table 4.1). Only single replicates of these experiments were performed, and thus conclusions that can be drawn from them are limited. However, even with only this data it appears that little influence on CW molecular structure is associated with the deletion of individual CWR genes (Figure 4.2). The only minor alterations that were observed were the increase of peaks corresponding to the PGN monomer lacking a pentaglycine bridge and its L-Lys-L-Ala derivative in NCTCΔ*murP* (Figures 4.2 and 4.3), similar to changes seen in *S. aureus* mutants of Fem proteins, required for the polymerisation of pentaglycine stems [85], or in *S. aureus* inhibited in glycine uptake from the medium [502]. NCTCΔ*murQ* also appeared to show alteration in the abundance one unidentified peak and the appearance of several other small peaks at nearby retention times (Figure 4.2). It is currently unknown what these tentative CW alterations may mean for CW properties and repetition of these assays along with complementation of strains would be required to confirm them, but it seems unlikely that such small alterations would have large phenotypic effects.

Examination of CW ultrastructure of all of the selected PCM's however, revealed some potentially interesting phenotypes, ranging from abnormal septal morphology in some strains, again reminiscent of *S. aureus* Fem protein mutants [503], to a less well-stained PGN layer of more variable thickness in NCTCΔ*murQ* (Figure 4.5). Though these data are only preliminary, they could be potentially interesting and warrant further investigation. For example, NCTCΔ*nagA* and NCTCΔ*murQ* seemed to show increased variation in the thickness of their CW's (Table 4.1), which may be indicative of a role of aminosugar metabolism in CW homeostasis i.e. regulation of CW thickness [504, 460, 505, 344]. It has also been suggested that MurNAc recovered by cells during stationary phase may stabilise the CW [368]. The counter-staining of these samples with lead citrate and uranyl acetate (see Chpater 7) stains structures containing proteins, DNA, lipid membranes and other compartments of the cytoplasm, along with anionic structures such as WTA [506, 507], leaving PGN unstained [47, 48, 90]. Thus the reduced staining of the PGN layer of NCTCΔ*murQ* may be interlinked with its increased thickness; stained proteins normally present it the CW may be more diffuse in a thicker PGN layer. It also appeared that NCTCΔ*murQ* cultures contained an increased number of lysed cells (Figure 4.5, Figure C.2), an interesting observation in light of the report that at least one *S. aureus* Δ*murQ* mutant and a *B. subtilis* Δ*murQ* mutant appear to show reduced stationary phase viability [368]. When turning our attention to the abnormal septa observed, particularly in NCTCΔ*nagA* and NCTCΔ*oppA* samples, the swollen appearance of these septa is suggestive of possible

unrecovered turnover product accumulation in the MLZ of the SCW [90]. The seeming accumulation of poorly stained material beneath the membrane of some NCTCΔ*murP* cells does not offer such straightforward possible interpretations, though PGN-derived material is poorly stained during the TEM preparation used here (see Chapter 7), and this material may perhaps represent accumulation of PGN precursors at the inner surface of the plasma membrane. However, it is difficult to say whether these alterations are characteristic of these strains as this experiment was only performed once and complemented strains were unavailable. In short, these data are suggestive of potentially interesting effects of disruption of CWR or aminosugar metabolism on CW ultrastructural properties but little more can be said with certainty at this stage.

Chapter 5

Putative roles for cell wall recycling and extracellular PGN degradation in *S. aureus* host-pathogen interaction

5.1 *Introduction*

Alongside roles in determining cell shape and in protecting the cell from environmental challenges, the structure and composition of CW PGN plays a role in the ability of pathogenic bacteria to cause infection [508, 173]. Many modifications to the PGN are involved in the ability of pathogenic species to resist the hydrolytic activity of lysozyme [509, 181, 510], or to resist killing by host immune cells [511]. However, PGN may also be viewed as an 'Achilles heel' of many pathogenic bacteria in that it is both essential for the bacterium but also a potent pathogen associated molecular pattern (PAMP), well recognised by a multitude of host pattern recognition receptors (PRRs) [512, 498, 373, 513]. PGN may be recognised at the bacterial cell surface in Gram-positive bacteria [457, 293], or as soluble fragments of PGN released by either bacterial or host lytic enzymes [480, 514]. PRR's recognising PGN include the LysM domain proteins of plants [415], intracellular NOD receptors and hexokinase of mammals [391, 390, 390, 396, 404], and the peptidoglycan recognition proteins (PGRPs) of many taxa ranging from insects to mammals [399].

Bacteria in turn have evolved ways of evading host immune recognition. The OM of Gram-negative bacteria shields the PGN sacculus from host PRRs, but in Gram-positive bacteria, this outer membrane is absent. Instead, Gram-positives employ CW-anchored glycopolymers such as WTAs that cover the outer surface of the cell and can interfere with recognition of PGN [457]. Furthermore, autolytic enzymes such as the major autolysins of *S. aureus* and *S. pneumoniae*, may trim PGN strands protruding from the bacterial cell surface to

prevent binding by host PRRs [292, 293]. However, material trimmed from the cell surface may be subsequently recognised by circulating host PRRs, as may material shed during CW turnover. Most Gram-negative bacteria are able to efficiently recover and recycle released PGN fragments [194], hiding them from the innate immune system [480]. However, some Gram-negative bacteria such as *Neisseria* spp. and *B. pertussis* shed immunostimulatory PGN fragments during bacterial growth, apparently to their advantage [362, 363, 337], though may also alter the quantity and nature of such fragments through modulation of PGN hydrolase activity and the efficiency of fragment recovery during PR [364, 363, 337]. PR has also been directly implicated in regulating the virulence of the Gram-negative *S. typhimurium* through accumulation of recovered turnover products its cytoplasm [429].

It seems possible that other bacteria such as *S. aureus* may utilise similar strategies to modulate PGN shedding or modify the nature of shed fragments, or that products recovered during PR may affect the physiology of *S. aureus* in ways relevant to infection. Indeed, *S. aureus* Δ*atl* mutants demonstrate drastically reduced PGN turnover [324], and during the release of Staphylococcal protein A (SpA) from the CW, Atl and other PGN hydrolases trim its PGN anchor, likely to reduce its immunostimulatory capacity [322]. Other Gram-positive species such as *S. pneumoniae* shed almost no PGN-derived material despite demonstrating autolytic activity [333], either as a result of lower turnover or efficient fragment recovery [334]. However, *S. aureus* turnover products stimulate hyphal formation by cohabiting *C. albicans*, facilitating tissue invasion by *S. aureus* [426]. Thus shedding of PGN fragments may be of advantage in some situations, but not others, and modulation of PGN hydrolase activity or PGN recovery during PR may allow regulation of fragment shedding. Intriguingly, MurR, encoded by a gene located in an operon with *SAOUHSC_00156*, *murQ* and *murP* (Chapter 2) is also involved in regulation of virulence in *S. aureus* [472]. However, as with all aspects of putative Gram-positive PR, potential roles of PGN fragment recovery and reutilisation in host-pathogen interaction are little explored.

Drosophila melanogaster, the fruit fly, has proven useful in studying the role of PGN recognition in *S. aureus* pathogenesis [447, 458, 457, 293], and recognises Gram-positive bacteria using the PRRs PGRP-SA, PGRP-SD and GNBP1 to recognise of a variety of Gram-positive PGN structures [445, 452, 446]. Recognition of Gram-positive bacteria by PGRP-SA then stimulates the Toll-cascade immune signalling pathway, a pathway highly homologous to that of the TLR/IL-1 pathways of mammals [454, 385]. This culminates in the production of Drosomycin, an AMP responsible for the clearance of Gram-positive bacteria [445, 420]. *D. melanogaster* is also a versatile and tractable animal model for the study of *S. aureus* virulence

[432, 39, 433]. However, some limitations to this infection model exist, largely relating to the fact that *D. melanogaster* is not a natural host of *S. aureus*. Some known determinants of *S. aureus* virulence in mammals do not affect virulence in *D. melanogaster* [432]. Additionally, although the PGN monomer of *S. aureus*, a natural ligand for mammalian NOD2 [397], is bound by *D. melanogaster* PGRP-SA, PGRP-SA-dependent immune responses are only stimulated by dimeric or larger muropeptide fragments [447].

In order to obtain a preliminary understanding of how CWR *S. aureus* may influence host-pathogen interaction, *D. melanogaster* flies were infected with the PCM's selected in Chapter 3 identifying alterations to virulence in 3 of the 5 assayed mutants, though this did not appear to depend on the presence of PGRP-SA. Binding of PGRP-SA to the bacterial cell surface and *in vivo* assays of immune stimulation by spent culture supernatants revealed that recognition of these PCM's by the *Drosophila* immune system was seemingly unaltered. However, during these experiments it became apparent that NCTCΔ*atl* spent culture supernatant stimulated the *Drosophila* immune system in a PGRP-SA dependent manner, tentatively suggesting that degradation of released PGN fragments rather than recovery of released material is most important for evasion of PGN fragment recognition in *S. aureus*. Preliminary assessments of virulence factor production by PCM's also identified possible roles of MurNAc recovery and metabolism in the production of haemolysins, and may be indicative of a regulatory role of MurNAc-6-P in virulence.

5.2 *Results*

5.2.1 Putative cell wall recycling mutants do not differentially bind mCherry::PGRP-SA at the cell surface

In order to first determine whether CWR mutants may be differently recognised at the cell surface by *D. melanogaster* PGRP-SA, bacterial cells from 18h cultures were washed with PBS and incubated with fluorescently-tagged mCherry::PGRP-SA (Figure 5.1, mCherry::PGRP-SA purified by Gonçalo Covas). mCherry::PGRP-SA did not bind differentially to the surface of any PCM when compared to NCTC8325-4 (Figure 5.1), though it bound strongly to the surface of NCTCΔ*atl* as previously reported [293].

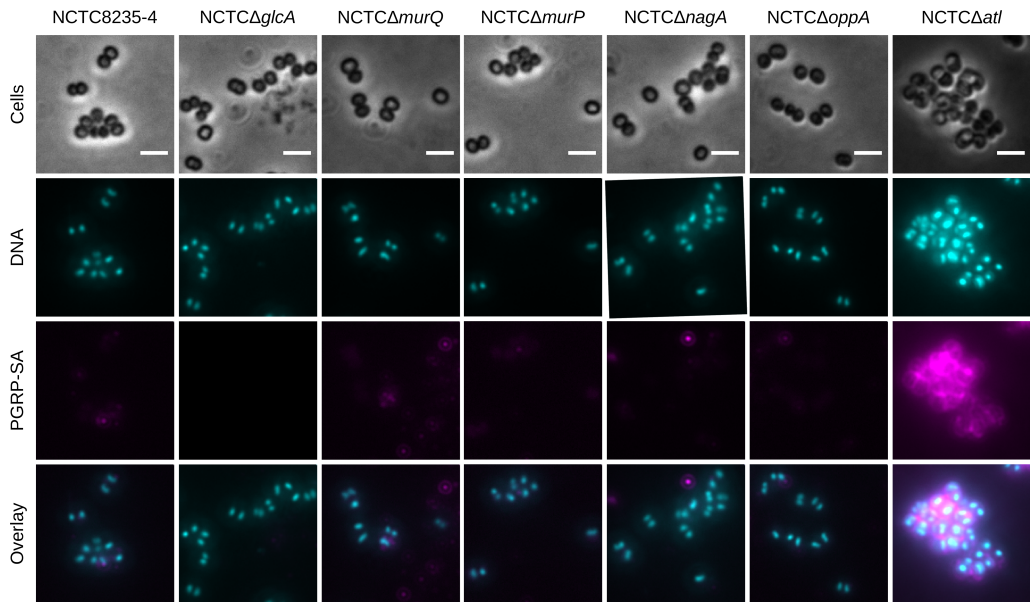


FIGURE 5.1: ***PGRP-SA binding to the surface of putative cell wall recycling mutants.*** *Bacteria were grown in TSB up to an OD_{600} of 0.5 (exponential phase), washed in PBS and incubated with mCherry::PGRP-SA before imaging on a widefield microscope. DNA is labelled with hoechst, and cells imaged in phase contrast. NCTCΔatl was included as a positive control known to bind mCherry::PGRP-SA strongly at the cell surface [293]. Scale bars represent 2µm.*

5.2.2 NCTCΔ*atl* spent supernatant, but not that of putative cell wall recycling mutants stimulates a PGRP-SA dependent immune response

In order to determine if turnover products of PCM's stimulated the *D. melanogaster* immune response differentially to NCTC8325-4 spent culture supernatants from overnight (18h) bacterial cultures were injected into *DD1* and *DD1*^{seml} flies. Spent culture supernatant of NCTCΔ*atl* was originally injected as a negative control, as *S. aureus* Atl mutants exhibit drastically reduced CW turnover [324]. As *DD1* flies contain a *drosomycin-gfp* (*drs-gfp*) reporter fusion construct [445], GFP signal from the bodies of the flies may be used a read-out of increased Drosomycin production and hence recognition of PGN by PGRP-SA [445]. *DD1*^{seml} flies possess a C80Y mutation in PGRP-SA, rendering it ineffective in recognising PGN [445] and thus should not produce Drosomycin in response to injection of Gram-positive PGN-derived material. Spent culture supernatant from PCM's did not stimulate increased Drosomycin::GFP signal relative to NCTC8325-4 in either *DD1* or *DD1* ^{seml} flies, but surprisingly, spent supernatant of NCTCΔ*atl* did in *DD1* flies (ANOVA; $F_{7,32}^{strain*fly_line}$ = 2.39, p = 0.044, Figure 5.2). This result was then confirmed by measurement of *drs* mRNA levels using qRT-PCR, again showing that NCTCΔ*atl* spent supernatant stimulated Toll-cascade activation in a functional-PGRP-SA-dependent manner (Figure 5.2, ANOVA; $F_{1,12}^{strain*fly_line}$ = 7.8936, p = 0.016).

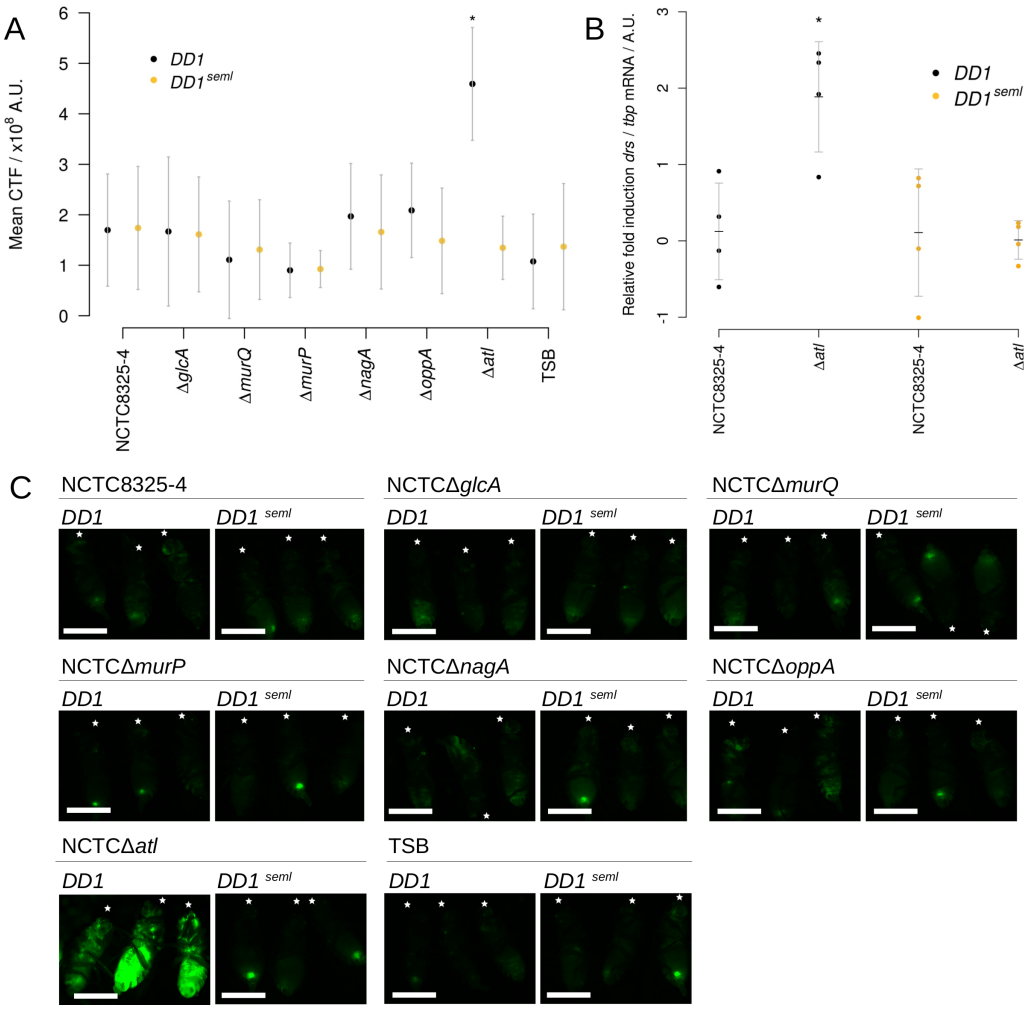


FIGURE 5.2: ***Drosomycin::GFP production in DD1 flies upon injection with spent culture supernatant of putative cell wall recycling mutants and NCTCΔatl.*** *NCTC8325-4, PCM's and NCTCΔatl were grown overnight (18h) in TSB before spent culture supernatants were collected, filter-sterilised and injected into D. melanogaster DD1 or DD1^{seml} flies (see text). TSB and 18h spent culture supernatant of NCTCΔatl were injected as negative controls. Drosomycin::GFP fluorescence was then quantified as mean corrected total fluorescence per fly (CTF, see Chapter 7) after incubation of injected flies at 30°C for 18h (A). In a separate experiment, flies were injected with NCTC8325-4 and NCTCΔatl spent supernatant as before, and drs mRNA levels quantified by qRT-PCR, relative to TSB-injected controls (B). qRT-PCR data are presented as Box-Cox [515] transformed data, and TATA-box binding protein mRNA (tbp) was used as an internal control. Representative wide-field microscopy images are shown in panel C and white stars in each image are placed by the heads of imaged flies. Mean CTF was calculated from fluorescence measurements of at least 3 flies per replicate (6 flies on average), and data points are representative of 3 independent biological replicates. Error bars represent 95% confidence intervals. Significance levels; * $p < 0.05$. The asterisks in panels A and B are representative of orthogonal contrasts. Bright spots of GFP are observed in the abdomen of some flies due to expression of drs in their ovaries (B). Scale bars represent 2mm. A.U.; abitrary units.*

5.2.3 Putative cell wall recycling mutants are impaired in virulence in *D. melanogaster* but *in vivo* bacterial growth is unaltered

In order to discern whether any PCM's might show altered virulence, the model host *D. melanogaster* was infected with each of these strains, alongside NCTCΔ*atl* and NCTC8325-4.

NCTCΔ*atl* was included as a control known to be impaired in its virulence in *D. melanogaster* due to its increased cell surface recognition by PGRP-SA [458, 293]. Bacteria were introduced via pulled glass capillary into the haemocoel (body cavity) of the wild-type (*25174*) and *25174*^{seml}) mutant flies (the latter produced by Dr. Magda Atilano), at an initial titre of ~100-200 colony forming units (CFU) per fly (Figure C.3). *25174*^{seml} flies do not possess functional PGRP-SA due to the same C80Y mutation present in *DD1*^{seml} flies [445]. Survival of infected flies was then monitored every 12h for 72h, and the number of surviving flies recorded. Both NCTCΔ*glcA* and NCTCΔ*oppA* killed infected 25174 flies more rapidly than NCTC8325-4, whereas NCTCΔ*murP* and NCTCΔ*atl* were impaired in virulence ($\chi^2{}_7{}^{strain}$ = 611.39, $p < 0.001$, see Figure 5.3, A for individual contrasts). Similar results were observed in 25174^{seml} flies (ANODE; $\chi^2{}_7{}^{strain}$ = 740.51, $p < 0.001$) though NCTCΔ*oppA* survival curves were statistically inseparable from NCTC8325-4 in 25174^{seml}. All strains killed *25174*^{seml} flies more quickly than *25174* flies (Figure 5.3). To further investigate the dynamics of infection, flies were infected as for survival assays and the bacterial load up to 48h post-infection in *25174* flies and 18h post infection in *25174*^{seml} flies was quantified by enumerating CFU in homogenates of 6 flies at each time-point (Figure 5.3, B). The number of CFU recovered from infected flies did not differ throughout the course of infection in either fly line, aside from NCTCΔ*atl* which showed reduced numbers of CFU in *25174* flies (*25174*; $\chi^2{}_6{}^{strain*time}$ = 80.7, $p < 0.001$, *25174*^{seml}; $\chi^2{}_6{}^{strain}$ = 4.76, $p = 0.403$, see Figure 5.3 B). NCTCΔ*atl* was already known to be impaired in its growth in *25174* flies [293], and as expected grew similarly to NCTC8325-4 in the 25174^{seml} background [293].

5.2.4 *S. aureus* cell wall recycling mutants appear to have an active virulence regulatory system, though haemolysis production by NCTCΔ*murQ* and NCTCΔ*murP* is altered

As survival of *D. melanogaster* infected with PCM's differed from those infected with NCTC8325-4 but *in vivo* growth of bacteria appeared to be similar between strains, a preliminary assessment of virulence factor production was made. Bacteria were grown overnight (18h), washed with PBS and spotted onto TSA plates containing 5% sheep's blood before incubation at 30°C for 24h. This was followed by a further incubation at 4°C for a further 24h to determine if any potential differences in β-haemolysin production (inner haemolysis zone; figure 5.4 C) were made clearer by temperature-shock-induced haemolysis [516]. The area of different zones of haemolysis produced by each strain was then measured as a proxy for haemolysin production (Figure 5.4). The accessory gene regulator *agr* (RNAIII), is critical for virulence in *S. aureus* [34] and an indicator of its functioning is the

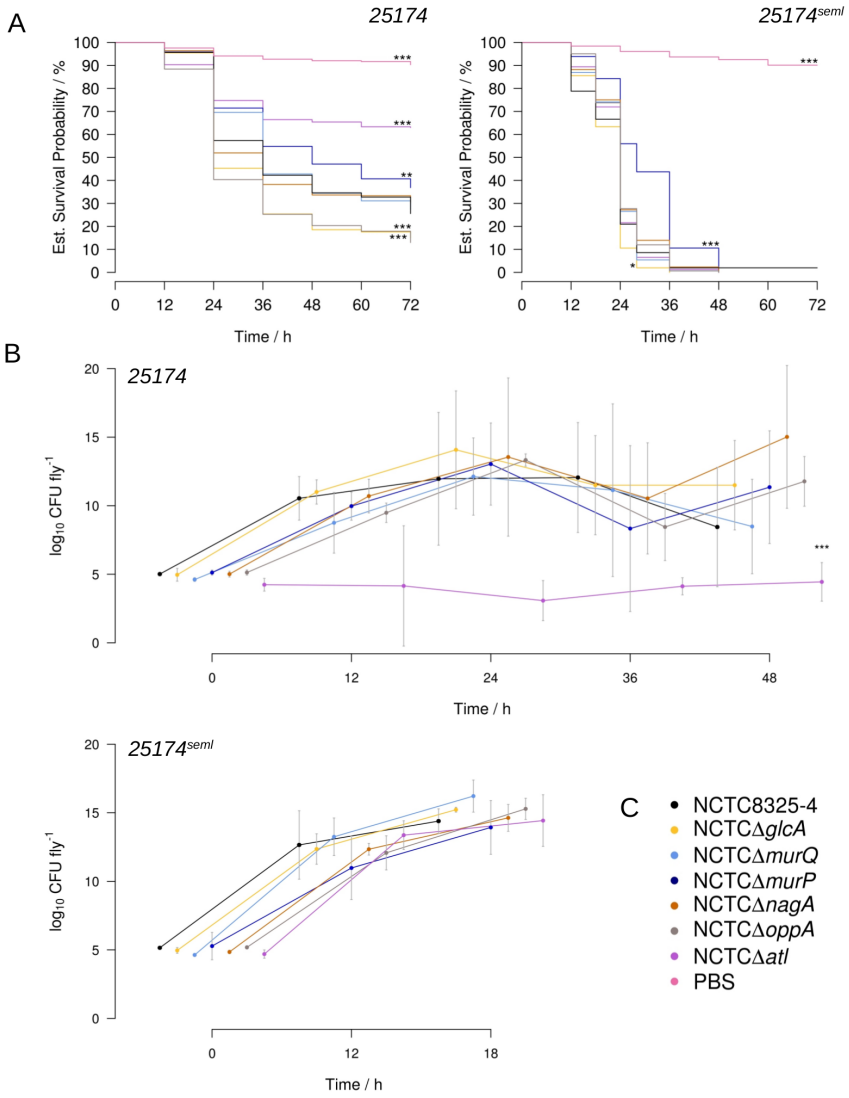


FIGURE 5.3: ***Survival of D. melanogaster upon infection with putative cell wall recycling mutants and in vivo growth of bacterial strains.*** *Bacterial strains were grown overnight (18h) in TSB, cells washed, resuspended in PBS and injected into D. melanogaster strain 25174 (wild-type) and its cognate PGRP-SA functional mutant (25174^{seml}). PBS alone was injected as a control. Following injection, flies were incubated at 30^{o}C and monitored for survival over 72h (A). Data are presented as Kaplan-Meier survival curves, as the estimated survival probability of flies at each time-point, and are representative of 6 independent biological replicates. Bacterial titres (CFU) were also monitored by infecting flies as for survival assays and then plating groups of 6 flies homogenised in TSB per timepoint (B). Data were log_{10} transformed before plotting. 25174 CFU were assayed in two blocks comprising 3 independent biological replicates of all mutants, including NCTCΔatl, with NCTC8325-4 included in both blocks (total of 6 NCTC8325-4 replicates). As NCTC8325-4 CFU did not differ between blocks (ANOVA; $F_{1,26}^{block} = 3.52$, $p = 0.072$) data were combined. 25174^{seml} CFU were assayed in in a single block again comprising 3 independent biological replicates. Panel C shows colours used in both panels A and B. Error bars in panel B represent 95% confidence intervals, some negative errors bars are present due to large variation in the data. 95% confidence intervals were omitted from panel A for clarity. Significance levels; ** $p < 0.01$, *** $p < 0.001$. Asterisks in panel A are representative of Dunnett's multiple comparisons (DMCs) and asterisks in panel B of orthogonal contrasts. All strains were compared to the wild-type NCTC8325-4.*

production of haemolysins, cytolytic enzymes present in >99.5% of human *S. aureus* isolates [517, 34]. All PCM's produced haemolysis zones of some description (Figure 5.4 A). All PCM's except NCTCΔ*murQ* produced a similar total area of haemolysis (α + β-haemolysis) on 5% sheep's blood TSA plates after both 24h incubation at 30°C or after a further 24h at 4°C (ANOVA; $F_{6,34}^{strain} = 5.78$, $p < 0.01$, Figure 5.4A, B). Further incubation at 4°C did not reveal any further differences in the area of haemolysis (ANOVA; $F_{1,34}^{time} = 1.63$, $p = 0.21$). Similar results were obtained for the area of α (ANOVA; $F_{6,34}^{strain} = 6.41$, $p < 0.001$) and β (ANOVA; $F_{6,34}^{strain} = 5.28$, $p < 0.001$) haemolysis zones (Figure 5.4A, C, D), though again no increase in the area of α or β-haemolysis was observed with time (α-hameolysis, ANOVA; $F_{1,34}time = 0.610$, $p = 0.44$, β-haemolysis, ANOVA; $F_{1,34}^{time} = 1.60$, $p = 0.21$). NCTCΔ*murP* also showed some qualitative differences in the appearance of the lysis zones produced, with a clearer β-haemolysis zone than the other strains that became more obvious after incubation at 4°C as well as a more diffuse α-haemolysis zone (Figure 5.4 A).

5.3 *Discussion*

PR is known to influence host-pathogen interaction in a number of Gram-negative bacteria. Gram-negative PR may modulate host recognition of turnover products [480], is involved in virulence regulation via accumulation of cytoplasmic recovery products [429], and may regulate the extent of host epithelial tissue damage by modulating release of cytotoxic muropeptides [362, 337]. However, no study to date has addressed the role of PR in host-pathogen interaction in any Gram-positive bacterium. Here, the first assessment of the role PR may play in virulence of the Gram-positive *S. aureus* is presented. PCM's known to be impaired in their ability to grow on or take-up CW aminosugars (NCTCΔ*glcA* and NCTCΔ*murP*) were found to be altered in their virulence relative to NCTC8325-4 during infection of the model host *D. melanogaster*, though the bacterial load of these mutants during infection was unchanged. NCTCΔ*oppA* was also found to have alterations in virulence, but again without alteration to bacterial load. Alterations in virulence did not seem to be associated with the ability of *D. melanogaster* to recognise the CW PGN of these mutants at the *S. aureus* cell surface, or indeed PGN fragments shed into culture medium during growth. All PCM's appeared to possess a functional virulence regulation system as signified by an ability to produce haemolysins, though the haemolysis of sheep's blood was altered in NCTCΔ*murQ* and NCTCΔ*murP*. Although pointing to a potential role of PR in virulence independent of host PGN recognition, the results of this Chapter do not rule out a role of PR in modulating *S. aureus* PGN fragment recognition in mammalian hosts. However, during

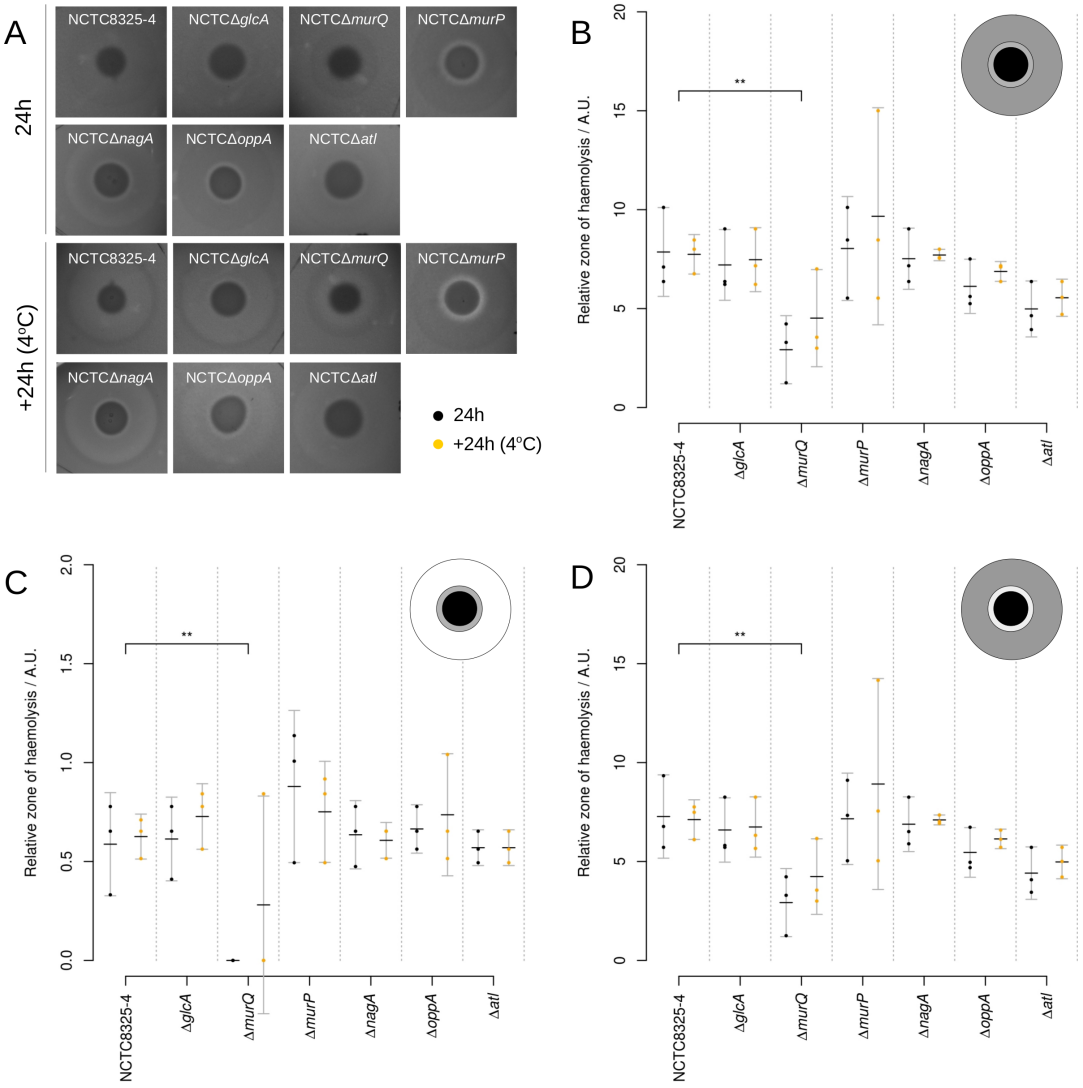


FIGURE 5.4: ***Haemolysis of sheep's blood is altered in NCTCΔmurQ and NCTCΔmurP.*** *NCTC8325-4, NCTCΔatl and PCM's were assayed for their ability to lyse sheep erythrocytes on 5% sheep's blood TSA (A). The key in the bottom right of panel A denotes the colours used in panels B-D. Zones of haemolysis were then measured and split into total area of haemolysis (B), the inner halo, representing β-haemolysis (complete lysis) (C) and the outer halo representing α-haemolysis (incomplete lysis) (D). The measured zones are depicted by grey areas of the inset in the top right of the respective panel. Areas (zones) of haemolysis are expressed relative to the area of the colony they surrounded (A.U.; arbitrary units). Panel A shows representative images of each strain. All data in panels B-D are representative of 3 independent biological replicates, and error bars represent 95% confidence intervals. The negative error bar in panel C is due to large variation in the data for NCTCΔmurQ. Significance levels; ** $p < 0.01$. Asterisks in panels B-D are representative of Dunnett's multiple comparisons (DMCs), with comparisons made to NCTC8325-4.*

the course of this study, it was found that NCTCΔ*atl* culture supernatant elicited an immune response, suggesting that correct degradation of released PGN fragments may act in immune evasion, either instead of, or in synergy with fragment recovery.

The fact that NCTCΔ*glcA*, NCTCΔ*murP* and NCTCΔ*oppA* demonstrated differential virulence to NCTC8325-4 in *D. melanogaster* is intriguing in a number of respects. First and

foremost, although these mutants showed little observable phenotype in other assays performed during this study they appeared to be affected in their ability to cause fatal infection in a model host (Figure 5.3 A). This in itself is extremely interesting, and suggests that PR or PGN fragment recovery may well have functions relevant to infection in *S. aureus*, as in Gram-negative bacteria [480, 429, 337]. However, without complementation of these strains and repetition of this assay, it is not yet possible to conclude that deletion of these genes is directly linked to alterations in virulence. Differences in the virulence of NCTCΔ*glcA* and NCTCΔ*murP* were observable in both *25174* and *25174*^{seml} flies, suggesting that possession of functional PGRP-SA by the host did not affect the ability of bacteria to cause their deaths. The fact that NCTCΔ*oppA* seemed to be similarly virulent to NCTC8325-4 in the *25174*^{seml} background seems likely to be due to the overall lower survival of flies lacking PGRP-SA and the subsequent loss of resolution between survival curves, rather than differential recognition of this mutant (Figures 5.1 and 5.2). Indeed, purified mCherry::PGRP-SA did not show any difference in binding to the surface of any PCM when compared to NCTC8325-4 (Figure 5.1) and injection of spent culture supernatants expected to contain turnover products of these mutants did not seem to stimulate Drosomycin::GFP production (Figure 5.2).

NCTCΔ*atl* on the other hand, bound PGRP-SA strongly at the cell surface as previously reported [293]. As *S. aureus* Δ*atl* mutants are also know to exhibit drastically reduced CW turnover [324], spent NCTCΔ*atl* culture supernatant was originally used as a negative control unlikely to stimulate the *D. melanogaster* immune system via PGRP-SA. Instead, it was found that spent culture supernatant from NCTCΔ*atl* strongly stimulated the Toll-cascade of *D. melanogaster* in a PGRP-SA-dependent manner (Figure 5.2). This is particularly interesting, as reduction of immune stimulation by shed PGN fragments may be reduced either by their recovery during PR [480], or by their degradation in the extracytoplasmic environment [364, 320]. It has been suggested that the MLAA (amidase) domain of Atl may be involved in trimming stem peptides from released muropeptides [293]. The presence of stem peptides is required for PGN detection by PGRPs [399], and by NOD receptors [391, 390, 396]. Thus, lack of stem peptide removal by Atl could increase immunostimulatory activity of turnover products. As Atl is the responsible for the bulk of turnover in *S. aureus* [324] and also liberates protruding strands of PGN from the cell surface of *S. aureus* [292, 293], it may also be possible that other PGN hydrolases that are up-regulated in its absence [518] may cleave this material in an abnormal way, again releasing immunostimulatory muropeptides. It seem possible that this may act as the main mechanism of turnover product

recognition avoidance, or that it may also complement PGN fragment recovery. As PGRP-SA of *D. melanogaster* is evidently able to bind artificially generated PGN monomers of *S. aureus* but not respond to them [447], this also suggests that whatever material is present in the supernatant of NCTCΔ*atl* is likely to be composed of dimeric or larger muropeptides.

As virulence was apparently not related to differential recognition of PCM's (Figures 5.1 and 5.2), nor simply the bacterial load present inside infected flies (Figure 5.3, B) this suggested that it may instead be due to differences in the production of virulence factors. Thus, a preliminary assessment of virulence factor production revealed that all PCM's appeared to have functional *agr* (RNAII) gene (Figure 5.4), which is vital for virulence in *S. aureus* [34]. At least α-haemolysin (*hla*) is expressed by *S. aureus* during infection of *D. melanogaster* [432, 433] and its expression is associated with virulence in this model [433]. Some alteration in haemolysin production relative to NCTC8325-4 was evident, with both NCTCΔ*murQ* producing an overall smaller area or haemolysis, and almost no β-hameolysis, and NCTCΔ*murP* producing a clearer zone of β-hameolysis, respectively. Though the *agr* system in all PCM's appeared to be functional, it is still possible that alterations in haemolysis, particularly in NCTCΔ*murQ*, may be indicative of some mutation in *agr*. Complementation of these mutations would again be useful in interpreting these results. However, these results may be potentially interesting. MurR (RpiRB), the gene for which is found in the same operon as *murQ* and *murP*, is a putative transcriptional regulator that may sense MurNAc-6-P (Chapter 2, [460]), and is known to be involved in regulation of *S. aureus* virulence [472]. It may be that interference with this hypothetical MurNAc-6-P mediated regulatory system through deletion of *murQ* and/or *murP* might alter virulence factor production. It is tempting to suggest that this may also underlie the attenuated virulence of NCTCΔ*murP* in *D. melanogaster*. However, differences in haemolysin production did not seem to correlate with the observed patterns of virulence (Figures 5.3 and 5.4), though haemolysins are far from the only virulence factors produced by *S. aureus* [34].

In short, it is difficult to know what may underlie the differences in virulence of these PCM's from the given data, but differences in the phagocytosis of these strains by fly haemocytes [519, 520], susceptibility to other immune effectors of *D. melanogaster* [420] or alterations to carbon source utilisation within the host [474] are just a few possible explanations. Regardless, this data suggests that there may be interesting influences of PR or aminosugar uptake and metabolism on host-pathogen interaction in *S. aureus*, unrelated to recognition of PGN, and possibly related to virulence factor expression. However, complementation of these strains would be required to confirm all of the phenotypes reported here and as *D.*

melanogaster is unable to respond to artificially generated monomeric *S. aureus* muropeptides [447], a possible role of CWR in avoidance of immune recognition in mammalian hosts is cannot be ruled out. *S. aureus* already employs multiple mechanisms of evasion of PGN recognition [457, 293, 509, 181, 510]. Here, a possible new mechanism of reducing turnover product recognition involving Atl has also been uncovered.

Chapter 6

General discussion and synthesis

The first aim of this thesis was to determine whether or not the Gram-positive pathogen *S. aureus* possessed the capacity for PR. This was achieved through bioinformatic identification and examination of putative CWR components (Chapter 2), and was followed by the generation of *S. aureus* NCTC8325-4 mutants lacking the identified components. The second major aim was to then identify which of the identified putative CWR components may actually be involved in *S. aureus* PR, and what influence PR may have on other aspects of *S. aureus* physiology and particularly PGN metabolism. This was achieved in part, through examination of the ability of bacteria to consume and utilise CW PGN components for growth, assessment of their general vigour and morphology, more in-depth assessment of the functions of some putative CWR components and an assessment of the possible influence of *S. aureus* PR on CW structure (Chapters 3 and 4). However, attempts to assess the impacts of putative PR on PGN turnover were unsuccessful. The final aim was to then to investigate what possible function PR may play in host-pathogen interaction of *S. aureus*. This was achieved by experimentally characterising the interaction between *S. aureus* and a model host; *D. melanogaster* (Chapter 5). Though most aims were met, verification of the results presented in this thesis through complementation of the generated mutants is still required. In the following sections, I first give a short summary of what was found during these studies regarding the nature of putative PR in *S. aureus* and its potential influences on the physiology and pathogenesis of this organism. This is followed by a more general discussion of whether Gram-positive bacteria truly 'recycle' PGN and an attempt to set these findings in the broader context of putative Gram-positive PR and its functions.

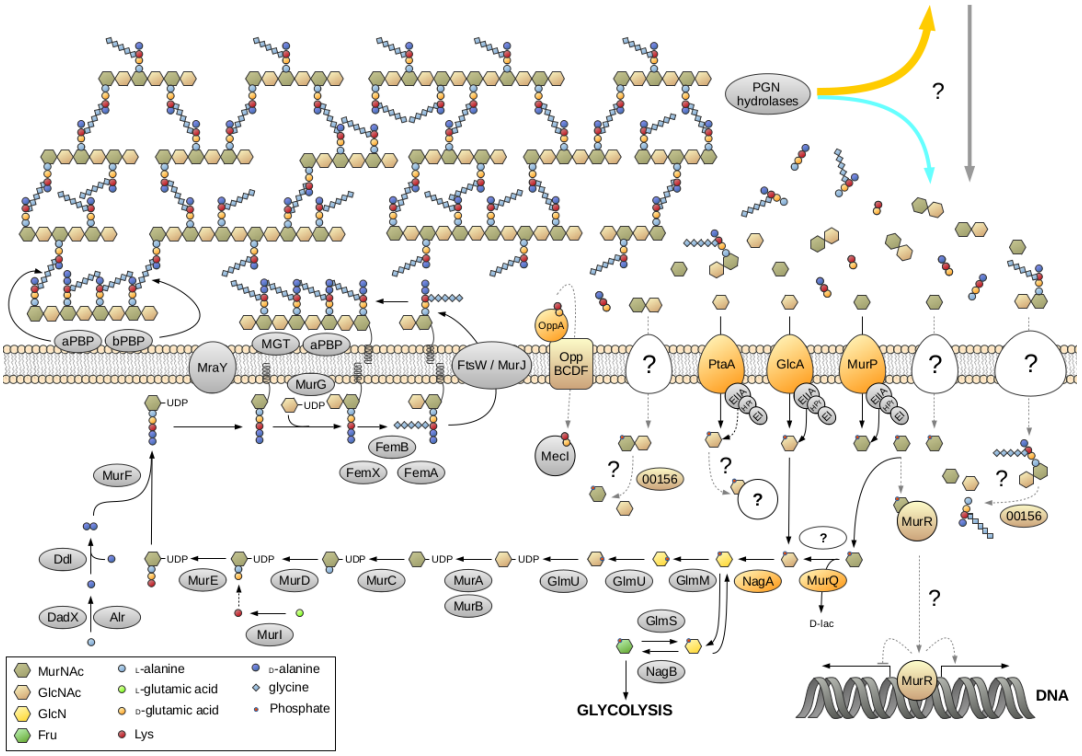


FIGURE 6.1: ***An overview of the putative peptidoglycan recycling pathways of S. aureus.*** *PGN fragments released during PGN turnover are known to be shed into the environment by growing S. aureus (thick orange arrow), but may also be recovered and recycled (thin blue arrow). PGN fragments shed from other cohabiting bacteria may also be recovered from the extracellular milieu (grey arrow). The nature of PGN fragments shed by S. aureus is currently unknown but possible structures are depicted. PGN fragments may be recovered through various routes, before being processed by a suite of catabolic cytoplasmic enzymes and eventually fed into the PGN biosynthetic or glycolytic pathways. It is also possible that recovered PGN-derived molecules may be sensed by various cytoplasmic proteins such as MurR or MecI that may act as transcriptional regulators. Proteins identified and studied in this thesis are depicted in orange, those identified but not studied further are depicted in beige, and hypothetical proteins in white. Dashed grey arrows represent hypothetical activities, and solid black arrows represent those known with some certainty to occur. Flat ended arrows represent possible repressive functions. Angled arrows on DNA represent gene transcription. Mechanisms of CCR have not been included in this diagram for clarity, but may also play a role in the regulation of PR in S. aureus.*

6.1 *Putative PR and its functions in S. aureus*

6.1.1 The putative peptidoglycan recycling pathways of *S. aureus*

One previous analysis had indicated that *S. aureus* contained orthologues of several *E. coli* PR proteins, namely MurP, 2 orthologues of NagE, MurQ, NagA and MppA [294]. Though the analysis performed in Chapter 2 largely confirmed this result (see Figure 6.1) it appeared that *S. aureus* does not possess a true orthologue of MppA, but instead possesses a similar protein; OppA (Chapter 2, Figure 6.1). Several further PTS components potentially involved in CW aminosugar recovery were identified by homology searching, along with a handful of further components encoded in operons that also encoded components identified by

homology searching (Chapter 2). It also seemed that in agreement with the previous analysis [294], *S. aureus*, like many Gram-positive bacteria, seems to lack pathways for possible recycling of anhMurNAc-containing PGN fragments.

One of these operons, including *murQ* and *murP* was published during the course of this study [368], alongside confirmation that MurP and MurQ are likely responsible for the uptake and metabolism of MurNAc, respectively [368] (Figure 6.1). The results presented in Chapter 3 regarding the growth of NCTCΔ*murQ* and NCTCΔ*murP* in CDM(MurNAc) complement this work, while also raising some interesting questions about MurNAc recovery and metabolism. While the aforementioned study suggested MurNAc recovery and utilisation in *S. aureus* occurred solely via MurP and MurQ [368], growth of NCTCΔ*murQ* and NCTCΔ*murP* in CDM(MurNAc) (Chapter 3), suggests this is not the case (Figure 6.1). MurNAc may also be recovered via one or more identified PTS components listed in Chapter 2, may be recovered via alternative mechanisms [358, 354, 355], or as a component of muropeptides. SAOUHSC_00156 is also encoded in this 4-gene operon, and is a putative cytoplasmic hydrolase predicted to cleave glycosidic or amide bonds such as those found in muropeptides (Chapter 2). The final protein encoded in this operon, MurR, is a putative transcriptional regulator implicated in virulence of *S. aureus* that may sense MurNAc-6-P [460, 472].

GlcA and PtaA were identified here as potential transporters for GlcNAc uptake in *S. aureus* (Figure 6.1). Another study subsequently identified GlcA as the sole GlcNAc transporter in this bacterium [474], though this also seemed not to be the case (Chapter 3). Results presented in Chapters 3 and 4 suggest that PtaA may primarily responsible for GlcNAc uptake and GlcA may aid this in stationary phase. However, the contribution of GlcA to GlcNAc uptake seemed to be minimal in rich media (Chapter 4). As no mutant lacking both *glcA* and *ptaA* was studied, other GlcNAc uptake routes in *S. aureus* cannot be ruled out. Accumulation of GlcNAc-6-P in the cytoplasm of NCTCΔ*nagA* and NCTCΔ*glcA*Δ*nagA* strongly suggested that the function of NagA is as a GlcNAc deacetylase (Figure 6.1), in agreement with growth profiles of *nagA* mutants in CDM(GlcNAc) (Chapter 3) and previous work [471]. Previous studies have concluded that PR in Gram-positive bacteria is most likely to occur in the stationary phase of growth [320, 368], though GlcNAc-6-P accumulation began during exponential phase (Chapter 4).

Verification of the function of OppA was not achieved in this study, but it may act in peptide uptake along with OppBCDF, encoded in the same operon (Chapter 2). *S. aureus* MecI, a transcriptional repressor of β-lactamase expression binds γ-D-Glu-L-Lys fragments

that may be taken up via this route [369] (Figure 6.1). OppA may also be involved in muropeptide uptake as MppA of *S. flexneri* [480]. Although only a preliminary result, the noted MLZ swelling in the SCW of NCTCΔ*oppA* is suggestive of turnover product accumulation between dividing cells, perhaps due to reduced recovery in the absence of OppA (Chapter 4).

6.1.2 Possible physiological functions of peptidoglycan recycling in *S. aureus*

Disruption of putative PR had little influence on the ability of bacteria to grow, or on their cell morphology in rich media (Chapters 3). It remains possible that potential phenotypes may have been somewhat masked by CCR (Chapter 2) [294], but this is as yet untested. Disruption of PR in *E. coli* also produces little obvious effect on growth or morphology in most cases [340, 194], and similar results have been obtained for other Gram-positive bacteria sporting mutations in putative PR/CWR components [320, 368]. However, one previous study had indicated that CW structure may be altered under perturbation of PR in *E. coli* [340]. Examination of the molecular structure of PCM CW PGN revealed almost no differences when compared to NCTC8325-4 (Chapter 4). This was not entirely surprising as bacteria still had access to sufficient nutrients for CW synthesis in these experiments [471].

Preliminary examination of PCM stationary phase CW ultrastructure revealed some more potentially interesting phenotypes, ranging from more variable CW thicknesses to abnormal septal morphologies (Chapter 4), suggesting a potential influence of PR on this aspect of *S. aureus* CW structure. However, these data were derived from only a single biological replicate with uncomplemented mutant strains and require verification. Independent experiments have also indicated that Δ*murQ* mutants of *S. aureus* and *B. subtilis* exhibit reduced survival during extended stationary phase [368]. Though this result was not replicated here, the putative abnormalities observed in the CW ultrastructure of NCTCΔ*murQ* were accompanied with what appeared to be increased numbers of lysed cells in stationary phase (Chapter 4). It also seemed that cells of this mutant may be larger than that of NCTC8325-4 (Chapter 3) in stationary phase. NCTCΔ*murP* and NCTCΔ*oppA* may also be smaller in size in stationary phase than NCTC8325-4. Assessment of stationary phase morphology would be useful in interpreting these results.

6.1.3 Peptidoglycan recycling may potentially play a role in *S. aureus* virulence, while Atl may have a novel role in immune evasion

NCTC8325Δ*glcA*, NCTC8325Δ*murP* and NCTC8325Δ*oppA* exhibited differential virulence when compared to NCTC8325-4 (Chapter 5). This was seemingly unrelated to the ability of flies to recognise PGN of these PCM's or their ability to grow *in vivo*. This was suggestive of a potential role of PR in host-pathogen interaction of *S. aureus*. It was also found that NCTC8325Δ*murQ* and NCTC8325Δ*murP* were affected in their production of haemolysins (Chapter 5) though this did not appear correlate with the ability of PCM's to cause fatal infection in *D. melanogaster*. During the course of this study it was coincidentally found that spent NCTC8325Δ*atl* supernatant stimulated the flies' immune system in a PGRP-SA-dependent manner, contrary to expectation [292, 324, 293]. This suggested that while PR may be somehow involved in virulence independent of PGN recognition, Atl may be involved in avoidance of immune recognition of shed PGN-derived material. However, a possible role of *S. aureus* PR in immune evasion in mammalian hosts could not be ruled out.

6.2 *Towards an broader understanding of the possible occurrence, nature and function of PR in S. aureus and other Gram-positive bacteria*

6.2.1 Do Gram-positive bacteria really 'recycle' peptidoglycan?

As many Gram-positive bacteria shed large quantities of turnover products [274, 313, 288, 314, 299, 312], it is possible that putative CWR components may be involved in scavenging this material from the extracellular milieu rather than specifically recycling what is shed from their own sacculus (Figure 6.1). Indeed, the question of how most Gram-positive bacteria may trap this material in the absence of an OM is still an outstanding one [294]. It is possible that there may be a combination of the two scenarios. In *S. aureus* for example, the SCW [90] formed between two cells during septal synthesis encloses the MLZ, an area in which extensive remodelling of the cell wall takes place [109, 192]. Any turnover products produced as a result of PGN hydrolysis may be trapped in this enclosed compartment from which *S. aureus* may be able to recycle the released fragments. Indeed, in Chaper 4, preliminary CW ultrastructural studies revealed that several PCM's exhibited what appeared to MLZ's swollen with possible turnover products. If this were the case, it may perhaps underlie the lower rate of turnover exhibited by *S. aureus* when compared to other bacteria such as *B. subtilis* [288, 314, 299, 274, 313].

However, it may be difficult to distinguish between these two scenarios experimentally. The scenario for *S. aureus* proposed above could be addressed by examining whether the MLZ does indeed sequester turnover products, and in turn whether removal of putative CWR components affects this. It would also be interesting to examine the turnover of *S. penumoniae* PGN in the absence of putative CWR components as this organism exhibits almost no shedding of PGN even though it has readily detectable autolytic activity [312, 334, 333]. For other bacteria such as *B. subtilis* which shed considerable amounts of PGN and possess no obvious structures that may trap turnover products, this may be much more difficult. Experiments examining turnover in strains lacking putative CWR transporters would be useful in determining the extent of turnover product recovery in Gram-positive bacteria [338, 339, 335, 363], but it would still be difficult to distinguish between recycling and scavenging scenarios. Conversely, quantification of PGN transfer from a donor strain to a receiving strain could determine if shed PGN is taken up by cohabiting cells, and to what extent this may occur. This could be achieved by labelling PGN of the donor strain and emplying a marker such as GFP to subsequently separate cells for analysis.

But, is this distinction important? If bacteria were recycling their own PGN, this may potentially give useful feedback to the cell on the status of its CW [338, 339] (c.f. Subsection 6.2.2 and Chapter 4), whereas PGN fragments from conspecific bacteria may act as potential quorum sensing signals if they could be differentiated from self [373, 521, 522, 505]. As bacteria are rarely found in monospecific populations [523], PGN fragments from other species of bacteria or indeed GlcNAc originating from other microorganisms may also be taken-up [505], potentially providing information to a given bacterium about community composition in its environment [523, 373, 521].

6.2.2 Aminosugar uptake and metabolism, and the possible regulatory functions of cell wall aminosugar-phosphates in *S. aureus*

It is now becoming apparent that Gram-positive bacteria possess the capacity for the uptake and metabolism of CW aminosugars, largely via PTS system components (Chapters 3 and 4) [471, 366, 367, 368]. Other bacteria are capable of MurNAc uptake via other mechanisms, but aminosugar phosphates are still produced in each mechanism [358, 357, 368, 355]. Whether the hypothesised alternative route for MurNAc utilisation in *S. aureus* may also involve the generation of MurNAc-6-P is however unknown. Uptake of aminosugars via PTS components adds to the cytoplasmic pools of GlcNAc-6-P and MurNAc-6-P, while their subsequent metabolism of then depletes these pools [368] (Chapter 4). GlcNAc-6-P

and MurNAc-6-P also play important signalling roles in *E. coli* and other Gram-negative bacteria [504, 460, 344, 505]. In *E. coli* both GlcNAc-6-P and MurNAc-6-P are respectively recognised by the intracellular transcriptional regulators NagC and MurR [504, 460, 344]. NagC represses transcription of genes encoding components involved in the uptake and metabolism of GlcNAc [524, 525, 526] while simultaneously activating transcription of the *glmUS* operon, encoding the PGN precursor synthesis enzymes GlmU and GlmS [527, 504]. The presence of GlcNAc (and hence GlcNAc-6-P) or mutation of either *nagA* or *nagC* results in the simultaneous derepression of the *nag* genes and activation of *glmUS* [527, 525]. Similarly, MurR represses transcription of *murQ* and *murP* in *E. coli*, which encode an orthologous system to MurQ and MurP of *S. aureus* [345, 346, 460] and the presence of MurNAc (and hence MurNAc-6-P) or mutation of MurR relieves this repression [460].

In *S. aureus*, MurR may play a similar role to MurR of *E. coli* [460, 472], but also plays a further role in regulation of *S. aureus* virulence factor synthesis and pentose phosphate metabolism [472]. A hypothetical transcriptional regulator may also exist in *S. aureus* allowing the apparent tight regulation of Glc and GlcNAc utilisation in this organism [471] (Figure 6.1). This hypothetical regulator is proposed to regulate the transcription of *glms*, and GlmS along with NagB control the allocation of Glc-6-P and GlcNAc-6-P between CW biosynthesis and glycolysis (see Figure 1.5) [471]. These phenomena may also be linked to CW biosynthesis. *S. aureus* WTA is composed largely of ribitol phosphate (a pentose phosphate) [52], and perturbation of pentose phosphate metabolism may potentially affect its synthesis [528]. WTA is also an important determinant of nasal colonisation and pathogenesis in this organism [510, 529]. The *S. aureus nagA* mutant from [471] was also shown to exhibit decreased resistance to a panel of CW synthesis targetting antibiotics including Oxacillin, Methicillin, Teicoplanin, Vancomycin and Fosfomycin, an effect exacerbated by the presence of GlcNAc in the medium [471]. Together, this information highlights possible links between CW aminosugar uptake and metabolism and CW biosynthesis, as well as virulence. Thus, there may be a possible regulatory role of aminosugar-phosphate accumulation in various aspects of *S. aureus* biology, ranging from CW biosynthesis to virulence.

The preliminary results presented in Chapter 4 regarding the variable thickness of the CW of NCTCΔ*murQ* and NCTCΔ*nagA* are consistent with this idea. Such variable CW thicknesses may be potentially indicative of disruption of normal CW homeostasis effected through perturbations of precursor synthesis induced by changes in cytoplasmic CW aminosugar-phosphate levels. Though CW ultrastructural features may potentially be altered following perturbation of aminosugar-phosphate concentrations (Chapter 4), this should not alter the

basic molecular structure of PGN in the presence of other sugars that may be used for CW biosynthesis. Indeed, glucose was present in the medium used to grow cells for CW PGN molecular structure experiments allowing normal CW biosynthesis [471]. The altered haemolysin production of NCTCΔ*murQ* and NCTCΔ*murP* and the altered virulence profile of NCTCΔ*murP* presented in Chapter 5 may result from altered cytoplasmic MurNAc-6-P concentration affecting virulence factor production via MurR [460, 472]. During infection by *S. aureus*, the presence of MurNAc in the environment could signal the presence of growing bacteria [373] and thus that the cell is in a rich nutritional environment such as host soft tissue [474]. Accumulation of cytoplasmic MurNAc-6-P may then affect regulation of virulence factor production via MurR, and this may act in a quorum sensing-type manner [472, 522]. Investigation of these possibilities in *S. aureus* and other Gram-positive pathogens could prove an interesting avenue for future research.

6.2.3 A re-evaluation of the possible functions of putative Gram-positive PR

Two previous studies on the topic of Gram-positive PR had identified phenotypes suggesting that PR in *S. aureus* and *B. subtilis* may influence stationary phase viability [320, 368]. The first of these two studies reported that a *B. subtilis* NagZ mutant showed a lytic phenotype in stationary phase, when expression of *nagz* was normally highest, and the latter implicated MurQ in stationary phase cell viability of both *S. aureus* and *B. subtilis*. The former study however, made no direct assessment of lysis or cell viability and neither study examined the mechanism by which viability may be altered. Interestingly however, in the latter study the addition of exogenous MurNAc to *S. aureus* cultures boosted cell viability of a wild-type strain, but not a Δ*murQ* mutant, whereas addition of MurNAc to *B. subtilis* cultures suppressed viability of both the wild-type and the Δ*murQ* mutant [368]. The explanations put forward by the authors for these phenomena were that MurNAc recovered during stationary phase may stabilise the CW of *S. aureus* and that exogenous MurNAc may stimulate lysis during sporulation of *B. subtilis* [368]. Here, it was seen that changes in PCM optical density did not correlate to the number of viable cells in the culture (Chapter 3), and that reduced stationary phase viability of the above described *S. aureus* Δ*murQ* mutant [368] was not reproducible under the experimental conditions used. However, in Chapter 4, it was observed that stationary phase cultures of NCTCΔ*murQ* displayed potential abnormalities in their CW ultrastructure and that increased numbers of lysed cells were present in the sample. When combined with the proposition that differences in optical density may instead

be indicative of altered size of bacterial cells (Chapter 3), this suggests that PR may still have some role in determining fitness of cells during stationary phase [268, 269]. However, this may be more important in the long term stationary phase populations of cells present in the natural environment than under standard laboratory conditions [486, 487]. Given the fact that GlcNAc-6-P accumulates during exponential phase in Δ*nagA* mutants (Chapter 4), there may also be functions for PR beyond those in stationary phase.

A possible role for PR in host-pathogen interaction was also uncovered in this study (Chapter 5). As the function of OppA is unknown, it is at present difficult to surmise why the virulence of NCTCΔ*oppA* was altered. It is tempting to speculate that due to the preliminary finding that NCTCΔ*oppA* seems to show MLZ swelling and that other *opp* mutants have been shown to shed Muramyl-pentapeptide fragments [480] that mass release of accumulated material from the MLZ of NCTCΔ*oppA* may cause a toxic-shock type response in *D. melanogaster*, leading to death [530]. The altered virulence of NCTCΔ*glcA* is difficult to interpret in the light of PR, as GlcA also transports glucose [474]. GlcA's absence may affect carbon utilisation preference of *S. aureus* in a way that is detrimental to the host. Indeed, *S. aureus* is in possession of a large number of carbohydrate transporters and appears to have evolved to maximise glycolytic flux during infection [474]. Though the decreased virulence of NCTCΔ*murP* was not consistent with its apparently increased haemolysin production, it seems possible that an inability to take-up MurNAc may play a role in virulence factor synthesis as described above (see Subsection 6.2.2).

6.3 *Concluding remarks and future perspectives*

It seems that *S. aureus* and a number of Gram-positive bacteria are able to recover and reutilise components of PGN, but at present it has not been established whether this constitutes true PR. Experiments such as those described in Subsection 6.2.1 may help to explore this possibility, and examination of PGN turnover in putative CWR mutants may give additional useful information on the possible roles of PR in regulating PGN fragment shedding in Gram-positive bacteria. It would also be of interest to characterise the nature of PGN fragments released by Gram-positive bacteria, which at the moment is almost completely unstudied. Regardless, it seems that uptake and metabolism of CW aminosugars may influence the fitness of bacteria in long-term low nutrient conditions in which most natural bacterial communities exist and that it may additionally affect CW homeostasis by

as yet uncharacterised mechanisms potentially regulated by cytoplasmic CW aminosugar-phosphate levels. It also remains possible that putative Gram-positive PR may play roles in β-lactamase expression and in resistance to other CW-synthesis-targetting antibiotics. In addition, it seems that putative Gram-positive PR may also play a role in host-pathogen interaction, again potentially regulated in part by cytoplasmic CW aminosugar-phosphate concentration. Future research into the role of CW-aminosugar-mediated regulation of various aspects of Gram-positive physiology and pathogenesis thus promises potentially interesting results. The investigation of the function of components unstudied here such as SAOUHSC_00156, OppA and additional PTS components potentially involved in MurNAc uptake could also be particularly illuminating with regards to understanding what other components of PGN may be potentially recycled in *S. aureus*. Similarly, investigation of components occupying further putative PR operons in other species may shed further light on the putative PR capabilities of Gram-positive bacteria as a whole. Finally, investigation of Gram-positive PR under more natural conditions may clarify the potential functions of this process, particularly with regards to its roles in stationary phase survival and pathogenesis.

Chapter 7

Materials and methods

7.1 *Bioinformatics*

7.1.1 Putative cell wall recycling gene identification in *S. aureus*

Putative CWR genes were identified in *S. aureus* by use of Best Reciprocal Blast (BRB) analysis [531]. Protein sequences for all 15 *E. coli* (Str K-12, Substr W3110) recycling components were downloaded from NCBI (https://www.ncbi.nlm.nih.gov/) and used as queries using NCBI's `blastp` (protein-protein BLAST) algorithm to find putative homologues in the reference proteome of NCTC8325 (non-redundant protein database), as no proteome for NCTC8325-4 is available via NCBI. NCTC8325-4 is the 'wild-type' strain of *S. aureus* used in this study and is derived from NCTC8325 through curing of 3 prophages [477]. It is almost identical to NCTC8325 in genome sequence [532]. Protein sequences of homologues found in *S. aureus* NCTC8325 were then used as queries to BLAST search back against *E. coli* K-12 W3110, and those homologues returning the original query sequence were taken as orthologues of *E. coli* PR proteins.

To expand this search and find potential aminosugar PTS transporters that were more distant orthologues of those found in *E. coli* functional families (FunFams) FunFam2607 (GlcNAc specific EIIBC PTS component domain) and FunFam2608 (MurNAc specific EIIBC PTS component domain) from the CATH protein structure classification database [462], were used to create alignments using ClustalOmega [465]. These alignments were then used as queries for HMM searching of the *S. aureus* NCTC8325 proteome using the `hmmsearch` webtool of HMMER [461] to identify proteins containing putative GlcNAc or MurNAc specific PTS domains. A cutoff expect value (e-value) of $1x10^{-9}$ was used to delimit search results.

7.1.2 Identification of putative peptidoglycan recycling operons, *cre* site regulatory elements and protein domains

In order to identify putative PR operons in *S. aureus*, the genomic context of putative PR protein encoding genes was mapped using the Microbial Genome-context Viewer (MGcV; http://mgcv.cmbi.ru.nl/, [463]) run by the Netherlands Bioinformatic Centre (nbic). NCBI locus tags were provided as queries and regions spanning 10,000bp either side of each gene were mapped. To identify putative *cre* sites the consensus sequence for *cre* sites in *B subtilis*; 'WWTGNAARCGNWWWCAWW' (N, W and R stand for 'any base', 'A or T' and 'G or A', respectively) [464] was aligned with the CDS and flanking 200bp regions of the GOIs using ClustalOmega and mapped onto genomic context maps. Figures were then prepared using MGcV, and the open source graphics programs GNU Image Manipulation Program (GIMP; https://www.gimp.org/) and LibreOffice Draw (LOD; https://www.libreoffice.org/discover/draw/). Protein domain maps were constructed using Interpro and Pfam domain annotations. Figures were built using GIMP and LOD.

7.1.3 Identification of putative cell wall recycling protein orthologues in other Staphylococci

Prokaryotic-specific COGs were downloaded from the EggNOG 4.5.1 database [475]. With the help of Dr Aino Jarvelin protein identifiers belonging to all available Staphylococcal species in each COG were extracted using a `bash` script, and subsequently subject to a local BLAST+ `blastp` search of these genes against a custom BLAST database built from the proteome of *E. coli* (UP000000625-Ecoli-K12-taxid83333) downloaded from Uniprot (http://www.uniprot.org/). BLAST searches were called from `R` [488] for each group of species extracted from each COG and results collected. Proteins found to match the original sequence query from *E. coli* K-12 W3110 were counted as orthologues. Subsequent alignments were made with ClustalOmega and genomic organisation maps made with MGcV. Alignment figures were created with Jalview [533].

7.1.4 Primer design

Primers were designed using Primer3plus (http://www.bioinformatics.nl/cgi-bin/primer3plus/primer3plus.cgi/), ReverseComplement (http://www.bioinformatics.org/sms/rev_comp.html) and OligoCalc (http://biotools.nubic.northwestern.edu/OligoCalc.html). Deletion regions were selected using SnapGene software with care to avoid putative ribosomal binding sites (RBS's) and to avoid removing parts of other genes. This meant that some

genes were not completely deleted, and short fragments were left behind in the chromosome following deletion (Table B.3). All primers were purchased from Life Technologies (now Thermo-Fisher Scientific).

7.2 *Molecular biology*

7.2.1 *S. aureus* DNA extraction

DNA was extracted from *S. aureus* for deletion fragment amplification. 2 full 10μL loops of confluent growth from a TSA plate were resuspended in 50μL of EDTA (50mM, pH 8.0) with 1μL Lysostaphin (10mg mL^{-1}) and 2μL RNase A (10mg mL^{-1}) before shaking at 1200rpm at 37^{o}C for 30 minutes. 200μL more EDTA and 250μL nuclei lysis solution (Promega) were added and mixed by pipetting. This mixture was incubated at 80^{o}C for 10 minutes and then cooled to room temperature (RT). 100μL protein precipitation solution (Promega) was added and samples were vigorously vortexed. Samples were then incubated on ice for 10 minutes and pelleted at 16,000*g* for 10 minutes at RT. Supernatant was transferred to a fresh tube and mixed with 420μL propan-2-ol to a final volume of 500μL and mixed by inversion. Samples were then centrifuged at 16,000*g* for 10 minutes at RT. Supernatant was carefully removed and samples air-dried. 250μL of 70% (v/v) ethanol was then added to the pellet and tubes inverted several times. This was then centrifuged again at 16,000*g* for 3 minutes at RT, ethanol carefully removed and samples air-dried before dissolving DNA in 100μL distilled water. DNA concentrations were measured using a Nanodrop1000 (Thermo-Fisher Scientific).

7.2.2 PCR, agarose gel electrophoresis, PCR product purification and gel imaging

All PCRs were performed using a T100 Thermal Cycler (Biorad). For amplification of fragments used in vector construction, Phusion High-Fidelity DNA Polymerase (Thermo-Fisher Scientific) was used with 0.2mM dNTPs, primers at a final concentration of 10μM and Diethylpyrocarbonate (DEPC) treated water (DEPCW) to dilute to the final reaction volume. Where necessary Dimethyl sulfoxide (DMSO) or additional $MgCl_2$ were added to aid in template amplification.

PCR colony screening and PCR to produce fragments for sequencing was performed using GoTaq Green Master Mix (M712, Promega), with primers used at a final concentration of 10μM and DEPCW to dilute to the final reaction volume. *S. aureus* cells are resistant to

boiling and standard colony PCR techniques are variable in their effectiveness. Thus, DNA for colony screening was extracted from individual isolated colonies through resuspension in alkaline wash solution (0.05M Sodium citrate, 0.5M NaOH) for 20 minutes, followed by washing with 500μL 0.5M Tris-HCl (pH 8.0), before resuspension in 100μL of nuclease-free water (NFW) and boiling at 100^{o}C for 10 minutes.

DNA fragments were purified by AGE, typically using 0.8% (w/v) Agarose in TAE (4.84g L^{-1} Tris, 0.372 g L^{-1} di-sodium EDTA·$2H_2O$, 1.14% (v/v) acetic acid) with ethidium bromide included in the gel at a concentration of 1:10000 (v/v). GoTaq Green PCRs were loaded directly into the gel, but PCR mixes not already containing loading dye were first mixed with DNA loading dye (NEB) in a 1:5 ratio before loading. Gels were run at 50-80V for 1-3h in TAE buffer depending on the degree of separation required. Bands were detected using UV radiation at 285nm and gel slices were excised using a razor blade and purified using a QIAquick Gel Extraction Kit (Qiagen). When purification by AGE was not required a QIAquick PCR Purification Kit (Qiagen) was used.

7.2.3 Restriction digests, vector construction and plasmid purification

Deletion fragments and pMAD digestions were made using restriction endonucleases (New England Biolabs; NEB) specific to each fragment (Table A.3) and their respective buffers. Reactions were optimised for double digestions where possible (https://www.neb.com/tools-and-resources/interactive-tools/double-digest-finder). Digested plasmid backbone was treated with Antarctic phosphatase (NEB) to prevent self-ligation and deletion fragments inserted into the pMAD backbone using T4 DNA ligase (NEB). After transformation of DH5α competent cells (Subsection 7.3.2), plasmids were purified from 12-16h overnight cultures using a QIAprep Spin Miniprep Kit (Qiagen).

7.3 *Microbiological methods*

7.3.1 Bacterial strains, general growth conditions, growth analyses and frozen stock preparation

Strains used in this thesis are listed in Tables 2.3 and A.4. *S. aureus* strains were routinely grown in TSB (Difco) or on TSA (Sigma Aldrich), unless otherwise stated. Growth was monitored by optical density at 600nm (OD_{600}) using an Amersham Pharmacia Biochrom Ultrospec 2100 spectrophotometer. Liquid cultures were grown at 30^{o}C, with agitation at 180rpm. Cultures were always maintained at 30^{o}C to keep *in vitro* and *in vivo D. melanogaster*

infection experiments consistent. *D. melanogaster* survival is already affected at 37°C, and the normal rearing temperature of 25°C for *D. melanogaster* prevents rapid bacterial growth during infection, while incubation at 30°C permits meaningful infection experiments to be carried out. For assessment of growth on aminosugars strains were grown in CDM (Table 7.1) supplemented with various carbohydrate sources. Overnight pre-cultures for CDM experiments were always grown in 50mM CDM(Glc), pelleted at 3000*g* for 10 minutes at RT, washed with PBS (137mM NaCl, 2.7mM KCl, 10mM Na_2HPO_4, 1.8mM KH_2PO_4, pH 7.4), pelleted again and inoculated at an initial density of OD_{600} 0.05. Aminosugar growth experiments were performed in 3mL cultures of CDM containing either 25mM Glc, 25mM GlcNAc or 25mM MurNAc. NTIML strains (except JE2) were always grown in the presence of 25μg mL^{-1} Erythromycin (Ery).

In order to analyse different growth phase parameters, such the r_0 of bacterial strains and stationary phase density measurements, bacterial growth curves (both OD_{600} and CFU) were partitioned into different data sets for analysis. For r_0 analyses, r_0 values were extracted using the `R` package `grofit` [489]. This package fits growth data to pre-determined parametric growth models and in addition provides a model free spline method to circumvent systematic errors that might occur within application of parametric methods. For the analyses presented in this study the model-free spline was utilised as fluctuations in low OD_{600} measurements or erratic increases in CFU lead to spurious results when fitting data to pre-determined models. After generation of r_0 values, data were analysed as detailed in Section 7.8. For stationary phase analyses, the section of the bacterial growth curve after which bacteria were no longer growing was taken for specific analysis of stationary phase dynamics. This was post-24h, unless otherwise specified. Data were then analysed as detailed in Section 7.8.

Overnight pre-cultures for experiments were grown for between 16-18h in 3mL media. Bacterial stocks were made by mixing 700μL of overnight culture with 300μL of 50% (v/v) glycerol and snap freezing in liquid nitrogen. Those confirmed not to contain mutations in the deletion region were kept for further studies. Stocks were stored at -80°C.

7.3.2 Preparation and transformation of *E. coli* DH5α competent cells

E. coli DH5α were grown overnight at 37°C, 180rpm, in Luria-Bertani broth (LBB; Difco), and reinoculated into fresh LBB at an optical density (OD_{600}) of 0.05. Cells were grown until OD_{600} ~0.3 and placed in an ice bath for 15 minutes before pelleting at 5000*g* at 4°C for 15

TABLE 7.1: Composition of chemically defined medium without carbon sources.

Basal solution	86% (v/v)[1]
Component	**[2]Conc / mM**
KH_2PO_4	25.4
K_2HPO_4	16.4
Diammonium citrate	3.09
Sodium Acetate	15.2
L-Tyrosine	1.93
L-Cysteine-HCl	6.98
Sodium bicarbonate	2.62

Amino acids	8% (v/v)[1]
Component	**[2]Conc / mM**
L-Alanine	1.12
L-Arginine	0.574
L-Aspartatic acid	0.751
L-Glutamic acid	0.492
L-Glutamine	0.684
Glycine	1.33
L-Histidine-HCl	0.644
L-Isoleucine	0.762
L-Leucine	0.762
L-Lysine-HCl	0.547
L-Methionine	0.670
L-Phenylalanine	0.605
L-Proline	0.869
L-Serine	0.952
L-Threonine	1.68
L-Tryptophan	0.490
L-Valine	0.854
L-Hydroxiproline	0.763

Nitrogenous bases	2% (v/v)[1]
Component	**[2]Conc / mM**
Adenine-HCl	0.117
Guanine	0.132
Uracil	0.178

Vitamins	1% (v/v)[1]
Component	**[2]Conc / μM**
Na 4-aminobenzoate	1.26
Biotin	0.819
Folic acid	1.81
Nicotinamide	8.19
D-Pantothenic acid	8.39
Pyridoxine-HCl	4.86
Pyridoxal-HCl	4.91
Riboflavin	5.31
Thiamine-HCl	2.96
Cyanocobolamine	0.0738

Micronutrients	1% (v/v)[1]
Component	**[2]Conc / μM**
$MgSO_4 \cdot 7H_2O$	2840
$CaCl_2 \cdot 2H_2O$	63.1
$FeSO_4 \cdot 7H_2O$	7.50
$ZnCl_2$	0.510
$MnCl_2 \cdot 4H_2O$	0.500
$CoCl_2$	1.46
$NiCl_2$	0.100
$Na_2MoO_4 \cdot 4H_2O$	0.148
$CuSO_4 \cdot 5H_2O$	1.50

[1] % of the total solution volume (v/v). Carbohydrate sources (Glc, GlcNAc or MurNAc) were supplied in the remaining 2% of the solution volume. The composition of this medium was adapted from [491]. [2] Conc; concentration.

minutes. Cells were then resuspended in Buffer RF1 (12g L^{-1} $RbCl_2$, 9.9g L^{-1} $MnCl_2$, 1.5g L^{-1} $CaCl_2$, 2.95g L^{-1} CH_3CO_2K, 15% (v/v) glycerol) and incubated for a further 15 minutes on ice. Suspensions were pelleted again before resuspension in buffer RF2 (1.2g L^{-1} $RbCl_2$, 11g L^{-1} $CaCl_2$, 2.09g L^{-1} 3-morpholinopropane-1-sulphonic acid (MOPS), 10% v/v glycerol) to final OD_{600} of ~12. Aliquots of 50μL were then snap frozen in liquid nitrogen and stored at -80ºC.

DH5α competent cells were transformed by thermal shock at 42ºC. Cells were recovered in LBB for 1h at 37ºC and then plated on Luria-Bertani broth agar (LBA) containing 100μg mL^{-1}

Ampicillin (Amp) and incubated overnight at 37°C.

7.3.3 Preparation and electroporation of *S. aureus* RN4220 electrocompetent cells

S. aureus RN4220 were grown overnight in TSB at 37°C, 180rpm, and reinoculated into fresh TSB at an OD_{600} of 0.05. Cells were grown until OD_{600} ~0.4 before pelleting at 5000*g* at 4°C for 10 minutes. Cells were then washed with 0.5M sucrose and pelleted again. Pellets were then resuspended again in fresh 0.5M sucrose and incubated on ice for 15 minutes. Cells were pelleted a further time and resuspended in fresh 0.25M sucrose with 50% (v/v) glycerol to a final OD_{600} of ~150. Aliquots of 50μL were then snap frozen in liquid nitrogen and stored at -80°C.

RN4220 competent cells were electroporated using a MicroPulser 165-2100 system (BioRad; 2500V, 25μF, 100Ω), ensuring that the time constant was within the 2.5ms range. Cells were recovered in TSB for 1h at 30°C and then plated on TSA containing 10μg mL^{-1} Ery and incubated overnight at 30°C.

7.3.4 Phage lysate preparation and phage transduction of NCTC8325-4

pMAD donor strains were streaked on TSA Ery^{10}, X-gal^{100} (5-bromo-4-chloro-3-indolyl-β-D-galactopyranoside) and grown overnight at 30°C to create a rich confluent growth. Cells were then collected with a 10μL loop and resuspended in TSB containing 5mM $CaCl_2$. 10μL of cell suspension as then incubated with 10μL of several dilutions of empty phage 80α lysate and 3mL of phage top agar (3g L^{-1} casamino acids, 3g L^{-1} yeast extract, 5.9g L^{-1} NaCl and 5g L^{-1} agar, pH 7.8) at ~46°C before quickly pouring onto plates containing 20mL phage bottom agar (top agar plus 10g L^{-1} agar). Top agar was allowed to set and plates incubated at 30°C overnight. Plates with confluent lysis of cells were chosen and 4mL of phage buffer (1mM $MgSO_4$, 4mM $CaCl_2$, 50mM Tris pH 7.8, 5.9g L^{-1} NaCl, 1g L^{-1} gelatine) was added to plates followed by 1h incubation at 4°C. Top agar was then collected by scraping and deposited in a 50mL centrifuge tube (Greiner) and agar disrupted by vortexing. Top agar homogenates were then incubated for 1h at 4°C to allow phage transfer to the buffer. Agar was then sedimented by centrifugation at 2000*g* for 15 minutes at 4°C before recovery of supernatant and filtration through a 0.45μm filter. Lysates were checked for sterility and stored at 4°C before further use.

To transduce NCTC8325-4 a single colony of this strain was grown overnight at 30°C to produce rich confluent growth. Plates to recover transductions were poured containing 10mL 0.3GI bottom agar (3g L^{-1} casamino acids, 3g L^{-1} yeast extract, 5.9gL^{-1} NaCl, 0.5g L^{-1} trisodium citrate, 3.3mL L^{-1} Sodium DL-lactate syrup 60% (w/w), 2mL L^{-1} 50% (v/v) glycerol, 7.5g L^{-1} agar) with 30μg mL^{-1} Ery and left to set. Cells were scraped from the NCTC8325-4 overnight plate and again resuspended in TSB containing 5mM $CaCl_2$. Bottom agar plates then have a further 20mL 0.3GI bottom agar added and were allowed to set, and used within 1h. 100μL of cell suspension, 100μL of phage buffer containing 5mM $CaCl_2$ and 100μL of several phage lysate dilutions containing the plasmid of interest were incubated at 37°C for 20 minutes with agitation, mixed with 3mL of 0.3GI top agar (0.3GI bottom agar with only 7.5g L^{-1} agar) and poured onto the set 0.3GI bottom agar plates. The top agar layer was allowed to set and plates incubated at 30°C for 48h.

7.3.5 Construction of markerless gene deletion mutants in *S. aureus* NCTC8325-4

Markerless deletion mutants were constructed using the methods of Arnaud *et al.* [476] (see Figure 7.1). Briefly, genomic regions flanking either side of the GOI were amplified by PCR using gene specific p1/p2 and p3/p4 primer sets (Table A.3). Primers were designed to produce complementary overhangs at the ends of each flanking fragment closest to the GOI CDS and restriction endonuclease (RE) sites (+3bp) were included at the opposite end of each fragment. PCR products were subjected to AGE and purified. Overlap PCR using the gene specific p1/p4 primer sets was then used to ligate the two fragments together, creating a deletion fragment encoding the two flanking regions of the gene and in some cases short fragments of the GOI CDS, capped at either end by RE sites (Table A.3). Resulting fragments were purified and inserted into the pMAD *E. coli-S. aureus* shuttle vector pMAD [476] (Tables A.4 and 2.3, Figure 7.1).

The resulting plasmids were then transformed into *E. coli* DH5α (Table 2.3) competent cells (Subsection 7.3.2). Ampicillin resistant colonies were screened by colony PCR using gene specific p1/p4 primer sets (Table A.3). Colonies containing the correct plasmid were then grown overnight (12-16h) and plasmid DNA purified. Purified plasmids were then sequenced using gene specific p1/p4 primer sets by Source Bioscience and sequence data analysed using SnapGene software.

NCTC8325-4, as with other *S. aureus* strains is naturally non-transformable and so cannot be electroporated. Plasmids must first be electroporated into the *S. aureus* RN4220 donor

strain (Table A.4) and transduced using phage 80α to NCTC8325-4. Thus, plasmids bearing the correct sequence were then electroporated into *S. aureus* RN4220 electrocompetent cells. Colonies displaying a blue colour and hence indicating the presence of pMAD were picked, isolated and screened to confirm the identity of the plasmid contained within. Phage lysates for transduction of the plasmid to NCTC8325-4 were then prepared for each vector and transduced to NCTC8325-4 as detailed in Subsection 7.3.4. Colonies were picked and re-streaked onto TSA Ery^{10} X-gal^{100} and screened for blue colour to confirm plasmid presence. Phage lysates were then used to transduce NCTC8325-4 (Subsection 7.3.4).

Colonies displaying blue colour were then selected for integration of the plasmid into the chromosome of NCTC8325-4. Single colonies were inoculated into TSB Ery^{10} and grown overnight at 30°C. Cultures were then back-diluted 1:1000 and grown for a further 12h at

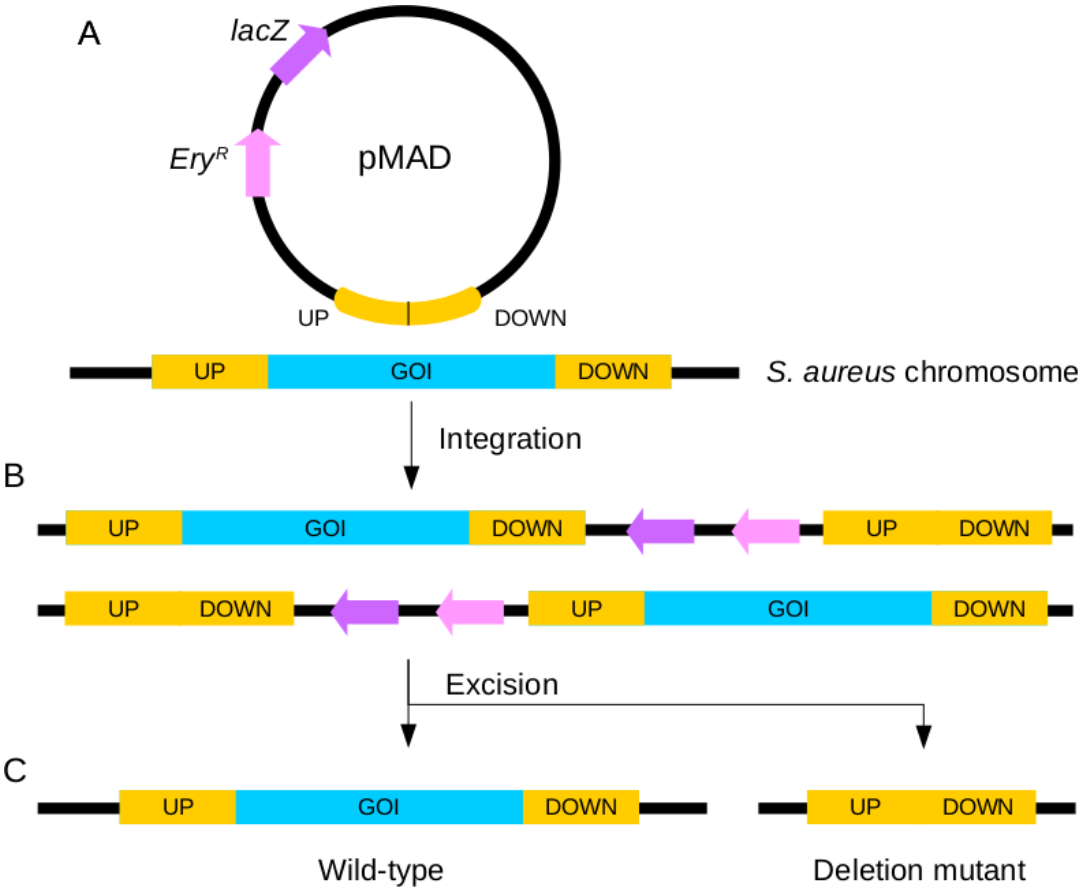


FIGURE 7.1: ***Construction of S. aureus deletion mutants.*** *pMAD constructs containin the upstream and downstream flanking regions of the GOI (UP / DOWN) were introduced into NCTC8325-4 (A). pMAD was then integrated into the chromosome, through recombination at either the UP region or DOWN region, producing strains containing one of the two depicted chromosomal integration types (B). Following integration, pMAD contructs were then excised, producing either clones possessing the original 'Wild-type' chromosomal sequence with no deletion, or deletion mutants lacking the GOI (C). Ery^R and lacZ genes respectively provide Ery resistance and β-galactosidase acitivity to strains carrying pMAD either in the cytoplasm or integrated into the chromosome, allowing selection of mutants.*

30°C to allow replication of pMAD. To select for integrants cultures were then back-diluted 1:100 and shifted to 43°C for 16h before plating on TSA Ery^{10} X-gal^{100} and incubation at 43°C overnight. This selects for bacteria containing integrated plasmid as pMAD has a temperature sensitive origin of replication not active at 43°C [476]. Cultures were plated on TSA Ery^{10} X-gal^{100} and incubated overnight at 43°C. Integration was then confirmed by screening colonies as described in Subsection 7.2.2 using GOI specific integration primers (Table A.2, see Figure 7.1).

To excise plasmids again, and to remove the GOI, correctly integrated colonies were then grown overnight in TSB at 30°C and plated on TSA X-gal^{100} without Ery. This culture was then back-diluted 1:500 in TSB, grown for a further 12h and plated on TSA X-gal^{100} again. This was repeated once more, with cultures grown for 16h. All plates were recovered at 43°C to encourage selective loss of pMAD in the absence of Ery. Non-blue colonies were then picked, and gene deletion screened using integration primers (see Figure 7.1). Colonies bearing the desired deletion were then sequenced using the Sanger Sequencing Service at Source Bioscience using GOI specific sequencing primers (Table B.1) to confirm that no mutations were present in the deletion region. Overnight cultures of deletion mutants were grown and frozen stocks made.

7.3.6 Streptozotocin resistance assay

Overnight bacterial cultures were used to inoculate fresh TSB at an initial OD_{600} of 0.05 and allowed to grow until OD_{600} ~0.5. Samples were then placed on ice and diluted with fresh TSB to an exact OD of 0.5 before swabbing onto TSA plates. Media was supplemented with 25μg mL^{-1} Ery for NTIML mutants. Streptozotocin (MP Biomedicals) was prepared fresh by dissolving in sterile distilled water and transferred to 6mm antibiotic assay discs (VWR) at a concentration of 20μg per disc, determined by pre-tests with NCTC8325-4 (data not shown). Discs were then placed onto swabbed areas of the plate and plates incubated for 18h at 30°C. Plates were then photographed and the diameter of the zone of inhibition measured. See Section 7.8 for details of statistical analysis.

7.3.7 Stationary phase viable cell count assay

Bacteria from overnight cultures were inoculated into 20mL fresh TSB at an initial OD_{600} of 0.05 and grown as detailed in Subsection 7.3.1 in TSB. 1mL culture samples were taken every 3h until 12h, and then every 12h until 72h along with complimentary OD_{600} measurements.

Samples were placed on ice, serially diluted in fresh ice cold TSB and 100μL of pre-determined dilutions (data not shown) were plated on TSA to achieve colony counts of ~30-300 colonies in at least one of the plated dilutions. Platings were made in duplicate. Plates were then incubated for 24-30h at 30^{o}C and then photographed. Colonies were enumerated using the automatic colony counting program OpenCFU [534] with manual inspection to ensure accurate counting. See Section 7.8 for details of statistical analysis.

7.3.8 Haemolysis assay

5μL of overnight bacterial cultures was spotted onto TSA containing 5% v/v defibrinogenated sheep's blood (Oxoid) and incubated at 30^{o}C for 24h. Plates were then photographed, transferred to 4^{o}C for a further 24h and photographed again. Diameters of the zones of haemolysis were measured and the area of each zone calculated relative to the size of the spotted colony. See Section 7.8 for details of statistical analysis.

7.4 *Microscopy*

7.4.1 Live cell imaging of bacterial cells

Bacteria from overnight cultures were inoculated into 20mL fresh TSB at an initial OD_{600} of 0.05 and grown as detailed in Subsection 7.3.1 in TSB. For morphological observations, 1mL culture samples were taken and 1μL of hoechst trihydrochloride trihydrate (10mg mL^{-1}, Life technologies) added. Samples were then incubated at 30^{o}C for 5 minutes with agitation (1200rpm) in an Eppendorf Thermomixer. Samples were then pelleted at 8000g for 5 minutes, resuspended in 30μL PBS and 2μL transferred to an PBS agarose (1.2% w/v) slide and covered with a glass coverslip. Fluorescence microscopy was performed using a Zeiss Axio Observer microscope with a Plan-Apochromat 100x/1.4 oil Ph3 objective. Images were acquired with a Retiga R1 CCD camera (QImaging) using ZEN software (black edition, 2012, version 8.1.0.484).

For PGRP-SA binding experiments 1mL culture samples were pelleted at 8000g for 5 minutes at RT, washed with PBS (pH 6.0), pelleted again and resuspended in 100μL PBS (pH6.0) containing 0.15mg mL^{-1} mCherry::PGRP-SA (see Subsection 7.5.3) and incubated for 5 minutes at RT. Cells were pelleted once again, washed twice with 1mL PBS and finally resuspended in 30μL PBS. 2μL were then added to an agarose slide and imaged in the same manner as detailed above. Image analyses were carried out using Fiji [500].

7.4.2 Live imaging of *Drosophila melanogaster*

After injection with spent bacterial culture supernatant (see Subsection 7.7.2), living *D. melanogaster* flies were anaesthetised on a CO_2 pad and imaged using an Olympus SZX-TLGAD microscope with a MVPLAPO 1X lens. Samples were illuminated using a Cool LED pE-2 coIlluminator and photographed using a RETIGA R3 MONO camera.

7.4.3 Transmission electron microscopy

Bacteria from overnight cultures were inoculated into 20mL fresh TSB at an initial OD_{600} of 0.05 and grown as detailed in Subsection 7.3.1 in TSB for 24h. 1mL culture samples were then taken and pelleted at 5000*g* for 5 minutes, RT. Pellets were then immediately resuspended in 1mL 1% glutaraldehyde (w/v) and 1% osmium tetroxide (w/v) in 0.1M PIPES buffer on ice (0.058g L^{-1} NaCl, 0.3g L^{-1} piperazine-*N*,*N*′bis[2-ethanesulfonic acid], 0.02g L^{-1} $MgCl_2{\cdot}6H_2O$, 0.1M NaOH) and then incubated at 4°C for 1h. Subsequent TEM sample preparation and imaging were carried out by Anna Pielach at the Sir William Dunn School of Pathology EM facility. Fixed samples were washed once with PIPES buffer and then washed 4 times with MilliQ water, incubated for 5-10 minutes during each wash. Samples were then embedded in agarose to maintain pellet integrity and incubated in 0.5% uranyl acetate overnight at 4°C in the dark. Samples were then rinsed with MilliQ water for 10 minutes. To dehydrate samples they were serially incubated on ice in ice cold 30%, 50%, 70%, 80%, 90% (all v/v) anhydrous ethanol followed by two incubations in 100% anhydrous ethanol, each for 10 minutes. Samples were then placed in anhydrous ice-cold acetone and left at room temperature for 10 minutes. Samples were then transferred to room temperature anhydrous acetone for a further 20 minutes. Samples were then infiltrated with low viscosity resin (TLVR; TAAB Laboratory and Microscopy equipment) through incubation in 3:1 acetone:TLVR for 1h and then 1:1 acetone:TLVR for for 2h and finally 1:3 acetone:TLVR with rotation. Samples were then incubated in TLVR overnight at RT. Resin was changed the next morning and again after another 4h. Samples were then embedded in Beem capsules filled with TLVR and resin was polymerised at 60°C for 24h. Sample blocks were then removed from capsules using a razor blade and ultra-thin sections taken using a Diatome diamond knife using a Leica UC7 ultramicrotome and mounted onto 200 mesh Cu grids. Grids were then placed section-side down on a droplet of Reynolds lead-citrate and incubated at RT for 5 minutes. Grids were washed by passing over a droplet of degassed MilliQ water, 5 times. Grids were then blotted on dry and left to dry completely. Imaging was performed at 120kV using an FEI Technai

12 transmission electron microscope and images acquired using a Gatan OneView CMOS camera with Digital Micrograph 3.0 software. CW layer thickness was measured using the line-profile tool in Fiji [500], taking 5 measurements per cell and averaging for each cell. Grey values (as a proxy for electron density) were calculated by the taking the average grey value from profile plots created from the line profiles.

7.5 *Biochemical methods*

7.5.1 Extraction of *S. aureus* cytoplasmic content

Bacteria from overnight cultures were inoculated into 200mL fresh TSB at an initial OD_{600} of 0.05 and grown at 30°C with shaking. Samples were then collected at 6h, 12h and 24h post-inoculation and chilled in an ice-ethanol bath for 10 minutes. OD_{600} was measured and entire cultures pelleted at 5000*g* for 15 minutes before pellets were snap frozen in liquid nitrogen, ensuring supernatants were completely removed by aspiration before freezing. Samples were then stored at -80°C before further processing. Cell samples were then resuspended to a final OD_{600} of 250 on ice and 1mL of sample homogenised with 0.25g of fine acid-washed glass beads. Homogenisation was performed using a FastPrep-24 *Classic*, with 4 cycles of homogenisation at 6.5m s^{-1} for 35s each time and incubation on ice for 2 minutes after the first two cycles. Homogenised samples were then pelleted at 16,000*g* for 10 mins at 4°C. 500μL of supernatant was then passed through 0.5mL 3kDa molecular weight cut-off filters pre-washed with sterile MilliQ water by centrifugation at 14,000*g* for 20 minutes at 4°C. Filtered supernatants were then lyophilised at 55°C in a CentriVap Benchtop Centrifugal Vacuum Concentrator (Labconco) until complete dryness (~4h). Samples were then stored at -20°C.

7.5.2 CW PGN purification

Bacteria from overnight cultures were inoculated into 1L TSB at an initial OD_{600} of 0.001 to allow at least 10 rounds of cell division before harvesting bacteria to purify CW samples. Upon reaching an OD_{600} of 0.5-0.9 for exponential phase samples (~6-7h), and after 24h for stationary phase samples, cultures were submerged in an ice-ethanol bath, chilled for 10 minutes and transferred to 500mL centrifuge tubes (polystyrene; PS) before harvesting at 13000*g* for 5 minutes in an Avanti J-26 XP High-Performance Centrifuge at 4°C. Supernatant was discarded and the pellet resuspended in 20mL of MilliQ water before transferring to 40mL boiling 8% (w/v) sodium dodecyl sulphate (SDS) with stirring. Tubes were rinsed

with a further 20mL cold MilliQ and added to the SDS sample. Samples were then boiled for 30 minutes before cooling to RT. Samples were stored at RT overnight before resuming purification the next morning. Samples were transferred to 50mL centrifuge tubes (PS) and pelleted before filling with the remaining sample and pelleting again at 20000*g* for 10 minutes each time. Supernatant was discarded and the pellet resuspended in warm MilliQ water to wash out SDS. This was repeated iteratively until the absence of SDS could be determined using the Hayashi method [535]. Briefly, 250μL of sample supernatant was added to 125μL of methylene blue solution (0.05% (w/v) methylene blue, 0.665mM sodium phosphate buffer pH 7.2, 5% (v/v) choloroform), vortexed for 30s and the aqueous phase checked against a water only control to determine lack of blue colour and thus SDS absence. Samples were stored at -80ºC at this point.

The SDS-free pellets were then defrosted and resuspended in MilliQ water and transferred to a 2.2mL screw cap tube containing ~250mg acid-washed glass beads and homogenised using a FastPrep-24 *Classic*, with 10 cycles of homogenisation at 4.5m s^{-1} for 30s each time. Samples were chilled on ice for 2 minutes between each cycle. Unbroken cells and glass beads were pelleted at 500*g* for 10 minutes at 4ºC and supernatants transferred to a 50mL centrifuge tube (PS). Glass beads were washed three times with 2mL MilliQ water and subsequent supernatants transferred to the same tube, taking care not to transfer glass beads. Tubes were then filled with MilliQ water and centrifuged at 10000*g* for 10 minutes at 4ºC. Supernatant was carefully removed and samples resuspended in 10mL 50mM Tris-HCl (pH 7.0). $MgSO_4$ was added to a concentration of 20mM and then DNAse I and RNAse A added to final concentrations of 10μg mL^{-1} and 50μg mL^{-1}, respectively and incubated at 37ºC for 2h with shaking at 180rpm. $CaCl_2$ was then added to a final concentration of 10mM and Trypsin to 100μg mL^{-1} and incubated at 37ºC with shaking at 180rpm.

SDS was then added to the samples to a final concentration of 1% (w/v) and samples boiled for 15 minutes. Samples were then centrifuged at 20000*g* for 15 minutes at RT. Samples were washed once with warm MilliQ water and then resuspended in 10mL LiCl (8M) and incubated at 37ºC for 15 minutes. Samples were pelleted again and resuspended in 10mL EDTA (100mM, pH 7.0) and incubated for a further 15 minutes at 37ºC. Samples were pelleted again and washed with warm MilliQ water before resuspension in 10mL Acetone and placed in a sonication bath for 5 minutes. Samples were then washed twice more with warm MilliQ before resuspension in 1mL of MilliQ water. Samples were then lyophilised overnight at 30ºC in pre-weighed 2mL tubes in a CentriVap Benchtop Centrifugal Vacuum Concentrator (Labconco) and dry mass of CW preparations calculated. Samples were

resuspended to a final concentration of 20mg mL^{-1} and frozen at -20°C until further use.

To remove wall teichoic acids from the CW preparations, 10mg samples were treated with 2mL of concentrated hydrofluoric acid (46% v/v) and incubated with rocking at 4°C for 48h. Samples were then diluted to a final volume of 15mL with 100mM Tris-HCl (pH7.0) and transferred to a 50mL centrifuge tube (PS). Centrifuge tubes were then filled with Tris-HCl and centrifuged at 20000*g* for 30 minutes at 4°C. Samples were iteratively washed with Tris-HCl until the pH of the supernatant reached pH 7.0-7.5. Samples were then washed with MilliQ water twice. Samples were finally resuspended in 1mL of MiliQ water and lyophilised overnight as before and PGN samples resuspended to a final concentration of 20mg mL^{-1}. PGN samples were frozen at -20°C until further use.

7.5.3 Purification of mCherry::PGRP-SA

Purification of PGRP-SA was carried out by Gonçalo Covas. *E. coli* BL21a(DE3) were transformed with a pET21a derivative carrying the mCherry::PGRP-SA construct and plated in LBA Amp^{100}. 50mL overnight cultures were grown in LBB supplemented with Amp^{100} and back-diluted to OD_{600} 0.05 in 1L LBB Amp^{100} then grown at 25°C at 120rpm until OD ~0.5. Induction of mCherry::PGRP-SA expression was initiated with the addition of 1mM isopropyl β-D-1-thiogalactopyranoside (IPTG) and grown for a further 16h. Bacteria were harvested in 500mL centrifuge tubes (PS) at 8700*g* for 7 minutes at 4°C and washed once with 20mL equilibration buffer (50mM Na_2PO_4 pH 7.4, 300mM NaCl) before pelleting again. Pellets were then resuspended in 40mL equilibration buffer and lysed through 3 cycles in French Press apparatus at 1000psi. Lysates were pelleted at 30000*g* for 20 minutes at 4°C. The pellet was then resuspended in 20mL resuspension buffer (50mM Na_2PO_4 pH 7.4, 500mM NaCl, 8M urea) and incubated at 4°C with rocking for ~60h until the suspension appeared homogeneous. Samples were pelleted again, diluted to 4M urea using dilution buffer (50mM Na_2PO_4 pH 7.4, 500mM NaCl) and incubated at 4°C with rocking for a further 24h. Samples were then pelleted at 1500*g* for 10 minutes at 4°C and mixed with 10mL pre-washed metal affinity resin (Talon) and incubated at 4°C with rocking for 1h. Resin with bound mCherry::PGRP-SA was then recovered by centrifugation at 1500*g* for 2 minutes at 4°C. Resin was then washed once with 30mL wash solution (50mM Na_2PO_4 pH 7.4, 300mM NaCl, 4M urea) and then three times with 5mL wash solution. Resin was then washed once with 10mL wash solution containing 5mM imadazole and then once with 10mL wash solution containing 10mM imadazole. Protein was eluted from the resin using 5mL elution buffer (50mM Na_2PO_4 pH 7.4, 300mM NaCl, 150mM imadzole) at 4°C

with rocking for 1h. Resin was separated by centrifugation at 1500*g* for 2 minutes at 4°C. Supernatant was collected and washing repeated twice more with 5mL and then 2mL elution buffer. Combined supernatants were dialysed overnight against 5L PBS (pH 6.0), three times. Aliquots of purified mCherry::PGRP-SA were snap frozen in liquid nitrogen and stored at -80°C.

7.6 *Chromatography and mass spectrometry*

7.6.1 Analysis of cytoplasmic GlcNAc-6-P levels by LC-MS/MS

Samples prepared as in Subsection 7.5.1 were thawed on ice and dissolved in 80% (v/v) methanol. Subsequent analysis of cytoplasmic metabolite content was performed by Elisabete Pires of the McCullagh Group (Chemistry Research Laboratory, University of Oxford). Metabolite analysis was performed using a Thermo Scientific ICS-5000+ ion chromatography system coupled directly to a Q-Exactive HF Hybrid Quadrupole-Orbitrap mass spectrometer (MS) with a HESI II electrospray ionisation source (Thermo Scientific, San Jose, CA). This system incorporates an electrolytic anion generator (KOH) which was programmed to produce an OH- gradient from 5-100mM over 37 minutes (Figure 7.2 A). An in-line electrolytic suppressor was employed to remove OH^- ions and cations from the post-column eluent prior to eluent delivery to the electrospray ion source of the MS system (Thermo Scientific Dionex AERS 500). A 10μL partial loop injection was used for all analyses and the chromatographic separation was performed using a Thermo Scientific Dionex IonPac AS11-HC 2 x 250mm ion chromatography (IC) column, (4μm particle size) with a Dionex Ionpac AG11-HC 4μm 2 x 50mm guard column in-line. The flow rate was 0.250mL min^{-1} and the hydroxide ion gradient was as depicted in Figure 7.2 A. Analysis was performed in negative ion mode using a scan range from 80-900 and resolution set to 70,000. The tune file source parameters were set as follows: sheath gas flow; 60 ms^{-1}, auxillary gas flow; 20ms^{-1}, spray voltage; 3.6 V, capillary temperature; 320°C, S-lens retardation factor value; 70, heater temperature; 450°C. The automatic gain control target was set to $1x10^6$ and the maximum ionisation time value was 250ms. The column temperature was kept at 30°C throughout the experiment and full scan data were acquired in continuum mode across a mass-to-charge ratio (m/z) range of 60-900. The m/z of a GlcNAc-6-P standard was determined as 300.04892 with a column retention time of 12.41 minutes (data not shown). This information was used to identify the peaks of interest in the data and raw abundance data were collected (counts per second; cps). See Section 7.8 for details of statistical analysis.

7.6.2 Analysis of cell wall peptidoglycan structure by RP-HPLC

Muropeptides were prepared for analysis by RP-HPLC by digestion of 0.5mg purified PGN (see Subsection 7.5.2) in 12.5mM $NaHPO_4$ (pH 5.5) containing 0.5mg mL^{-1} Mutanolysin. Samples were incubated at 37°C for 16h before adding 100μL MilliQ water and boiling for 5 minutes. Samples were pelleted at 16000g for 5 minutes and supernatants kept. Muropeptides were reduced by adding an equal volume of borate buffer (100mM $Na_2B_4O_7$-HCl, 150mM NaCl, pH 9.0) was added to samples along with 50μL freshly prepared $NaBH_4$ (50mg mL^{-1}) and incubated at RT for 2h. After 2h the reaction was ended by adding orthophosphoric acid (85% v/v) to adjust the pH to 2.0. Samples were centrifuged at 13000g for 5 minutes to remove undigested material and supernatants used for injection into the HPLC apparatus.

Eluents A (100mM $NaHPO_4$, 5% v/v methanol, pH2.0) and B (100mM $NaHPO_4$, 30% methanol, pH2.0) were prepared to elute muropeptides, filtered through a 0.2μm filter and thoroughly degassed through sonication for 15 minutes. Samples were injected into a Hypersil ODS C-18 column (125mmx4mm, Thermo Electron Corporation) (50μL) using a Shimadzu Prominence HPLC system. Samples were eluted at a flow rate of 0.5mL min^{-1} with a profile as shown in Figure 7.2. Sample absorbance was measured at 206nm. Data analysis was performed using Shimadzu prominence software and peaks identified where possible from comparison to previous work [84, 85] and reference HPLC profiles from the

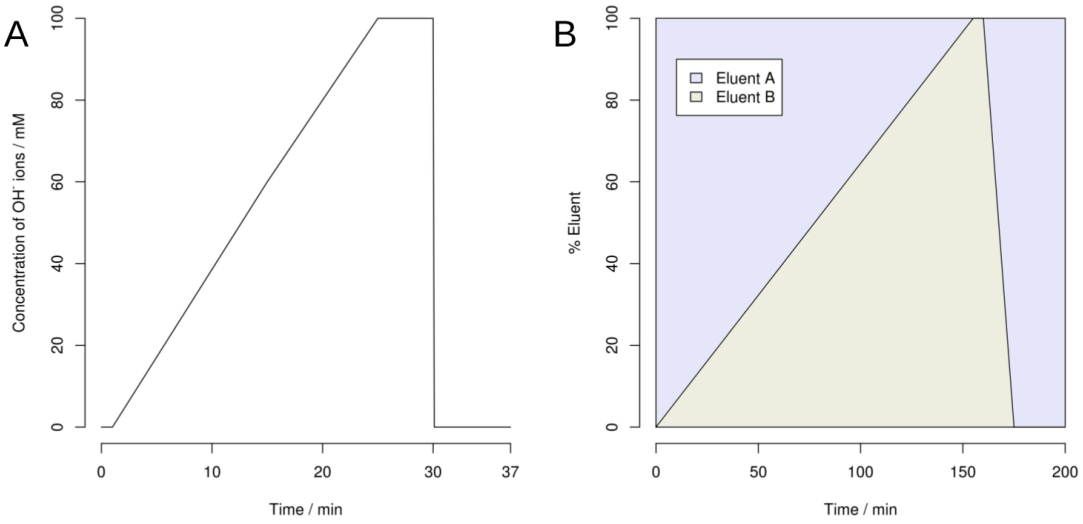


FIGURE 7.2: ***Elution profiles for ion chromatography and RP-HPLC.*** *The OH^- ion profile used for IC (Subsection 7.6.1) was as depicted in panel A (0mins; 0mM, 1min; 0mM, 15mins; 60mM, 25mins; 100mM, 30mins; 100mM, 30.1mins; 0mM, 37mins; 0mM). The elution profile used for RP-HPLC was as depicted in panel B (0min; 100% eluent A, 155min; 100% eluent B, 160min; 100% eluent B, 175min; 100% eluent A, 200min; 100% eluent A).*

Bacterial Cell Surfaces and Pathogenesis Lab (S. Filipe, ITQB, Oeiras, Portugal).

7.7 *Host-pathogen interaction*

7.7.1 Drosophila culture

D. melanogaster flies were raised at 25ºC with a 12h light:dark cycle. Flies were fed on food produced by the Media and Glassware Sterilisation Lab (New Biochemistry, University of Oxford). Food contained 7.69g L^{-1} agar, 34.6g L^{-1} maize, 4.15g L^{-1} soya, 7.04g L^{-1} yeast, 69.2g L^{-1} malt, and 19.2 mL L^{-1} molasses. Agar was first dissolved in water by heating to 95ºC with stirring, and once at temperature the remaining ingredients were added, cooked for 2-4 minutes and then cooled to 75ºC. Then orthophosphoric acid was added to 0.12% (v/v), propionic acid to 1.92% (v/v), and Nipagin to 3% (w/v) and the mixture stirred well. Food was then poured into bottles and cool to RT. Flies were routinely cultures in bottles containing ~50mL food, but following infection were transferred to vials containing ~10mL food for observation.

7.7.2 Bacterial inoculate preparation, spent supernatant preparation and injection of *Drosophila melanogaster*

Bacteria were grown in TSB as detailed in Subsection 7.3.1 overnight in 20mL cultures. After 18h of growth, entire cultures were pelleted at 5000*g* for 10 minutes at 4ºC, washed twice with PBS (pH 7.4) and finally resuspended in PBS and diluted to pre-determined concentrations to ensure injection of ~200 CFU per fly in a 13.8nL injection (see below). All inoculate preparation was done on ice. Spent bacterial culture supernatants were saved from similar overnight cultures, and filtered through 0.2μm filters before injection into *Drosophila*.

Bacterial cells and spent culture supernatant samples were injected into *Drosophila* via the anepisternum (a soft area of the thorax, below the wing) of adult flies using a Nanoject II microinjector (Drummond Scientific) via pulled glass capillary tubes. Flies were always used 3-5 days post-eclosion as adults, and kept in groups of 15-20 in vials. Prior to infection, flies were shifted to 30ºC for 24h, and kept at 30ºC post-infection.

7.7.3 Survival assays and determination of infection bacterial titres

After infection, survival was assayed at 0h, 3h, 6h, 12h and then every 12h for 72h. Those flies dying within the first 6h of infection were excluded from analysis as they likely represent

casualties after injection. The number of flies excluded was normally between 0-2 and did not exceed 4 on any occasion. Survival data was analysed using the `survival` package [536] for `R`. Survival data was taken from 6 independent survival assays for each *Drosophila* strain (25174 and 25174^{seml}), resulting in sample sizes of ~330 flies per strain in 25174 and ~240 flies per strain in 25174^{seml}. See Section 7.8 for details of statistical analysis.

Bacterial infection titres were determined by collecting groups of 6 flies infected in the same way as for survival experiments at 0h and then every 12h for 48h. Flies were homogenised in ice cold TSB on ice and homogenates serially diluted in fresh ice cold TSB. 100μL of pre-determined dilutions (data not shown) were plated on TSA to achieve colony counts of ~30-300 colonies in at least one of the plated dilutions. Platings were made in duplicate. Plates were then incubated for 24-30h at 30^{o}C and plates photographed. Colonies were then enumerated using the automatic colony counting program OpenCFU [534] with manual inspection to ensure accurate counting. Data were collected in two blocks, as practical issues made it very difficult assay all strains at once but as CFU counts of NCTC8325-4 were similar between blocks data were combined (see Figure C.4). See Section 7.8 for details of statistical analysis.

7.7.4 Assessment of Drosomycin::GFP production and *drs* transcription levels

D. melanogaster DD1 and *DD1*^{seml} flies were injected with spent culture supernatant as detailed in Subsection 7.7.2, and 18h after injection, groups of 6 flies were collected and either imaged as in Subsection 7.4.2 for assessment of Drosomycin::GFP production or snap-frozen in liquid nitrogen for isolation of RNA and assessment of *drs* transcription levels. For those flies that were imaged, Drosomycin::GFP signal was quantified by selecting the areas of the images occupied by flies and taking measurements of the measured area (A), the integrated density (ID) of the area (the product of the area measured and the mean grey value of that area), and mean grey value of the background (GB) before calculating CTF as follows; `CTF = ID - (A x GB)`. These values were then averaged over the number of flies imaged in each replicated for each strain/fly line combination and analysed as described in Section 7.8).

For RNA extraction flies were defrosted on ice and homogenised in Buffer RL (Norgen). Debris was pelleted by centrifugation at 14000*g* for 2 minutes and supernatant used for RNA extraction using a Norgen Total RNA purification kit (Biotek Corporation). Final RNA concentration was measured using a Nanodrop1000 and cDNA sythesised using a

SensiFAST cDNA synthesis kit (Bioline) using 500ng of RNA. cDNA was then stored at -80°C until further use. qRT-PCR was carried out using a SensiFAST SYBR No-ROX kit (Bioline) in a Rotor-Gene Q qRT-PCR machine (Qiagen). A thermal profile of 95°C for 2min, followed by 40 cycles of 95°C for 5s, 60°C for 10s, 72°C for 10s was employed, followed by a final melt curve analysis. Fold change of *drs* expression was calculated relative to *tbp* (TATA-box binding-protein) mRNA levels, previously validated as a reliable internal control [457, 293], using the $2^{\Delta\Delta\text{-CT}}$ method [537], relative to TSB control injected flies. See Section 7.8 for details of statistical analysis.

7.8 *Statistical analyses*

All statistical analyses were performed using `R` [488]. All statistical models were built including all possible interactions first (maximal model), and where appropriate (i.e. where model terms had little or no explanatory power) iterative model simplification was performed via likelihood ratio testing (LRT) [538] with highest order non-significant interactions removed first. Non-significant interaction effects were incrementally removed and the goodness of fit of the original model and simplified model to the data compared by ANOVA to ensure the minimum adequate model was used for analysis. Model simplification by LRT was performed as erroneous inclusion of interaction effects can lead to incorrect model interpretation. If removal of any interaction effect reduced the explanatory power of the model, model simplification was halted and the resulting minimum adequate model was used for analysis. Table 7.2 lists the minimum adequate models used for statistical analysis, indexed by the respective Figure that the given model refers to. For the most part, general linear models (`lm`) were employed, but where data exhibited violations of the assumptions of general linear modelling, data were transformed to conform to assumptions (e.g. F3.1 C in Table 7.2) or generalised linear models (`glm`; e.g. F3.5 A in Table 7.2) were used in their place with appropriately defined error structures and link functions. For analysis of *drs* mRNA levels following injection of spent culture supernatants (F5.2 B in Table 7.2), data was first transformed by Box-Cox transformation [515] using the `MASS` package for `R` [539] as it was not possible to satisfactorily fit raw fold-change data to any attempted model.

Error structures and link functions were chosen for generalised linear models following interpretation of diagnostics of general linear models specifying the same relationship and through iterative improvement of model fitting to the data. Gamma error distributions

(with the canonical 'log' link function for this distribution) were used when data exhibited an increasing mean~variance relationship with an asymmetry between the positive and negative residuals and a non-normal distribution of errors. Link functions specify the relationship between the linear predictor (e.g. time) with the mean of the given error distribution, and in some cases non-canonical link functions (e.g. identity, inverse) were used to better match the the mean of the error distribution for a given data set. A quasipossion distribution and 'log' link function was used in analysis of CFU counts in F3.6 (see Table 7.2) to account for the non-normality, 0-bounded cut-off and over-dispersion of the data [538]. However, the same error structure was not used for later CFU analyses in F5.3 (see Table 7.2) as models using this error structure fit the data poorly and instead Gamma error structures with 'log' link functions were employed. Where appropriate (e.g. F3.6 F, Table 7.2) a quadratic relationship between the linear predictor and the response variable was specified to take into account non-linearity of the response. For survival analysis, a Cox's proportional hazards model applied to a Kaplan-Meier survival object (see Table 7.2) was employed to assess the influence of bacterial strain on the rate of fly death at a particular point in time. Kaplan–Meier survival objects are complex objects comprising discrete stepped survivorship data accrued as each death occurs (see Figure 5.3) and information on whether an individual had died at a particular time, or whether it was simply last seen alive at that time (status; see Table 7.2).

Assessment of overall treatment effects was made using ANOVA where general linear models were used and ANODE for generalised linear models. In the case of assessment of *in vivo* growth of PCM's in *D. melanogaster 25174* data were analysed using ANOVA for an unbalanced design (Type-3 errors, due to extra NCTC8325-4 replicates from the blocked design) using the `car` package for R [540]. Where multiple comparisons were required, DMC's were used where responses of strains were compared to that of the wild-type bacterium (NCTC8325-4 or JE2), TKMC's where similar comparisons between multiple strains were desirable, or OC's where comparisons were made between predictor~response relationships of different strains. Multiple comparisons were made using the `mutlcomp` package [541].

TABLE 7.2: Summary of statistical models used for data analysis.

Figure/Table	Figure Panel[1]	Model specification in R.[2]	Test	Contrasts
F3.1	B	`lm(r0~strain)`	ANOVA	-
	C	`lm(log(OD)~time+strain)`	ANOVA	DMC's
F3.3/FC.1	A; TSB	`lm(log(OD)~time*strain)`	ANOVA	DMC's / OC's
	A; G, MN B; TSB, G, GN C; G, GN D; TSB, GN	`lm(log(OD)~time+strain)`	ANOVA	DMC's
	C; TSB	`glm(OD~time*strain, family = Gamma(link = log))`	ANODE	DMC's / OC's
	D; GN	`glm(OD~time+strain, family = Gamma(link = identity))`	ANODE	DMC's
T3.1	A; TSB, G B; TSB, G C; TSB, G D; TSB	`lm(r0~strain)`	ANOVA	DMC's
	A; MN B; GN C; GN D; G, GN	`glm(r0~strain, family = Gamma(link = log))`	ANODE	DMC's
F3.5	A	`glm(zoi~strain, family= Gamma(link = inverse))`	ANODE	TKMC's
	C	`lm(zoi~strain)`	ANOVA	TKMC's
F3.6	B	`lm(r0~strain)`	ANOVA	DMC's
	C	`lm(log(OD)~time+strain)`	ANOVA	DMC's
	E	`lm(r0~strain)`	ANOVA	-
	F	`glm(CFU~time+I(time^2)+strain, family = quasipoisson(link = log))`	ANODE	-
F4.1	-	`glm(G6P_abd~time+strain, family = Gamma(link = log))`	ANODA	TKMC's
F5.2	A	`lm(CTF~treat*fly_line)`	ANOVA	OC's
	B	`lm(mRNA~treat*fly_line)`	ANOVA	OC's
F5.3	A; *25174*, *25174*^{seml}	`coxph(Surv(time,status)~strain)`	ANOVA	DMC's
	B; *25174*	`glm(cfu_fly~time+I(time^2)*strain, family = Gamma(link = log))`	ANODE	DMC's
	B; *25174*^{seml}	`glm(cfu_fly~time+I(time^2)+strain, family = Gamma(link = log))`	ANODE	-
F5.4	A-C	`lm(zoh~strain+time)`	ANOVA	DMC's
FC.3	-	`lm(CFU~strain)`	ANOVA	-
FC.4	-	`lm(cfu_fly~time*block)`	ANOVA	-

[1] MN; MurNAc, GN; GlcNAc. [2] `lm`; linear model, ~; "as a function of", `log`; $\log_{10}$, `OD`; OD_{600}, `+`; "with an additive effect of", `*`; 'with an interaction effect of', `glm`; generalised linear model, `family`; error structure/distribution family (`Gamma`, `quasipoisson`), `link`; link function (`log`, `identity`, `inverse`), `zoi`; zone of inhibition, `+I(time^2`; "fitting 'y' as a quadratic function of time", `G6P_abd`; GlcNAc-6-P abundance, `proportion_OD`; proportion of original OD_{600}, `CTF`; corrected total fluorescence, `mRNA`; Box-Cox transformed *drs* fold-change data, `treat`; treatment, `fly_line`; *D. melanogaster* fly line, `coxph`; Cox proportional hazards model, `Surv`; Kaplan-Meier survival object, `zoh`; zone of haemolysis, `block`; experimental block.

Appendix A

Additional primers and strains used in this study

TABLE A.1: Additional miscellaneous primers.

Primer ID	Sequence	Use	Source
pMAD 1	CTCCTCCGTAACAAATTGAGG	pMAD screening / sequencing	M. Atilano
pMAD 2	CGTCATCTACCTGCCTGGAC	pMAD screening / sequencing	M. Atilano
ptagOFw	CGAGTGAGAAGAAATGCC	*tagO* deletion screening	M. Atilano
ptagORv	CAAACGATTTATAGTCATGTC	*tagO* deletion screening	M. Atilano
p1atl	ATATAAGGTACTATCAAACG	*atl* deletion screening	M. Atilano
p2atl	CGAAACAATGAAATCACTTAGC	*atl* deletion screening	M. Atilano
qPCR_drs_fwd	GTACTTGTTCGCCCTCTTCG	qRT-PCR of *drs* mRNA	M. Atilano
qPCR_drs_rev	TTAGCATCCTTCGCACCAG	qRT-PCR of *drs* mRNA	M. Atilano
qPCR_tbp_fwd	GGCAAAGAGTGAGGACGACT	qRT-PCR of *tbp* mRNA	M. Atilano
qPCR_tbp_rev	GAGCCGACCATGTTTTGAAT	qRT-PCR of *tbp* mRNA	M. Atilano

TABLE A.2: Primers used to confirm intergation of pMAD constructs.

Primer ID	Sequence
glcA_int_A	CAGTAATGATGATAGGCTGCTT
glcA_int_B	CTTTAAACCCTGTGCCATTAT
murQ_int_A	AAGAAGATGACGAGACAAAATATC
murQ_int_B	CACTAAATACGCCACCAATAC
murP_int_A	GGAGTGTAAGAAGTGATGGAA
murP_int_B	CAAGCAACTGAATCACATCA
ptsG_int_A	CTGCACGCTTTAGATTATTGT
ptsG_int_B	CTACCCAAATATTGAATTCTGCT
treP_int_A	CGAAGGTACAGAACCAACAG
treP_int_B	CTGATCATGATTACACCAGAA
nagA_int_A	CAGGTTTCTTAGCAGGTTACTT
nagA_int_B	TTCCAGAAGCGTATTCAGTT
oppA_int_A	TCGTTCAATGAAAAATGATGA
oppA_int_B	GGCTTACCTTGCCAATAATC
ccpA_int_A	GCTTCACATGGCATTATCAG
ccpA_int_B	TGAAGTGGCTGATGAGTATTTAG
glvC_int_A	ATTGTTAATCCCATACCTAACATAA
glvC_int_B	AGCTAGAATAGTCTGTACCATCAGTT
scrA_int_A	ATGGATTAATGTAGTAGAACCAGA
scrA_int_B	TGGTATCTTCTAACATCATGAAAC

TABLE A.3: Primers used to create deletion constructs.

Primer ID	Sequence	RE*
glcA_p1	TGC**CCATGG**AATTTCAGAGATTGCGACAT	NcoI
glcA_p2	ACGTATTGGTAAAGCGCTAGATCAATTATTTGAAGCTAAATAA	-
glcA_p3	TTATTTAGCTTCAAATAATTGATCTAGCGCTTTACCAATACGT	-
glcA_p4	TGC**GAATTC**TGGATTAGCATCTATGAGGTAAG	EcoRI
murQ_p1	TGC**CCATGG**ACAATATGATGCACAATTTATGA	NcoI
murQ_p2	TCGTTTAACAATGTCACCATTCACTTCTTACACTCCCTAGTTT	-
murQ_p3	AAACTAGGGAGTGTAAGAAGTGAATGGTGACATTGTTAAACGA	-
murQ_p4	TGC**AGATCT**CGTTACAATAATATCAATCGCA	BglII
murP_p1	TGC**CCATGG**CAAGTCCCGTTAGCAGTTCG	NcoI
murP_p2	CATCGCCTTTGTCGTTCCTTAAATCCCTCCTAAGGTTGTCTATC	-
murP_p3	GATAGACAACCTTAGGAGGGATTTAAGGAACGACAAAGGCGATG	-
murP_p4	TGC**GGATCC**GCCATTTTCGATTGGGTTAT	BamHI
ptsG_p1	TGC**CCATGG**TCAACCTTTGAAGACATTACTTG	NcoI
ptsG_p2	ATAATTAGGAGGGATGTTGATGATCAAAAATGAAATTGAAGAATTG	-
ptsG_p3	CAATTCTTCAATTTCATTTTTGATCATCAACATCCCTCCTAATTAT	-
ptsG_p4	TGC**GGATCC**TAAGAGGACCTGTCGCTACA	BamHI
treP_p1	TGC**CCATGG**CTAGACGTGGTCAAAGTTTAGT	NcoI
treP_p2	AACGCCCCTTTTTTATTTTATTACATATATTTCACTCCCTTAATGTCT	-
treP_p3	AGACATTAAGGGAGTGAAATATATGTAATAAAATAAAAAAGGGGCGTT	-
treP_p4	TGC**AGATCT**TCACCATCAACATAATCAACC	BglII
nagA_p1	TGC**CCATGG**CACCAGCATCTTGGTTAAAT	NcoI
nagA_p2	GATTATTTATTAGCTAAATGTGTGGTATAAACCCTTCTTTATTTAT	-
nagA_p3	ATAAATAAAGAAGGGTTTATACCACACATTTAGCTAATAAATAATC	-
nagA_p4	TGC**GAATTC**GTAATTCGTCTACATTAAAAGGTT	EcoRI
oppA_p1	TGC**GGATCC**GGGAAACATTAGGTTTAGTAGGAG	BamHI
oppA_p2	CCAGCCTAATTTACAAAGCATATTACATTGCATTTCCCCCTTC	-
oppA_p3	GAAGGGGGAAATGCAATGTAATATGCTTTGTAAATTAGGCTGG	-
oppA_p4	TGC**CCATGG**CGCTAAATCTTTAATTGGTACATCT	NcoI
ptaA_p1	TGC**GGATCC**AATACCTAATTCGAAACCAGCAC	BamHI
ptaA_p2	TTTAAGAAGGATGACATTCAATGTAAAATTTAAACAGCTAAAGCGCAAA	-
ptaA_p3	TTTGCGCTTTAGCTGTTTAAATTTTACATTGAATGTCATCCTTCTTAAA	-
ptaA_p4	TGC**CCATGG**GTGGCACAATGTATTCAGTGATTAGT	NcoI
ccpA_p1	TGC**ACGCGT**CAGATCTTATTATGTCAGGCAAA	MluI
ccpA_p2	ACGTTTACAAGGAGGAAATTATGTAAATTCACAAAATTAGGCATTC	-
ccpA_p3	GAATGCCTAATTTTGTGAATTTACATAATTTCCTCCTTGTAAACGT	-
ccpA_p4	TGC**CCATGG**AATCGAAGAGTTTGTTTATGCA	NcoI
glvC_p1	TGC**GTCGAC**ACTCTTCGTGGCAAATATACTC	SalI
glvC_p2	GATATGGAGGGAATAGAAGATGTAATACAAAAAAAGACACATCACTAT	-
glvC_p3	ATAGTGATGTGTCTTTTTTTGTATTACATCTTCTATTCCCTCCATATC	-
glvC_p4	TGC**CCATGG**TGTCTAAGTTGAAGCAAGTTTG	NcoI
scrA_p1	TGC**GGATCC**GACGAAGATACTGGTTACTCATT	BamHI
scrA_p2	TCTGGTACAGGGGAATAAAGTATAAAAAAAAGAGGTATGACAGTAATCAA	-
scrA_p3	TTGATTACTGTCATACCTCTTTTTTTATACTTTATTCCCCTGTACCAGA	-
scrA_p4	TGC**CCATGG**CCGTTACAACTAAAGTTTCAATC	NcoI
glcB_p1	TGC**GGATCC**TGGTAAAACGGCATGACA	BamHI
glcB_p2	TTGAGATAGGGGATGTTTATATGTAATGATTAAAAATGAAACAGCA	-
glcB_p3	TGCTGTTTCATTTTTAATCATTACATATAAACATCCCCTATCTCAA	-
glcB_p4	TGC**CCATGG**AAATGGATGGAACAAGATAAA	NcoI

*RE; Restriction enzyme. RE sites are shown in bold, and additional sequence to aid in cleavage underlined.

TABLE A.4: Additional strains and plasmids used in this study.

Strain / plasmid	**Relevant characteristics**	**Source**
DH5α	*E. coli* cloning strain	Lab stock
pMAD	*E. coli* - *S. aureus* shuttle vector with a thermosensitive origin of replication in Gram-positive bacteria; Amp^R Ery^R $LacZ^+$	[476]
RN4220	Restriction deficient derivative of NCTC82325-4	R. Novick
JE2	MRSA; USA300 isolate	[490]
NE172	JE2 SAUSA300_0191 *bursa aurealis* insertion	[490]
NE395	JE2 SAUSA300_0686 *bursa aurealis* insertion	[490]
NE1457	JE2 SAUSA300_1672 *bursa aurealis* insertion	[490]
NE39	JE2 SAUSA300_2476 *bursa aurealis* insertion	[490]
NCTCΔ*atl*	NCTC8325-4 *atl* null mutant	[293]
NCTCΔ*tagO*	NCTC8325-4 *tagO* null mutant	[542]

Appendix B

Sequencing primers and sequencing results

TABLE B.1: Sequencing primers used in this study.

Primer ID	Sequence
glcA_SEQ	TGATGCTGCAAAATACAATAGC
glcA_SEQ2	AGTGTAAGGTCAAGGAAGTTGA
murQ_SEQ	TGCAAATTGTGAGACAAACG
murQ_SEQ_2	ACCTACTGCAGCAATAATTCGTT
murP_SEQ	AGGTATCTGAGCATGATGTGAAAG
ptsG_SEQ_1	CATTAAACGACGAAGAACAAAG
ptsG_SEQ_2	ATCCGATATGCCTTATCAACCTA
treP_SEQ	TAACGCAATTGTAGCGAGGA
nagA_SEQ	ACGGTAGCTTATACAAAGCTGTAA
nagA_SEQ_2	ACGAATTACTGCGCCACAT
nagA_SEQ_3	CTACTCGTCCATTGATTTTGAA
nagA_SEQ_4	CTGATGGTGCACACTTACTTCA
oppA_SEQ	GATGAAGCAAATAATCATTTAAGAC
oppA_SEQ_2	ATCAGCCATTCCACAACCT
ptaA_SEQ	ACGCCATCAACATCAAATAAA
ccpA_SEQ	CAATAAGTAACCTAATCTGCAACG
ccpA_SEQ_2	AAGTAACCTAATCTGCAACGAT
ccpA_SEQ3	TAGATTCACACATTTGTTGCTG
glvC_SEQ	AAATATCGACATTCTATCTGCCAAT
glvC_SEQ_2	GTCAATGTCGTTGTAGGTGTGTA
glvC_SEQ_3	TCAACTTGAACAAAATTAAGTCACCT
scrA_SEQ	AGGTATTTCATTAATTCTTGTCGTA
glcB_SEQ	TGTAACGTATTCTCTTTCAACTCG
glcB_SEQ_2	ACCGCAACCCATTGTACCT
glcB_SEQ_3	CCTATCTCAATTTCCGCTTCCA
glcB_SEQ_4	CACAAATGATCGTACTGAATTGAT
scrA_genF	ACTTAAGTAATACTCGCTTTTCCTA
scrA_genR	AAGACAGGCATCCACATCTAA
scrA_genSEQ1	ATCATGATTACTTCATTCAGACAT
scrA_genSEQ2	GCACATTCATACCGAAGAAACTAA
scrA_genSEQ3	TTGAAAATAACCAAGCCATC
scrA_genSEQ4	CACTAAAACGGGTGGATCAT
scrA_genSEQ5	TCTGTAATACCAAGTAATGCTGAA
scrA_genSEQ6	ATCTTTGTTCCGATTATACCA
scrA_genSEQ7	TATCATTTCAGCTAATCCAGCA
scrA_genSEQ8	CCACATATGATCAAAAGCATTA
scrA_genSEQ9	TACACAGTCAACAGTCTCACCAA
scrA_genSEQ10	GCTAACACCTAACATCAAAGAAT

TABLE B.2: Results of sequencing of pMAD constructs.

Plasmid	SNPs	Deletions	Insertions
pMADΔ*glcA*	-	-	-
pMADΔ*murQ*	-	-	-
pMADΔ*murP*	-	-	-
pMADΔ*ptsG*	-	-	-
pMADΔ*treP*	-	-	-
pMADΔ*nagA*	-	-	-
pMADΔ*oppA*	-	-	-
pMADΔ*oppBCDF*	-	-	-
pMADΔ*oppABCDF*	-	-	-
pMADΔ*ptaA*	-	-	-
pMADΔ*glvC*	-	-	-
pMADΔ*scrA*	A6578T	6281 C	6819 G
		G6589A	7058 G
		G6826T	7094 A
		G6973A	
		G7056T	
		G7057C	
pMADΔ*glcB*	-	-	-

TABLE B.3: Results of sequencing of final mutant strains.

Strain	CDS deletion*	SNPs	Deletions	Insertions
NCTCΔ*glcA*	10bp remaining	-	-	-
NCTCΔ*murQ*	1bp remaining	-	-	-
NCTCΔ*murP*	complete	-	-	-
NCTCΔ*ptsG*	complete	-	-	-
NCTCΔ*treP*	12bp remaining	-	-	-
NCTCΔ*nagA*	15bp remaining	-	-	-
NCTCΔ*oppA*	complete	-	-	-
NCTCΔ*glvC*	complete	-	-	-
NCTCΔ*scrA*	48bp remaining	-	-	-

*In some cases short stretches of CDS were left to avoid deleting parts of other genes or putative ribosomal binding sites.

Appendix C

Supplementary data

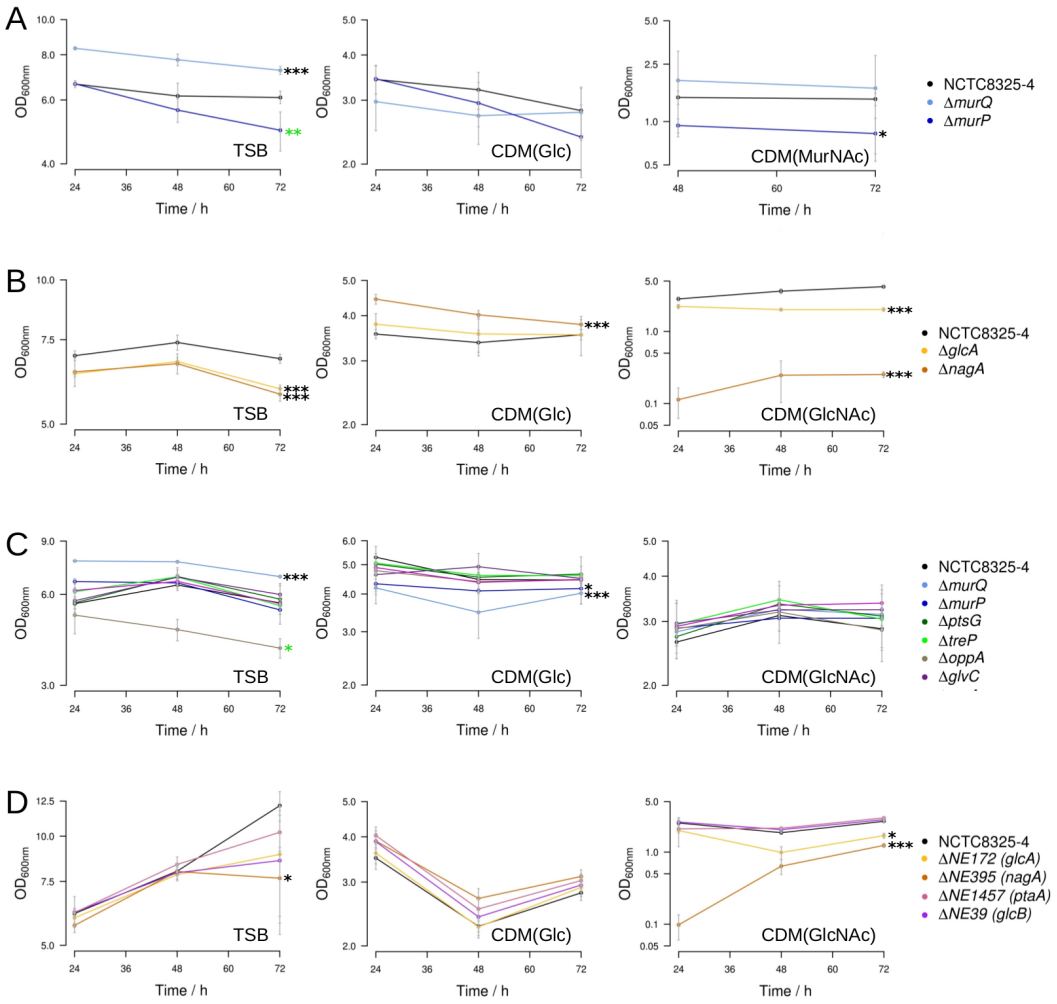


FIGURE C.1: ***Enlargements of panels from Figure 3.3 to more clearly show stationary phase OD_{600} dynamics.*** *Analyses of stationary phase dynamics in Figure 3.3 were conducted on OD_{600} data from 24-72h, except for those in CDM(MurNAc) which were conducted on data from 48-72h. Plots correspond to those in Figure 3.3 and represent an enlargement of the OD_{600} traces for the analysed time periods. All data points are representative of 3 independent biological replicates and error bars represent 95% confidence intervals. Significance levels; * $p < 0.05$, ** $p < 0.01$, *** $p < 0.001$. Black asterisks denote DMC's comparing PCM's to their respective parental strain, and green asterisks denote orthogonal contrasts (OC's) representing interaction effects between time and strain, again relative to the parental strain. See Figure 3.3 and Subsection 3.2.2 for further details.*

TABLE C.1: Output of statitical analyses for r_0 and stationary phase OD_{600} from Figure 3.3 and Table 3.1.

Panel[1]	**Medium**	**Analysis**[2]	**Test**	**Output**	**Response**[3]
A	TSB	r_0	ANOVA	$F_{2,6} = 2.31$, $p = 0.18$	strain
	TSB	SP	ANOVA	$F_{1,21} = 53.9$, $p < 0.001$ ***	time
				$F_{2,21} = 88.6$, $p < 0.001$	strain
				$F_{2,21} = 7.22$, $p < 0.01$ **	time*strain
	CDM(Glc)	r_0	ANOVA	$F_{2,6} = 14.9$, $p < 0.01$ **	strain
	CDM(Glc)	SP	ANOVA	$F_{1,23} = 11.7$, $p < 0.01$ **	time
				$F_{2,23} = 1.63$, $p = 0.22$	strain
B	TSB	r_0	ANOVA	$F_{2,6} = 19.1$, $p < 0.01$ **	strain
	TSB	SP	ANOVA	$F_{1,23} = 6.31$, $p < 0.05$ *	time
				$F_{2,23} = 12.8$, $p = < 0.001$ ***	strain
	CDM(Glc)	r_0	ANOVA	$F_{2,6} = 15.8$, $p < 0.01$ **	strain
	CDM(Glc)	SP	ANOVA	$F_{1,23} = 6.67$, $p < 0.05$ *	time
				$F_{2,23} = 6.67$, $p < 0.001$ ***	strain
C	TSB	r_0	ANOVA	$F_{7,16} = 3.94$, $p < 0.05$ *	strain
	TSB	SP	ANODE	$\chi^2_7 = 0.0830$, $p < 0.01$ **	time
				$\chi^2_7 = 1.08$, $p < 0.001$ ***	strain
				$\chi^2_7 = 0.130$, $p < 0.05$ *	time*strain
	CDM(Glc)	r_0	ANOVA	$F_{7,16} = 1.50$, $p = 0.24$	strain
	CDM(Glc)	SP	ANOVA	$F_{1,63} = 11.1$, $p < 0.01$ **	time
				$F_{7,63} = 7.63$, $p < 0.001$ ***	strain
D	TSB	r_0	ANOVA	$F_{4,10} = 19.9$, $p < 0.001$ ***	strain
	TSB	SP	ANOVA	$F_{1,39} = 63.7$, $p < 0.01$ **	time
				$F_{4,39} = 2.52$, $p < 0.05$ *	strain
	CDM(Glc)	r_0	ANODE	$\chi^2_4 = 0.00720$, $p = 0.77$	strain
	CDM(Glc)	SP	ANOVA	$F_{1,39} = 15.4$, $p < 0.001$ ***	time
				$F_{4,39} = 0.960$, $p = 0.44$	strain

[1] Panel; the panel to which testing corresponds in Figure 3.3, [2] Analysis; SP - stationary phase OD_{600}, r_0; maximum growth rate, [3] Response; the effect within the model to which the result given in the 'Output' column refers. All F values are given to 3 significant figures (S.F.) and p-values to 2 S.F's where appropriate.

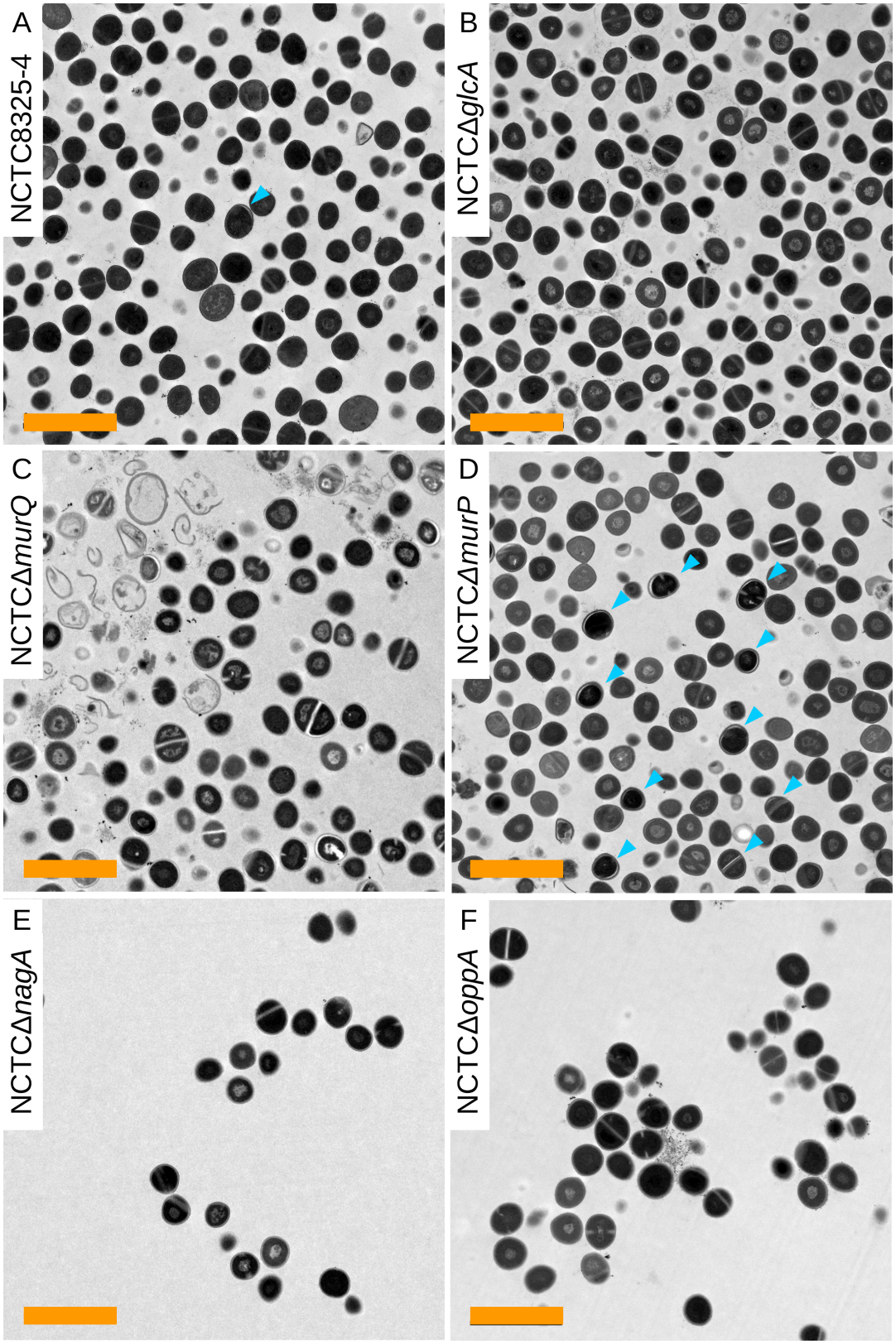


FIGURE C.2: ***Transmission electron microscopy field images of putative cell wall recycling mutants.*** *TEM studies of stationary phase (24h) cultures revealed a larger proportion of lysed cells in NCTCΔmurQ samples (C) and an increased proportion of cells in NCTCΔmurP cultures that appeared to accumulate poorly stained material beneath the plasma membrane (D; blue arrowheads). These cells were also observed in NCTC8325-4 cultures (A; blue arrowhead), but were far fewer in number. These data complement that presented in Figure 4.5. Scale bars represent 2µm.*

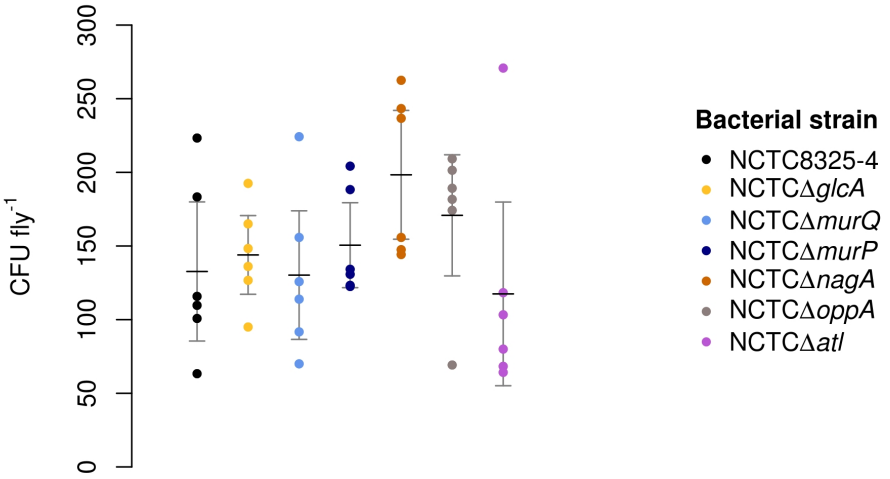


FIGURE C.3: ***Initial infection titres for D. melanogaster survival experiments.*** *D. melanogaster 25174 and 25174^{seml} flies were inoculated with ~100-200 CFU fly^{-1} for survival experiments (see Figure 5.3. Bacterial titres were assayed by plating 6 homogenised flies on TSA at the beginning of the experiment. Subsequent enumeration was conducted using Open CFU [534]. All inoculates were approximately equal (ANOVA; $F_{6,35}^{strain}$ = 1.55, p = 0.19). Data are representative of 6 independent biological replicates and presented with 95% confidence intervals.*

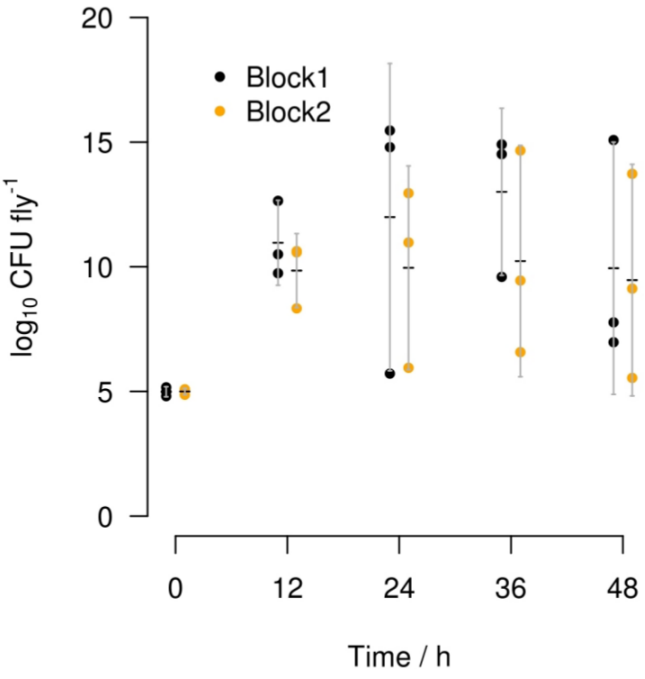


FIGURE C.4: ***In vivo growth of NCTC8325-4 in 25174 flies in different experimental blocks.*** *For assessment of bacterial in vivo growth in 25174 flies in Figure 5.3, experiments were split into two experimental blocks (see Chapter 7) as it was not possible to assess all mutants at once. As the bacterial titres of NCTC8325-4 included in both blocks was not statistically different (ANOVA; $F_{1,26}^{strain}$ = 3.52, p < 0.071), blocks were combined for analysis. Data points are representative of 3 independent biological repeats and error bars represent 95% confidence intervals.*

Bibliography

[1] Philip C J Donoghue and Jonathan B Antcliffe. "Origins of multicellularity". In: *Nature* 466.July (2010), pp. 41–42.

[2] Naji M Bassil, Nicholas Bryan, and Jonathan R Lloyd. "Microbial degradation of isosaccharinic acid at high pH". In: *The ISME Journal* 9.2 (2015), pp. 310–320. DOI: 10.1038/ismej.2014.125.

[3] J. R. Porter. "Antony van Leeuwenhoekl: Tercentenary of His Discovery of Bacteria". In: *Bacteriological Reviews* 40.2 (1976), pp. 260–269.

[4] R J Salton. "The Anatomy of the Bacterial Cell Surface". In: *Bacteriological Reviews* 25 (1961), pp. 77–99.

[5] S Mudd et al. "Bacterial Morphology as Shown by the Electron Microscope". In: *Journal of Bacteriology* 42.2 (1941), pp. 251–264.

[6] P. D. Cooper, D. Rowley, and I. M. Dawson. "Location of Radioactive Penicillin in Staphylococcus aureus after Contact with the Drug". In: *Nature* 164 (1949), p. 842.

[7] James T. Park and Marvin J. Johnson. "Accumualtion of labile phosphate in Staphylococcus aureus grown in the presence of penicillin". In: *Journal of Biological Chemistry* 179 (1949), pp. 585–592.

[8] M. R. J. Salton and R. W. Horne. "Studies of the Bacterial Cell Wall I. Electron microscopical observations on heated bacteria". In: *Biochimica et Biophysica Acta* 7 (1951), pp. 19–42.

[9] M. R. J. Salton and R. W. Horne. "Studies of the Bacterial Cell Wall II. Methods of preparation and some properties of cell walls". In: *Biochimica et Biophysica Acta* 7 (1951), pp. 177–197.

[10] M. R. J. Salton. "Studies of the Bacterial Cell Wall IV. The composition of the cell walls of some Gram-positive and Gram-negative bacteria". In: *Biochimica et Biophysica Acta* 10 (1953), pp. 512–523.

[11] C S Cummins and H Harris. "The Chemical Composition of the Cell Wall in some Gram-positive Bacteria and its Possible Value as a Taxonomic Character". In: *Journal of General Microbiology* 14 (1956), pp. 583–600.

[12] Mitchell L. Cohen. "Staphylococcus aureus: Biology, mechanisms of virulence, epidemiology". In: *The journal of Pediatrics* 108.5 (1986), pp. 796–799.

[13] Sharon J. Peacock, Ishani De Silva, and Franklin D. Lowy. "What determines nasal carriage of Staphylococcus aureus?" In: *Trends in Microbiology* 9.12 (2001), pp. 605–610. DOI: 10.1016/S0966-842X(01)02254-5.

[14] Heiman F L Wertheim et al. "The role of nasal carriage in Staphylococcus aureus infections". In: *Lancet Infectious Diseases* 5 (2005), pp. 751–762.

[15] J Kluytmans, Alex van Belkum, and Henri Verbrugh. "Nasal Carriage of Staphylococcus aureus : Epidemiology , Underlying Mechanisms , and Associated Risks". In: *Clinical Microbiology Reviews* 10.3 (1997), pp. 505–520.

[16] Steven Y C Tong et al. "Staphylococcus aureus Infections: Epidemiology, Pathophysiology, Clinical Manifestations, and Management". In: *Clinical Microbiology Reviews* 28.3 (2015), pp. 603–661. DOI: 10.1128/CMR.00134-14.

[17] Guy E Thwaites et al. "Clinical management of Staphylococcus aureus bacteraemia". In: *Lancet Infectious Diseases* 11.3 (2011), pp. 208–222. DOI: 10.1016/S1473-3099(10)70285-1.

[18] T J Foster. "Immune evasion by staphylococci". In: *Nature Reviews Microbiology* 3 (2005), pp. 948–958. DOI: 10.1038/nrmicro1289.

[19] Alfonso Zecconi and Federico Scali. "Staphylococcus aureus virulence factors in evasion from innate immune defenses in human and animal diseases". In: *Immunology Letters* 150.1-2 (2013), pp. 12–22. DOI: 10.1016/j.imlet.2013.01.004.

[20] Tomasz K. Prajsnar et al. "A privileged intraphagocyte niche is responsible for disseminated infection of staphylococcus aureus in a zebrafish model". In: *Cellular Microbiology* 14.10 (2012), pp. 1600–1619. DOI: 10.1111/j.1462-5822.2012.01826.x.

[21] Jessica Horn et al. "Inside job: Staphylococcus aureus host-pathogen interactions [Ahead of print]". In: *International Journal of Medical Microbiology* (2018), pp. 1–18. DOI: 10.1016/j.ijmm.2017.11.009.

[22] Timothy J Foster and Magnus Höök. "Surface protein adhesins of Staphylococcus aureus". In: *Trends in Microbiology* 6.98 (1998), pp. 484–488.

[23] Eric P Skaar and Olaf Schneewind. "Iron-regulated surface determinants (Isd) of Staphylococcus aureus: stealing iron from heme". In: *Microbes and Infection* 6 (2004), pp. 390–397. DOI: 10.1016/j.micinf.2003.12.008.

[24] Martin M Dinges, Paul M Orwin, and Patrick M Schlievert. "Exotoxins of Staphylococcus aureus". In: *Clinical Microbiology Reviews* 13.1 (2000), pp. 16–34.

[25] Katherine O Riordan and Jean C Lee. "Staphylococcus aureus Capsular Polysaccharides". In: *Clinical Microbiology Reviews* 17.1 (2004), pp. 218–234. DOI: 10.1128/CMR.17.1.218.

[26] Ing-marie Nilsson et al. "The Role of Staphylococcal Polysaccharide Microcapsule Expression in Septicemia and Septic Arthritis". In: *Infection and Immunity* 65.10 (1997), pp. 4216–4221.

[27] Manoj Thakker et al. "Staphylococcus aureus Serotype 5 Capsular Polysaccharide Is Antiphagocytic and Enhances Bacterial Virulence in a Murine Bacteremia Model". In: *Infection and Immunity* 66.11 (1998), pp. 5183–5189.

[28] Carla J C De Haas et al. "Chemotaxis Inhibitory Protein of Staphylococcus aureus, a Bacterial Antiinflammatory Agent". In: *Journal of Experimental Medicine* 199.5 (2004), pp. 687–695. DOI: 10.1084/jem.20031636.

[29] Suzan H M Rooijakkers et al. "Immune evasion by a staphylococcal complement inhibitor that acts on C3 convertases". In: *Nature Immunology* 6.9 (2005), pp. 920–927. DOI: 10.1038/ni1235.

[30] Kok P M van Kessel, Jovanka Bestebroer, and Jos A G van Strijp. "Neutrophil-mediated phagocytosis of Staphylococcus aureus". In: *Frontiers in Immunology* 5 (2014), pp. 1–12. DOI: 10.3389/fimmu.2014.00467.

[31] Margareta Verdrengh and Andrzej Tarkowski. "Role of Neutrophils in Experimental Septicemia and Septic Arthritis Induced by Staphylococcus aureus". In: *Infection and Immunity* 65.7 (1997), pp. 2517–2521.

[32] Lena Molne, Margareta Verdrengh, and Andrzej Tarkowski. "Role of Neutrophil Leukocytes in Cutaneous Infection Caused by Staphylococcus aureus". In: *Infection and Immunity* 68.11 (2000), pp. 6162–6167.

[33] M Strobel et al. "Post-invasion events after infection with Staphylococcus aureus are strongly dependent on both the host cell type and the infecting

S. aureus strain". In: *Clinical Microbiology and Infection* 22 (2016), pp. 799–809. DOI: 10.1016/j.cmi.2016.06.020.

[34] Divya Balasubramanian et al. "Staphylococcus aureus pathogenesis in diverse host environments". In: *Pathogens and Disease* 75.1 (2017), pp. 1–13. DOI: 10.1093/femspd/ftx005.

[35] Sarah Dubrac et al. "A matter of life and death: cell wall homeostasis and the WalKR (YycGF) essential signal transduction pathway". In: *Molecular Microbiology* 70.6 (2008), pp. 1307–1322. DOI: 10.1111/j.1365-2958.2008.06483.x.

[36] Aurélia Delauné et al. "The WalKR system controls major staphylococcal virulence genes and is involved in triggering the host inflammatory response". In: *Infection and Immunity* 80.10 (2012), pp. 3438–3453. DOI: 10.1128/IAI.00195-12.

[37] J Kajimura et al. "Identification and molecular characterization of an N-acetylmuramyl-L-alanine amidase Sle1 involved in cell separation of Staphylococcus aureus". In: *Mol.Microbiol.* 58.4 (2005), pp. 1087–1101. DOI: 10.1111/j.1365-2958.2005.04881.x.

[38] Andrew Watts et al. "Staphylococcus aureus strains that express serotype 5 or serotype 8 capsular polysaccharides differ in virulence". In: *Infection and Immunity* 73.6 (2005), pp. 3502–3511. DOI: 10.1128/IAI.73.6.3502-3511.2005.

[39] Patricia Reed et al. "Staphylococcus aureus Survives with a Minimal Peptidoglycan Synthesis Machine but Sacrifices Virulence and Antibiotic Resistance." In: *PLoS Pathogens* 11.5 (2015), e1004891. DOI: 10.1371/journal.ppat.1004891.

[40] H de Lencastre et al. "Antibiotic resistance as a stress response: complete sequencing of a large number of chromosomal loci in Staphylococcus aureus strain COL that impact on the expression of resistance to methicillin." In: *Microbial Drug Resistance* 5.3 (1999), pp. 163–175. DOI: 10.1089/mdr.1999.5.163.

[41] Krzysztof Sieradzki and Alexander Tomasz. "Inhibition of cell wall turnover and autolysis by vancomycin in a highly vancomycin-resistant mutant of Staphylococcus aureus". In: *Journal of Bacteriology* 179.8 (1997), pp. 2557–2566.

[42] Chie Yanagisawa et al. "Rapid depletion of free vancomycin in medium in the presence of β-lactam antibiotics and growth restoration in Staphylococcus aureus strains with β-lactam-induced vancomycin resistance". In: *Antimicrobial Agents and Chemotherapy* 53.1 (2009), pp. 63–68. DOI: 10.1128/AAC.00762-08.

[43] Shinsuke Ikeda et al. "Identification of the active component that induces vancomycin resistance in MRSA." In: *The Journal of antibiotics* 63.9 (2010), pp. 533–8. DOI: 10.1038/ja.2010.75.

[44] Yuriko Hirao et al. "Low level ß-lactamase production in methicillin-resistant staphylococcus aureus strains with ß-lactam antibiotics-induced vancomycin resistance." In: *BMC microbiology* 12.1 (2012), p. 69. DOI: 10.1186/1471-2180-12-69.

[45] Losee L Ling et al. "A new antibiotic kills pathogens without detectable resistance". In: *Nature* 517.7535 (2015), pp. 455–459. DOI: 10.1038/nature14098.

[46] Timothy J Foster. "Antibiotic resistance in Staphylococcus aureus. Current status and future prospects". In: *FEMS Microbiology Reviews* 41 (2017), pp. 430–449. DOI: 10.1093/femsre/fux007.

[47] V. R F Matias and Terry J. Beveridge. "Cryo-electron microscopy reveals native polymeric cell wall structure in Bacillus subtilis 168 and the existence of a periplasmic space". In: *Molecular Microbiology* 56.1 (2005), pp. 240–251. DOI: 10.1111/j.1365-2958.2005.04535.x.

[48] Valério R F Matias and Terry J. Beveridge. "Native cell wall organization shown by cryo-electron microscopy confirms the existence of a periplasmic space in Staphylococcus aureus". In: *Journal of Bacteriology* 188.3 (2006), pp. 1011–1021. DOI: 10.1128/JB.188.3.1011-1021.2006.

[49] V R F Matias et al. "Cryo-Transmission Electron Microscopy of Frozen-Hydrated Sections of Escherichia coli and Pseudomonas aeruginosa". In: *Journal of Bacteriology* 185.20 (2003), pp. 6112–6118. DOI: 10.1128/JB.185.20.6112.

[50] By Audrey M Glauert. "The topography of the bacterial cell wall". In: *Annual Reviews Microbiology* 23 (1969), pp. 159–198.

[51] Jeremy C Henderson et al. "The Power of Asymmetry: Architecture and Assembly of the Gram-Negative Outer Membrane Lipid Bilayer". In: *Annual Reviews Microbiology* 70 (2016), pp. 255–278. DOI: 10.1146/annurev-micro-102215-095308.

[52] C Weidenmaier and A Peschel. "Teichoic acids and related cell-wall glycopolymers in Gram-positive physiology and host interactions". In: *Nature Reviews Microbiology* 6 (2008), pp. 276–287. DOI: 10.1038/nrmicro1861.

[53] Guoqing Xia, Thomas Kohler, and Andreas Peschel. "The wall teichoic acid and lipoteichoic acid polymers of Staphylococcus aureus". In: *International Journal of Medical Microbiology* 300.2-3 (2010), pp. 148–154. DOI: 10.1016/j.ijmm.2009.10.001.

[54] P J Brennan. "Structure, function, and biogenesis of the cell wall of Mycobacterium tuberculosis". In: *Tuberculosis* 83 (2003), pp. 91–97. DOI: 10.1016/S1472-9792(02)00089-6.

[55] Patrick Brennan. "The envelope of mycobacteria". In: *Annual Reviews Biochemistry* 64 (1995), pp. 29–63.

[56] William Wiley Navarre and Olaf Schneewind. "Surface Proteins of Gram-Positive Bacteria and Mechanisms of Their Targeting to the Cell Wall Envelope". In: *Molecular and Molecular Biology Reviews* 63.1 (1999), pp. 174–229.

[57] Nathalie T. Reichmann and Angelika Gründling. "Location, synthesis and function of glycolipids and polyglycerolphosphate lipoteichoic acid in Gram-positive bacteria of the phylum Firmicutes". In: *FEMS Microbiology Letters* 319.2 (2011), pp. 97–105. DOI: 10.1111/j.1574-6968.2011.02260.x.

[58] Jonathan G Swoboda et al. "Wall Teichoic Acid Function, Biosynthesis, and Inhibition". In: *Chembiochem* 11.1 (2010), pp. 35–45. DOI: 10.1002/cbic.200900557.Wall.

[59] Silke Litzinger and Christoph Mayer. *The murein sacculus (Chapter 1). In: König H, Claus H, Varma A (Eds)*. Berlin: Springer, 2010, pp. 3–54. DOI: 10.1007/978-3-642-05062-6.

[60] Katherine O'Riordan and Jean C Lee. "Staphylococcus aureus Capsular Polysaccharides". In: *Clinical Microbiology Reviews* 17.1 (2004), pp. 218–234. DOI: 10.1128/CMR.17.1.218.

[61] G W Liechti et al. "A new metabolic cell-wall labelling method reveals peptidoglycan in Chlamydia trachomatis." In: *Nature* 506.7489 (2014), pp. 507–10. DOI: 10.1038/nature12892. arXiv: 15334406.

[62] Olga Jeske et al. "Planctomycetes do possess a peptidoglycan cell wall". In: *Nature Communications* 6.7116 (2015), pp. 1–7. DOI: 10.1038/ncomms8116.

[63] Sharanjeet Atwal et al. "Evidence for a peptidoglycan-like structure in Orientia tsutsugamushi". In: *Molecular Microbiology* 105.3 (2017), pp. 1–13. DOI: 10.1111/mmi.13709.

[64] Naoki Sato and Hiroyoshi Takano. "Diverse origins of enzymes involved in the biosynthesis of chloroplast peptidoglycan". In: *Journal of Plant Research* 130.4 (2017), pp. 635–645. DOI: 10.1007/s10265-017-0935-3.

[65] Hélène Barreteau et al. "Cytoplasmic steps of peptidoglycan biosynthesis". In: *FEMS Microbiology Reviews* 32 (2008), pp. 168–207. DOI: 10.1111/j.1574-6976.2008.00104.x.

[66] Ahmed Bouhss et al. "The biosynthesis of peptidoglycan lipid-linked intermediates". In: *FEMS Microbiology Reviews* 32.April (2008), pp. 208–233. DOI: 10.1111/j.1574-6976.2007.00089.x.

[67] Jean van Heijenoort. "Lipid Intermediates in the Biosynthesis of Bacterial Peptidoglycan". In: *Microbiology and Molecular Biology Reviews* 71.4 (2007), pp. 620–635. DOI: 10.1128/MMBR.00016-07.

[68] Eric Sauvage et al. "The penicillin-binding proteins: structure and role in peptidoglycan biosynthesis". In: *FEMS Microbiology Reviews* 32 (2008), pp. 234–258. DOI: 10.1111/j.1574-6976.2008.00105.x.

[69] Waldemar Vollmer and Stephen J Seligman. "Architecture of peptidoglycan: more data and more models". In: *Trends in Microbiology* 18.2 (2010), pp. 59–66. DOI: 10.1016/j.tim.2009.12.004.

[70] Waldemar Vollmer. "Structural variation in the glycan strands of bacterial peptidoglycan". In: *FEMS Microbiology Reviews* 32.2 (2008), pp. 287–306. DOI: 10.1111/j.1574-6976.2007.00088.x.

[71] K H Schleifer and O Kandler. "Peptidoglycan types of bacterial cell walls and their taxonomic implications." In: *Bacteriological Reviews* 36.4 (1972), pp. 407–477.

[72] Daniela Munch et al. "Identification and in vitro Analysis of the GatD / MurT Enzyme-Complex Catalyzing Lipid II Amidation in Staphylococcus aureus". In: *PLoS Pathogens* 8.1 (2012), pp. 1–11. DOI: 10.1371/journal.ppat.1002509.

[73] Teresa A. Figueiredo et al. "Identification of genetic determinants and enzymes involved with the amidation of glutamic acid residues in the peptidoglycan of Staphylococcus aureus". In: *PLoS Pathogens* 8.1 (2012). DOI: 10.1371/journal.ppat.1002508.

[74] Athanasios Typas et al. "Regulation of peptidoglycan synthesis by outer-membrane proteins". In: *Cell* 143.7 (2010), pp. 1097–1109. DOI: 10.1016/j.cell.2010.11.038.

[75] Waldemar Vollmer, Didier Blanot, and Miguel A. De Pedro. "Peptidoglycan structure and architecture". In: *FEMS Microbiology Reviews* 32.2 (2008), pp. 149–167. DOI: 10.1111/j.1574-6976.2007.00094.x.

[76] Boris A Dmitriev, Stefan Ehlers, and Ernst Th. Rietschel. "Layered murein revisited: a fundamentally new concept of bacterial cell wall structure , biogenesis and function". In: *Medical Micrbiology and Immunology* 187 (1999), pp. 173–181.

[77] Joachim-Volker Holtje. "Growth of the Stress-Bearing and Shape-Maintaining Murein Sacculus of Escherichia coli". In: *Microbiology and Molecular Biology Reviews* 62.1 (1998), pp. 181–203.

[78] Boris Dmitriev, Filip Toukach, and Stefan Ehlers. "Towards a comprehensive view of the bacterial cell wall". In: *Trends in Microbiology* 13.12 (2005), pp. 569–574. DOI: 10.1016/j.tim.2005.10.001.

[79] Arthur L Koch and Steven Woeste. "Elasticity of the Sacculus of Escherichia coli". In: *Journal of Bacteriology* 174.14 (1992), pp. 4811–4819.

[80] Gerhard Barnickel et al. "Conformational Energy Calculation on the Peptide Part of Murein". In: *European Journal of Biochemistry* 95 (1979), pp. 157–165.

[81] Abdelmadjid Atrih et al. "Structural Analysis of Bacillus subtilis 168 Endospore Peptidoglycan and Its Role during Differentiation". In: *Journal of Bacteriology* 178.21 (1996), pp. 6173–6183.

[82] Abdelmadjid Atrih et al. "Analysis of peptidoglycan structure from vegetative cells of Bacillus subtilis 168 and role of PBP 5 in peptidoglycan maturation". In: *Journal of Bacteriology* 181.13 (1999), pp. 3956–3966.

[83] Michael A Snowden and Harold R Perkins. "Peptidoglycan cross-linking in Staphylococcus aureus, an apparent random polymerisation process". In: *European Journal of Biochemistry* 191 (1990), pp. 373–377.

[84] Boudewijn L M De Jonge et al. "Peptidoglycan composition of a highly methicillin-resistant Staphylococcus aureus strain: The role of penicillin binding protein 2A". In: *Journal of Biological Chemistry* 267.16 (1992), pp. 11248–11254.

[85] Boudewijn L M de Jonge et al. "Peptidoglycan Composition in Heterogeneous Tn551 Mutants of a Methicillin-resistant Staphylococcus aureus strain". In: *Journal of Biological Chemistry* 267.16 (1992), pp. 11255–11259.

[86] Ivo G Boneca et al. "Characterization of Staphylococcus aureus Cell Wall Glycan Strands, Evidence for a New B-N-Acetylglucosaminidase Activity". In: *Journal of Biological Chemistry* 275.14 (2000), pp. 9910–9918.

[87] H Labischinski et al. "Confirmational and topological aspects of the three-dimensional architecture of bacterial peptidoglycan". In: *Annals of the Intitute Pasteur / Micrbiology* 136 A (1985), pp. 45–50.

[88] B Leps. "Conformational Behavior of the Polysaccharide Backbone of Murein". In: *Biopolymers* 26 (1987), pp. 1391–1406.

[89] Samy O Meroueh et al. "Three-dimensional structure of the bacterial cell wall peptidoglycan". In: *Proceedings of the National Academy of Sciences* 103.12 (2006), pp. 4404–4409.

[90] Valério R F Matias and Terry J Beveridge. "Cryo-electron microscopy of cell division in Staphylococcus aureus reveals a mid-zone between nascent cross walls". In: *Molecular Microbiology* 64.1 (2007), pp. 195–206. DOI: 10.1111/j.1365-2958.2007.05634.x.

[91] Bernd Glauner, Joachim-Volker Höltje, and Uli Schwarz. "The Composition of the Murein of Escherichia coli". In: *The Journal of Biological Chemistry* 263.21 (1988), pp. 10088–10095.

[92] Emma J Hayhurst et al. "Cell wall peptidoglycan architecture in Bacillus subtilis". In: *Proceedings of the National Academy of Sciences* 105.38 (2008), pp. 14603–14608.

[93] Robert D Turner et al. "Cell wall elongation mode in Gram-negative bacteria is determined by peptidoglycan architecture". In: *Nature Communications* 4 (2013), pp. 1496–1498. DOI: 10.1038/ncomms2503.

[94] Robert D Turner et al. "Peptidoglycan architecture can specify division planes in Staphylococcus aureus." In: *Nature Communications* 1.3 (2010), p. 26. DOI: 10.1038/ncomms1025.

[95] Bernd Glauner and Joachim-Volker Holtje. "Growth Pattern of the Murein Sacculus of Escherichia". In: *The Journal of Biological Chemistry* 265.31 (1990), pp. 18988–18997.

[96] Robert D Turner et al. "Molecular imaging of glycan chains couples cell-wall polysaccharide architecture to bacterial cell morphology". In: *Nature Communications* 9 (2018), p. 1263. DOI: 10.1038/s41467-018-03551-y.

[97] Richard Wheeler et al. "Super-resolution microscopy reveals cell wall dynamics and peptidoglycan architecture in ovococcal bacteria". In: *Molecular Microbiology* 82.5 (2011), pp. 1096–1109. DOI: 10.1111/j.1365-2958.2011.07871.x.

[98] P Demchick and Arthur L Koch. "The Permeability of the Wall Fabric of Escherichia coli and Bacillus subtilis". In: *Journal of Bacteriology* 178.3 (1996), pp. 768–773.

[99] David Pink et al. "On the Architecture of the Gram-Negative Bacterial Murein Sacculus". In: *Journal of Bacteriology* 182.20 (2000), pp. 5925–5930.

[100] Boris A Dmitriev et al. "Tertiary Structure of Bacterial Murein: the Scaffold Model". In: *Journal of Bacteriology* 185.11 (2003), pp. 3458–3468. DOI: 10.1128/JB.185.11.3458.

[101] Boris A Dmitriev et al. "Tertiary Structure of Staphylococcus aureus Cell Wall Murein". In: *Journal of Bacteriology* 186.21 (2004), pp. 7141–7148. DOI: 10.1128/JB.186.21.7141.

[102] Hartmann Harz, Knut Burgdorf, and Joachim-Volker Holtje. "Isolation and Separation of the Glycan Strands from Murein of Escherichia coli by Reversed-Phase High-Performance Liquid Chromatography". In: *Analytical Biochemistry* 190 (1990), pp. 120–128.

[103] Waldemar Vollmer and Joachim-volker Holtje. "The Architecture of the Murein (Peptidoglycan) in Gram-Negative Bacteria: Vertical Scaffold or Horizontal Layer(s)?" In: *Journal of Bacteriology* 186.18 (2004), pp. 5978–5987. DOI: 10.1128/JB.186.18.5978.

[104] Lu Gan, Songye Chen, and Grant J Jensen. "Molecular organization of Gram-negative peptidoglycan". In: *Proceedings of the National Academy of Sciences* 105.48 (2008), pp. 18953–18957.

[105] R W H Verwer et al. "Arrangement of Glycan Chains in the Sacculus of Escherichia coli". In: *Journal of Bacteriology* 1.2 (1978), pp. 723–729.

[106] Richard J. Wheeler, Eva Gluenz, and Keith Gull. "The cell cycle of Leishmania: Morphogenetic events and their implications for parasite biology". In: *Molecular Microbiology* 79.3 (2011), pp. 647–662. DOI: 10.1111/j.1365-2958.2010.07479.x.

[107] Guillaume Andre et al. "Imaging the nanoscale organization of peptidoglycan in living Lactococcus lactis cells". In: *Nature Communications* 1.27 (2010), pp. 1–8. DOI: 10.1038/ncomms1027.

[108] Kazunobu Amako and Akiko Umeda. "Concentric Circular Structure of the Cell Wall of Staphylococcus epidermidis Revealed by the Scanning Electron Microscope". In: *Journal of Electron Microscopy* 27.2 (1978), pp. 147–148.

[109] João M Monteiro et al. "Cell shape dynamics during the staphylococcal cell cycle". In: *Nature Communications* 6 (2015), pp. 1–12. DOI: 10.1038/ncomms9055.

[110] Bernard Badet et al. "Glucosamine Synthetase from Escherichia coli: Purification, Properties, and Glutamine-Utilizing Site Location". In: *Biochemistry* 26.7 (1987), pp. 1940–1948. DOI: 10.1021/bi00381a023.

[111] Dominique Mengin-Lecreulx, Jean van Heijenoort, and James T Park. "Identification of the mpl Gene Encoding UDP- N -Acetylmuramate: L-Alanyl- y-D-Glutamyl-meso-Diaminopimelate Ligase in Escherichia coli and Its Role in Recycling of Cell Wall Peptidoglycan". In: *Journal of Bacteriology* 178.18 (1996), pp. 5347–5352.

[112] Laure Jolly et al. "Autophosphorylation of Phosphoglucosamine Mutase from Escherichia coli". In: *Journal of Bacteriology* 182.5 (2000), pp. 1280–1285.

[113] Dominique Mengin-Lecreulx and Jean Van Heijenoort. "Identification of the glmU Gene Encoding N-Acetylglucosamine-1-Phosphate Uridyltransferase in Escherichia coli". In: *Journal of Bacteriology* 175.19 (1993), pp. 6150–6157.

[114] Dominique Mengin-Lecreulx and Jean van Heijenoort. "Copurification of Glucosamine-1-Phosphate Acetyltransferase and N-Acetylglucosamine-1-Phosphate Uridyltransferase Activities of Escherichia coli: Characterization of the glmU Gene Product as a Bifunctional Enzyme Catalyzing Two Subsequent Steps in the Pat". In: *Journal of Bacteriology* 176.18 (1994), pp. 5788–5795.

[115] John L Marquardt et al. "Cloning and Sequencing of Escherichia coli murZ and Purification of Its Product, a UDP-N-Acetylglucosamine Enolpyruvyl Transferase". In: *Journal of Bacteriology* 174.17 (1992), pp. 5748–5752.

[116] Michael J Pucci, Linda F Discotto, and Thomas J Dougherty. "Cloning and Identification of the Escherichia coli murB DNA Sequence, Which Encodes UDP-N-Acetylenolpyruvoylglucosamine Reductase". In: *Journal of Bacteriology* 174.5 (1992), pp. 1690–1693.

[117] Kenneth Duncan, Jean Van Heijenoort, and Christopher T Walsh. "Purification and Characterization of the D-Alanyl-D-alanine-Adding Enzyme from Escherichia coli". In: *Biochemistry* 29.9 (1990), pp. 2379–2386. DOI: 10.1021/bi00461a023.

[118] Clyde A Smith. "Structure, Function and Dynamics in the mur Family of Bacterial Cell Wall Ligases". In: *Journal of Molecular Biology* (2006), pp. 640–655. DOI: 10.1016/j.jmb.2006.07.066.

[119] M Ikeda et al. "The Escherichia coli mraY Gene Encoding UDP-N-Acetylmuramoyl-Acetylmuramoyl-Pentapeptide Transferase". In: *Journal of Bacteriology* 173.3 (1991), pp. 1021–1026.

[120] Dominique Mengin-Lecreulx et al. "The murG Gene of Escherichia coli Codes for the UDP-N- Acetylglucosamine: N-Acetylmuramyl-(Pentapeptide) Pyrophosphoryl-Undecaprenol N-Acetylglucosamine Transferase Involved in the Membrane Steps of Peptidoglycan Synthesis". In: *Journal of Bacteriology* 173.15 (1991), pp. 4625–4636.

[121] Boudewijn L M de Jonge et al. "Altered Muropeptide Composition in Staphylococcus aureus Strains with an Inactivated femA Locus". In: *Journal of Bacteriology* 175.9 (1993), pp. 2779–2782.

[122] U Henze et al. "Influence of femB on Methicillin Resistance and Peptidoglycan Metabolism in Staphylococcus aureus". In: *Journal of Bacteriology* 175.6 (1993), pp. 1612–1620.

[123] Kerstin Ehlert, Werner Schroder, and Harald Labischinski. "Specificities of FemA and FemB for Different Glycine Residues: FemB Cannot Substitute for FemA in Staphylococcal Peptidoglycan Pentaglycine Side Chain Formation". In: *Journal of Bacteriology* 179.23 (1997), pp. 7573–7576.

[124] S Rohrer et al. "The essential Staphylococcus aureus gene fmhB is involved in the first step of peptidoglycan pentaglycine interpeptide formation". In: *Proceedings of the National Academy of Sciences* 96 (1999), pp. 9351–9356.

[125] Ursula Kopp et al. "Staphylococcal Peptidoglycan Interpeptide Bridge Biosynthesis: A Novel Antistaphylococcal Target?" In: *Microbial Drug Resistance* 2.1 (1996), pp. 29–41.

[126] Alex Dajkovic et al. "Hydrolysis of peptidoglycan is modulated by amidation of meso-diaminopimelic acid and Mg2+ in Bacillus subtilis". In: *Molecular Microbiology* 104.6 (2017), pp. 972–988. DOI: 10.1111/mmi.13673.

[127] Tamimount Mohammadi et al. "Identification of FtsW as a transporter of lipid- linked cell wall precursors across the membrane". In: *The EMBO journal* 30.8 (2011), pp. 1425–1432. DOI: 10.1038/emboj.2011.61.

[128] Tamimount Mohammadi et al. "Specificity of the Transport of Lipid II by FtsW in Escherichia coli". In: *Journal of Biological Chemistry* 289.21 (2014), pp. 14707–14718. DOI: 10.1074/jbc.M114.557371.

[129] Lok-To Sham et al. "MurJ is the flippase of lipid-linked precursors for peptidoglycan biogenesis". In: *Science* 719.6193 (2014), pp. 220–222.

[130] Joann Huber et al. "Chemical Genetic Identification of Peptidoglycan Inhibitors Potentiating Carbapenem Activity against Methicillin-Resistant Staphylococcus aureus". In: *Chemistry & Biology* 16.8 (2009), pp. 837–848. DOI: 10.1016/j.chembiol.2009.05.012.

[131] João M Monteiro et al. "Peptidoglycan synthesis drives and FtsZ-treadmilling-independent step of cytokinesis". In: *Nature* 554.7693 (2018), pp. 528–532. DOI: 10.1038/nature25506.

[132] Alexander J Meeske et al. "MurJ and a novel lipid II flippase are required for cell wall biogenesis in Bacillus subtilis". In: *Proceedings of the National Academy of Sciences* 112.20 (2015), pp. 6437–6442. DOI: 10.1073/pnas.1504967112.

[133] Andrew L Lovering et al. "Structural Insight into the Transglycosylation Step of Bacterial Cell Wall Biosynthesis". In: *Science* 315 (2007), pp. 1402–1406.

[134] Yanqiu Yuan et al. "Crystal structure of a peptidoglycan glycosyltransferase suggests a model for processive glycan chain synthesis". In: *Proceedings of the National Academy of Sciences* 104.13 (2007), pp. 5348–5353.

[135] Beate Henrichfreise, Melanie Brunke, and Patrick H Viollier. "Bacterial Surfaces : The Wall that SEDS Built". In: *Current Biology* 26.21 (2016), R1158–R1160. DOI: 10.1016/j.cub.2016.09.028.

[136] Sylvia A Denome et al. "Escherichia coli Mutants Lacking All Possible Combinations of Eight Penicillin Binding Proteins: Viability, Characteristics, and Implications for Peptidoglycan Synthesis". In: *Journal of Bacteriology* 181.13 (1999), pp. 3981–3993.

[137] Catherine Paradis-bleau et al. "Lipoprotein Cofactors Located in the Outer Membrane Activate Bacterial Cell Wall Polymerases". In: *Cell* 143.7 (2010), pp. 1110–1120. DOI: 10.1016/j.cell.2010.11.037.

[138] Barry J Hartman and Alexander Tomasz. "Low-Affinity Penicillin-Binding Protein Associated with r-Lactam Resistance in Staphylococcus aureus". In: *Journal of Bacteriology* 158.2 (1984), pp. 513–516.

[139] M. G. Pinho et al. "Complementation of the essential peptidoglycan transpeptidase function of penicillin-binding protein 2 (PBP2) by the drug resistance protein PBP2A in Staphylococcus aureus". In: *Journal of Bacteriology* 183.22 (2001), pp. 6525–6531. DOI: 10.1128/JB.183.22.6525-6531.2001.

[140] Mariana G Pinho, Hermínia De Lencastre, and Alexander Tomasz. "An acquired and a native penicillin-binding protein cooperate in building the cell wall of drug-resistant staphylococci". In: *Proceedings of the National Academy of Sciences* 98.19 (2001), pp. 10886–10891.

[141] Andrew K Fenton et al. "CozE is a member of the MreCD complex that directs cell elongation in Streptococcus pneumoniae". In: *Nature Microbiology* 2.16237 (2016), pp. 1–9. DOI: 10.1038/nmicrobiol.2016.237.

[142] Marco Di Berardino et al. "The monofunctional glycosyltransferase of Escherichia coli is a member of a new class of peptidoglycan-synthesising enzymes". In: *FEBS Letters* 392 (1996), pp. 184–188.

[143] B G Spratt et al. "Monofunctional biosynthetic peptidoglycan transglycosylases". In: *Molecular Microbiology* 19 (1996), pp. 639–647.

[144] Q M A Y Wang et al. "Identification and Characterization of a Monofunctional Glycosyltransferase from Staphylococcus aureus". In: *Journal of Bacteriology* 183.16 (2001), pp. 4779–4785. DOI: 10.1128/JB.183.16.4779.

[145] Patricia Reed et al. "Monofunctional Transglycosylases Are Not Essential for Staphylococcus aureus Cell Wall Synthesis". In: *Journal of Bacteriology* 193.10 (2011), pp. 2549–2556. DOI: 10.1128/JB.01474-10.

[146] F Kunst et al. "The complete genome sequence of the Gram-positive bacterium Bacillus subtilis". In: *Nature* 390 (1997), pp. 249–256.

[147] Ana Arbeloa et al. "Role of Class A Penicillin-Binding Proteins in PBP5-Mediated B-Lactam Resistance in Enterococcus faecalis". In: *Journal of Bacteriology* 186.5 (2004), pp. 1221–1228. DOI: 10.1128/JB.186.5.1221.

[148] Mohammed Terrak and Martine Nguyen-Disteche. "Kinetic Characterization of the Monofunctional Glycosyltransferase from Staphylococcus aureus". In: *Journal of Bacteriology* 188.7 (2006), pp. 2528–2532. DOI: 10.1128/JB.188.7.2528.

[149] M Kuroda et al. "Whole genome sequencing of meticillin-resistant Staphylococcus aureus." In: *Lancet (London, England)* 357.9264 (2001), pp. 1225–40. DOI: 10.1016/S0140-6736(00)04403-2.

[150] Derrell C Mcpherson and David L Popham. "Peptidoglycan Synthesis in the Absence of Class A Penicillin-Binding Proteins in Bacillus subtilis". In: *Journal of Bacteriology* 185.4 (2003), pp. 1423–1431. DOI: 10.1128/JB.185.4.1423.

[151] Fumitoshi Ishino et al. "Peptidoglycan Synthetic Activities in Membranes of Escherichia coli Caused by Overproduction of Penicillin-binding Protein 2 and RodA Protein". In: *The Journal of Biological Chemistry* 261.15 (1986), pp. 7024–7031.

[152] Alexander J Meeske et al. "SEDS proteins are a widespread family of bacterial cell wall polymerases". In: *Nature* 537 (2016), pp. 634–638. DOI: 10.1038/nature19331.

[153] Kaveh Emami et al. "RodA as the missing glycosyltransferase in Bacillus subtilis and antibiotic discovery for the peptidoglycan polymerase pathway". In: *Nature Microbiology* 2.0 (2017), p. 16253. DOI: 10.1038/nmicrobiol.2016.253.

[154] Warawan Eiamphungporn and John D. Helmann. "The Bacillus subtilis sigma M Regulon and its Contribution to Cell Envelope Stress Responses". In: *Molecular Microbiology* 67.4 (2008), pp. 830–848. DOI: 10.1111/j.1365-2958.2007.06090.x.The.

[155] Ana Yepes et al. "Reconstruction of mreB expression in staphylococcus aureus via a collection of new integrative plasmids". In: *Applied and Environmental Microbiology* 80.13 (2014), pp. 3868–3878. DOI: 10.1128/AEM.00759-14.

[156] Hongbaek Cho et al. "Bacterial cell wall biogenesis is mediated by SEDS and PBP polymerase families functioning semi-autonomously." In: *Nature Microbiology* 1.9 (2016), pp. 1–8. DOI: 10.1038/nmicrobiol.2016.172.

[157] Heng Zhao et al. "Don't let sleeping dogmas lie: new views of peptidoglycan synthesis and its regulation". In: *Molecular Microbiology* 106.6 (2017), pp. 847–860. DOI: 10.1111/mmi.13853.

[158] Sophie Magnet et al. "Specificity of L,D-Transpeptidases from Gram-positive Bacteria Producing Different Peptidoglycan Chemotypes". In: *Journal of Biological Chemistry* 282.18 (2007), pp. 13151–13159. DOI: 10.1074/jbc.M610911200.

[159] Sophie Magnet et al. "Identification of the L,D-Transpeptidases for Peptidoglycan Cross-Linking in Escherichia coli". In: *Journal of Bacteriology* 190.13 (2008), pp. 4782–4785. DOI: 10.1128/JB.00025-08.

[160] Jean-luc Mainardi et al. "A Novel Peptidoglycan Cross-linking Enzyme for a B-Lactam-resistant Transpeptidation Pathway". In: *Journal of Biological Chemistry* 280.46 (2005), pp. 38146–38152. DOI: 10.1074/jbc.M507384200.

[161] Carlos Quintela, Marta Caparrhs, and Miguel A De Pedro. "Variability of peptidoglycan structural parameters in Gram-negative bacteria". In: *FEMS Microbiology Letters* 125 (1995), pp. 95–100.

[162] Marie Lavollay et al. "The Peptidoglycan of Stationary-Phase Mycobacterium tuberculosis Predominantly Contains Cross-Links Generated". In: *Journal of Bacteriology* 190.12 (2008), pp. 4360–4366. DOI: 10.1128/JB.00239-08.

[163] Jean-luc Mainardi et al. "Novel Mechanism of B-Lactam Resistance Due to Bypass of DD-Transpeptidation in Enterococcus faecium". In: *Journal of Biological Chemistry* 275.22 (2000), pp. 16490–16496. DOI: 10.1074/jbc.M909877199.

[164] Jean-luc Mainardi et al. "Balance between Two Transpeptidation Mechanisms Determines the Expression of B-Lactam Resistance in Enterococcus faecium". In: *Journal of Biological Chemistry* 277.39 (2002), pp. 35801–35807. DOI: 10.1074/jbc.M204319200.

[165] Jonathan Dworkin. "Ser/Thr phosphorylation as a regulatory mechanism in bacteria". In: *Current Opinion in Microbiology* 24 (2015), pp. 47–52. DOI: 10.1016/j.mib.2015.01.005.

[166] Sylvie Manuse et al. "Role of eukaryotic-like serine / threonine kinases in bacterial cell division and morphogenesis". In: *FEMS Microbiology Reviews* 40 (2016), pp. 41–56. DOI: 10.1093/femsre/fuv041.

[167] Greg Jones and Paul Dyson. "Evolution of Transmembrane Protein Kinases Implicated in Coordinating Remodeling of Gram-Positive Peptidoglycan: Inside versus Outside". In: *Journal of Bacteriology* 188.21 (2006), pp. 7470–7476. DOI: 10.1128/JB.00800-06.

[168] Mushtaq Mir et al. "The Extracytoplasmic Domain of the Mycobacterium tuberculosis Ser/Thr Kinase PknB Binds Specific Muropeptides and Is Required for PknB Localization". In: *PLoS Pathogens* 7.7 (2011), e1002182. DOI: 10.1371/journal.ppat.1002182.

[169] Amit Parikh et al. "PknB-Mediated Phosphorylation of a Novel Substrate , N-acetylglucosamine-1-Phosphate Uridyltransferase , Modulates Its Acetyltransferase Activity". In: *Journal of Molecular Biology* 386.2 (2009), pp. 451–464. DOI: 10.1016/j.jmb.2008.12.031.

[170] Christine L Gee et al. "A Phosphorylated Pseudokinase Complex Controls Cell Wall Synthesis in Mycobacteria". In: *Science Signalling* 5.208 (2012), pp. 1–13.

[171] Karen J Kieser et al. "Phosphorylation of the Peptidoglycan Synthase PonA1 Governs the Rate of Polar Elongation in Mycobacteria". In: *PLoS Pathogens* (2015), pp. 1–28. DOI: 10.1371/journal.ppat.1005010.

[172] Cara C Boutte et al. "A cytoplasmic peptidoglycan amidase homologue controls mycobacterial cell wall synthesis". In: *eLife* 5.e14590 (2016), pp. 1–22. DOI: 10.7554/eLife.14590.

[173] Kimberly M Davis and Jeffrey N Weiser. "Modifications to the Peptidoglycan Backbone Help Bacteria To Establish Infection". In: *Infection and Immunity* 79.2 (2011), pp. 562–570. DOI: 10.1128/IAI.00651-10.

[174] Abdelmadjid Atrih and Simon J Foster. "In vivo roles of the germination-specific lytic enzymes of Bacillus subtilis 168". In: *Microbiology* 146 (2001), pp. 2925–2932.

[175] Margreet A Wolfert, Abhijit Roychowdhury, and Geert-jan Boons. "Modification of the Structure of Peptidoglycan Is a Strategy To Avoid Detection by Nucleotide-Binding Oligomerization Domain Protein 1". In: *Infection and Immunity* 75.2 (2007), pp. 706–713. DOI: 10.1128/IAI.01597-06.

[176] Ge Wang et al. "Oxidative Stress-induced Peptidoglycan Deacetylase in Helicobacter pylori". In: *Journal of Biological Chemistry* 284.11 (2009), pp. 6790–6800. DOI: 10.1074/jbc.M808071200.

[177] M Inês Crisóstomo et al. "Attenuation of penicillin resistance in a peptidoglycan O-acetyl transferase mutant of Streptococcus pneumoniae". In: *Molecular Microbiology* 61.6 (2006), pp. 1497–1509. DOI: 10.1111/j.1365-2958.2006.05340.x.

[178] Jon B Raymond et al. "Identification of the namH Gene , Encoding the Hydroxylase Responsible for the N-Glycolylation of the Mycobacterial Peptidoglycan". In: *Journal of Biological Chemistry* 280.1 (2005), pp. 326–333. DOI: 10.1074/jbc.M411006200.

[179] Emmanuel Psylinakis et al. "Peptidoglycan N-Acetylglucosamine Deacetylases from Bacillus cereus, Highly Conserved Proteins in Bacillus anthracis". In: *Journal of Biological Chemistry* 280.35 (2005), pp. 30856–30863. DOI: 10.1074/jbc.M407426200.

[180] J Bonnet et al. "Peptidoglycan O-acetylation is functionally related to cell wall biosynthesis and cell division in Streptococcus pneumoniae". In: *Molecular Microbiology (Ahead of print)* (2017). DOI: 10.1111/mmi.13849.

[181] Agnieszka Bera et al. "The Presence of Peptidoglycan O-Acetyltransferase in Various Staphylococcal Species Correlates with Lysozyme Resistance and Pathogenicity". In: *Infection and Immunity* 74.8 (2006), pp. 4598–4604. DOI: 10.1128/IAI.00301-06.

[182] Felipe Cava et al. "Distinct pathways for modification of the bacterial cell wall by non-canonical D-amino acids". In: *The EMBO Journal* 30.16 (2011), pp. 3442–3453. DOI: 10.1038/emboj.2011.246.

[183] Tania J Lupoli et al. "Transpeptidase-Mediated Incorporation of D-Amino Acids into Bacterial Peptidoglycan". In: *Journal of the American Chemical Society* 133 (2011), pp. 10748–10751. DOI: 10.1021/ja2040656.

[184] Hubert Lam et al. "D-Amino Acids Govern Stationary Phase Cell Wall Remodeling in Bacteria". In: *Science* 325.September (2009), pp. 1552–1556.

[185] Ilana Klodkin-Gal et al. "D-Amino Acids Trigger Biofilm Disassembly". In: *Science* 328 (2010), pp. 627–630.

[186] Waldemar Vollmer et al. "Bacterial peptidoglycan (murein) hydrolases". In: *FEMS Microbiology Reviews* 32.2 (2008), pp. 259–286. DOI: 10.1111/j.1574-6976.2007.00099.x.

[187] Alexander J F Egan et al. "Regulation of bacterial cell wall growth". In: *The FEBS Journal* (2016), pp. 1–17. DOI: 10.1111/febs.13959.

[188] Waldemar Vollmer and Ute Bertsche. "Murein (peptidoglycan) structure, architecture and biosynthesis in Escherichia coli". In: *Biochimica et Biophysica Acta - Biomembranes* 1778.9 (2008), pp. 1714–1734. DOI: 10.1016/j.bbamem.2007.06.007.

[189] Athanasios Typas et al. "From the regulation of peptidoglycan synthesis to bacterial growth and morphology". In: *Nature Reviews Microbiology* 10.2 (2012), pp. 123–136. DOI: 10.1038/nrmicro2677. arXiv: NIHMS150003.

[190] Manuel Pazos, Katharina Peters, and Waldemar Vollmer. "Robust peptidoglycan growth by dynamic and variable multi-protein complexes". In: *Current Opinion in Microbiology* 36 (2017), pp. 55–61. DOI: 10.1016/j.mib.2017.01.006.

[191] Richard Wheeler et al. "Bacterial Cell Enlargement Requires Control of Cell Wall Stiffness Mediated by Peptidoglycan Hydrolases". In: *mBio* 6.4 (2015), pp. 1–10. DOI: 10.1128/mBio.00660-15.Editor.

[192] Victoria A Lund et al. "Molecular coordination of Staphylococcus aureus cell division". In: *eLife* 7 (2018), e32057.

[193] Alexander J F Egan et al. "Activities and regulation of peptidoglycan synthases". In: *Philosophical Transactions of the Royal Society B: Biological Sciences* 370 (2015), p. 20150031.

[194] James T Park and Tsuyoshi Uehara. "How Bacteria Consume Their Own Exoskeletons (Turnover and Recycling of Cell Wall Peptidoglycan)". In: *Microbiology and Molecular Biology Reviews* 72.2 (2008), pp. 211–227. DOI: 10.1128/MMBR.00027-07.

[195] Tsuyoshi Uehara and Thomas G. Bernhardt. "More than just lysins: Peptidoglycan hydrolases tailor the cell wall". In: *Current Opinion in Microbiology* 14.6 (2011), pp. 698–703. DOI: 10.1016/j.mib.2011.10.003. arXiv: NIHMS150003.

[196] Stéphane Mesnage et al. "Molecular basis for bacterial peptidoglycan recognition by LysM domains." In: *Nature communications* 5.4269 (2014), pp. 1–11. DOI: 10.1038/ncomms5269.

[197] June R Scott and Timothy C Barnett. "Surface proteins of gram-positive bacteria and how they get there". In: *Annual Review of Microbiology* 60.60 (2006), pp. 397–423. DOI: 10.1146/annurev.micro.60.080805.142256.

[198] Tadashi Baba and Olaf Schneewind. "Targeting of muralytic enzymes to the cell division site of Gram-positive bacteria: Repeat domains direct autolysin to the equatorial surface ring of Staphylococcus aureus". In: *EMBO Journal* 17.16 (1998), pp. 4639–4646. DOI: 10.1093/emboj/17.16.4639.

[199] Martin Schlag et al. "Role of staphylococcal wall teichoic acid in targeting the major autolysin Atl". In: *Molecular Microbiology* 75.4 (2010), pp. 864–873. DOI: 10.1111/j.1365-2958.2009.07007.x.

[200] Paola Bisicchia et al. "The essential YycFG two-component system controls cell wall metabolism in Bacillus subtilis". In: *Molecular Microbiology* 65.1 (2007), pp. 180–200. DOI: 10.1111/j.1365-2958.2007.05782.x.

[201] Aurelia Delaune et al. "Peptidoglycan Crosslinking Relaxation Plays an Important Role in Staphylococcus aureus WalKR- Dependent Cell Viability". In: *PLoS ONE* 6.2 (2011), e17054. DOI: 10.1371/journal.pone.0017054.

[202] T Oshida et al. "A Staphylococcus aureus autolysin that has an N-acetylmuramoyl-L-alanine amidase domain and an endo-beta-N-acetylglucosaminidase domain: cloning, sequence analysis, and characterization." In: *Proceedings of the National Academy of Sciences of the United States of America* 92.1 (1995), pp. 285–289.

[203] M Sugai et al. "Identification of endo-beta-N-acetylglucosaminidase and N-acetylmuramyl-L-alanine amidase as cluster-dispersing enzymes in Staphylococcus aureus." In: *Journal of Bacteriology* 177.6 (1995), pp. 1491–1496.

[204] H Komatsuzawa et al. "Subcellular localization of the major autolysin, ATL and its processed proteins in Staphylococcus aureus." In: *Microbiology and Immunology* 41.6 (1997), pp. 469–479.

[205] Jeffrey L Bose et al. "Contribution of the Staphylococcus aureus Atl AM and GL Murein Hydrolase Activities in Cell Division, Autolysis, and Biofilm Formation". In: *PLoS ONE* 7.7 (2012), e42244. DOI: 10.1371/journal.pone.0042244.

[206] Matthew B. Frankel et al. "LytN, a murein hydrolase in the cross-wall compartment of Staphylococcus aureus, is involved in proper bacterial growth and envelope assembly". In: *Journal of Biological Chemistry* 286.37 (2011), pp. 32593–32605. DOI: 10.1074/jbc.M111.258863.

[207] Christoph Heidrich et al. "Involvement of N -acetylmuramyl- L -alanine amidases in cell separation and antibiotic-induced autolysis of Escherichia coli". In: *Molecular Microbiology* 41 (2001), pp. 167–178.

[208] Christoph Heidrich et al. "Effects of Multiple Deletions of Murein Hydrolases on Viability , Septum Cleavage, and Sensitivity to Large Toxic Molecules in Escherichia coli". In: *Journal of Bacteriology* 184.22 (2002), pp. 6093–6099. DOI: 10.1128/JB.184.22.6093.

[209] David E Nelson and Kevin D Young. "Penicillin Binding Protein 5 Affects Cell Diameter, Contour, and Morphology of Escherichia coli". In: *Journal of Bacteriology* 182.6 (2000), pp. 1714–1721.

[210] David E Nelson and Kevin D Young. "Contributions of PBP 5 and DD-Carboxypeptidase Penicillin Binding Proteins to Maintenance of Cell Shape in Escherichia coli". In: *Journal of Bacteriology* 183.10 (2001), pp. 3055–3064. DOI: 10.1128/JB.183.10.3055.

[211] Jeff Errington. "Regulation of endospore formation in Bacillus subtilis". In: *Nature Reviews Microbiology* 1 (2003), pp. 117–127. DOI: 10.1038/nrmicro750.

[212] Patrick J Piggot and David W Hilbert. "Sporulation of Bacillus subtilis". In: *Current Opinion in Microbiology* 7 (2004), pp. 579–586. DOI: 10.1016/j.mib.2004.10.001.

[213] G Koraimann. "Cellular and Molecular Life Sciences Lytic transglycosylases in macromolecular transport systems of Gram-negative bacteria". In: *Cellular and Molecular Life Sciences* 60 (2003), pp. 2371–2388. DOI: 10.1007/s00018-003-3056-1.

[214] Kenneth W Bayles. "The biological role of death and lysis in biofilm development". In: *Nature Reviews Microbiology* 5 (2007), pp. 721–726.

[215] Hiroki Yamamoto et al. "Post-translational control of vegetative cell separation enzymes through a direct interaction with specific inhibitor IseA in Bacillus subtilis". In: *Molecular Microbiology* 70.1 (2008), pp. 168–182. DOI: 10.1111/j.1365-2958.2008.06398.x.

[216] Chelsea A Clarke, Edie M Scheurwater, and Anthony J Clarke. "The Vertebrate Lysozyme Inhibitor Ivy Functions to Inhibit the Activity of Lytic". In: *The Journal of Biological Chemistry* 285.20 (2010), pp. 14843–14847. DOI: 10.1074/jbc.C110.120931.

[217] Tsuyoshi Uehara et al. "Daughter cell separation is controlled by cytokinetic ring-activated cell wall hydrolysis". In: *The EMBO Journal* 29.8 (2010), pp. 1412–1422. DOI: 10.1038/emboj.2010.36.

[218] Nick T Peters, Thuy Dinh, and Thomas G Bernhardt. "A Fail-Safe Mechanism in the Septal Ring Assembly Pathway Generated by the Sequential Recruitment of Cell Separation Amidases and Their Activators". In: *Journal of Bacteriology* 193.18 (2011), pp. 4973–4983. DOI: 10.1128/JB.00316-11.

[219] Erik De Leeuw et al. "Molecular characterization of Escherichia coli FtsE and FtsX". In: *Molecular Microbiology* 31.3 (1999), pp. 983–993.

[220] Desirée C Yang et al. "An ATP-binding cassette transporter-like complex governs cell-wall hydrolysis at the bacterial cytokinetic ring". In: *Proceedings of the National Academy of Sciences* 108.45 (2011), E1052–E1060. DOI: 10.1073/pnas.1107780108/-/DCSupplemental.www.pnas.org/cgi/doi/10.1073/pnas.1107780108.

[221] Sergio G Bartual et al. "Structural basis of PcsB-mediated cell separation in Streptococcus pneumoniae". In: *Nature Communications* 5.3842 (2014), pp. 1–12. DOI: 10.1038/ncomms4842.

[222] Ruchika Bajaj et al. "Biochemical characterization of essential cell division proteins FtsX and FtsE that mediate peptidoglycan hydrolysis by PcsB in Streptococcus pneumoniae". In: *MicrobiologyOpen* (2016). DOI: 10.1002/mbo3.366.

[223] Maria-halima Laaberki et al. "O -Acetylation of Peptidoglycan Is Required for Proper Cell Separation and S-layer Anchoring in Bacillus anthracis". In: *The Journal of Biological Chemistry* 286.7 (2011), pp. 5278–5288. DOI: 10.1074/jbc.M110.183236.

[224] A Gogos et al. "A Quorum Sensing-Regulated Protein Binds Cell Wall Components and Enhances Lysozyme Resistance in Streptococcus pyogenes". In: *Journal of Bacteriology* 200.11 (2018), e00701–17.

[225] Santosh Kumar Singh et al. "Regulated proteolysis of a cross-link–specific peptidoglycan hydrolase contributes to bacterial morphogenesis". In: *Proceedings of the National Academy of Sciences* 112.35 (2015), pp. 10956–10961. DOI: 10.1073/pnas.1507760112.

[226] Arthur L Koch and Ronald J Doyle. "Inside-to-outside Growth and Turnover of the Wall of Gram-positive Rods". In: *Journal of Theoretical Biology* 117 (1985), pp. 137–157.

[227] Rut Carbadillo-Lopez et al. "Actin Homolog MreBH Governs Cell Morphogenesis by Localization of the Cell Wall Hydrolase LytE". In: *Developmental Cell* 11 (2006), pp. 399–409. DOI: 10.1016/j.devcel.2006.07.017.

[228] Ute Meisel, Joachim-volker Ho, and Waldemar Vollmer. "Overproduction of Inactive Variants of the Murein Synthase PBP1B Causes Lysis in Escherichia coli". In: *Journal of Bacteriology* 185.18 (2003), pp. 5342–5348. DOI: 10.1128/JB.185.18.5342.

[229] Jean-emmanuel Hugonnet et al. "Factors essential for L,D-transpeptidase-mediated peptidoglycan cross-linking and B-lactam resistance in Escherichia coli". In: *eLife* 5 (2016), e19469. DOI: 10.7554/eLife.19469.

[230] Alexander J F Egan and Waldemar Vollmer. "The physiology of bacterial cell division". In: *Annals of the New York Academy of Sciences* 1277 (2013), pp. 8–28. DOI: 10.1111/j.1749-6632.2012.06818.x.

[231] Sven Van Teeffelen et al. "The bacterial actin MreB rotates, and rotation depends on cell-wall assembly". In: *Proceedings of the National Academy of Sciences* 108.38 (2011), pp. 15822–15827. DOI: 10.1073/pnas.1108999108.

[232] Randy M Morgenstein et al. "RodZ links MreB to cell wall synthesis to mediate MreB rotation and robust morphogenesis". In: *Proceedings of the*

National Academy of Sciences 112.40 (2015), pp. 12510–12515. DOI: 10.1073/pnas.1509610112.

[233] A Bisson-Filho et al. "Treadmilling by FtsZ filaments drives peptidoglycan synthesis and bacterial cell division". In: *Science* 355 (2017), pp. 1–6.

[234] H M Pooley. "Turnover and Spreading of Old Wall During Surface Growth of Bacillus subtilis". In: *Journal of Bacteriology* 125.3 (1976), pp. 1127–1138.

[235] Ethan C Garner et al. "Coupled, Circumferential Motions of the Cell Wall Synthesis Machinery and MreB Filaments in B. subtilis". In: *Science* 333 (2011), pp. 222–226.

[236] Julia Dominguez-Escobar et al. "Processive Movement of MreB-Associated Cell Wall Biosynthetic Complexes in Bacteria". In: *Science* 333 (2011), pp. 225–228.

[237] Laura J F Jones, Rut Carballido-Lopez, and Jeffery Errington. "Control of Cell Shape in Bacteria: Helical , Actin-like Filaments in Bacillus subtilis". In: *Cell* 104 (2001), pp. 913–922.

[238] Thomas Kruse et al. "Dysfunctional MreB inhibits chromosome segregation in Escherichia coli". In: *EMBO Journal* 22.19 (2003), pp. 5283–5292.

[239] Yu-ling Shih, Trung Le, and Lawrence Rothfield. "Division site selection in Escherichia coli involves dynamic redistribution of Min proteins within coiled structures that extend between the two cell poles". In: *Proceedings of the National Academy of Sciences* 100.13 (2003), pp. 7865–7870.

[240] Rainer M Figge, Arun V Divakaruni, and James W Gober. "MreB, the cell shape-determining bacterial actin homologue, co-ordinates cell wall morphogenesis in Caulobacter crescentus". In: *Molecular Microbiology* 51.5 (2004), pp. 1321–1332. DOI: 10.1046/j.1365-2958.2003.03936.x.

[241] Thomas Kruse, Jette Bork-jensen, and Kenn Gerdes. "The morphogenetic MreBCD proteins of Escherichia coli form an essential membrane-bound complex". In: *Molecular Microbiology* 55.1 (2005), pp. 78–89. DOI: 10.1111/j.1365-2958.2004.04367.x.

[242] Yoshikazu Kawai, Richard A Daniel, and Jeffery Errington. "Regulation of cell wall morphogenesis in Bacillus subtilis by recruitment of PBP1 to the MreB helix". In: *Molecular Microbiology* 71.5 (2009), pp. 1131–1144. DOI: 10.1111/j.1365-2958.2009.06601.x.

[243] Manuel Banzhaf et al. "Cooperativity of peptidoglycan synthases active in bacterial cell elongation". In: *Molecular Microbiology* 85.1 (2012), pp. 179–194. DOI: 10.1111/j.1365-2958.2012.08103.x.

[244] Timothy K Lee et al. "Single-molecule imaging reveals modulation of cell wall synthesis dynamics in live bacterial cells". In: *Nature Communications* 7 (2016), p. 13170. DOI: 10.1038/ncomms13170.

[245] Arun V Divakaruni et al. "The cell shape proteins MreB and MreC control cell morphogenesis by positioning cell wall synthetic complexes". In: *Molecular Microbiology* 66.1 (2007), pp. 174–188. DOI: 10.1111/j.1365-2958.2007.05910.x.

[246] Sandy Favini-stabile et al. "MreB and MurG as scaffolds for the cytoplasmic steps of peptidoglycan biosynthesis". In: *Environmental Microbiology* 15.12 (2013), pp. 3218–3228. DOI: 10.1111/1462-2920.12171.

[247] Courtney L White, Aleksandar Kitich, and James W Gober. "Positioning cell wall synthetic complexes by the bacterial morphogenetic proteins MreB and MreD". In: *Molecular Microbiology* 76.3 (2010), pp. 616–633. DOI: 10.1111/j.1365-2958.2010.07108.x.

[248] Anne Stéphanie Rueff et al. "An early cytoplasmic step of peptidoglycan synthesis is associated to MreB in Bacillus subtilis". In: *Molecular Microbiology* 91.2 (2014), pp. 348–362. DOI: 10.1111/mmi.12467.

[249] René Van Der Ploeg et al. "Colocalization and interaction between elongasome and divisome during a preparative cell division phase in Escherichia coli". In: *Molecular Microbiology* 87.5 (2013), pp. 1074–1087. DOI: 10.1111/mmi.12150.

[250] Andrew K Fenton and Kenn Gerdes. "Direct interaction of FtsZ and MreB is required for septum synthesis and cell division in Escherichia coli". In: *The EMBO Journal* 32.13 (2013), pp. 1953–1965. DOI: 10.1038/emboj.2013.129.

[251] Mirjam E G Aarsman et al. "Maturation of the Escherichia coli divisome occurs in two steps". In: *Molecular Microbiology* 55.6 (2005), pp. 1631–1645. DOI: 10.1111/j.1365-2958.2005.04502.x.

[252] Michelle Aaron et al. "The tubulin homologue FtsZ contributes to cell elongation by guiding cell wall precursor synthesis in Caulobacter crescentus". In: *Molecular Micorbiology* 64.4 (2007), pp. 938–952. DOI: 10.1111/j.1365-2958.2007.05720.x.

[253] Miguel A de Pedro et al. "Murein Segregation in Escherichia coli". In: *Journal of Bacteriology* 179.9 (1997), pp. 2823–2834.

[254] Keri L N Mercer and David S Weiss. "The Escherichia coli Cell Division Protein FtsW Is Required To Recruit Its Cognate Transpeptidase, FtsI (PBP3), to the Division Site". In: *Journal of Bacteriology* 184.4 (2002), pp. 904–912. DOI: 10.1128/JB.184.4.904.

[255] Ute Bertsche et al. "Interaction between two murein (peptidoglycan) synthases , PBP3 and PBP1B, in Escherichia coli". In: *Molecular Microbiology* 61.3 (2006), pp. 675–690. DOI: 10.1111/j.1365-2958.2006.05280.x.

[256] Nathan W Goehring, Mark D Gonzalez, and Jon Beckwith. "Premature targeting of cell division proteins to midcell reveals hierarchies of protein interactions involved in divisome assembly". In: *Molecular Microbiology* 61.1 (2006), pp. 33–45. DOI: 10.1111/j.1365-2958.2006.05206.x.

[257] Xinxing Yang et al. "GTPase activity – coupled treadmilling of the bacterial tubulin FtsZ organizes septal cell wall synthesis". In: *Science* 355 (2017), pp. 744–747.

[258] Masaki Osawa, David E Anderson, and Harold P Erickson. "Reconstitution of Contractile FtsZ Rings in Liposomes". In: *Science* 320.5877 (2008), pp. 792–794. DOI: 10.1126/science.1154520.Reconstitution.

[259] Masaki Osawa, David E Anderson, and Harold P Erickson. "Curved FtsZ protofilaments generate bending forces on liposome membranes". In: *The EMBO Journal* 28.22 (2009), pp. 3476–3484. DOI: 10.1038/emboj.2009.277.

[260] Daniel O Daley, Ulf Skoglund, and Bill Söderström. "FtsZ does not initiate membrane constriction at the onset of division". In: *Scientific Reports* 6.33183 (2016), pp. 1–6. DOI: 10.1038/srep33138.

[261] Carla Coltharp and Jie Xiao. "Beyond force generation: Why is a dynamic ring of FtsZ polymers essential for bacterial cytokinesis?" In: *Bioessays* 39.1 (2016), pp. 1–11. DOI: 10.1002/bies.201600179.

[262] Carla Coltharp et al. "Defining the rate-limiting processes of bacterial cytokinesis". In: *Proceedings of the National Academy of Sciences* (2016), E1044–E1053. DOI: 10.1073/pnas.1514296113.

[263] Hao Yang et al. "Characterization of the tertiary structure of the peptidoglycan of Enterococcus faecalis". In: *BBA - Biomembranes* 1859 (2017), pp. 2171–2180. DOI: 10.1016/j.bbamem.2017.08.003.

[264] Dennis Claessen et al. "Control of the cell elongation – division cycle by shuttling of PBP1 protein in Bacillus subtilis". In: *Molecular Microbiology* 68.4 (2008), pp. 1029–1046. DOI: 10.1111/j.1365-2958.2008.06210.x.

[265] Victoria R Steele et al. "Multiple essential roles for EzrA in cell division of Staphylococcus aureus". In: *Molecular Microbiology* 80.2 (2011), pp. 542–555. DOI: 10.1111/j.1365-2958.2011.07591.x.

[266] Gouzel Karimova, Nathalie Dautin, and Daniel Ladant. "Interaction Network among Escherichia coli Membrane Proteins Involved in Cell Division as Revealed by Bacterial Two-Hybrid Analysis". In: *Journal of Bacteriology* 187.7 (2005), pp. 2233–2243. DOI: 10.1128/JB.187.7.2233.

[267] Bing Liu et al. "Roles for both FtsA and the FtsBLQ subcomplex in FtsN-stimulated cell constriction in Escherichia coli". In: *Molecular Microbiology* 95.January (2015), pp. 945–970. DOI: 10.1111/mmi.12906.

[268] Jue D Wang and Petra A Levin. "Metabolism, cell growth and the bacterial cell cycle". In: *Nature Reviews Microbiology* 7.11 (2009), pp. 822–827. DOI: 10.1038/nrmicro2202.

[269] Sattar Taheri-Araghi et al. "Cell-Size Control and Homeostasis in Bacteria". In: *Current Biology* 25 (2015), pp. 385–391.

[270] Richard B Weart et al. "A Metabolic Sensor Governing Cell Size in Bacteria". In: *Cell* 130 (2007), pp. 335–347. DOI: 10.1016/j.cell.2007.05.043.

[271] An-chun Chien et al. "Changes in the oligomerization potential of the division inhibitor UgtP co-ordinate Bacillus subtilis cell size with nutrient availability". In: *Molecular Microbiology* 86.3 (2012), pp. 594–610. DOI: 10.1111/mmi.12007.

[272] Boris Gorke, Elodie Foulquier, and Anne Galinier. "YvcK of Bacillus subtilis is required for a normal cell shape and for growth on Krebs cycle intermediates and substrates of the pentose phosphate pathway". In: *Microbiology* 151 (2005), pp. 3777–3791. DOI: 10.1099/mic.0.28172-0.

[273] Elodie Foulquier et al. "The YvcK protein is required for morphogenesis via localization of PBP1 under gluconeogenic growth conditions in Bacillus subtilis". In: *Molecular Microbiology* 80.March (2011), pp. 309–318. DOI: 10.1111/j.1365-2958.2011.07587.x.

[274] John Mauck and Luis Glaser. "Turnover of the cell wall of bacillus subtilis W-23 during logarithmic growth". In: *Biochemical and Biophysical Research Communications* 39.4 (1970), pp. 699–706. DOI: 10.1016/0006-291X(70)90261-5.

[275] Aude Antignac, Krzysztof Sieradzki, and Alexander Tomasz. "Perturbation of cell wall synthesis suppresses autolysis in Staphylococcus aureus: Evidence for coregulation of cell wall synthetic and hydrolytic enzymes". In: *Journal of Bacteriology* 189.21 (2007), pp. 7573–7580. DOI: 10.1128/JB.01048-07.

[276] Birgitte H Kallipolitis and Hanne Ingmer. "Listeria monocytogenes response regulators important for stress tolerance and pathogenesis". In: *FEMS Microbiology Letters* 204 (2001), pp. 111–115.

[277] Lynn E Hancock and Marta Perego. "Systematic Inactivation and Phenotypic Characterization of Two-Component Signal Transduction Systems of Enterococcus faecalis V583". In: *Journal of Bacteriology* 186.23 (2004), pp. 7951–7958. DOI: 10.1128/JB.186.23.7951.

[278] Zhiqiang Qin et al. "Structure-based discovery of inhibitors of the YycG histidine kinase: New chemical leads to combat Staphylococcus epidermidis

infections". In: *BMC Microbiology* 96.6 (2006), pp. 1–18. DOI: 10.1186/1471-2180-6-96.

[279] Sarah Dubrac et al. "New insights into the WalK/WalR (YycG/YycF) essential signal transduction pathway reveal a major role in controlling cell wall metabolism and biofilm formation in Staphylococcus aureus". In: *Journal of Bacteriology* 189.22 (2007), pp. 8257–8269. DOI: 10.1128/JB.00645-07.

[280] Tatsuya Fukushima et al. "A sensor histidine kinase co-ordinates cell wall architecture with cell division in Bacillus subtilis". In: *Molecular Microbiology* 69.3 (2008), pp. 621–632. DOI: 10.1111/j.1365-2958.2008.06308.x.

[281] Patrick Hardt et al. "The cell wall precursor lipid II acts as a molecular signal for the Ser/Thr kinase PknB of Staphylococcus aureus". In: *International Journal of Medical Microbiology* 307 (2017), pp. 1–10. DOI: 10.1016/j.ijmm.2016.12.001.

[282] Manuel Liebeke et al. "A metabolomic view of staphylococcus aureus and its ser/thr kinase and phosphatase deletion mutants: Involvement in cell wall biosynthesis". In: *Chemistry and Biology* 17.8 (2010), pp. 820–830. DOI: 10.1016/j.chembiol.2010.06.012.

[283] Makoto Kuroda et al. "Two-component system VraSR positively modulates the regulation of cell-wall biosynthesis pathway in Staphylococcus aureus". In: *Molecular Microbiology* 49.3 (2003), pp. 807–821. DOI: 10.1046/j.1365-2958.2003.03599.x.

[284] Michael Meehl et al. "Interaction of the GraRS Two-Component System with the VraFG ABC Transporter To Support Vancomycin-Intermediate Resistance in Staphylococcus aureus". In: *Antimicrobial Agents and Chemotherapy* 51.8 (2007), pp. 2679–2689. DOI: 10.1128/AAC.00209-07.

[285] Wei Sun et al. "Ultra-deep profiling of alternatively spliced Drosophila Dscam isoforms by circularization- assisted multi-segment sequencing". In: *The EMBO Journal* 32.May (2013), pp. 2029–2038. DOI: 10.1038/emboj.2013.144.

[286] Ahmed Touhami, Manfred H Jericho, and Terry J Beveridge. "Atomic Force Microscopy of Cell Growth and Division in Staphylococcus aureus". In: *Journal of Bacteriology* 186.11 (2004), pp. 3286–3295. DOI: 10.1128/JB.186.11.3286.

[287] Xiaoxue Zhou et al. "Mechanical crack propagation drives millisecond daughter cell separation in Staphylococcus aureus". In: *Science* 348.6234 (2015), pp. 574–578.

[288] W. Wong, F. E. Young, and A. N. Chatterjee. "Regulation of bacterial cell walls: turnover of cell wall in Staphylococcus aureus." In: *Journal of Bacteriology* 120.2 (1974), pp. 837–843.

[289] Mariana G. Pinho and Jeff Errington. "Dispersed mode of Staphylococcus aureus cell wall synthesis in the absence of the division machinery". In: *Molecular Microbiology* 50.3 (2003), pp. 871–881. DOI: 10.1046/j.1365-2958.2003.03719.x.

[290] Mariana G Pinho, Morten Kjos, and Jan-Willem Veening. "How to get (a)round: mechanisms controlling growth and division of coccoid bacteria." In: *Nature Reviews Microbiology* 11.9 (2013), pp. 601–14. DOI: 10.1038/nrmicro3088.

[291] Mariana G Pinho and Jeff Errington. "Recruitment of penicillin-binding protein PBP2 to the division site of Staphylococcus aureus is dependent on its transpeptidation substrates". In: *Molecular Microbiology* 55.3 (2005), pp. 799–807. DOI: 10.1111/j.1365-2958.2004.04420.x.

[292] S J Foster. "Molecular characterization and functional analysis of the major autolysin of Staphylococcus aureus 8325/4". In: *J.Bacteriol.* 177.0021-9193 (Print) (1995), pp. 5723–5725.

[293] Magda Luciana Atilano et al. "Bacterial autolysins trim cell surface peptidoglycan to prevent detection by the Drosophila innate immune system". In: *eLife* 3 (2014), e02277. DOI: 10.7554/eLife.02277.

[294] Jan Reith and Christoph Mayer. "Peptidoglycan turnover and recycling in Gram-Positive bacteria". In: *Applied Microbiology and Biotechnology* 92.1 (2011), pp. 1–11. DOI: 10.1007/s00253-011-3486-x.

[295] J Chaloupka. "Changes in the character of the cell wall in growth of Bacillus megaterium cultures". In: *Folia Microbiologica* 7.5 (1962), pp. 269–270.

[296] J Chaloupka. "Synthesis and degradation of surface structures by growing and non-growing Bacillus megaterium". In: *Folia Microbiological* 12.3 (1963), pp. 3–4.

[297] J Chaloupka, L Rihova, and P Kreckova. "Degradation and turnover of bacterial cell wall mucopeptides in growing bacteria". In: *Folia Microbiologica* 9.1 (1964), pp. 9–15.

[298] Jarrod W. Johnson, Jed F. Fisher, and Shahriar Mobashery. "Bacterial cell-wall recycling". In: *Annals of the New York Academy of Sciences* 1277.1 (2013), pp. 54–75. DOI: 10.1111/j.1749-6632.2012.06813.x.

[299] Peter Blumel, Wilhelm Uecker, and Peter Giesbrecht. "Zero order kinetics of cell wall turnover in Staphylococcus aureus". In: *Archives of Microbiology* 121 (1979), pp. 103–110.

[300] I C Hancock and C M Cox. "Turnover of cell surface-bound capsular polysaccharide in Staphylococcus aureus." In: *FEMS Microbiology Letters* 61.1 (1991), pp. 25–30.

[301] E. W. Goodell. "Recycling of murein by Escherichia coli". In: *Journal of Bacteriology* 163.1 (1985), pp. 305–310.

[302] E. W. Goodell and U. Schwarz. "Release of cell wall peptides into culture medium by exponentially growing Escherichia coli". In: *Journal of Bacteriology* 162.1 (1985), pp. 391–397.

[303] Tsuyoshi Uehara and James T. Park. "Growth of Escherichia coli: Significance of peptidoglycan degradation during elongation and septation". In: *Journal of Bacteriology* 190.11 (2008), pp. 3914–3922. DOI: 10.1128/JB.00207-08.

[304] Lars G Burman, Judith Raichler, and James T Park. "Evidence for Diffuse Growth of the Cylindrical Portion of the Escherichia coli Murein Sacculus". In: *Journal of Bacteriology* 155.3 (1983), pp. 983–988.

[305] Henk Engel, Bert Kazemier, and Wolfgang Keck. "Murein-Metabolizing Enzymes from Escherichia coli: Sequence Analysis and Controlled Overexpression of the slt Gene, Which Encodes the Soluble Lytic Transglycosylase". In: *Journal of Bacteriology* 173.21 (1991), pp. 6773–6782.

[306] Richa Priyadarshini, David L Popham, and Kevin D Young. "Daughter Cell Separation by Penicillin-Binding Proteins and Peptidoglycan Amidases in Escherichia coli". In: *Journal of Bacteriology* 188.15 (2006), pp. 5345–5355. DOI: 10.1128/JB.00476-06.

[307] Tsuyoshi Uehara and James T Park. "An Anhydro-N-Acetylmuramyl-L-Alanine Amidase with Broad Specificity Tethered to the Outer Membrane of Escherichia coli". In: *Journal of Bacteriology* 189.15 (2007), pp. 5634–5641. DOI: 10.1128/JB.00446-07.

[308] J. T. Park. "Why does Escherichia coli recycle its cell wall peptides?" In: *Molecular Microbiology* 17.3 (1995), pp. 421–426. DOI: 10.1111/j.1365-2958.1995.mmi_17030421.x.

[309] Bernd Glauner. "Separation and Quantification of Muropeptides with High-Performance Liquid Chromatography". In: *Analytical Biochemistry* 172 (1988), pp. 451–464.

[310] Derek Boothby et al. "Turnover of Bacterial Cell Wall Peptidoglycans". In: *Journal of Biological Chemistry* 248 (1973), pp. 2161–2169.

[311] Ronald J. Doyle, Milwood A. Motley, and Per H B Carstens. "Turnover of cell wall in Listeria monocytogenes". In: *Carbohydrate Research* 104.1 (1982), pp. 147–152. DOI: 10.1016/S0008-6215(00)82227-2.

[312] R Jennings Doyle, Jiri Chaloupka, and Vladimir Vinter. "Turnover of Cell Walls in Microorganisms". In: *Microbiological Reviews* 52.4 (1988), pp. 554–567.

[313] John Mauck, Lawrence Chan, and Luis Glaser. "Turnover of the Cell of Gram-positive Bacteria". In: *Journal of Biological Chemistry* 246.6 (1971), pp. 1820–1827.

[314] W Wong, A N Chatterjee, and F E Young. "Regulation of Bacterial Cell Walls: Correlation Between Autolytic Activity and Cell Wall Turnover in Staphylococcus aureus". In: *Journal of Bacteriology* 134.2 (1978), pp. 555–561.

[315] R. W. Gilpin et al. "Autolysis in Staphylococcus aureus: preferential release of old cell walls". In: *Journal of Bacteriology* 119.3 (1974), pp. 672–676.

[316] Thomas J Smith, Steve A Blackman, and Simon J Foster. "Autolysins of Bacillus subtilis: Multiple enzymes with multiple functions". In: *Microbiology* 146.2 (2000), pp. 249–262. DOI: 10.1115/1.4026364.

[317] Philippe Margot and Dimitri Karamata. "Identification of the structural genes for N-acetylmuramoyl-L-alanine amidase and its modifier in Bacillus subtilis 168: inactivation of these genes by insertional mutagenesis has no effect on growth or cell separation". In: *Molecular and General Genetics* 232 (1992), pp. 359–366.

[318] Steve A Blackman, Thomas J Smith, and Simon J Foster. "The role of autolysins during vegetative growth of Bacillus subtilis". In: *Microbiology* 144 (1998), pp. 73–82.

[319] Philippe Margot, Marco Pagni, and Dimitri Karamata. "Bacillus subtilis 168 gene LytF encodes a 7-D- muropeptidase expressed by the alternative vegetative sigma factor , cD". In: *Microbiology* 145 (1999), pp. 57–65.

[320] Silke Litzinger et al. "Muropeptide rescue in Bacillus subtilis involves sequential hydrolysis by B-N-acetylglucosaminidase and N-acetylmuramyl-L-alanine amidase". In: *Journal of Bacteriology* 192.12 (2010), pp. 3132–3143. DOI: 10.1128/JB.01256-09.

[321] Lakshmi Ramadurai and Radheshyam K Jayaswal. "Molecular Cloning, Sequencing, and Expression of lytM, a Unique Autolytic Gene of Staphylococcus aureus". In: *Journal of Bacteriology* 179.11 (1997), pp. 3625–3631.

[322] Samuel Becker et al. "Release of protein A from the cell wall of Staphylococcus aureus." In: *Proceedings of the National Academy of Sciences of the United States of America* 111.4 (2014), pp. 1574–9. DOI: 10.1073/pnas.1317181111.

[323] Melanie R. Stapleton et al. "Characterization of IsaA and SceD, two putative lytic transglycosylases of Staphylococcus aureus". In: *Journal of Bacteriology* 189.20 (2007), pp. 7316–7325. DOI: 10.1128/JB.00734-07.

[324] Junko Takahashi et al. "Molecular Characterization of an atl Null Mutant of Staphylococcus aureus". In: *Microbiology and Immunology* 46.9 (2002), pp. 601–612.

[325] Christian Croux et al. "Purification and characterization of an extracellular muramidase of Clostridium acetobutylicum ATCC 824 that acts on Non-N-acetylated peptidoglycan". In: *Applied and Enviromental Microbiology* 58.4 (1992), pp. 1075–1081.

[326] Yoshiyuki Takahara, Eiichi Machigaki, and Sawao Murao. "General Properties of Endo-N-acetylmuramidase of Bacillus subtilis YT-25". In: *Agricultural and Biological Chemsitry* 38.12 (1974), pp. 2357–2365. DOI: 10.1080/00021369.1974.10861519.

[327] Chien-peng Chu et al. "Cloning and Sequence Analysis of the Muramidase-2 Gene from Enterococcus hirae". In: *Journal of Bacteriology* 174.5 (1992), pp. 1619–1625.

[328] Reiko Kariyama and Gerald D Shockman. "Extracellular and Cellular Distribution of Muramidase-2 and Muramidase-1 of Enterococcus hirae ATCC 9790". In: *Journal of Bacteriology* 174.10 (1992), pp. 3236–3241.

[329] Girbe Buist et al. "Molecular Cloning and Nucleotide Sequence of the Gene Encoding the Major Peptidoglycan Hydrolase of Lactococcus lactis, a Muramidase Needed for Cell Separation". In: *Journal of Bacteriology* 177.6 (1995), pp. 1554–1563.

[330] Shannon A Carroll et al. "Identification and Characterization of a Peptidoglycan Hydrolase, MurA, of Listeria monocytogenes, a Muramidase Needed for Cell Separation". In: *Journal of Bacteriology* 185.23 (2003), pp. 6801–6808. DOI: 10.1128/JB.185.23.6801.

[331] Pablo Meyer et al. "Cell wall synthesis is necessary for membrane dynamics during sporulation of Bacillus subtilis". In: *Molecular Microbiology* 76.4 (2010), pp. 956–970. DOI: 10.1111/j.1365-2958.2010.07155.x.

[332] Cecile Morlot et al. "A highly coordinated cell wall degradation machine governs spore morphogenesis in Bacillus subtilis". In: *Genes and Development* 24 (2010), pp. 411–422. DOI: 10.1101/gad.1878110.enzymes.

[333] Stéphane Mesnage et al. "Role of N-acetylglucosaminidase and N-acetylmuramidase activities in Enterococcus faecalis peptidoglycan metabolism". In: *Journal of Biological Chemistry* 283.28 (2008), pp. 19845–19853. DOI: 10.1074/jbc.M802323200.

[334] Michael J. Boersma et al. "Minimal Peptidoglycan (PG) Turnover in Wild-Type and PG Hydrolase and Cell Division Mutants of Streptococcus pneumoniae D39 Growing Planktonically and in Host-Relevant Biofilms". In: *Journal of Bacteriology* 197.21 (2015), pp. 3472–3485. DOI: 10.1128/JB.00541-15.Editor.

[335] Daniel L. Garcia and Joseph P. Dillard. "Mutations in ampG or ampD affect peptidoglycan fragment release from Neisseria gonorrhoeae". In: *Journal of Bacteriology* 190.11 (2008), pp. 3799–3807. DOI: 10.1128/JB.01194-07.

[336] Katelynn L. Woodhams et al. "Peptidoglycan fragment release from neisseria meningitidis". In: *Infection and Immunity* 81.9 (2013), pp. 3490–3498. DOI: 10.1128/IAI.00279-13.

[337] J M Chan and J P Dillard. "Attention seeker: Production, modification, and release of inflammatory peptidoglycan fragments in Neisseria". In: *Journal of Bacteriology* (2017), pp. 1–29. DOI: 10.1128/JB.00354-17.

[338] C Jacobs et al. "Bacterial cell wall recycling provides cytosolic muropeptides as effectors for beta-lactamase induction." In: *The EMBO journal* 13.19 (1994), pp. 4684–4694.

[339] Christine Jacobs et al. "AmpD, essential for both B-lactamase regulation and cell wall recycling, is a novel cytosolic N-acetylmuramyl-L-alanine amidase". In: *Molecular Microbiology* 15.3 (1995), pp. 553–559.

[340] Markus F Templin, Astrid Ursinus, and Joachim-volker Holtje. "A defect in cell wall recycling triggers autolysis during the stationary growth phase of Escherichia coli". In: *The EMBO Journal* 18.15 (1999), pp. 4108–4117.

[341] Qiaomei Cheng et al. "Molecular Characterization of the B-N-Acetylglucosaminidase of Escherichia coli and Its Role in Cell Wall Recycling". In: *Journal of Bacteriology* 182.17 (2000), pp. 4836–4840.

[342] Tsuyoshi Uehara and James T Park. "The N-Acetyl-D-Glucosamine Kinase of Escherichia coli and Its Role in Murein Recycling". In: *Journal of Bacteriology* 186.21 (2004), pp. 7273–7279. DOI: 10.1128/JB.186.21.7273.

[343] Tsuyoshi Uehara et al. "Recycling of the Anhydro-N-Acetylmuramic Acid Derived from Cell Wall Murein Involves a Two-Step Conversion to N-Acetylglucosamine-Phosphate". In: *Journal of Bacteriology* 187.11 (2005), pp. 3643–3649. DOI: 10.1128/JB.187.11.3643.

[344] Jacqueline Plumbridge. "An Alternative Route for Recycling of N-Acetylglucosamine from Peptidoglycan Involves the N-Acetylglucosamine Phosphotransferase System in Escherichia coli". In: *Journal of Bacteriology* 191.18 (2009), pp. 5641–5647. DOI: 10.1128/JB.00448-09.

[345] Ulrike Dahl et al. "Identification of a Phosphotransferase System of Escherichia coli Required for Growth on N-Acetylmuramic Acid". In: *Journal of Bacteriology* 186.8 (2004), pp. 2385–2392. DOI: 10.1128/JB.186.8.2385.

[346] Tina Jaeger et al. "Scission of the Lactyl Ether Bond of N-Acetylmuramic Acid by Escherichia coli "Etherase"". In: *Journal of Biological Chemistry* 280.34 (2005), pp. 30100–30106. DOI: 10.1074/jbc.M502208200.

[347] T Jaeger and C Mayer. "N-acetylmuramic acid 6-phosphate lyases (MurNAc etherases): role in cell wall metabolism, distribution, structure, and mechanism". In: *Cellular and Molecular Life Sciences* 65 (2008), pp. 928–939. DOI: 10.1007/s00018-007-7399-x.

[348] R. J. White. "Control of Amino Sugar Metabolism in Escherichia coli and Isolation of Mutants Uable to Degrade Amino Sugars". In: *Biochemical Journal* 106 (1968), pp. 847–858.

[349] R. J White and C. A. Pasternak. "The Purification and Properties of N-Acetylglucosamine-6-Phosphate Deacetylase from Escherichia coli". In: *Biochemical Journal* 105 (1967), pp. 121–125.

[350] Dominique Mengin-Lecreulx, Jean Van Heijenoort, and James T Park. "Identification of the mpl Gene Encoding UDP-N-Acetylmuramate: L-Alanyl-y-D-Glutamyl-meso-Diaminopimelate Ligase in Escherichia coli and Its Role in Recycling of Cell Wall Peptidoglycan". In: *Journal of Bacteriology* 178.18 (1996), pp. 5347–5352.

[351] J. T. Park. "Turnover and recycling of the murein sacculus in oligopeptide permease- negative strains of Escherichia coli: Indirect evidence for an alternative permease system and for a monolayered sacculus". In: *Journal of Bacteriology* 175.1 (1993), pp. 7–11. DOI: 0021-9193/93/010007-05$02.00/0.

[352] James T Park et al. "MppA, a Periplasmic Binding Protein Essential for Import of the Bacterial Cell Wall Peptide L-Alanyl-y-D-Glutamyl-meso-Diaminopimelate". In: *Journal of Bacteriology* 180.5 (1998), pp. 1215–1223.

[353] Ellen Z Baum et al. "Identification of a Dithiazoline Inhibitor of Escherichia coli L , D -Carboxypeptidase A". In: *Antimicrobial Agents and Chemotherapy* 49.11 (2005), pp. 4500–4507. DOI: 10.1128/AAC.49.11.4500.

[354] Jonathan Gisin et al. "A cell wall recycling shortcut that bypasses peptidoglycan de novo biosynthesis." In: *Nature Chemical Biology* 9 (2013), pp. 491–3. DOI: 10.1038/nchembio.1289.

[355] Marina Borisova, Jonathan Gisin, and Christoph Mayer. "The N -Acetylmuramic Acid 6-Phosphate Phosphatase MupP Completes the Pseudomonas Peptidoglycan Recycling Pathway Leading to Intrinsic Fosfomycin Resistance". In: *mBio* 8.2 (2017), pp. 1–12.

[356] Coralie Fumeaux and Thomas G Bernhardt. "Identification of MupP as a New Peptidoglycan Recycling Factor and Antibiotic Resistance Determinant in Pseudomonas aeruginosa". In: *mBio* 8.2 (2017), pp. 1–13.

[357] Angela Ruscitto et al. "Regulation and Molecular Basis of Environmental Muropeptide Uptake and Utilization in Fastidious Oral Anaerobe Tannerella forsythia". In: *Frontiers in Microbiology* 8 (2017), pp. 1–9. DOI: 10.3389/fmicb.2017.00648.

[358] Angela Ruscitto et al. "Identification of a Novel N -Acetylmuramic Acid Transporter in Tannerella forsythia". In: *Journal of Bacteriology* 198.22 (2016), pp. 3119–3125. DOI: 10.1128/JB.00473-16.Editor.

[359] Pavel Kotrba, Masayuki Inui, and Hideaki Yukawa. "Bacterial phosphotransferase system (PTS) in carbohydrate uptake and control of carbon metabolism". In: *Journal of Bioscience and Bioengineering* 92.6 (2001), pp. 502–517. DOI: 10.1016/S1389-1723(01)80308-X.

[360] Bruce H Hebeler and Frank E Young. "Chemical Composition and Turnover of Peptidoglycan in Neisseria gonorrhoeae". In: *Journal of Bacteriology* 126.3 (1976), pp. 1180–1185.

[361] Raoul S Rosenthal. "Release of Soluble Peptidoglycan from Growing Gonococci : Hexaminidase and Amidase Activities". In: *Infection and Immunity* 24.3 (1979), pp. 869–878.

[362] William E Goldman, David G Klapper, and Joel B Baseman. "Detection, Isolation, and Analysis of a Released Bordetella pertussis Product Toxic to Cultured Tracheal Cells". In: *Infection and Immunity* 36.2 (1982), pp. 782–794.

[363] Jia Mun Chan and Joseph P. Dillard. "Neisseria gonorrhoeae crippled its peptidoglycan fragment permease to facilitate toxic peptidoglycan monomer release". In: *Journal of Bacteriology* 198.21 (2016), pp. 3029–3040. DOI: 10.1128/JB.00437-16.

[364] Karen A. Cloud and Joseph P. Dillard. "A lytic transglycosylase of Neisseria gonorrhoeae is involved in peptidoglycan-derived cytotoxin production". In: *Infection and Immunity* 70.6 (2002), pp. 2752–2757. DOI: 10.1128/IAI.70.6.2752-2757.2002.

[365] Silke Litzinger et al. "Structural and Kinetic Analysis of Bacillus subtilis N -Acetylglucosaminidase Reveals a Unique Asp-His Dyad". In: *Journal of Biological Chemistry* 285.46 (2010), pp. 35675–35684. DOI: 10.1074/jbc.M110.131037.

[366] Jan Reith, Anne Berking, and Christoph Mayer. "Characterization of an N-acetylmuramic acid/N-acetylglucosamine kinase of Clostridium acetobutylicum". In: *Journal of Bacteriology* 193.19 (2011), pp. 5386–5392. DOI: 10.1128/JB.05514-11.

[367] Jan Reith and Christoph Mayer. "Characterization of a glucosamine/glucosaminide N-acetyltransferase of Clostridium acetobutylicum". In: *Journal of Bacteriology* 193.19 (2011), pp. 5393–5399. DOI: 10.1128/JB.05519-11.

[368] Marina Borisova et al. "Peptidoglycan recycling in gram-positive bacteria is crucial for survival in stationary phase". In: *mBio* 7.5 (2016), pp. 1–10. DOI: 10.1128/mBio.00923-16.

[369] Ana Amoroso et al. "A peptidoglycan fragment triggers B-lactam resistance in Bacillus licheniformis". In: *PLoS Pathogens* 8.3 (2012). DOI: 10.1371/journal.ppat.1002571.

[370] Jan Reith. "Characterization of peptidoglycan-recovering enzymes of Clostridium acetobutylicum". PhD thesis. 2012.

[371] Joachim Volker Höltje et al. "The negative regulator of / 3-1actamase induction AmpD is a N-acetyl-anhydromuramyl-L-alanine amidase". In: *FEMS Microbiology Letters* 122 (1994), pp. 159–164.

[372] Boris Görke and Jörg Stülke. "Carbon catabolite repression in bacteria: many ways to make the most out of nutrients." In: *Nature reviews. Microbiology* 6.8 (2008), pp. 613–24. DOI: 10.1038/nrmicro1932.

[373] Marc A. Boudreau, Jed F. Fisher, and Shahriar Mobashery. "Messenger functions of the bacterial cell wall-derived muropeptides". In: *Biochemistry* 51.14 (2012), pp. 2974–2990. DOI: 10.1021/bi300174x. arXiv: NIHMS150003.

[374] Jessica B Warner and Juke S Lolkema. "CcpA-Dependent Carbon Catabolite Repression in Bacteria". In: *Microbiology and Molecular Biology Reviews* 67.4 (2003), pp. 475–490. DOI: 10.1128/MMBR.67.4.475.

[375] Tina M. Henkin. "The role of the CcpA transcriptional regulator in carbon metabolism in Bacillus subtilis". In: *FEMS Microbiology Letters* 135 (1996), pp. 9–15.

[376] J Stulke and W Hillen. "Carbon catabolite repression in bacteria." In: *Current opinion in microbiology* 2.2 (1999), pp. 195–201. DOI: 10.1016/S1369-5274(99)80034-4.

[377] Josef Deutscher, Christof Francke, and Pieter W Postma. "How Phosphotransferase System-Related Protein Phosphorylation Regulates Carbohydrate Metabolism in Bacteria". In: *Microbiol. Mol. Biol. Rev.* 70.4 (2006), pp. 939–1031. DOI: 10.1128/mmbr.00024-06.

[378] Josef Deutscher. "The mechanisms of carbon catabolite repression in bacteria". In: *Current Opinion in Microbiology* 11.2 (2008), pp. 87–93. DOI: 10.1016/j.mib.2008.02.007.

[379] Maria A Schumacher et al. "Structural Mechanism for the Fine-tuning of CcpA Function by The Small Molecule Effectors Glucose 6-Phosphate and Fructose 1 , 6-Bisphosphate". In: *Journal of Molecular Biology* 368 (2007), pp. 1042–1050. DOI: 10.1016/j.jmb.2007.02.054.

[380] Hans-matti Blencke et al. "Transcriptional profiling of gene expression in response to glucose in Bacillus subtilis: regulation of the central metabolic pathways". In: *Metabolic Engineering* 5 (2003), pp. 133–149. DOI: 10.1016/S1096-7176(03)00009-0.

[381] Jade Leiba et al. "A novel mode of regulation of the Staphylococcus aureus catabolite control protein A (CcpA) mediated by Stk1 protein phosphorylation". In: *Journal of Biological Chemistry* 287.52 (2012), pp. 43607–43619. DOI: 10.1074/jbc.M112.418913.

[382] Ishita M. Shah et al. "A Eukaryotic-like Ser/Thr Kinase Signals Bacteria to Exit Dormancy in Response to Peptidoglycan Fragments". In: *Cell* 135.3 (2008), pp. 486–496. DOI: 10.1016/j.cell.2008.08.039. arXiv: NIHMS150003.

[383] Qianqian Wang et al. "A Comprehensive Study of the Interaction between Peptidoglycan Fragments and the Extracellular Domain of Mycobacterium

tuberculosis Ser / Thr Kinase PknB". In: *ChemBioChem* 18 (2017), pp. 2094–2098. DOI: 10.1002/cbic.201700385.

[384] Brian P. Lazzaro and Jens Rolff. "Danger, Microbes, and Homeostasis". In: *Science* 332.6025 (2011), pp. 43–44. DOI: 10.1126/science.1200486.

[385] Catherine Chaput and Ivo G. Boneca. "Peptidoglycan detection by mammals and flies". In: *Microbes and Infection* 9.5 (2007), pp. 637–647. DOI: 10.1016/j.micinf.2007.01.022.

[386] Helen Sarantis and Sergio Grinstein. "Subversion of phagocytosis for pathogen survival". In: *Cell Host and Microbe* 12.4 (2012), pp. 419–431. DOI: 10.1016/j.chom.2012.09.001.

[387] Jerome Viala et al. "Nod1 responds to peptidoglycan delivered by the Helicobacter pylori cag pathogenicity island". In: *Nature Immunology* 5.11 (2004), pp. 1166–1174. DOI: 10.1038/ni1131.

[388] Richard Wheeler et al. "The biology of bacterial peptidoglycans and their impact on host immunity and physiology". In: *Cellular Microbiology* 16.7 (2014), pp. 1014–1023. DOI: 10.1111/cmi.12304.

[389] Donggi Paik et al. "SLC46 Family Transporters Facilitate Cytosolic Innate Immune Recognition of Monomeric Peptidoglycans". In: *The Journal of Immunology* (2017), pp. 1–9. DOI: 10.4049/jimmunol.1600409.

[390] Stephen E Girardin et al. "Nod2 Is a General Sensor of Peptidoglycan through Muramyl Dipeptide (MDP) Detection *". In: *The Journal of Biological Chemistry* (2003), pp. 8869–8873. DOI: 10.1074/jbc.C200651200.

[391] Stephen E Girardin et al. "Nod1 detects a unique muropeptide from gram-negative bacterial peptidoglycan." In: *Science (New York, N.Y.)* 300.5625 (2003), pp. 1584–1587. DOI: 10.1126/science.1084677. arXiv: 1002.1037.

[392] Mathias Chamaillard et al. "An essential role for NOD1 in host recognition of bacterial peptidoglycan containing diaminopimelic acid". In: *Nature Immunology* 4.7 (2003), pp. 702–707.

[393] Mizuho Hasegawa et al. "Differential release and distribution of Nod1 and Nod2 immunostimulatory molecules among bacterial species and environments". In: *Journal of Biological Chemistry* 281.39 (2006), pp. 29054–29063. DOI: 10.1074/jbc.M602638200.

[394] Yukari Fujimoto and Koichi Fukase. "Structures, Synthesis, and Human Nod1 Stimulation of Immunostimulatory Bacterial Peptidoglycan Fragments in the Environment". In: *Journal of Natural Products* 74 (2011), pp. 518–525. DOI: 10.1021/np100795d.

[395] Ruslan Medzhitov and Charles A Janeway. "How does the immune system distinguish self from nonself?" In: *Seminars in Immunology* 12 (2000), pp. 185–188. DOI: 10.1006/smim.2000.0230.

[396] Stephen E Girardin et al. "Peptidoglycan Molecular Requirements Allowing Detection by Nod1 and Nod2". In: *The Journal of Biological Chemistry* 278.43 (2003), pp. 41702–41708. DOI: 10.1074/jbc.M307198200.

[397] Thomas Volz et al. "Natural Staphylococcus aureus-derived peptidoglycan fragments activate NOD2 and act as potent costimulators of the innate immune system exclusively in the presence of TLR signals". In: *FASEB Journal* 24.10 (2010), pp. 4089–4102. DOI: 10.1096/fj.09-151001.

[398] Andrea A Gust et al. "Plant LysM proteins : modules mediating symbiosis and immunity". In: *Trends in Plant Science* 17.8 (2012), pp. 495–502. DOI: 10.1016/j.tplants.2012.04.003.

[399] Roman Dziarski and Dipika Gupta. "The peptidoglycan recognition proteins (PGRPs)." In: *Genome biology* 7.8 (2006), p. 232. DOI: 10.1186/gb-2006-7-8-232.

[400] Nicholas J Gay et al. "Assembly and localization of Toll-like receptor signalling complexes". In: *Nature Reviews Immunology* 14.8 (2014), pp. 546–558. DOI: 10.1038/nri3713.

[401] Andrea J Wolf and David M Underhill. "Peptidoglycan recognition by the innate immune system". In: *Nature Reviews Immunology* (2018), pp. 1–12. DOI: 10.1038/nri.2017.136.

[402] Fabio Martinon et al. "Identification of Bacterial Muramyl Dipeptide as Activator of the NALP3 / Cryopyrin Inflammasome". In: *Current Biology* 14 (2004), pp. 1929–1934. DOI: 10.1016/j.

[403] Matija Hedl and Clara Abraham. "NLRP1 and NLRP3 inflammasomes are essential for distinct outcomes of decreased cytokines but enhanced bacterial killing upon chronic Nod2 stimulation". In: *American Journal of Physiology. Gastrointestinal and Liver Physiology* 304.6 (2013), pp. 583–596. DOI: 10.1152/ajpgi.00297.2012.

[404] Andrea J Wolf et al. "Hexokinase Is an Innate Immune Receptor for the Detection of Bacterial Peptidoglycan Article Hexokinase Is an Innate Immune Receptor for the Detection of Bacterial Peptidoglycan". In: *Cell* 166.3 (2016), pp. 624–636. DOI: 10.1016/j.cell.2016.05.076.

[405] Leonardo H Travassos et al. "Toll-like receptor 2-dependent bacterial sensing does not occur via peptidoglycan recognition". In: *EMBO Reports* 5.10 (2004), pp. 1000–1006. DOI: 10.1038/sj.embor.7400248.

[406] M A Muller-Anstett et al. "Staphylococcal Peptidoglycan Co-Localizes with Nod2 and TLR2 and Activates Innate Immune Response via Both Receptors in Primary Murine Keratinocytes". In: *PLoS ONE* 5.10 (2010), e13153. DOI: 10.1371/journal.pone.0013153.

[407] Roman Dziarski and Dipika Gupta. "Staphylococcus aureus Peptidoglycan Is a Toll-Like Receptor 2 Activator : a Reevaluation Staphylococcus aureus Peptidoglycan Is a Toll-Like Receptor 2 Activator : a Reevaluation". In: *Infection and Immunity* 73.8 (2005), pp. 5212–5216. DOI: 10.1128/IAI.73.8.5212.

[408] Jinkeng Asong et al. "Binding and Cellular Activation Studies Reveal That Toll-like Receptor 2 Can Differentially Recognize Peptidoglycan from Gram-positive and Gram-negative Bacteria". In: *The Journal of Biological Chemistry* 284.13 (2009), pp. 8643–8653. DOI: 10.1074/jbc.M806633200.

[409] Mohamed Lamkanfi and Vishva M Dixit. "Mechanisms and Functions of Inflammasomes". In: *Cell* 157.5 (2014), pp. 1013–1022. DOI: 10.1016/j.cell.2014.04.007.

[410] Barry S Schonwetter, Ethan D Stolzenberg, and Michael A Zasloff. "Epithelial Antibiotics Induced at Sites of Inflammation". In: *Science* 267.March (1995), pp. 1645–1648.

[411] Ivan Tattoli et al. "NLRX1 is a mitochondrial NOD-like receptor that amplifies NF-kB and JNK pathways by inducing reactive oxygen species production". In: *EMBO Reports* 9.3 (2008), pp. 293–300. DOI: 10.1038/sj.embor.7401161.

[412] Georg Felix and Thomas Boller. "Molecular Sensing of Bacteria in Plants". In: *The Journal of Biological Chemistry* 278.8 (2003), pp. 6201–6208. DOI: 10.1074/jbc.M209880200.

[413] Andrea A Gust et al. "Bacteria-derived Peptidoglycans Constitute Pathogen-associated Molecular Patterns Triggering Innate Immunity in Arabidopsis". In: *The Journal of Biological Chemistry* 282.44 (2007), pp. 32338–32348. DOI: 10.1074/jbc.M704886200.

[414] Gitte Erbs et al. "Article Peptidoglycan and Muropeptides from Pathogens Agrobacterium and Xanthomonas Elicit Plant Innate Immunity: Structure and Activity". In: *Chemistry and Biology* May (2008), pp. 438–448. DOI: 10.1016/j.chembiol.2008.03.017.

[415] Girbe Buist et al. "Micro Review LysM , a widely distributed protein motif for binding to (peptido) glycans". In: *Molecular Microbiology* 68.4 (2008), pp. 838–847. DOI: 10.1111/j.1365-2958.2008.06211.x.

[416] Roland Willmann et al. "Arabidopsis lysin-motif proteins LYM1 LYM3 CERK1 mediate bacterial peptidoglycan sensing and immunity to bacterial infection". In: *Proceedings of the National Academy of Sciences* 108.49 (2011), pp. 19824–19829. DOI: 10.1073/pnas.1112862108/-/DCSupplemental.www.pnas.org/cgi/doi/10.1073/pnas.1112862108.

[417] Yusuke Kouzai et al. "Targeted Gene Disruption of OsCERK1 Reveals Its Indispensable Role in Chitin Perception and Involvement in the Peptidoglycan Response and Immunity in Rice". In: *Molecular Plant-Mirobe Interactions* 27.9 (2014), pp. 975–982.

[418] Julien Royet, Dipika Gupta, and Roman Dziarski. "Peptidoglycan recognition proteins: modulators of the microbiome and inflammation." In: *Nature Reviews Immunology* 11.12 (2011), pp. 837–51. DOI: 10.1038/nri3089.

[419] Min-sung Kim, Minji Byun, and Byung-ha Oh. "Crystal structure of peptidoglycan recognition protein LB from Drosophila melanogaster". In: *Nature Immunology* 4.8 (2003), pp. 787–793.

[420] Bruno Lemaitre and Jules Hoffmann. "The Host Defense of Drosophila melanogaster". In: *Annual Review of Immunology* 25 (2007), pp. 697–743. DOI: 10.1146/annurev.immunol.25.022106.141615.

[421] Sangwoo Cho et al. "Structural insights into the bactericidal mechanism of human peptidoglycan recognition proteins." In: *Proceedings of the National Academy of Sciences of the United States of America* 104.21 (2007), pp. 8761–6. DOI: 10.1073/pnas.0701453104.

[422] Des Raj Kashyap et al. "Peptidoglycan recognition proteins kill bacteria by activating protein-sensing two-component systems." In: *Nature medicine* 17.6 (2011), pp. 676–83. DOI: 10.1038/nm.2357.

[423] François Coulombe et al. "Increased NOD2-mediated recognition of N-glycolyl muramyl dipeptide". In: *Journal of Experimental Medicine* 206.8 (2009), pp. 1–8. DOI: 10.1084/jem.20081779.

[424] Li-chung Hsu et al. "A NOD2–NALP1 complex mediates caspase-1-dependent IL-1B secretion in response to Bacillus anthracis infection and muramyl dipeptide". In: *Proceedings of the National Academy of Sciences* 105.22 (2008), pp. 7803–7808.

[425] Nikolaos Mavrogiorgos et al. "Activation of NOD receptors by Neisseria gonorrhoeae modulates the innate immune response". In: *Innate Immunity* 20.4 (2014), pp. 377–389. DOI: 10.1177/1753425913493453.

[426] Brian M. Peters et al. "Microbial interactions and differential protein expression in Staphylococcus aureus -Candida albicans dual-species biofilms". In: *FEMS Immunology and Medical Microbiology* 59.3 (2010), pp. 493–503. DOI: 10.1111/j.1574-695X.2010.00710.x.

[427] Allia K. Lindsay and Deborah A. Hogan. "Candida albicans: Molecular interactions with Pseudomonas aeruginosa and Staphylococcus aureus". In: *Fungal Biology Reviews* 28.4 (2014), pp. 85–96. DOI: 10.1016/j.fbr.2014.10.002.

[428] Xiao-li Xu et al. "Article Bacterial Peptidoglycan Triggers Candida albicans Hyphal Growth by Directly Activating the Adenylyl Cyclase Cyr1p". In: *Cell Host & Microbe* 4 (2008), pp. 28–39. DOI: 10.1016/j.chom.2008.05.014.

[429] Anders Folkesson et al. "Components of the peptidoglycan-recycling pathway modulate invasion and intracellular survival of Salmonella enterica serovar Typhimurium". In: *Cellular Microbiology* 7.1 (2005), pp. 147–155. DOI: 10.1111/j.1462-5822.2004.00443.x.

[430] Kenji Kurokawa et al. "Biochemical characterization of evasion from peptidoglycan recognition by Staphylococcus aureus d-alanylated wall teichoic acid in insect innate immunity". In: *Developmental and Comparative Immunology* 35.8 (2011), pp. 835–839. DOI: 10.1016/j.dci.2011.03.001.

[431] Jack Dorling, Caroline Moraes, and Jens Rolff. "Recognition, survival and persistence of Staphylococcus aureus in the model host Tenebrio molitor". In: *Developmental and Comparative Immunology* 48.2 (2015), pp. 284–290. DOI: 10.1016/j.dci.2014.08.010.

[432] Andrew J. Needham et al. "Drosophila melanogaster as a model host for Staphylococcus aureus infection". In: *Microbiology* 150.7 (2004), pp. 2347–2355. DOI: 10.1099/mic.0.27116-0.

[433] Kaiyu Wu et al. "Assessment of virulence diversity of methicillin-resistant Staphylococcus aureus strains with a Drosophila melanogaster infection model". In: *BMC Microbiology* 12.1 (2012), p. 274. DOI: 10.1186/1471-2180-12-274.

[434] Ronen Ben-Ami et al. "Drosophila melanogaster as a model to explore the effects of methicillin-resistant Staphylococcus aureus strain type on virulence and response to linezolid treatment". In: *Microbial Pathogenesis* 55.1 (2013), pp. 16–20. DOI: 10.1016/j.micpath.2012.11.012.

[435] Rongjin Guan et al. "Structural basis for peptidoglycan binding by peptidoglycan recognition proteins". In: *Proceedings of the National Academy of Sciences* 101.49 (2004), pp. 17168–17173.

[436] Peter Mellroth and H Steiner. "PGRP-SB1: An N -acetylmuramoyl L-alanine amidase with antibacterial activity". In: *Biochemical and Biophysical Research Communications* 350 (2006), pp. 994–999. DOI: 10.1016/j.bbrc.2006.09.139.

[437] Anna Zaidman-Remy et al. "The Drosophila Amidase PGRP-LB Modulates the Immune Response to Bacterial Infection". In: *Immunity* 24.4 (2006), pp. 463–473. DOI: 10.1016/j.immuni.2006.02.012.

[438] Marie Gottar et al. "The Drosophila immune response against Gram-negative bacteria is mediated by a peptidoglycan recognition protein." In: *Nature* 416.6881 (2002), pp. 640–644. DOI: 10.1038/nature734.

[439] Takashi Kaneko et al. "PGRP-LC and PGRP-LE have essential yet distinct functions in the drosophila immune response to monomeric DAP-type peptidoglycan". In: *Nature Immunology* 7.7 (2006), pp. 715–723. DOI: 10.1038/ni1356.

[440] Jae-hong Lim et al. "Structural Basis for Preferential Recognition of Diaminopimelic Acid-type Peptidoglycan by a Subset of Peptidoglycan Recognition Proteins". In: *Journal of Biological Chemistry* 281.12 (2006), pp. 8286–8295. DOI: 10.1074/jbc.M513030200.

[441] Frederic Maillet et al. "Article The Drosophila Peptidoglycan Recognition Protein PGRP-LF Blocks PGRP-LC". In: *Cell Host & Microbe* 3 (2008), pp. 293–303. DOI: 10.1016/j.chom.2008.04.002.

[442] Aya Takehana et al. "Peptidoglycan recognition protein (PGRP)-LE and PGRP-LC act synergistically in Drosophila immunity". In: *The EMBO Journal* 23.23 (2004), pp. 4690–4700. DOI: 10.1038/sj.emboj.7600466.

[443] Takashi Kaneko et al. "Monomeric and Polymeric Gram-Negative Peptidoglycan but Not Purified LPS Stimulate the Drosophila IMD Pathway". In: *Immunity* 20 (2004), pp. 637–649.

[444] Tamaki Yano et al. "Autophagic control of listeria through intracellular innate immune recognition in drosophila". In: *Nature Immunology* 9.8 (2008), pp. 908–916. DOI: 10.1038/ni.1634.

[445] T Michel et al. "Drosophila Toll is activated by Gram-positive bacteria through a circulating peptidoglycan recognition protein." In: *Nature* 414.6865 (2001), pp. 756–759. DOI: 10.1038/414756a.

[446] Lihui Wang et al. "Peptidoglycan recognition protein-SD provides versatility of receptor formation in Drosophila immunity." In: *Proceedings of the National Academy of Sciences of the United States of America* 105.33 (2008), pp. 11881–6. DOI: 10.1073/pnas.0710092105.

[447] Sergio R Filipe, Alexander Tomasz, and Petros Ligoxygakis. "Requirements of peptidoglycan structure that allow detection by the Drosophila Toll pathway." In: *EMBO Reports* 6.4 (2005), pp. 327–33. DOI: 10.1038/sj.embor.7400371.

[448] Jean-baptiste Reiser, Luc Teyton, and Ian A Wilson. "Crystal Structure of the Drosophila Peptidoglycan Recognition Protein (PGRP)-SA at 1.56 A Resolution". In: *Journal of Molecular Biology* 340 (2004), pp. 909–917. DOI: 10.1016/j.jmb.2004.04.077.

[449] Chung I. Chang et al. "A Drosophila pattern recognition receptor contains a peptidoglycan docking groove and unusual L,D-carboxypeptidase activity". In: *PLoS Biology* 2.9 (2004). DOI: 10.1371/journal.pbio.0020277.

[450] Vincent Bischoff et al. "Function of the drosophila pattern-recognition receptor PGRP-SD in the detection of Gram-positive bacteria". In: *Nature Immunology* 5.11 (2004), pp. 1175–1180. DOI: 10.1038/ni1123.

[451] Philippe Leone et al. "Crystal structure of Drosophila PGRP-SD suggests binding to DAP-type but not lysine-type peptidoglycan". In: *Molecular Immunology* 45 (2008), pp. 2521–2530. DOI: 10.1016/j.molimm.2008.01.015.

[452] Lihui Wang et al. "Sensing of Gram-positive bacteria in Drosophila: GNBP1 is needed to process and present peptidoglycan to PGRP-SA." In: *The EMBO journal* 25.20 (2006), pp. 5005–14. DOI: 10.1038/sj.emboj.7601363.

[453] Bruno Lemaitre et al. "The Dorsoventral Regulatory Gene Cassette Spaetzle / Toll / cactus Controls the spa Potent Antifungal Response in Drosophila Adults". In: *Cell* 86 (1996), pp. 973–983.

[454] Lihui Wang and Petros Ligoxygakis. "Pathogen recognition and signalling in the Drosophila innate immune response". In: *Immunobiology* 211.4 (2006), pp. 251–261. DOI: 10.1016/j.imbio.2006.01.001.

[455] Marcia P Belvin, Yishi Jin, and Kathryn V Anderson. "Cactus protein degradation mediates Drosophila dorsal-ventral signaling". In: *Genes and Development* 9 (1995), pp. 783–793.

[456] J Yang and R Steward. "A multimeric complex and the nuclear targeting of the Drosophila Rel protein Dorsal". In: *Proceedings of the National Academy of Sciences* 94.12 (1997), pp. 14524–14529.

[457] Magda L. Atilano et al. "Wall teichoic acids of staphylococcus aureus limit recognition by the drosophila peptidoglycan recognition protein-SA to promote pathogenicity". In: *PLoS Pathogens* 7.12 (2011). DOI: 10.1371/journal.ppat.1002421.

[458] Yukichika Tabuchi et al. "Inhibitory role for D-alanylation of wall teichoic acid in activation of insect Toll pathway by peptidoglycan of Staphylococcus aureus." In: *The Journal of Immunology* 185.4 (2010), pp. 2424–2431. DOI: 10.4049/jimmunol.1000625.

[459] Chan Ki Min et al. "Genome-based construction of the metabolic pathways of Orientia tsutsugamushi and comparative analysis within the Rickettsiales order". In: *Comparative and Functional Genomics* 2008 (2008). DOI: 10.1155/2008/623145.

[460] Tina Jaeger and Christoph Mayer. "The transcriptional factors MurR and catabolite activator protein regulate N-acetylmuramic acid catabolism in Escherichia coli". In: *Journal of Bacteriology* 190.20 (2008), pp. 6598–6608. DOI: 10.1128/JB.00642-08.

[461] Robert D. Finn, Jody Clements, and Sean R. Eddy. "HMMER web server: Interactive sequence similarity searching". In: *Nucleic Acids Research* 39.SUPPL. 2 (2011), pp. 29–37. DOI: 10.1093/nar/gkr367.

[462] Ian Sillitoe et al. "New functional families (FunFams) in CATH to improve the mapping of conserved functional sites to 3D structures". In: *Nucleic Acids Research* 41.D1 (2013), pp. 490–498. DOI: 10.1093/nar/gks1211.

[463] Lex Overmars et al. "MGcV: the microbial genomic context viewer for comparative genome analysis". In: *BMC Genomics* 14.209 (2013), pp. 1–9.

[464] Y Miwa et al. "Evaluation and characterization of catabolite-responsive elements (cre) of Bacillus subtilis." In: *Nucleic acids research* 28.5 (2000), pp. 1206–10. DOI: 10.1093/nar/28.5.1206.

[465] Fabian Sievers et al. "Fast, scalable generation of high-quality protein multiple sequence alignments using Clustal Omega". In: *Molecular Systems Biology* 539 (2011). DOI: 10.1038/msb.2011.75.

[466] Evgeni M Zdobnov and Rolf Apweiler. "InterProScan - an integration platform for the signature-recognition methods in InterPro". In: *Bioinformatics* 17.9 (2001), pp. 847–848.

[467] Marco Punta et al. "The Pfam protein families database". In: *Nucleic Acids Research* 40 (2012), pp. 290–301. DOI: 10.1093/nar/gkr1065.

[468] Christophe Merlin et al. "The Escherichia coli metD Locus Encodes an ABC Transporter Which Includes Abc (MetN), YaeE (MetI), and YaeC (MetQ)". In: *Journal of Bacteriology* 184.19 (2002), pp. 5513–5517. DOI: 10.1128/JB.184.19.5513.

[469] Barbara G Hogarth and Christopher F Higgins. "Genetic Organization of the Oligopeptide Permease (opp) Locus of Salmonella typhimurium and Escherichia coli". In: *Journal of Bacteriology* 155.3 (1983), pp. 1548–1551.

[470] C Mathiopoulos et al. "A Bacillus subtilis dipeptide transport system expressed early during sporulation". In: *Molecular Microbiology* 5.8 (1991), pp. 1903–1913.

[471] Hitoshi Komatsuzawa et al. "The gate controlling cell wall synthesis in Staphylococcus aureus". In: *Molecular Microbiology* 53.4 (2004), pp. 1221–1231. DOI: 10.1111/j.1365-2958.2004.04200.x.

[472] Yefei Zhu et al. "RpiR Homologues May Link Staphylococcus aureus RNAIII Synthesis and Pentose Phosphate Pathway Regulation". In: *Journal of Bacteriology* 193.22 (2011), pp. 6187–6196. DOI: 10.1128/JB.05930-11.

[473] Ping Wang and Joseph Heitman. "Protein family review The cyclophilins". In: *Genome Biology* 6.7 (2005), pp. 266.1–266.6. DOI: 10.1186/gb-2005-6-7-226.

[474] Nicholas P. Vitko et al. "Expanded glucose import capability affords Staphylococcus aureus optimized glycolytic flux during infection". In: *mBio* 7.3 (2016), pp. 1–11. DOI: 10.1128/mBio.00296-16.

[475] Jaime Huerta-cepas et al. "eggNOG 4 . 5 : a hierarchical orthology framework with improved functional annotations for eukaryotic , prokaryotic and viral sequences". In: *Nucleic Acids Research* 44.10 (2017), pp. 286–293. DOI: 10.1093/nar/gkv1248.

[476] Maryvonne Arnaud, Arnaud Chastanet, and Michel De. "New Vector for Efficient Allelic Replacement in Naturally Gram-Positive Bacteria New Vector for Efficient Allelic Replacement in Naturally Gram-Positive Bacteria". In: *Applied and Enviromental Microbiology* 70.11 (2004), pp. 6887–6891. DOI: 10.1128/AEM.70.11.6887.

[477] Silvia Herbert et al. "Repair of global regulators in Staphylococcus aureus 8325 and comparative analysis with other clinical isolates". In: *Infection and Immunity* 78.6 (2010), pp. 2877–2889. DOI: 10.1128/IAI.00088-10.

[478] W Kundig, S Ghosh, and S Roseman. "PHOSPHATE BOUND TO HISTIDJNE IN A PROTEIN AS AN INTERMEDIATE IN A NOVEL PHOSPHOTRANSFERASE SYSTEM * Phosphoenolypyruvate (PEP) + HPr Phosphohistidine-". In: *Proceedings of the National Academy of Sciences* 52 (1964), pp. 1067–1074.

[479] Divya Balasubramanian et al. "Staphylococcus aureus Coordinates Leukocidin Expression and Pathogenesis by Sensing Metabolic Fluxes via RpiRc". In: *mBio* 7.3 (2016), pp. 1–13. DOI: 10.1128/mBio.00818-16.Editor.

[480] Giulia Nigro et al. "Muramylpeptide shedding modulates cell sensing of Shigella flexneri". In: *Cellular Microbiology* 10.3 (2008), pp. 682–695. DOI: 10.1111/j.1462-5822.2007.01075.x.

[481] Mireille Hervé et al. "Biochemical Characterization and Physiological Properties of Escherichia coli UDP-N-Acetylmuramate : L-Alanyl-gamma-D-Glutamyl-meso-Diaminopimelate Ligase". In: *Journal of Bacteriology* 189.11 (2007), pp. 3987–3995. DOI: 10.1128/JB.00087-07.

[482] Karen A Cloud-Hansen et al. "Neisseria gonorrhoeae Uses Two Lytic Transglycosylases To Produce Cytotoxic Peptidoglycan Monomers". In: *Journal of Bacteriology* 190.17 (2008), pp. 5989–5994. DOI: 10.1128/JB.00506-08.

[483] Yolande A Chan et al. "The Lytic Transglycosylases of Neisseria gonorrhoeae". In: *Microbial Drug Resistance* 18.3 (2012). DOI: 10.1089/mdr.2012.0001.

[484] Tanya A Koropatnick et al. "Microbial factor-mediated development in a host-bacterial mutulaism". In: *Science* 306.11 (2004), pp. 1186–1189.

[485] Dawn M Adin et al. "Mutations in ampG and Lytic Transglycosylase Genes Affect the Net Release of Peptidoglycan Monomers from Vibrio fischeri". In: *Journal of Bacteriology* 191.7 (2009), pp. 2012–2022. DOI: 10.1128/JB.01547-08.

[486] Steven E Finkel. "Long-term survival during stationary phase: evolution and the GASP phenotype". In: *Nature Reviews Microbiology* 4.2 (2006), pp. 113–120. DOI: 10.1038/nrmicro1340.

[487] María Mercedes et al. "Microbial Competition: Escherichia coli Mutants That Take Over Stationary Phase Cultures". In: *Science* 259.5102 (2012), pp. 1757–1760.

[488] R Core Team. *R: A Language and Environment for Statistical Computing*. Vienna, Austria, 2015.

[489] Matthias Kahm et al. "Grofit: Fitting biological growth curves". In: *Journal of Statistical Software* 33.7 (2010), pp. 1–21. DOI: 10.1038/npre.2010.4508.1.

[490] Taeok Bae, Elizabeth M Glass, and Olaf Schneewind. "Generating a Collection of Insertion Mutations in the Staphylococcus aureus Genome Using bursa aurealis". In: *Methods in Molecular Biology*. Vol. 416. 7. 2008, pp. 103–116.

[491] Maria Teresa Ferreira et al. "Effect of Oxygen on Glucose Metabolism: Utilization of Lactate in Staphylococcus Aureus as Revealed by In Vivo NMR Studies". In: *PLoS ONE* 8.3 (2013). DOI: 10.1371/journal.pone.0058277.

[492] R A Proctor et al. "Small colony variants: a pathogenic form of bacteria that facilitates persistent and recurrent infections". In: *Nature Reviews Microbiology* 4.4 (2006), pp. 295–305. DOI: 10.1038/nrmicro1384.

[493] J Lengeler. "Streptozotocin, an antibiotic superior to penicillin in the selection of rare bacterial mutations". In: *FEMS Microbiology Letters* 5.161 (1979), pp. 417–419. DOI: DOI10.1111/j.1574-6968.1979.tb03371.x.

[494] J. Ammer et al. "Phosphorylation of Streptozotocin during uptake via the phosphoenolpyruvate: Sugar phosphotransferase system in Escherichia coli". In: *Antimicrobial Agents and Chemotherapy* 16.6 (1979), pp. 801–807. DOI: 10.1128/AAC.16.6.801.

[495] Alejandro F. Alice, Gaspar Pérez-Martínez, and Carmen Sánchez-Rivas. "Phosphoenolpyruvate phosphotransferase system and N-acetylglucosamine metabolism in Bacillus sphaericus". In: *Microbiology* 149.7 (2003), pp. 1687–1698. DOI: 10.1099/mic.0.26231-0.

[496] Yvonne G Y Chan et al. "Staphylococcus aureus mutants lacking the lytr-cpsa-Psr family of enzymes release cell wall teichoic acids into the extracellular medium". In: *Journal of Bacteriology* 195.20 (2013), pp. 4650–4659. DOI: 10.1128/JB.00544-13.

[497] Cullen L Myers et al. "Identification of Two Phosphate Starvation-induced Wall Teichoic Acid Hydrolases Provides First Insights into the Degradative Pathway of a Key Bacterial Cell Wall". In: *Journal of Biological Chemistry* 291.50 (2016), pp. 26066–26082. DOI: 10.1074/jbc.M116.760447.

[498] Ivo G. Boneca. "The role of peptidoglycan in pathogenesis". In: *Current Opinion in Microbiology* 8.1 (2005), pp. 46–53. DOI: 10.1016/j.mib.2004.12.008.

[499] Akiko Umeda et al. "Location of Peptidoglycan and Teichoic Acid on the Cell Wall Surface of Staphylococcus aureus as Determined by Immunoelectron Microscopy". In: *Journal of Electron Microscopy* 41 (1992), pp. 46–52.

[500] Johannes Schindelin et al. "Fiji : an open-source platform for biological-image analysis". In: *Nature Methods* 9.7 (2012), pp. 676–682. DOI: 10.1038/nmeth.2019.

[501] James T Park. "Identification of a dedicated recycling pathway for anhydro-N-acetylmuramic acid and N-acetylglucosamine derived from Escherichia coli cell wall murein". In: *Journal of Bacteriology* 183.13 (2001), pp. 3842–3847. DOI: 10.1128/JB.183.13.3842.

[502] Mette Thorsing et al. "Thioridazine Induces Major Changes in Global Gene Expression and Cell Wall Composition in Methicillin- Resistant Staphylococcus aureus USA300". In: *PLoS ONE* 8.5 (2013), pp. 1–13. DOI: 10.1371/journal.pone.0064518.

[503] Shasad Sharif et al. "Characterization of Peptidoglycan in Fem-Deletion Mutants of Methicillin-Resistant Staphylococcus aureus by Solid-State NMR". In: *Biochemistry* 48 (2009), pp. 3100–3108.

[504] Jacqueline Plumbridge. "Co-ordinated regulation of amino sugar biosynthesis and degradation: the NagC repressor acts as both an activator and a repressor for the transcription of the glmUS operon and requires two separated NagC binding sites". In: *The EMBO Journal* 14.16 (1995), pp. 3958–3965. DOI: 10.1002/j.1460-2075.1995.tb00067.x.

[505] Shamoon Naseem and James B. Konopka. "N-acetylglucosamine Regulates Virulence Properties in Microbial Pathogens". In: *PLOS Pathogens* 11.7 (2015), e1004947. DOI: 10.1371/journal.ppat.1004947.

[506] Edward S Reynolds. "The use of lead citrate at high pH as an electron-opaque stain in electron microscopy". In: *Journal of Cell Biology* 17.1 (1963), pp. 208–212.

[507] L T Threadgold. *The Ultrastructure of the Animal Cell*. 2nd Editio. Oxford: Pergamon Press, 1976.

[508] Carlos Quintela et al. "Peptidoglycan structure of Salmonella typhimurium growing within cultured mammalian cells". In: *Molecular Microbiology* 23.4 (1997), pp. 693–704.

[509] Agnieszka Bera et al. "Why are pathogenic staphylococci so lysozyme resistant ? The peptidoglycan O-acetyltransferase OatA is the major determinant for lysozyme resistance of Staphylococcus aureus". In: *Molecular Microbiology* 55 (2005), pp. 778–787. DOI: 10.1111/j.1365-2958.2004.04446.x.

[510] Agnieszka Bera et al. "Influence of wall teichoic acid on lysozyme resistance in Staphylococcus aureus". In: *Journal of Bacteriology* 189.1 (2007), pp. 280–283. DOI: 10.1128/JB.01221-06.

[511] Nahuel Fittipaldi et al. "Significant contribution of the pgdA gene to the virulence of Streptococcus suis". In: *Molecular Microbiology* 70.5 (2008), pp. 1120–1135. DOI: 10.1111/j.1365-2958.2008.06463.x.

[512] R. Dziarski. "Recognition of bacterial peptidoglycan by the innate immune system". In: *Cellular and Molecular Life Sciences* 60.9 (2003), pp. 1793–1804. DOI: 10.1007/s00018-003-3019-6.

[513] Ute Bertsche et al. "Peptidoglycan perception - Sensing bacteria by their common envelope structure". In: *International Journal of Medical Microbiology* 305.2 (2015), pp. 217–223. DOI: 10.1016/j.ijmm.2014.12.019.

[514] Mary W Vermeulen and Gary R Gray. "Processing of Bacillus subtilis peptidoglycan by a mouse macrophage cell line Processing of Bacillus subtilis Peptidoglycan by a Mouse". In: *Infection and Immunity* 46.2 (1984), pp. 476–483.

[515] G E P Box and D R Cox. "An Analysis of Transformations". In: *Journal of the Royal Statistical Society B; Methodological* 26.2 (1964), pp. 211–252.

[516] G M Wiseman. "Some characteristics of the beta-haemolysin of Staphylococcus aureus". In: *The Journal of Pathology* 89.1 (1965), pp. 187–207.

[517] Katrina Traber and Richard Novick. "A slipped-mispairing mutation in AgrA of laboratory strains and clinical isolates results in delayed activation of agr and failure to translate δ- and α-haemolysins". In: *Molecular Microbiology* 59.5 (2006), pp. 1519–1530. DOI: 10.1111/j.1365-2958.2005.04986.x.

[518] Linda Pasztor et al. "Staphylococcal major autolysin (Atl) is involved in excretion of cytoplasmic proteins". In: *Journal of Biological Chemistry* 285.47 (2010), pp. 36794–36803. DOI: 10.1074/jbc.M110.167312.

[519] John E. McGonigle, Joanne Purves, and Jens Rolff. "Intracellular survival of Staphylococcus aureus during persistent infection in the insect Tenebrio molitor". In: *Developmental and Comparative Immunology* 59 (2016), pp. 34–38. DOI: 10.1016/j.dci.2016.01.002.

[520] Naoaki Shinzawa et al. "p38 MAPK-Dependent Phagocytic Encapsulation Confers Infection Tolerance in Drosophila". In: *Cell Host and Microbe* 6.3 (2009), pp. 244–252. DOI: 10.1016/j.chom.2009.07.010.

[521] Jonathan Dworkin. "The Medium Is the Message: Interspecies and Interkingdom Signaling by Peptidoglycan and Related Bacterial Glycans." In: *Annual Review of Microbiology* 68 (2014), pp. 137–154. DOI: 10.1146/annurev-micro-091213-112844.

[522] Eric J G Pollitt et al. "Cooperation, quorum sensing, and evolution of virulence in Staphylococcus aureus". In: *Infection and Immunity* 82.3 (2014), pp. 1045–1051. DOI: 10.1128/IAI.01216-13.

[523] Kim A Brogden, Janet M Guthmiller, and Christopher E Taylor. "Human polymicrobial infections". In: *The Lancet* 365 (2005), pp. 253–255.

[524] Jacqueline Plumbridge. "CAP and Nag repressor binding to the regulatory regions of the nagE-B and manX genes of Escherichia coli". In: *Journal of Molecular Biology* 217 (1991), pp. 661–679.

[525] Jacqueline Plumbridge. "Repression and induction of the nag regulon of Escherichia coli K-12: the roles of nagC and nagA in maintenance of the uninduced state". In: *Molecular Microbiology* 5.8 (1991), pp. 2053–2062.

[526] Jacqueline Plumbridge and Annie Kolb. "DNA loop formation between Nag repressor molecules bound to its two operator sites is necessary for repression of the nag regulon of Escherichia coli in vivo". In: *Molecular Microbiology* 10.5 (1993), pp. 973–981.

[527] J A Plumbridge et al. "Coordinated Regulation of Amino Sugar-Synthesizing and -Degrading Enzymes in Escherichia coli K-12". In: *Journal of Bacteriology* 175.16 (1993), pp. 4951–4956.

[528] Stephanie Brown, John P. Santa Maria, and Suzanne Walker. "Wall Teichoic Acids of Gram-Positive Bacteria". In: *Annual Review of Microbiology* 67.1 (2013), pp. 313–336. DOI: 10.1146/annurev-micro-092412-155620. arXiv: NIHMS150003.

[529] Volker Winstel et al. "Wall Teichoic Acid Glycosylation Governs Staphylococcus aureus Nasal Colonization". In: *mBio* 6.4 (2015), e00632–15. DOI: 10.1128/mBio.00632-15.

[530] Jacob E Wang et al. "Peptidoglycan and lipoteichoic acid in Gram-positive bacterial sepsis: receptors, signal transduction, biological effects, and synergism". In: *Shock* 20.5 (2003), pp. 402–414.

[531] Aaron E Hirsh and Hunter B Fraser. "Protein dispensability and rate of evolution". In: *Nature* 411.6 (2001), pp. 1046–1049.

[532] Kristoffer T. Baek et al. "Genetic Variation in the Staphylococcus aureus 8325 Strain Lineage Revealed by Whole-Genome Sequencing". In: *PLoS ONE* 8.9 (2013), pp. 1–16. DOI: 10.1371/journal.pone.0077122.

[533] Andrew M Waterhouse et al. "Jalview Version 2 — a multiple sequence alignment editor and analysis workbench". In: *Bioinformatics* 25.9 (2009), pp. 1189–1191. DOI: 10.1093/bioinformatics/btp033.

[534] Quentin Geissmann. "OpenCFU, a New Free and Open-Source Software to Count Cell Colonies and Other Circular Objects". In: *PLoS ONE* 8.2 (2013), pp. 1–10. DOI: 10.1371/journal.pone.0054072.

[535] Kenshi Hayashi et al. "A rapid determination of sodium dodecyl sulphate with methylene blue". In: *Analytical Biochemistry* 67 (1975), pp. 503–506.

[536] Terry M. Therneau and Patricia M. Grambsch. *Modeling Survival Data: Extending the Cox Model*. New York: Springer, 2000.

[537] Thomas D Schmittgen and Kenneth J Livak. "Analyzing real-time PCR data by the comparative CT method". In: *Nature Protocols* 3.6 (2008), pp. 1101–1108. DOI: 10.1038/nprot.2008.73. arXiv: 1003.3921v1.

[538] Michael J Crawley. *The R Book*. 2nd. Somerset: John Wiley & Sons, Incorporated, 2012.

[539] W. N. Venables Ripley and B. D. *Modern Applied Statistics with S*. Fourth. New York: Springer, 2002.

[540] John Fox and Sanford Weisberg. *An (R) Companion to Applied Regression*. Second. Thousand Oaks, CA: Sage, 2011.

[541] Torsten Hothorn, Frank Bretz, and Peter Westfall. "Simultaneous Inference in General Parametric Models". In: *Biometrical Journal* 50.3 (2008), pp. 346–363.

[542] M L Atilano et al. "Teichoic acids are temporal and spatial regulators of peptidoglycan cross-linking in Staphylococcus aureus". In: *Proc.Natl.Acad.Sci.U.S.A* 107.44 (2010), pp. 18991–18996. DOI: 10.1073/pnas.1004304107.